New polypyridine anchoring ligands for coordination complexes and surface functionalization

Inauguraldissertation

zur

Erlangung der Würde eines Doktors der Philosophie

vorgelegt der

Philosophisch-Naturwissenschaftlichen Fakultät

der Universität Basel

von

Steffen Müller

aus Steinen, Deutschland

Lörrach, 2015

Genehmigt von der Philosophisch–Naturwissenschaftlichen Fakultät auf Antrag von:

Prof. Dr. Edwin C. Constable

Prof. Dr. Oliver S. Wenger

Basel, den 09.12.2014

Prof. Dr. Jörg Schibler
Dekan

In der Wissenschaft gleichen wir alle nur den Kindern,

die am Rande des Wissens hie und da einen Kiesel aufheben,

während sich der weite Ozean des Unbekannten

vor unseren Augen erstreckt.

Isaac Newton

Contents

Acknowledgements **iv**

Abbreviations **vi**

Table of compounds **ix**

Abstract **xii**

1 Introduction **1**

1.1 General 1

1.2 Dye-Sensitized Solar Cells (DSSCs) 4

1.3 Light-emitting electrochemical cells (LECs) 8

1.4 Sensing 10

1.5 Catalysis 12

1.6 Polymers 14

2 Coordinating anchoring ligands **17**

2.1 Abstract 17

2.2 Synthetic strategy and synthesis 18

2.2.1 Ligand L1 18

2.2.2 Ligand L3 19

2.2.3 Ligands L2 and L4 19

2.2.4 Activation of ligands L2 and L4 21

2.2.5 Thioacetate ligands S1 to S4 22

2.2.6 Ligands S5 and S6 for polymer functionalization 24

2.3 Photophysical properties 25

2.3.1 Absorption spectra 25

2.3.2 Photoluminescene 28

2.4 XRD 32

2.4.1 L4-CMe 32

2.5 Concluding remarks 34

2.5.1 Ligand L1 34
2.5.2 Ligand L3 34
2.5.3 Ligands L2 and L4 34

3 Complexes for ion detection 37

3.1 Abstract 37
3.2 Synthetic strategy and synthesis 37
3.2.1 Complex C1 37
3.2.2 Complexes C2 and C2* 37
3.2.3 Complex C3 39
3.2.4 Complexes C4 and C5 39
3.3 Photophysical properties 40
3.3.1 Absorption spectra 40
3.3.2 Photoluminescence 47
3.4 Concluding remarks 54
3.4.1 Complex C1 54
3.4.2 Complex C2* 54
3.4.3 Complex C4 57
3.4.4 Complex C5 59
3.5 Summary 60

4 Surface functionalization 61

4.1 Abstract 61
4.2 TiO_2 62
4.2.1 Preparation and functionalization of TiO_2 surfaces 62
4.2.2 Photophysical properties 62
4.2.3 Time dependence 66
4.3 Metal ion sensing with MeO-tpy 68
4.3.1 Complex synthesis 68
4.3.2 Photophysical properties 68
4.4 Gold nanoparticles 71

4.4.1 Synthesis and functionalization 71
4.4.2 Photophysical properties 71
4.5 Iridium(III) complexes 75
4.5.1 Synthetic strategy and synthesis 75
4.5.2 Photophysical properties 76
4.6 Concluding remarks 79
4.6.1 TiO_2 79
4.6.2 Metal ion sensing with MeO-tpy 79
4.6.3 Gold nanoparticles 80
4.6.4 Iridium(III) complexes 80

5 Diverse ligands **81**
5.1 Abstract 81
5.2 DSSC anchoring ligands 81
5.2.1 ALP 81
5.2.2 ALP2 84
5.3 TA-PEG, TA-TEG 86
5.4 Detector ligand L6 87
5.5 Concluding remarks 89
5.5.1 ALP 89
5.5.2 ALP2 89
5.5.3 TA-PEG, TA-TEG 89
5.5.4 Detector ligand L6 89

6 Summary **91**

7 Experimental **93**
7.1 General 93
7.2 Synthesis of ligands 94
7.3 Synthesis of complexes 117
7.4 Diverse ligands 130

References **140**

Acknowledgements

In the first place, I would like to thank my supervisors *Prof. Dr. Edwin C. Constable* and *Prof. Dr. Catherine E. Housecroft* for giving me the opportunity to do my PhD thesis in their research group. I am deeply grateful for the last nearly four years, in which I had the chance to work with a lot of freedom on diverse interesting projects in a well-equipped lab and a great research atmosphere. I also want to thank for excellent support during my work and always very helpful advices.

I thank *Prof. Dr. Oliver S. Wenger* for the co-examination of this thesis.

I would like to thank the whole "Werkstatt-Team" for their work and maintenance, *Markus Hauri* and *Roy Lips* for the material and chemical supply and *Beatrice Erismann* for her administrative work and help. Also, I want to thank *Dr. Bernhard Jung* for the IT support and the great time in the Praktikum.

For measuring and solving my crystal structure, I thank *Jennifer A. Zampese.* For the measurements of the elemental analyis, thanks go to *Werner Kirsch* and *Sylvie Mittelheiser.*

For maintaining the NMR infrastructure and for the microTXI measurements I want to thank *PD Dr. Daniel Häußinger*, *Dr. Heiko Gsellinger* and *Kaspar Zimmermann.*

Big thanks goes to the following people for measuring my samples: *Dr. Sven Brauchli*, *Dr. Collin Morris* and *Dr. Gabriel Schneider-Joerg* for ESI-MS, *Cathrin Ertl*, *Sarah Keller*, *Dr. Jonas Schönle* and *Roché Walliser* for 500 MHz NMR spectroscopy and *Dr. Jonas Schönle* for the quantum yield measurements.

I am very thankful to *Dr. Iain A. Wright* and *Dr. Colin J. Martin* for their support and advice in the lab and for the great time working on the HYSENS-project. I also want to acknowledge for the synthesis and supply of several compounds and *Dr. Colin J. Martin* for the calculations of K_d-values. Thanks goes also to *Ralph Stoop* for the great and easy collaboration in the HYSENS-project.

For proofreading this thesis, I would like to thank *Prof. Dr. Catherine E. Housecroft* , *Dr. Colin J. Martin*, *Sarah Keller*, *Dr. Jonas Schönle* and *Dr. Heiko Gsellinger.*

I want to give thanks to *Fabian Brunner* for the work and the obtained results during his Praktikum.

For the great time during the studies, I like to thank *Beat A. Amrein*, *Andreas Buck*, *Dr. Heiko Gsellinger*, *Bernadette Hammer*, *Michel Rickhaus*, *Daniel Rösch*, *Anna-Catherina Senn*, *Kim von Allmen* and all other members of the Team 2006. Special thanks goes to the members of the coffee-break and lunch group for the great time outside the lab.

I would like to thank all current and former members of the Constable-Housecroft research group, especially (in alphabetical order): *Dr. Sven Brauchli, Andreas Bünzli, Annika Büttner, Cathrin Ertl, Sebastian Fürer, Nik Hostettler, Sarah Keller, Yannik M. Klein, Dr. Peter Kopecky, Frederik Malzner, Dr. Colin J. Martin*, *Dr. Collin Morris*, *Daniel Ris, Dr. Pirmin Rösel*, *Ralph Schmitt*, *Dr. Gabriel Schneider-Joerg, Ewald Schönhofer*, *Dr. Jonas Schönle, Dr. Marketa Smidkova, Roché Walliser, Dr. Markus Willgert and Dr. Iain A. Wright* for the nice working atmosphere,

the helpful support and the great time in- and outside the lab.

For financial support, the University of Basel and the European Commission under the FP7-NMP project HYSENS (263091) have to be acknowledged.

Finally, I want to express my gratitude to my family and friends for their constant support during my entire studies.

Abbreviations

A	AcO	acetate
	AIBN	azobisisobutyronitrile
	aq.	aqueous
	a.u.	arbitrary unit
B	bpy	2,2′-bipyridine
	B3LYP	hybrid functional
C	calc.	calculated
	cm	centimetre
	cod	1,5-cyclooctadiene
	conc.	concentration/concentrated
	°C	degree Celsius
D	d	doublet (NMR)
	DCC	*N,N'*-dicyclohexylcarbodiimide
	DFT	density functional theory
	dm	decimetre
	DMAP	4-dimethylaminopyridine
	dmbpy	6,6′-dimethyl-2,2′-bipyridine
	dmcbpy	dimethyl [2,2′ -bipyridine]-4,4′-dicarboxylate
	DMF	*N,N*-dimethylformamide
	DMSO	dimethylsulfoxide
	DOTA	1,4,7,10-tetraazacyclododecane-1,4,7,10-tetraacetic acid
	DSSC	dye sensitized solar cells
E	EA	elemental analysis
	EDTA	ethylenediaminetetraacetic acid
	EI	electron impact
	em.	emission
	eq.	equivalent
	ESI	electrospray ionisation
	et. al.	et alii (latin) = and others
	EWG	Eelectron withdrawing group
	exc.	excitation
	ε	extinction coefficient
F	FTO	fluorine doped tin oxide
G	g	gram
H	h	hour
	Hdfppy	2-(2,4-difluorophenyl)pyridine

	Hfppy	2-(4-fluorophenyl)pyridine
	HMBC	heteronuclear multiple bond coherence
	HMQC	heteronuclear multiple quantum coherence
	HOMO	highest occupied molecular orbital
	Hppy	2-phenylpyridine
	Hz	Hertz (1 Hz = 1 s^{-1})
I	IR	infrared
	ITO	indium tin oxide
J	J	coupling constant in Hz
K	K_d	dissociation constant
L	l	litre
	LANL2DZ	basis set
	LC	liquid chromatography
	LEC	light-emitting electrochemical cell
	LED	light-emitting diode
	LUMO	lowest unoccupied molecular orbital
M	M	molar ($mol\,l^{-1}$)
	m	multiplet (NMR) or medium (IR)
	MALDI	matrix-assisted laser desorption/ionization
	mCPBA	*meta*-chloroperoxybenzoic acid
	Me	methyl
	MeO-bpy	4,4′-dimethoxy-2,2′-bipyridine
	MeO-tpy	4′-(4-methoxyphenyl)-2,2′:6′,2″-terpyridine
	ml	millilitre
	MLCT	metal to ligand charge transfer
	mmol	millimole
	MP	melting point
	MS	mass spectrometry
	MW	microwave reactor
	m/z	mass-to-charge ratio (MS)
N	NBS	N-bromosuccinimide
	NHE	normal hydrogen elctrode
	NMR	nuclear magnetic resonance
	NP	nanoparticle
O	OH-bpy	[2,2′-bipyridine]-4,4′-diol
	OH-tpy	4-([2,2′:6′,2″-terpyridin]-4′-yl)phenol
	OLED	organic light-emitting diode

P	PEG	polyethylene glycol
	Ph	phenyl
	phen	1,10-phenanthroline
	phtpy	4′-phenyl-2,2′:6′,2″-terpyridine
	ppb	parts per billion
	ppm	parts per million
	pytpy	4′-(4-pyridyl)-2,2′:6′,2″-terpyridine
Q	QD	quantum dot
R	R_f	retardation factor
	rt	room temperature
S	s	singlet (NMR) or strong (IR)
	SPR	surface plasmon resonance
	SSL	solid state lighting
T	T	temperature
	t	triplet (NMR)
	TA	DL-thioctic acid
	TBA	tetrabutyl ammonium
	TEG	tetraethylene glycol
	TFA	trifluoroacetic acid
	THF	tetrahydrofuran
	THP	tetrahydropyran
	TOF	time-of-flight (MS)
	ttpy	4′-(4p-tolyl)-2,2′:6′,2″-terpyridine
U	USD	US Dollar
	UV-Vis	ultra violet and visible light
V	V	Volt
W	w	weak (IR)

Table of compounds

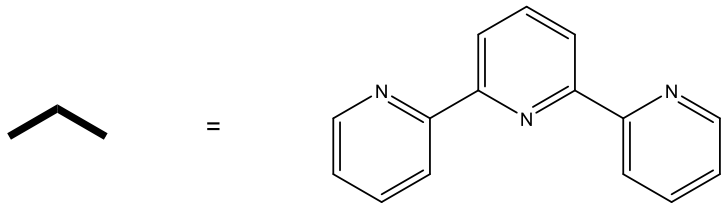

Ligands:

Label	Structure	Label	Structure
L1	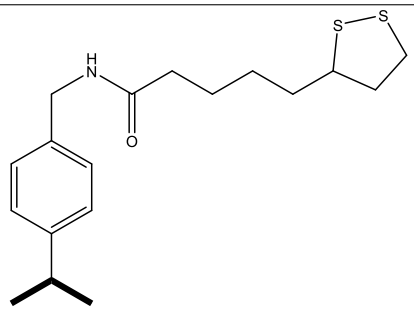	**L4**	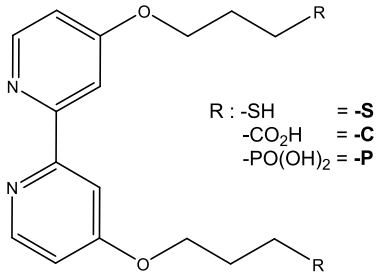
L2	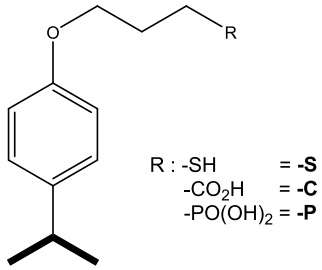	**L5**	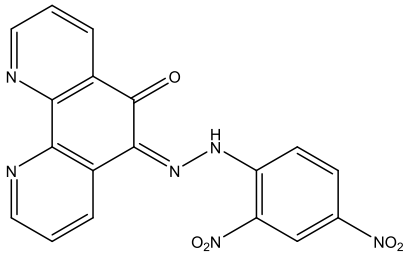
L3	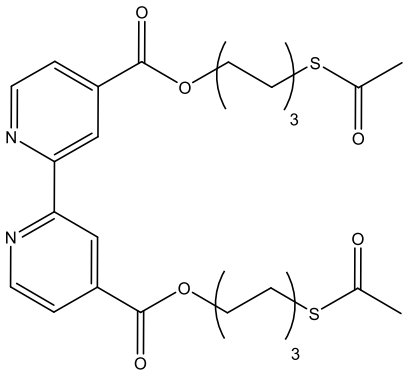	**L6**	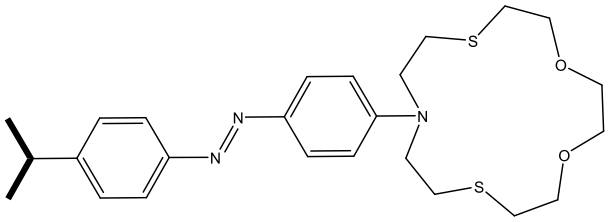

Complexes:

Label	Structure	Label	Structure
C1	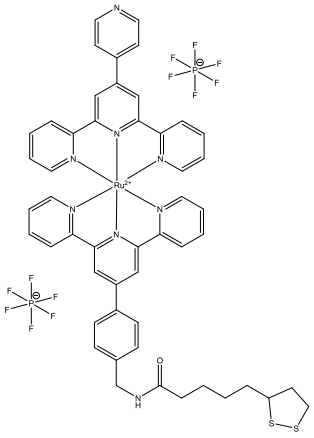	**C3**	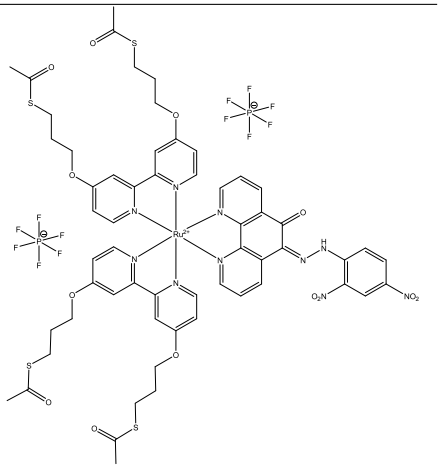
C2	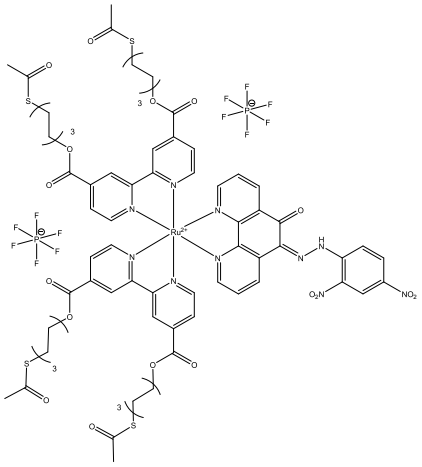	**C4**	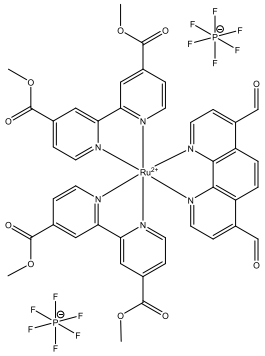
C2*	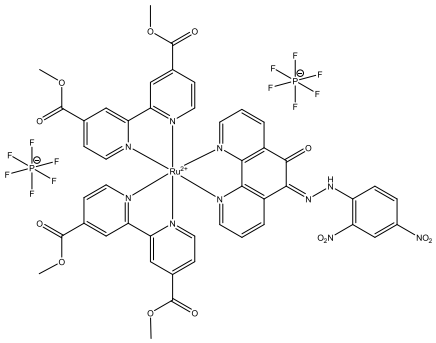	**C5**	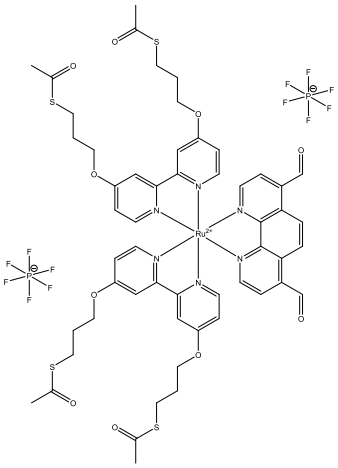

Label	Structure	Label	Structure
C6	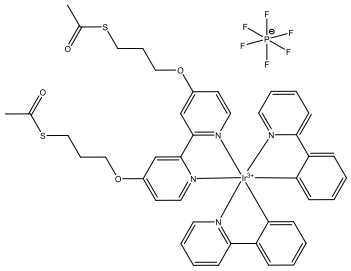	**C8**	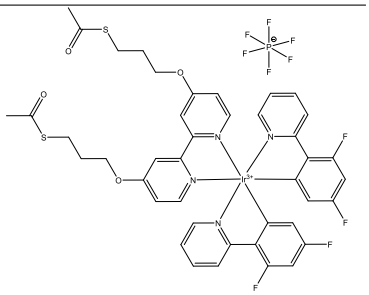
C7	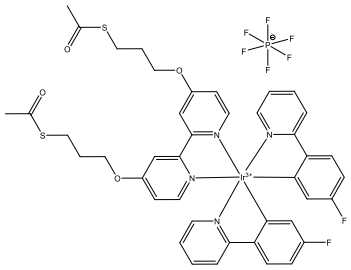		

Abstract

This PhD thesis focuses on the synthesis of new polypyridine anchoring ligands and several different applications. The ligands consist of a coordinating part, a flexible linker and an anchoring group. Due to the fact that different anchoring groups were used, the ligands can be applied for several types of surface-materials. Using these anchoring ligands, several coordination complexes were synthesized. Ruthenium-based complexes, bearing an ion-sensitive ligand, were tested towards their sensing properties. The photophysical properties of luminescent Ir(III)-complexes were investigated and compared to related compounds. Furthermore, different types of materials were functionalized with the coordinating anchoring ligands and characterized.

Chapter 1: Introduction

Chapter 1 gives background information about the different topics where the synthesized ligands and complexes can be applied.

Chapter 2: coordination anchoring ligands

Here, the synthesis of the anchoring ligands is presented. The photophysical properties and an X-ray structure are discussed.

Chapter 3: Complexes for detection

In this chapter, the synthesis and the photophysical properties of several ruthenium complexes are described. Titration experiments and sensing tests are described and the results are discussed.

Chapter 4: Surface functionalization

Chapter 4 shows different applications for the synthesized ligands. Functionalization of different surfaces is described as well as their photophysical characterization. Also the synthesis and the photophysical properties of luminescent Ir(III) complexes, bearing an anchoring ligand, are presented.

Chapter 5: Diverse other ligands

The synthetic routes for two DSSC anchoring ligands are shown in chapter 5. Furthermore, the syntheses of solvatation ligands for quantum dots and for a novel detection ligand are described.

1 Introduction

1.1 General

In 1893, Alfred Werner built the basis of modern coordination chemistry with his publication about the composition of cobalt complexes.[1] Since then, this field of chemistry has become very important with many different applications. Besides the metal and its oxidation state, the ligands have a key role, strongly influencing the properties of the complex. Due to their increased stability, multidentate chelating ligands are often preferred to simple monodentate ligands.[2] The vast class of chelating ligands ranges from flexible bidentate ligands like ethylenediamine to tetradentate ones like EDTA[3] and further to quite rigid structures like the octadentate DOTA. Among this huge variety, the family of polypyridines is often used. 1,10-Phenanthroline (phen) and especially the different isomers of bipyridine (bpy) and terpyridine (tpy) play probably the most prominent role. The most widely utilized isomers of the ligands are shown in *Fig. 1.1.* Particularly the chelating bidentate 2,2′-bipyridine and the tridentate 2,2′;6′,2″-terpyridine with their huge number of derivatives can be found in many areas of modern coordination chemistry and are applied for multiple applications. Complexes containing bpy and tpy have become one of the main classes of sensitizers in dye sensitized solar cells (DSSCs).[4, 5] Both bpy and tpy domains feature in ancillary ligands in complexes applied as the emitting layers in light-emitting electrochemical cells (LECs).[6, 7] In addition, functionalization of a wide range of polymers with bpy and tpy ligands and their metal complexes has been demonstrated, [8, 9] and polypyridyls have also been used as supporting and anchoring ligands in transition metal catalysts.[10, 11, 12]

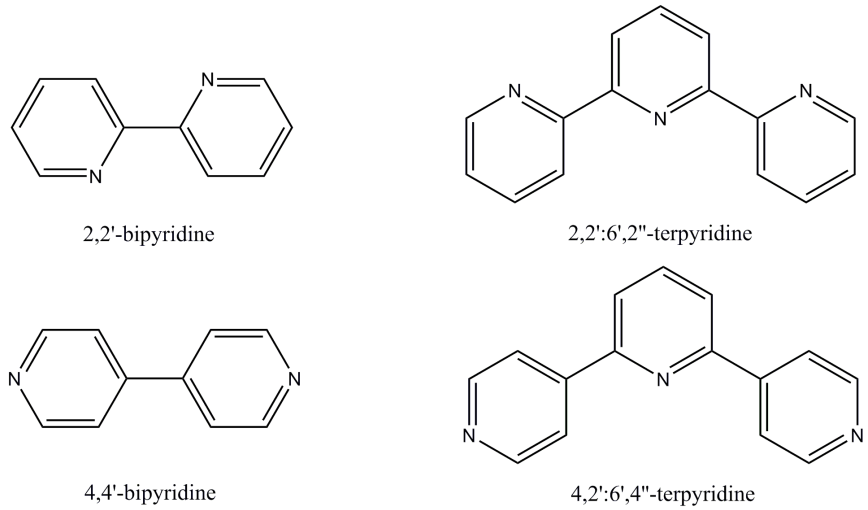

Figure 1.1: *isomers of the ligands bpy and tpy.*

From the synthetic point of view, these ligands offer several advantages. The unsubstituted bpy-ligand is commercially available in large quantities due to its use as precursor for the preparation of

Diquat insecticides.[13] Substitution at the 4,4′-positions by a standard procedure allows the introduction of different functional groups.[14] Also cross-coupling and lithiation reactions are possible to obtain asymmetric substitution or functionalize at the 5,5′ and 6,6′ positions.[15, 16, 17, 18] By using a *Kröhnke*-type synthesis, functional groups can be directly inserted during the reaction.[19] This method can also be used to obtain tpy-ligands with different substituents on several positions.[19, 20] Additionally the introduction of reactive groups allows further substitutions. Some of these ligands are also accessible by the method reported by *Wang* and *Hanan*.[21] This one-step synthesis is often used for different phenyl-substituted terpyridines because of the straightforward performance of the reaction and the easy purification.

The class of polypyridine ligands shows good chelating properties for many transition metals, mainly in the oxidation state +2 and +3.[13, 22] In contrast to other ligands like catechol or acetylacetonate, these ligands are neutral and thus allow the synthesis of charged coordination complexes.[23] Depending on the metal, thermodynamically stable $[M(tpy)_2]^{2+}$ complexes can be synthesized with stability constants of $\log K = 13.8$ for Fe^{2+} and $\log K = 11.1$ for Ni^{2+}.[8] For other metals like Co^{2+} ligand exchange in solution is known due to kinetic lability.[24, 25] Tpy coordination complexes for nearly every metal in the periodic table are known in the literature (*Fig. 1.2*). The synthesis can

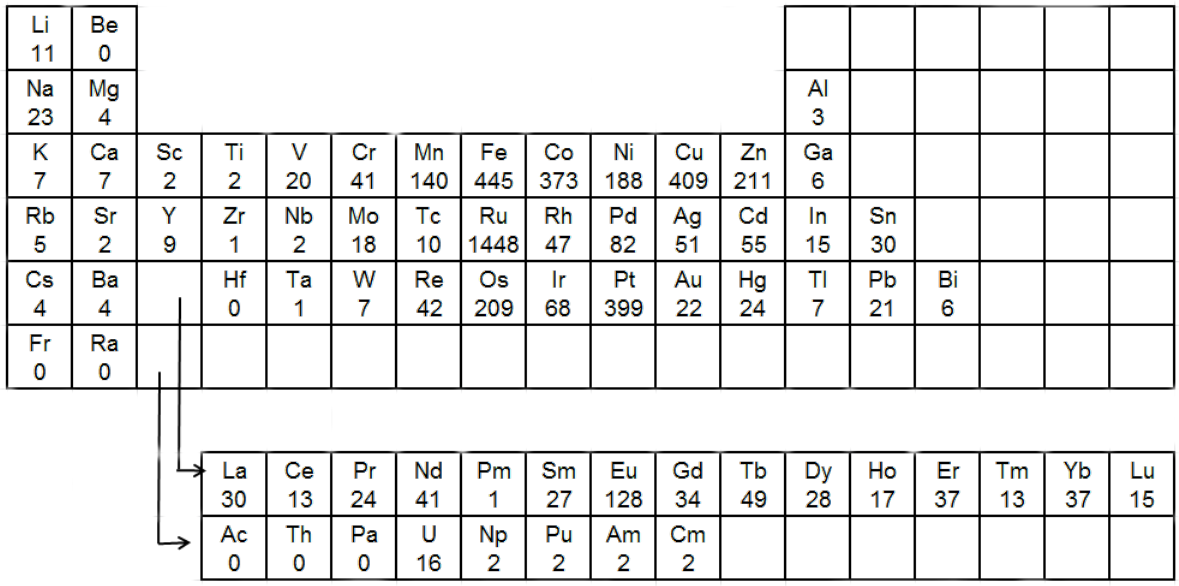

Figure 1.2: *Periodic table of elements (only metals are shown). The number indicates the number of scientific papers dealing with the respective terpyridine complexes (determined by SciFinder^{TM}, search performed 31st December 2010).*[8]

be performed in a one-step reaction to obtain the homoleptic complex or in a two-step procedure yielding the heteroleptic bis(terpyridine) complex, bearing two different ligands.[8] Homoleptic bpy complexes are known for most metals and different oxidation states.[13] For several metals there exist

bis-heteroleptic complexes and for some such as Ru(II) and Os(II) even tris-heteroleptic coordination complexes have been reported.[26, 27, 28, 29]

Metal	Number of publication
Mn	153
Fe	532
Co	426
Ni	163
Cu	262
Ru	1079
Os	160

Table 1.1: *The number of scientific publications dealing with the respective complex of 2,2′;6′,2″-terpyridine or 4′-substituted derivatives (determined by SciFinder^{TM}, search performed 8th October 2014).*

1.2 Dye-Sensitized Solar Cells (DSSCs)

Overcoming the world′s growing energy consumption is one of the main issues for the immediate future. For this, new technologies should be established because the current mainly used methods to produce electricity have several drawbacks. Oil and gas are limited resources. In addition the released CO_2 is influencing the global climate.[30] Nuclear energy produces highly toxic radioactive waste consisting of isotopes with half-lives of several thousands years or more. Furthermore, incidents in nuclear plants can lead to enormous environmental pollution as seen in 1986 in Chernobyl, Ukraine and in 2011 in Fukushima, Japan.[31] Therefore, to satisfy the energy demand, renewable sources should be used. Wind and water power are site dependent and limited, but solar energy is disposable all over the world and available in sufficient quantity.[30] To harvest the sunlight and convert it into electric power, solar cells are commonly used. Among the different existing types for the future, the third generation, the so-called Dye Sensitized Solar Cells (DSSC) are probably the most promising. Several advantages make them more favourable than the most commonly used first generation, based on silicon.[32] The production costs of a DSSC are much lower and application on diverse materials like flexible polymers is possible. Since they are transparent, they can also be used as stained glazing for houses.[33] Currently, these cells have shorter life-times and less efficiency than silicon-based cells, but much research is in progress to overcome these drawbacks.[34] The build-up and working principle of such a DSSC is shown in *Fig. 1.3*.

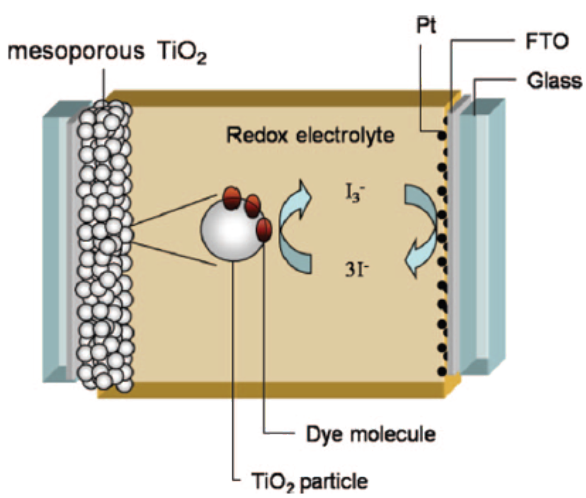

Figure 1.3: *Schematic overview of a dye-sensitized solar cell.*[34]

A layer of a mesoporous semiconducting (usually n-type) metal oxide like TiO_2 is deposited on a transparent conducting oxide (TCO) like fluorine doped tin oxide (FTO) on a plastic or glass substrate. The semiconducting oxide is loaded with a dye, which is excited by incident sunlight and injects an electron from its excited state into the conducting band of the metal oxide. The oxidized

dye is reduced back by the redox electrolyte which is then oxidized. The reduction of this electrolyte occurs at the counter electrode, which consists of a catalytic metal like platinum on a TCO coated glass or plastic substrate.[34, 35]

For sensitizing, transition metal complexes are often used due to several reasons. They have long excited state lifetimes, are stable in the oxidized as well as in the reduced form and have strong absorption in the visible range of the light spectrum. Furthermore they show no degradation or aggregation.[36] From the beginning, Ru(II) complexes have shown good efficiencies due to their broad absorption and good photovoltaic properties like fitting energy levels and stability. For these reasons, ruthenium is one of the mainly used metals in DSSCs. A detailed list of different Ru(II) polypyridine complexes has been developed,[34] the probably most prominent sensitizers of this class, N719 and N749 which is also called black dye, are illustrated as examples in *Fig. 1.4*.

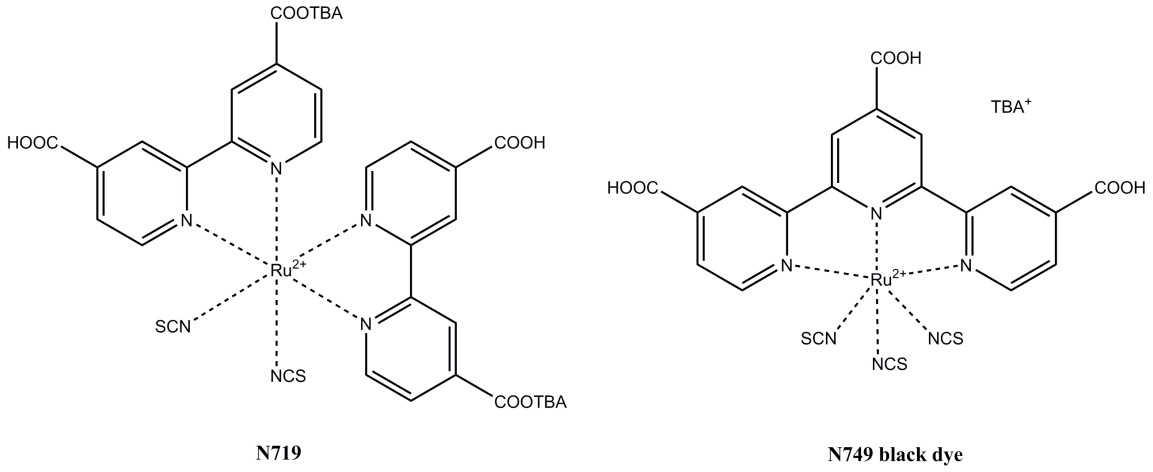

Figure 1.4: *Ru(II) based sensitizer N719 and N749 (TBA =* $^{n}Bu_4N^+$*).*[34]

Introduction of substituents to the ligands can have a strong influence on the performance of the dye. The efficiency can be improved in several ways. Insertion of chromophores like thiophene can lead to an increased molar extinction whereas long alkyl chains can decrease the aggregation of the dye. In addition substituents can be used to optimize the redox potential. In case of bpy ligands the functionalization is mainly concentrated on the 4,4′-position.[34]

This type of solar cell is by now so well established that companies from industry not only produce and sell some of these Ru(II) based dyes on a multi-gram scale,[37] but also offer fully manufactured cells for sale.[38, 39]

Despite the great performance of Ru(II)-based dyes, the major drawbacks are the low abundance of ruthenium in the Earth's crust and the high prices for this precious metal. As a consequence, there is a need for more abundant and cheaper alternatives. This is found in copper, which is far more common on earth and less expensive (*Tab. 1.2*). Also Cu(I) complexes show similar photophysical properties compared to Ru(II) complexes.

Metal	Abundance in earth's crust	Metal price
Ru	0.1 ppb	2765.27 USD/kg
Cu	25 ppm	8.85 USD/kg

Table 1.2: *Abundance on earth and metal prices for ruthenium and copper (18.08.2014).*[40, 41]

For copper, the majority of the reported dyes consist of bpy or phen-based ligands. The ligands bear on the 6,6′- and 2,9-position respectively sterically demanding groups like phenyl or alkyl chains to stabilize the tetraheadral geometry and prevent oxidation of the metal to Cu(II), which prefers a square planar coordination environment.[42]

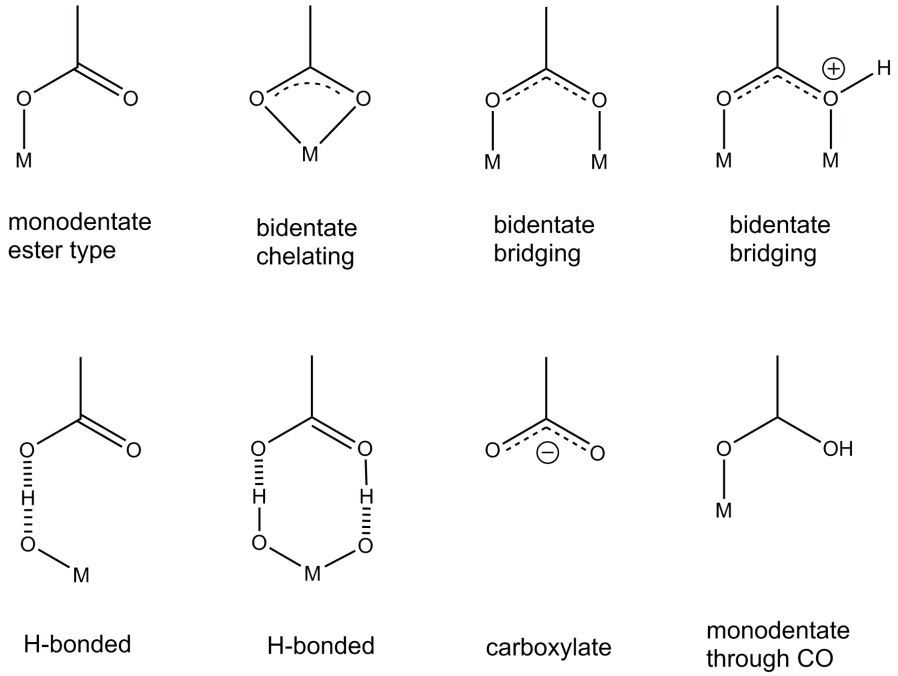

Figure 1.5: *Possible binding modes of COOH groups to a metal oxide (TiO_2).*[36]

Covalent binding of the sensitizer to the metal oxide is required for good electron injection, thus the coordination complexes comprise anchoring groups on the ligand. For TiO_2 and SiO_2, phosphonic and carboxylic acids exhibit the best performances and are most commonly used. For other metal oxides like SnO_2, anchoring groups like $SiCl_3$ are also possible.[36] Binding to the hydroxy groups of the metal oxide can occur in different ways. For carboxylates, this is shown in *Fig. 1.5.* The anchoring groups can be connected to the ligand by a linker. Whereas flexible saturated linkers can slow down the electron injection rate,[36] the insertion of conjugated, rigid linkers like phenyl groups can increase the efficiency.[43, 44]

The anchoring of ruthenium dyes like N719 or N749 (*Fig. 1.4*) on the metal oxide surface is performed

by immersing the electrodes into a solution of the complex for several hours or days.[45] When copper dyes are used, the electrodes are first immersed into a solution of the anchoring ligand for 1 day, washed and dried. Then, the functionalized electrodes are either immersed in a solution of a homoleptic Cu(I) complex or in a 1:1 mixture of ancillary ligand and $[Cu(MeCN)_4][PF_6]$ for several days.[46] With both methods, the heteroleptic copper(I) complex on the surface is obtained.

1.3 Light-emitting electrochemical cells (LECs)

Another approach to solve the global energy problem is to decrease the energy comsumption by using more efficient lighting devices. In the field of illumination, an immense progress was made by introducing solid-state lighting (SSL) which replaces the common but very inefficient tungsten filament light bulbs. The two main families of SSL are the light-emitting diodes (LEDs) and the organic light-emitting diods (OLEDs). These SSL devices are made of semiconducting materials which produce photons when an electric field is applied. This electroluminescence converts the energy mainly into light and not, like in light bulbs, into heat. This leads to very high efficiencies of such devices. Due to their working priciple, LEDs are built as light point sources whereas OLEDs are made as flat light devices. These devices consist of a multilayer stack (*Fig. 1.6*) and have quite demanding requirements for the materials used and the preparation of the devices. These requirements and the connected high production costs have so far prevented a breakthrough in the lighting market.[47, 48]

A new concept for building flat lighting devices are light-emitting electrochemical cells (LECs). Compared with OLEDs they have several eminent advantages, for example a much simplified architecture compared to OLEDs (*Fig. 1.6*).

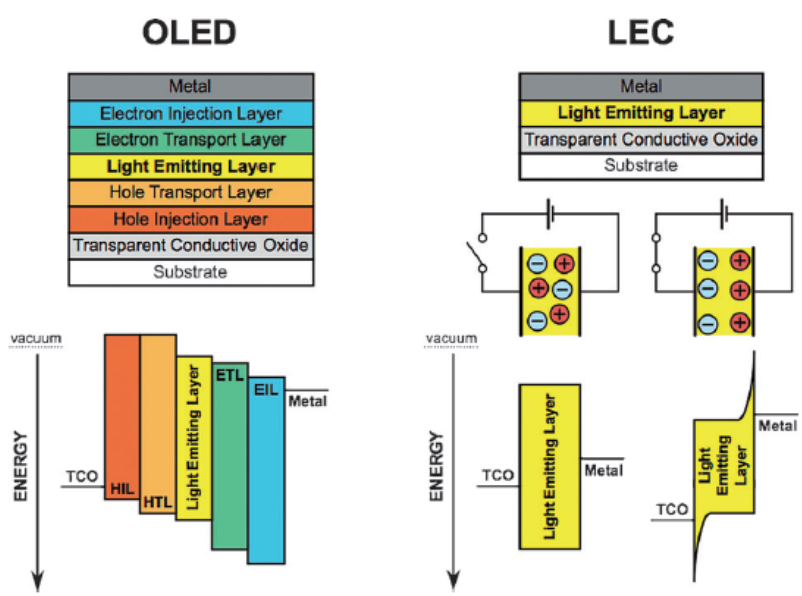

Figure 1.6: *Build-up of OLED (left) and LEC (right).*[48]

The opto-electronically active layers are reduced to just one and also the manufacturing is much easier. As active compound air and water stable materials can be used. Due to this, rigorous encapsulation of the devices can be omitted. As luminescent material in the emitting layer, either

light-emitting conjugated polymers or ionic transition metal complexes (iTMC) are used. Early research on iTMC-LECs was done with $[Ru(bpy)_3][PF_6]_2$ and other ruthenium(II) polypyridine complexes.[49] Today, mostly iridium(III) compounds are used due to their superior properties. With Ir(III) as metal center many different emission colours are possible which cover the whole visible light spectrum whereas with ruthenium(II) complexes only emission colours in the red-orange range are available. The used Ir(III) complexes usually consist of two cyclometalating C^N ligands and one ancillary N^N ligand. As C^N ligand phenylpyridine (ppy) or one of its derivatives is applied, whereas most of the ancillary ligands are bpy-based (*Fig. 1.7*).[48]

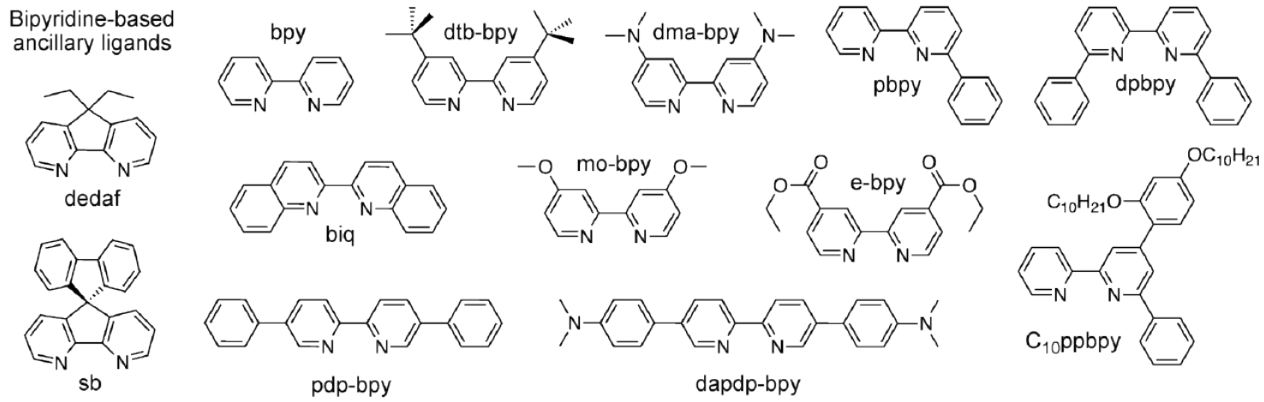

Figure 1.7: *Bipyridine-based ancillary ligands for iTMC-LECs.*[48]

The emission colour of the iridium(III) complexes can be tuned by the substituents on the ligands. Usually the frontier orbitals are located on different ligands. The LUMO is located on the ancillary ligand whereas the HOMO lies mainly on the cyclometalating ligands.[47] Therefore the energy of the frontier oritals can be changed almost independently by introducing electron-withdrawing or electron-donating groups to the ligands. By changing the HOMO-LUMO energy gap the emission colour of the complex can be tuned. The substituents on the ligands can also have an influence on the perfomance of the LEC device.

Beside the superior properties of Ir(III) as metal center for iTMC-LECs this metal has similar disadvantages as ruthenium. It is quite rare on earth with an abundance of only 0.05 ppb[41] and thus expensive. A more abundant and low-cost alternative could again be Cu(I) as metal center. The most investigated complexes consist of a N^N chelating ligand like bpy or phen and a P^P (bisphosphine) ligand. Cu(I)-based LEC devices with almost white-light emission and quite high brightness were build. Other examples demonstrated at low voltages performance comparable to Ru(II) or Ir(III) based LECs.[48]

1.4 Sensing

Ions play a substantial role in medicine, biology and chemistry. Some metal ions like iron or sodium are essential for basic processes in the body, other ions like cadmium or mercury can be highly toxic to organisms.[50] Thus it is very important to have reliable, specific and accurate methods for their detection. It would also be favourable if the used methods are low-price, fast and straightforward to operate, especially for medical applications. Advances were made by developing abiotic receptors with specific recognition to certain ions. These chemosensors can interact with the particular ion in different ways. For anions the reversible interaction can be either electrostatic, by formation of hydrogen bonds or working via coordination to a metal center. If the recognition occurs irreversibly through a reaction, the term chemodosimeter should be used.[51, 52] For cations the recognition can be done by large cyclic molecules such as crown ethers or cryptands.[50] This ion binding site is also connected to a signalling unit. This approach is shown in *Fig. 1.8*. It is desirable that the read-out occurs in the form of an easy-to-measure signal, for example a colour change induced by the ion which can be detected by absorption spectroscopy. The other possibility is a change in fluorescence. This is most widely used because it is more sensitive and offers fluorescence quenching, enhancement as well as a colour shift as signal read-out.

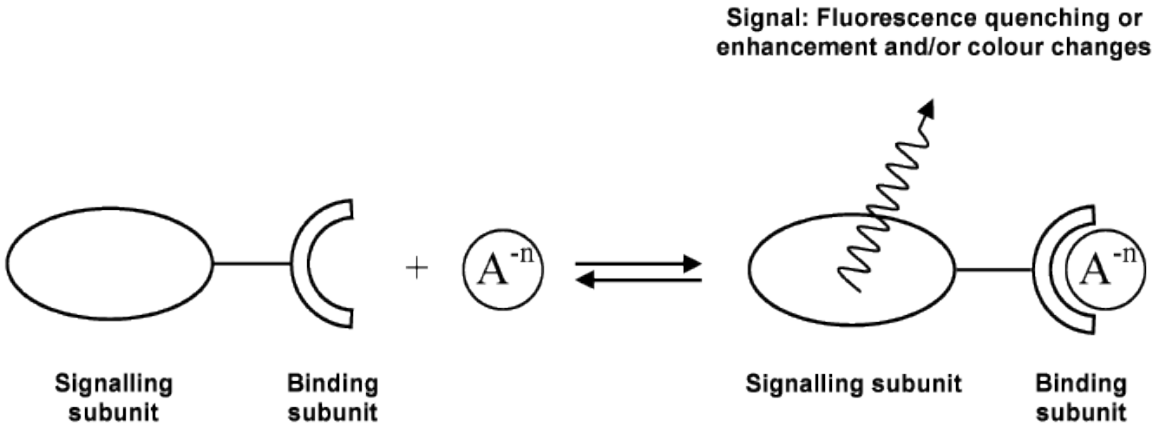

Figure 1.8: *Anion chemosensors based on the binding site-signaling subunit approach.*[51]

For fluorescence-based signal report organic molecules like anthracene, naphtalene or other aromatic heterocycles can be used. The emission of these molecules occurs near the UV region which could lead to matrix interference. To avoid this problem, transition metal complexes with emission in the visible region can be applied. Signalling subunits based on $Ir(tpy)_2{}^{3+}$ and $Ru(tpy)_2{}^{2+}$ are known, but most research was done with $Ru(bpy)_3{}^{2+}$-based reporting units.[51] Here, at least one of the three bpy ligands is functionalized at the 4,4′ -positions to introduce the covalent linkage to the binding site. Some examples for Cl^- and $H_2PO_4{}^-$ sensors with $Ru(bpy)_3{}^{2+}$ reporting units are shown in *Fig. 1.9*. In these cases, signal report occurs by fluorescene enhancement. It is presumed that the

presence of the anion changes the rigidity of the complex and thus reduces the non-radiative decay of the excited state,[53] resulting in more intense emission.

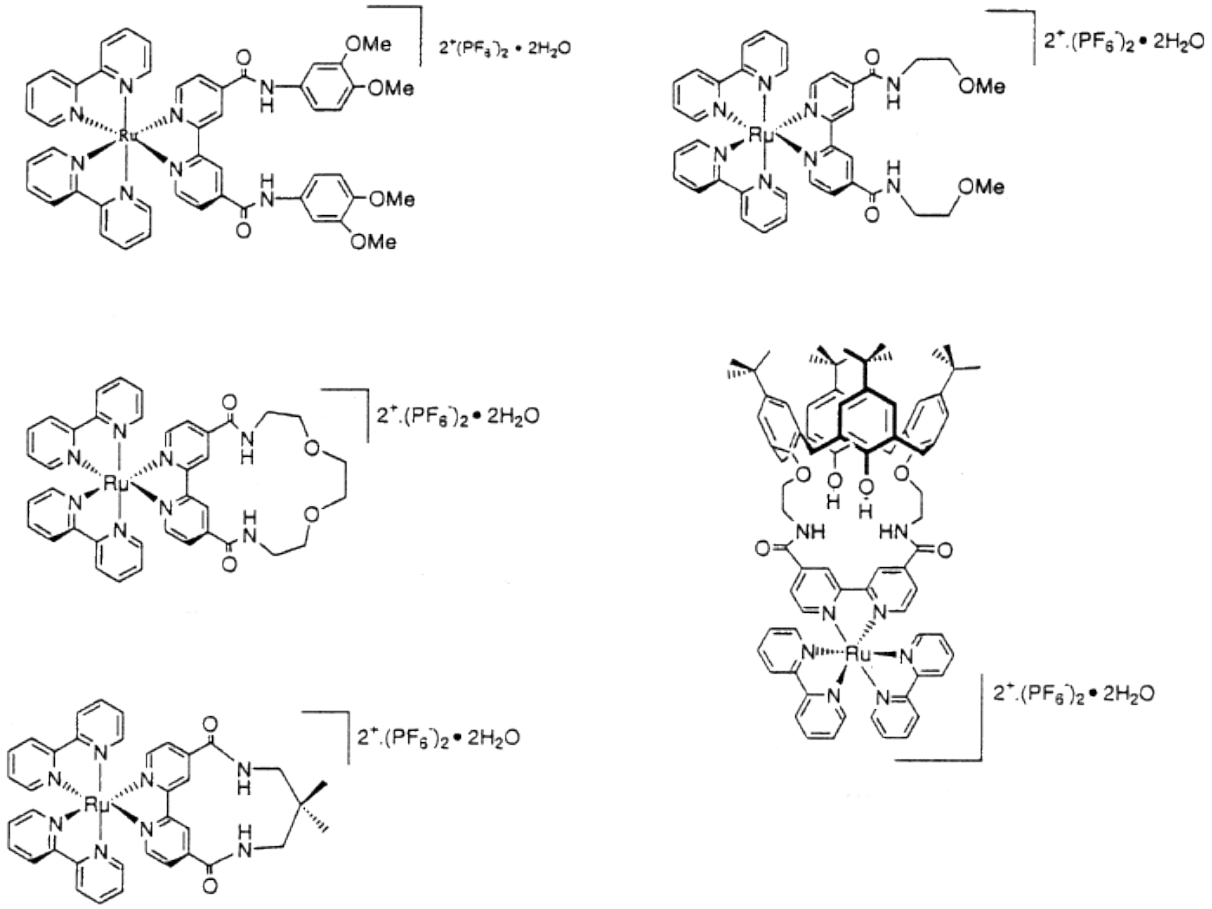

Figure 1.9: *Ru(II)bipyridine based sensors for Cl^- and $H_2PO_4^-$.* [53]

1.5 Catalysis

Polypyridine ligands also play a role in transition metal catalysis. In the field of water oxidation especially Ru(II) complexes have extensively been studied. The splitting of water into its components hydrogen and oxygen can be expressed rather simple (*equation 1*). But the chemical processes are complicated due to the required 4-electron reaction.

$$2H_2O + 4h\nu \rightarrow O_2 + 2H_2 \tag{1}$$

Several steps have to be carried out: (i) light absorption, followed by (ii) excited state electron transfer, (iii) directional long-range electron transfer and proton transfer and (iv) single electron activation of multielectron catalysis.[54] The requirements for the catalyst mimicing natural photosynthesis are thus rather demanding. The first working molecular catalyst was a oxygen-brigded $Ru(bpy)_2$-dimer, called "blue-dimer" (*Fig. 1.10*).

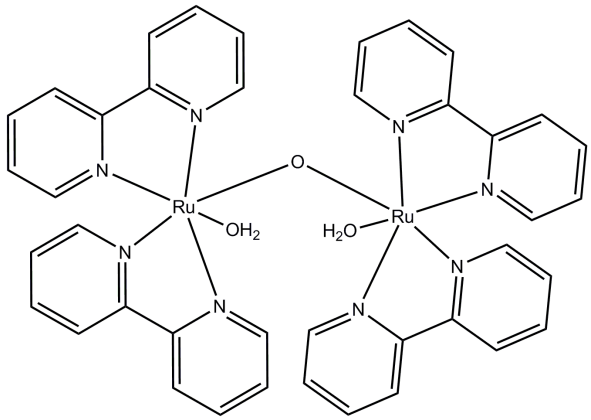

Figure 1.10: *Blue dimer, the first synthetic water-oxidizing catalyst.*[55]

Starting from that point, many other multimetallic molecular catalysts have been developed, but also catalysts based on one metal center have shown promising results. Many of the monometallic catalysts are based on $[Ru(bpy)_3]^{2+}$ due to the fitting properties. This complex class offers absorption in the visible region, a relatively long-lived excited-state lifetime, reversible redox processes and stability in the ground and excited states. Furthermore it has an oxidation potential of approximately 1.51 V vs NHE (normal hydrogen electrode). For the oxidation of water a potential of at least 1.23 V vs. NHE is needed, but a more positive potential is favourable.[55]
A different approach to water splitting is done with photoelectrochemical cells (PECs). The schematic build-up is shown in *Fig. 1.11*. The construction is comparable to the architecture of a DSSC. In such a cell the transition metal complex also acts as a sensitizer. The catalyst can be a transition metal oxide such as IrO_2 or Co_3O_4.[56]

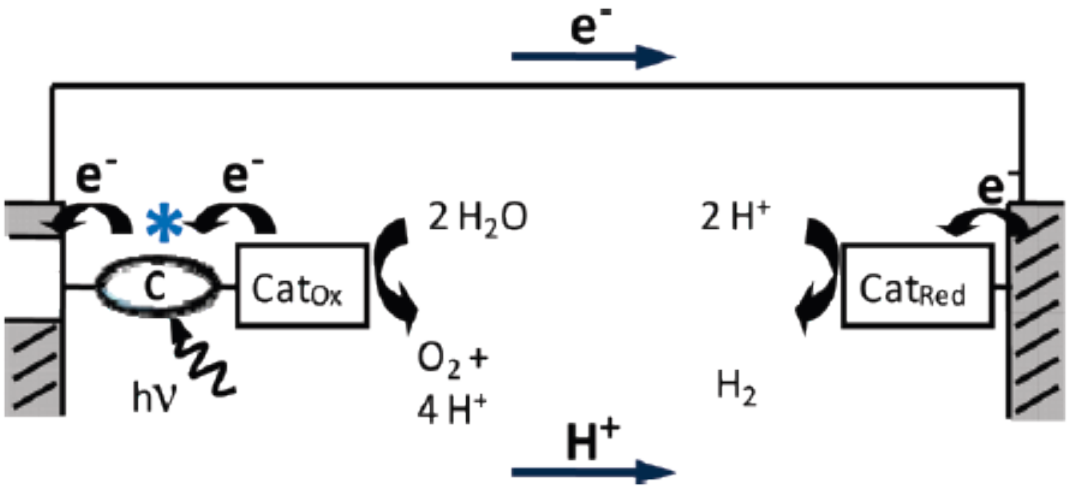

Figure 1.11: *Scheme of a photoelectrochemical cell (PEC) for water splitting: C is a chromophore, and Cat_{ox} and Cat_{Red} are catalysts for water oxidation and reduction.*[54]

The different derivatives of bpy and tpy can also act as ligands for transition metal catalysts in organic synthesis. They mainly play the role of ancillary ligands. The type of reactions in which these catalysts are successfully applied cover a broad range. Iridium catalyzed borylation using bipyridine ligands are known[57] as well as nickel-terpyridine catalysts for cross-coupling reactions.[58] Recently a molybdenum catalyst for phosphoester hydrolysis has been reported.[11] But the ligands can also be used as covalent linkers to a solid support like SiO_2[12, 10] or polymer beads. [59] With this method, the purification can be simplified because the heterogenous catalyst can be filtered off and is easily recycled.

1.6 Polymers

Bipyridine and terpyridine ligands have also proven to be useful for the functionalization of polymers. The synthesis can be carried out in different ways. One advance is the synthesis of bpy and tpy ligands bearing a functional group for polymerization. For this, groups like vinyl or acrylate can be used. With these functionalized ligands either homopolymers or, by addition of other monomers, copolymers can be synthesized. It is also possible to add the coordinating ligands to the ready-made polymer. This approach is done by reacting functional groups on the polymer with the ligands to yield a covalent linkage. The type and length of the linker can be varied to obtain different properties like energy transfer between the complex and the polymer backbone (*Fig. 1.12*). This usually yields lower ligand loading of the polymer than the first mentioned method. By adding transition metal ions to the functionalized polymers, cross-linked gels can be formed. But also compounds like $[Ru(bpy)_2Cl_2]$ or $[Ru(tpy)Cl_3]$ can be added to avoid cross-linking.[8, 23, 60]

These functionalized materials can be used for various applications. Bipyridine-decorated polymers can show selectivity to certain hazardous metal ions and thus be used for metal sorption. *Bartsch et al.* synthesized polymers which showed very good selectivities of Cu(II) over Co(II) and Ni(II) in competitive sorption and of Hg(II) over Cd(II) in single species sorption.[61]

Furthermore examples are known where polymers containing metal complexes can also act as catalysts. With palladium, hydrogenation of olefins at ambient temperature and pressure[23] is possible and cobalt-containing materials can act as oxidation catalysts for cyclic alkenes. $[Ru(bpy)_3]^{2+}$ -moiety containing polymers can be used as heterogeneous photocatalysts. These materials also have electroluminescent properties. [60]By adding lanthanides like Eu(III) and Tb(III) or transition metals like Ir(III) to tpy-decorated polymers, emissive polymers can be synthesized. These can be applied in the construction of polymer light-emitting diodes.[8]

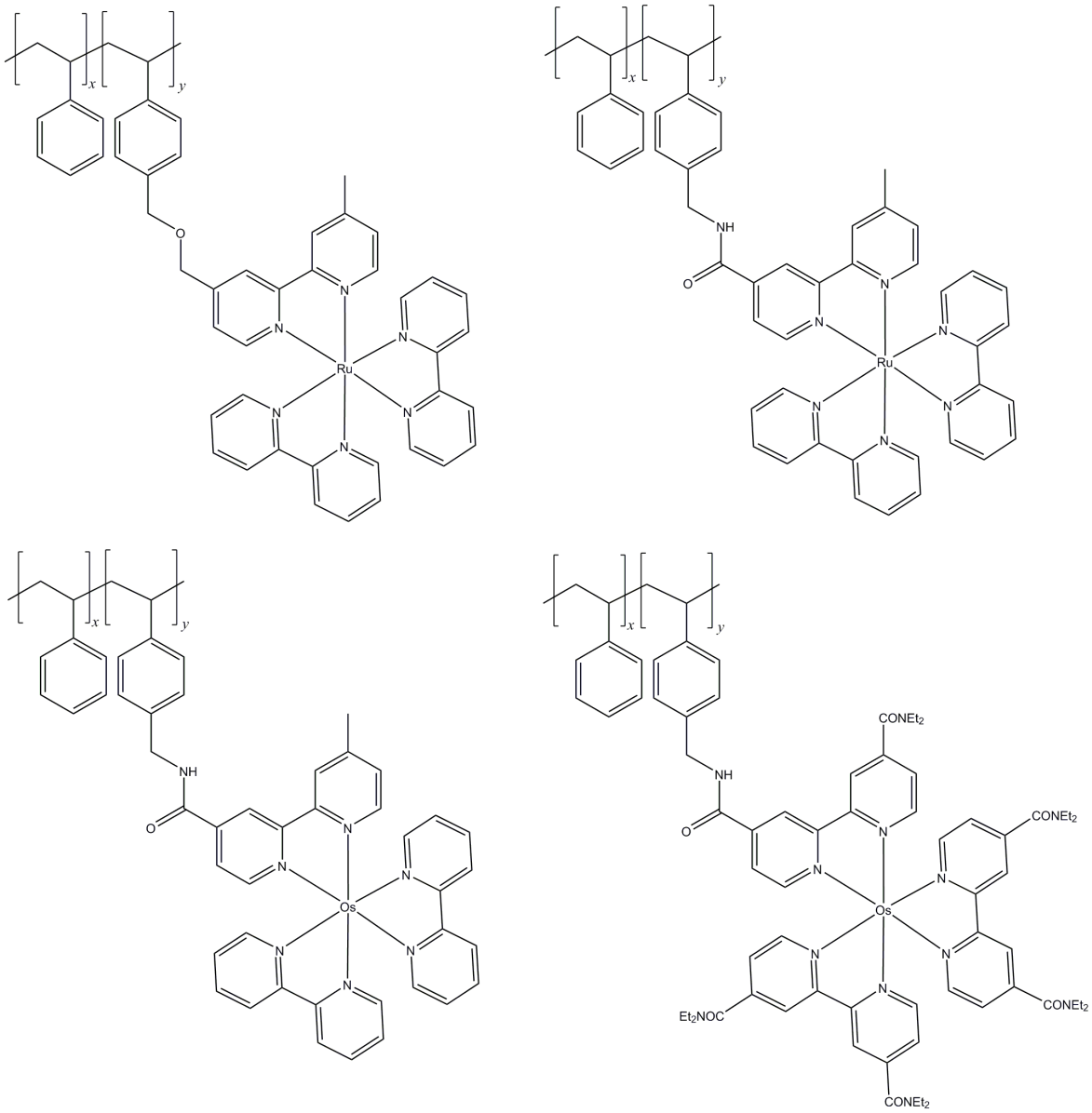

Figure 1.12: *Bipyridine ruthenium and -osmium complexes linked to polystyrene by different linkers.*[60]

2 Coordinating anchoring ligands

2.1 Abstract

In this chapter the synthesis, characterization as well as photophysical properties of a total of eight polypyridine-based anchoring ligands are described. The four 2,2′-bipyridine-based and four 2,2′:6′,2″-terpyridine-based compounds all contain flexible alkyl chains of different lengths as linkers between the anchoring group and the metal-coordinating domain. Protection of the anchoring group was necessary to avoid unwanted side reactions during synthesis but also simplified the purification, characterization and handling of the ligands. Deprotection was performed as the last step. Sulfur-containing groups were used as binding sites to gold (*section 4.4*) whereas phosphonic and carboxylic acids are used for tethering to metal oxides such as TiO_2 (*section 4.2*).

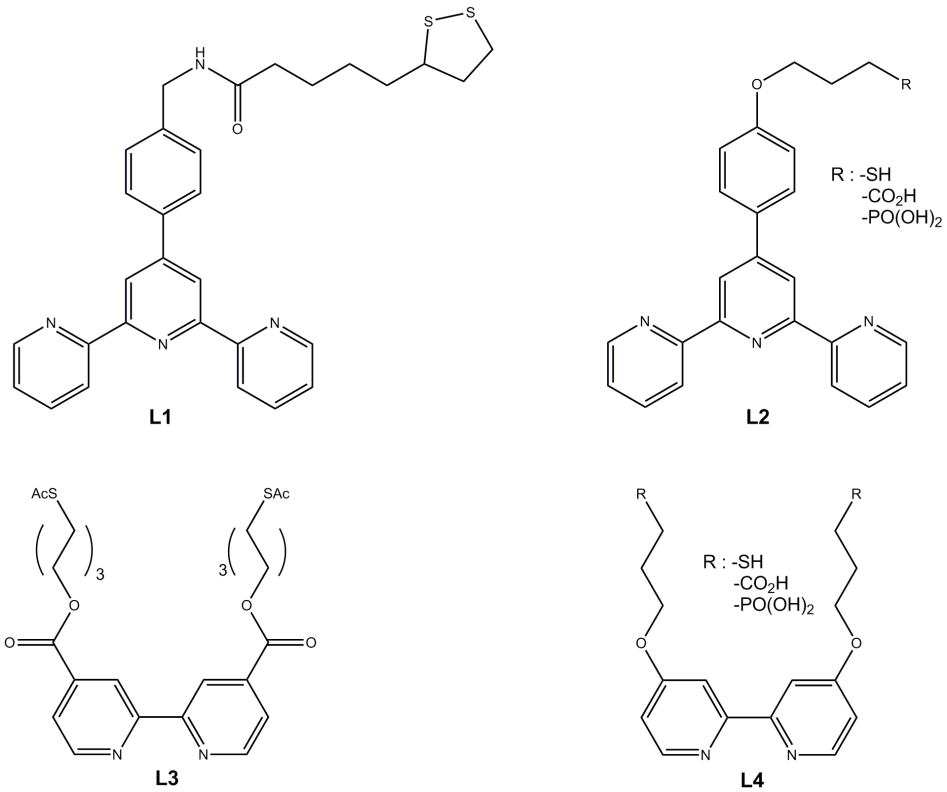

Scheme 2.1: *Terpyridine based ligands* ***L1*** *and* ***L2*** *and bipyridine based ligands* ***L3*** *and* ***L4***.

2.2 Synthetic strategy and synthesis

2.2.1 Ligand L1

The synthetic route to **L1** is shown in *Scheme 2.2*. The synthesis starts from 4′-(*p*-tolyl)- 2,2′:6′,2″-terpyridine (ttpy), prepared via the one-pot reaction reported by *Wang* and *Hanan*.[21] The substituted tridentate ligand is formed by an aldol condensation and *Michael* addition[62] of 2-acetylpyridine with an aryl aldehyde under basic conditions. Ammonia acts as the nitrogen source for the central pyridine during ring closure. The second step to intermediate P1 is an allylic bromination of the methyl group with *N*-bromosuccinimide (NBS). As radical starter azobisisobutyronitrile (AIBN) was used. To obtain the primary amine from the bromide compound, a *Gabriel* synthesis[63] was performed. This two-step synthesis via an imide is necessary due to the higher nucleophilicity of primary amines compared to ammonia. First, the bromide is substituted by a phtalimide (P2). Then, the nitrogen was reduced by hydrazine hydrate to obtain the primary amine P3.[64] In the last step, the amide with racemic thioctic acid (TA) was formed, mediated by *N*,*N*'-dicyclohexylcarbodiimide (DCC) as coupling reagent under mild conditions.[65] All intermediates are known in the literature and were characterized by ^{1}H and ^{13}C NMR spectroscopy and mass spectrometric methods. For **L1**, full characterization with absorption and photoluminescence spectroscopy (*section 2.3*), NMR spectroscopy, mass spectrometry, elemental analysis and IR spectroscopy (*section 7.2*) was performed.

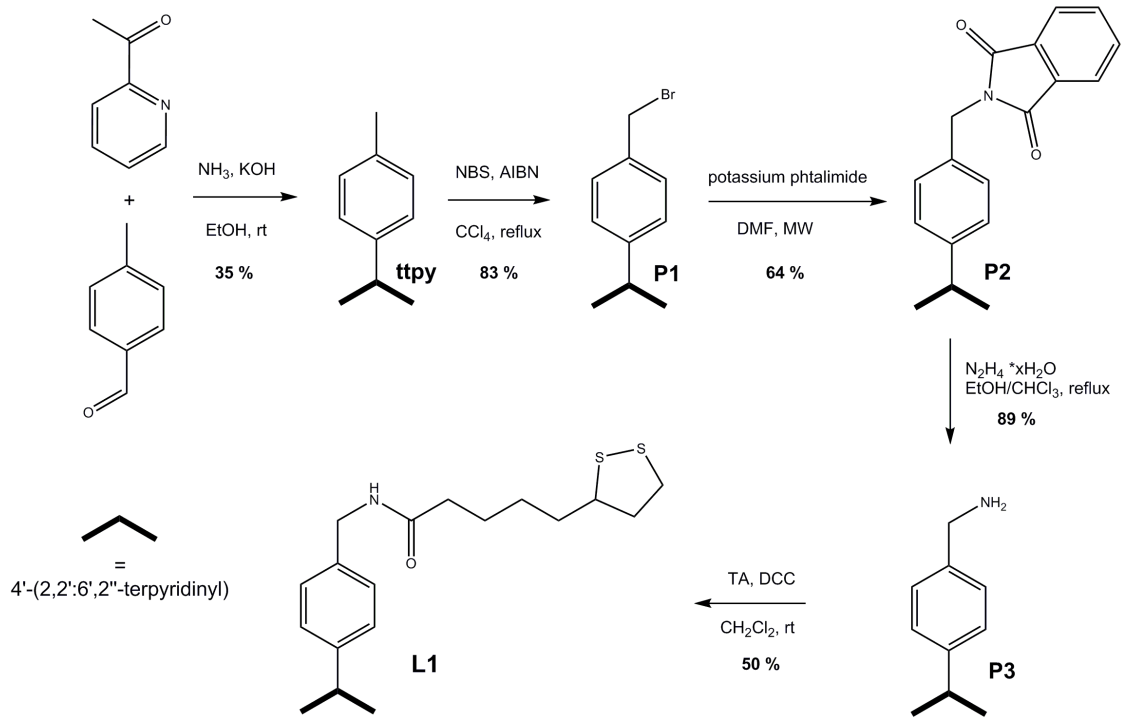

Scheme 2.2: *The synthesis of ligand* ***L1***.

2.2.2 Ligand L3

Scheme 2.3 shows the synthetic route to **L3**. The side chain **SC1** is prepared from 6-bromohexan-1-ol by a nucleophilic substitution with potassium thioacetate.[66] The commercially available 4,4′-dimethyl-2,2′-bipyridine is transformed into [2,2′-bipyridine]-4,4′-dicarboxylic acid (**dcbpy**) by oxidation with $KMnO_4$. The carboxyl groups were activated with $SOCl_2$ to yield the acid chloride. The reactive intermediate was not isolated and heated to reflux in toluene with **SC1** to yield the desired ester **L3**.[67] Triethylamine was added to neutralize the formed HCl and prevent hydrolysis. **L3** was characterized by absorption and photoluminescence spectroscopy (*section 2.3*), NMR spectroscopy, mass spectrometric methods, elemental analysis and IR spectroscopy (*section 7.2*).

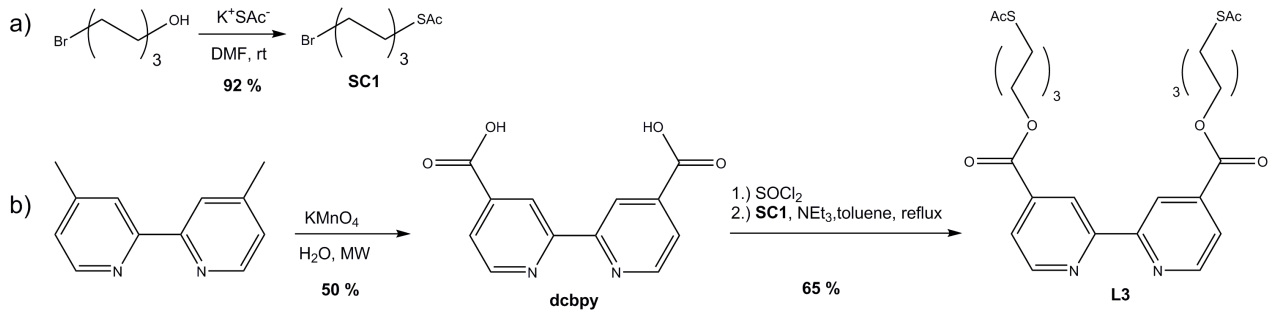

Scheme 2.3: *The synthesis of a) side chain **SC1** and b) ligand **L3**.*

2.2.3 Ligands L2 and L4

For the ligands **L2** and **L4**, a similar synthetic pathway was used, starting from the methoxy substituted 4,4′-dimethoxy-2,2′-bipyridine (MeO-bpy) and 4′-(4-methoxyphenyl)-2,2′:6′,2″-terpyridine (MeO-tpy), synthesized by literature methods,[21, 68] MeO-bpy was also commercially available. These precursors were converted into the corresponding hydroxy analogues 4-([2,2′:6′,2″-terpyridin]-4′-yl)phenol (OH-tpy) and [2,2′-bipyridine]-4,4′-diol (OH-bpy). For the bpy-compound, this was performed with HBr in acetic acid.[69] For OH-tpy a different approach, using pyridinium chloride in a microwave reactor, was used. The protected ligands **L2** and **L4** were obtained by a *Williamson* synthesis [63] of the hydroxy-compounds with the chains **SC2**, **SC3** and **SC4** in the presence of potassium carbonate.[70] (*Scheme 2.4*). The chains were synthesized and used with protected anchoring groups. This was necessary to avoid unwanted side reactions during synthesis and to simplify the purification, characterization and handling of the ligands. **SC2** and **SC3** were obtained starting from 1,3-dibromopropane (*Scheme 2.5*). For **SC2**, a nucleophilic substitution with potassium thioacetate similar to the preparation of **SC1** was used.[71] **SC3** was obtained by refluxing the starting material in triethyl phosphite, yielding the diethyl phosphonate.[72] **SC4** was commercially available.

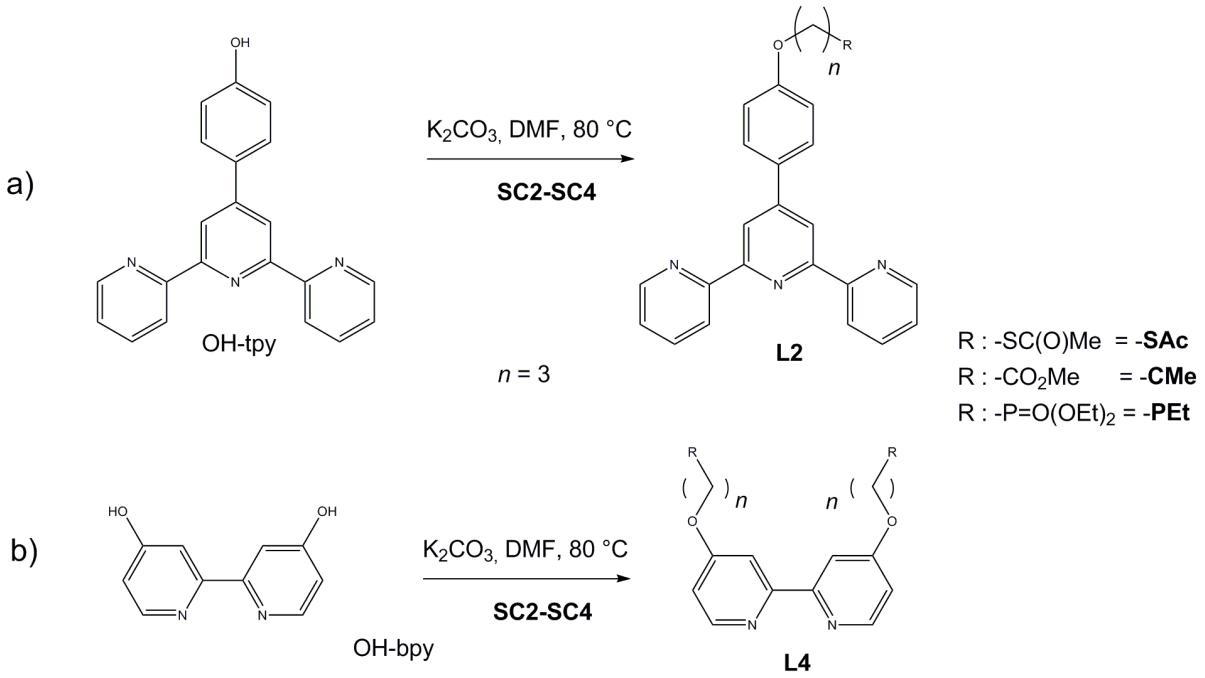

Scheme 2.4: *Preparation of the protected ligands* ***L2*** *and* ***L4*** *.*

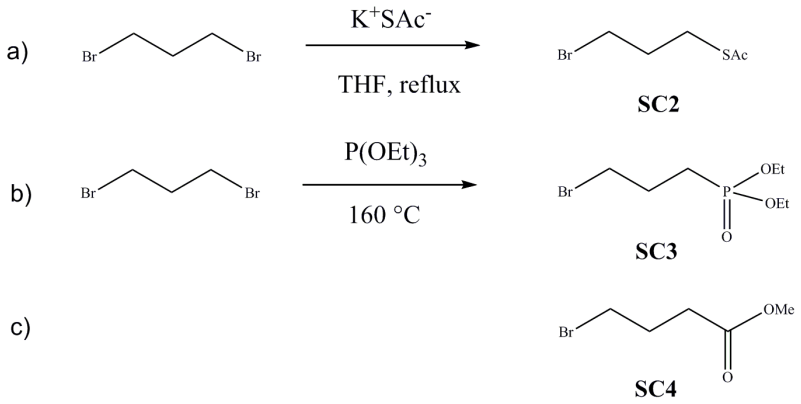

Scheme 2.5: *Synthesis of the side chains a)* ***SC2*** *and b)* ***SC3*** *; c) structure of side chain* ***SC4*** *.*

Full characterization with absorption and photoluminescence spectroscopy (*section 2.3*), NMR spectroscopy, mass spectrometry, elemental analysis and IR spectroscopy (*section 7.2*) of all 6 protected ligands **L2-SAc**, **-PEt**, **-CMe** and **L4-SAc**, **-PEt**, **-CMe** was performed.

2.2.4 Activation of ligands L2 and L4

Deprotection of the anchoring groups to yield the six activated ligands **L2-S**, **-P**, **-C** and **L4-S**, **-P**, **-C** was performed with different methods, shown in *Scheme 2.6*. The ligands **L2-S** and **L4-S** were obtained by treating the precursors **L2-SAc** and **L4-SAc** with sodium methoxide in anhydrous methanol at room temperature.[73] Hydrolysis of the phosphonates (**-PEt**) to the phosphonic acids (-P) was achieved using Me_3SiBr in CH_2Cl_2 at room temperature. The methyl carboxylates were hydrolyzed under basic conditions. For the conversion of **L2-CMe** to **L2-C**, K_2CO_3 in aqueous methanol at 80 °C was used. **L4-C** was obtained from refluxing **L4-CMe** in aqueous NaOH.[74] All activated ligands were isolated and characterized by NMR spectroscopy and mass spectrometric methods (*section 7.2*). For **L2-C** and **L4-C** elemental analysis was obtained, but satisfactory data could not be obtained for the remaining compounds.

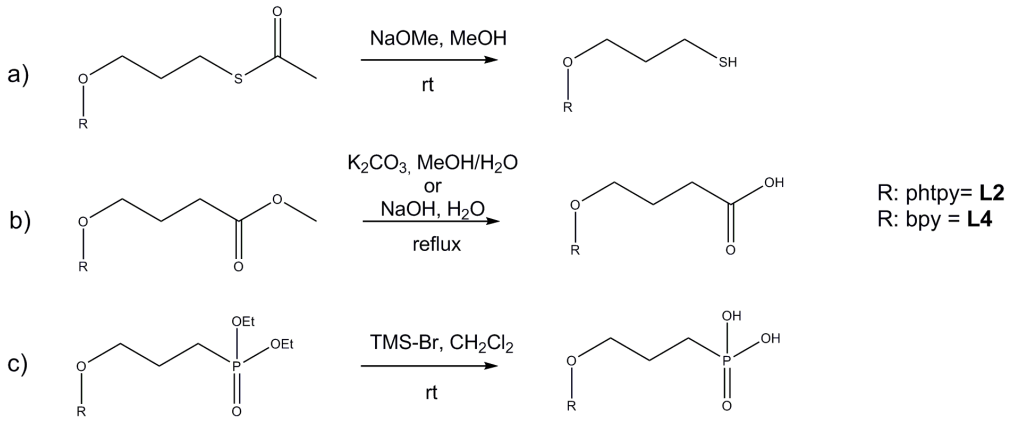

Scheme 2.6: *Reaction scheme to show the deprotection to give a) thiol* ***-S****, b)carboxylic acid* ***-C*** *and c) phosphonic acid* ***-P****.*

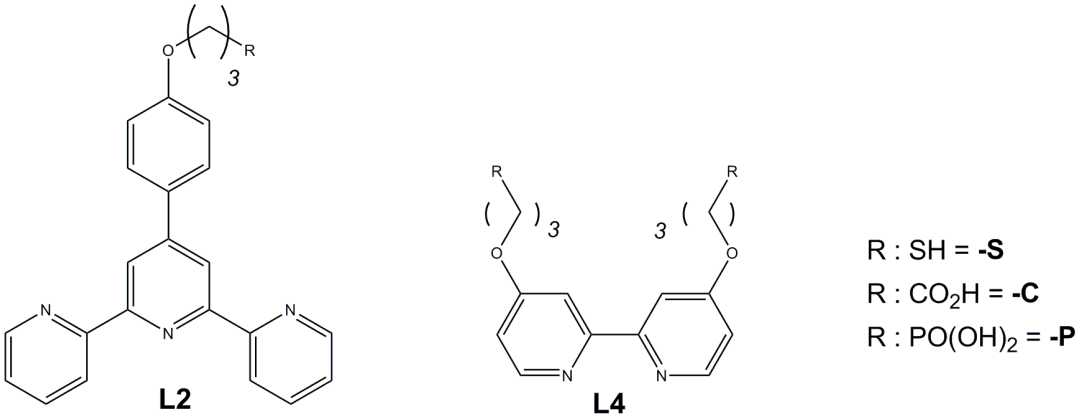

Scheme 2.7: *The deprotected ligands* ***L2*** *and* ***L4****.*

2.2.5 Thioacetate ligands S1 to S4

In addition to **L3**, the asymmetric analogue **S1** was synthesized. Several approaches were tried until the ligand was successfully synthesized. The first attempt started from 2-chloroisonicotinic acid, forming an ester with **SC1** in a *Steglich* esterification.[75] The ester was obtained, but the *Negishi* cross-coupling [63] with 2-pyridylzinc bromide was unsuccessful. In the second approach, [2,2′-bipyridine]-4-carboxylic acid could, in principle, be synthesized from 2-chloroisonicotinic acid and 2-pyridylzinc bromide, again by a *Negishi* cross-coupling reaction.[63] This attempt also did not work. The successful approach started again from 2-chloroisonicotinic acid, forming the methyl ester under *Steglich* conditions.[75] This step was necessary to increase the solubility and protect the carboxy group. Then, a *Negishi* cross-coupling[63] with 2-pyridylzinc bromide was performed, yielding methyl [2,2′-bipyridine]-4-carboxylate. The methyl ester was hydrolyzed under alkaline conditions and **S1** was obtained from a *Steglich* esterification[75] with **SC1**.

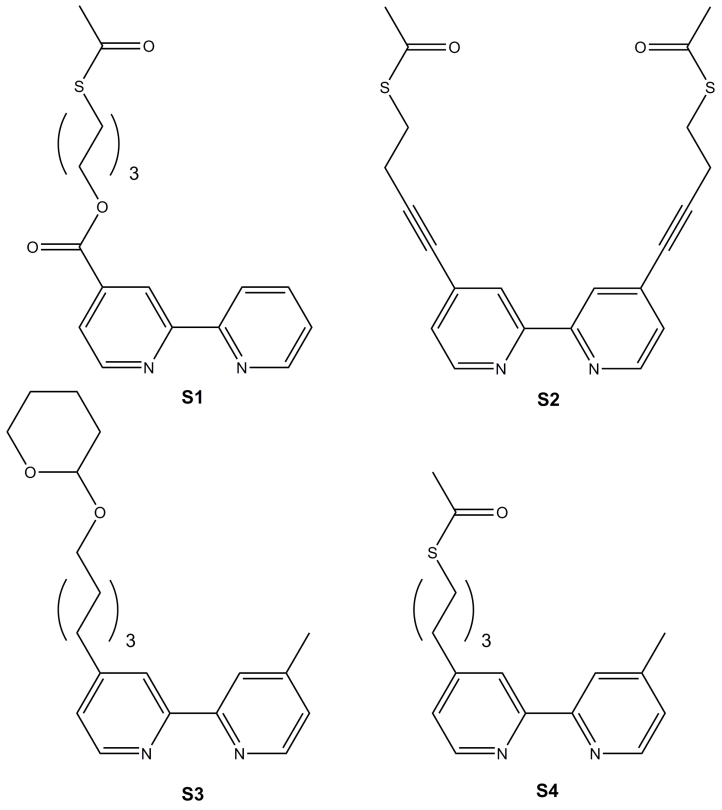

Scheme 2.8: *The 2,2′-bipyridine based ligands **S1-S4** with different substituents on the 4- and 4,4′-position.*

The ligand **S1** has several drawbacks. Due to its asymmetric nature it has only one anchoring group and thus presumably shows a weaker binding to surfaces compared to **L3**. If heteroleptic complexes are prepared, several isomers will be formed, which leads to complicated characterization.

Furthermore, the synthesis implies several steps with moderate yields. Because of these reasons the ligand **S1** was not used further.

Several attempts were made to synthesize bipyridine-based ligands with alkyl and alkynyl-bridged anchoring groups. The C-C bond should provide a strong connection. The thioacetate precursor for **S2** was synthesized in the same manner as **SC2**. A *Sonogashira* cross-coupling[62] with 4,4′-diiodo-2,2′-bipyridine was performed to yield the desired ligand. But only the mono-substituted compound was obtained, confirmed by NMR and MS methods. With optimized conditions the desired ligand was obtained.

Attempts to synthesize **S3** and **S4** followed the same strategy, shown in *Scheme 2.9*. Lithiation of 4,4′-dimethyl-2,2′-bipyridine and reaction with a bromo-substituted chain should lead to the desired C-C bond formation. The chains also bear reactive end groups for further functionalization. Chains with THP-protected hydroxy or bromo end groups were used, but none of the reactions succeeded. In the case of an alkenyl end group, the reaction to the mono-substituted bpy was successful. Attempts to obtain the symmetric ligand were made, but none yielded the desired product. Several attempts were made to functionalize the double-bond with a thioacetate. This included the reaction with thioacetic acid and AIBN in MeOH under reflux as well as in THF under light irradiation. All trials were unsuccessful.

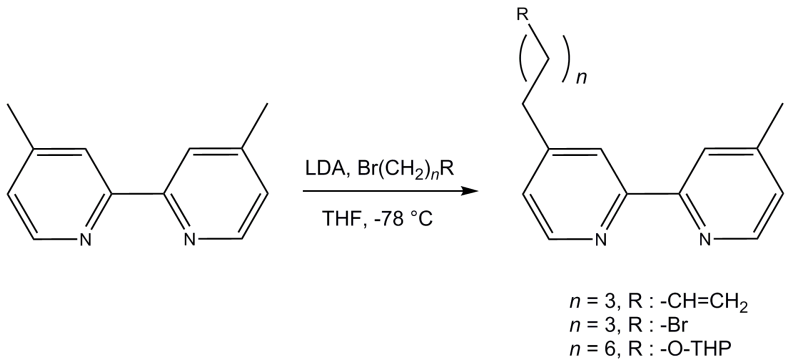

Scheme 2.9: *Reaction scheme for **S3** and two **S4**-precursors.*

2.2.6 Ligands S5 and S6 for polymer functionalization

The bipyridine based ligand **S5** comprises a long flexible chain connected via an ether bridge. The alkyl chain bears a hydroxyl group as the reactive site. **S6** is the symmetric analogue. The ligands are synthesized in the same way as the **L4** derivatives. Reaction of 10-bromodecan-1-ol with [2,2′-bipyridin]-4-ol or [2,2′-bipyridine]-4,4′-diol in the presence of potassium carbonate yields **S5** and **S6**, respectively. 10-Bromodecan-1-ol was synthesized by bromination of 1,10-decandiol.[76] The asymmetric bipyridine was obtained from 2,2′-bipyridine.[14, 77] Attempts to synthesize this precursor by a *Negishi* cross-coupling[63] between 4-methoxy-2-bromopyridine and 2-pyridylzinc bromide were performed but discarded as only low yields were obtained. The monofunctionalization of 2,2′-bipyridine was preferred as this synthetic route involved less steps and higher yields.

Attempts were made to functionalize the hydroxyl groups at the chain ends. Reaction of **S6** with methacrylic anhydride in THF at room temperature only partially yielded the desired ester.[78] With the ligand **S5** almost complete ester-formation was obtained, but due to the reactive character of the methacrylate, purification was not possible. Neither column chromatography nor recrystallization yielded the pure product.

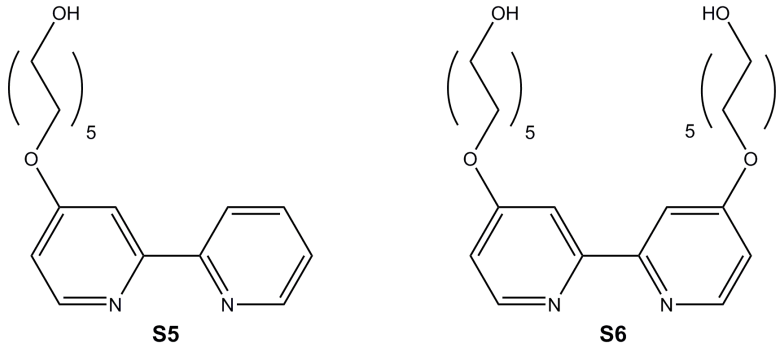

Scheme 2.10: *The ligands **S5** and **S6**.*

2.3 Photophysical properties

All absorption and photoluminescence spectra were recorded in $CHCl_3$. For the **L2** family, the protected compounds **L2-SAc**, **L2-CMe** and **L2-PEt** were used due to their good solubility which contrasts with the poor solubility of the deprotected compounds. Additionally, spectra of **MeO-tpy** were recorded to see if the alkyl chain and the anchoring group influence the photophysical properties. The same procedure was utilized for the **L4** family. For these ligands spectra of **L4-SAc**, **L4-CMe**, **L4-PEt** and **MeO-bpy** were recorded.

2.3.1 Absorption spectra

Ligand L1

The electronic absorption spectrum of **L1** (*Fig. 2.1*) shows a maximum at a wavelength of 280 nm with $\varepsilon = 31800\ dm^3\,mol^{-1}\,cm^{-1}$. This band arises from $\pi^* \leftarrow \pi$ transitions centred on the aromatic system. The spectrum also shows a shoulder at 315 nm.

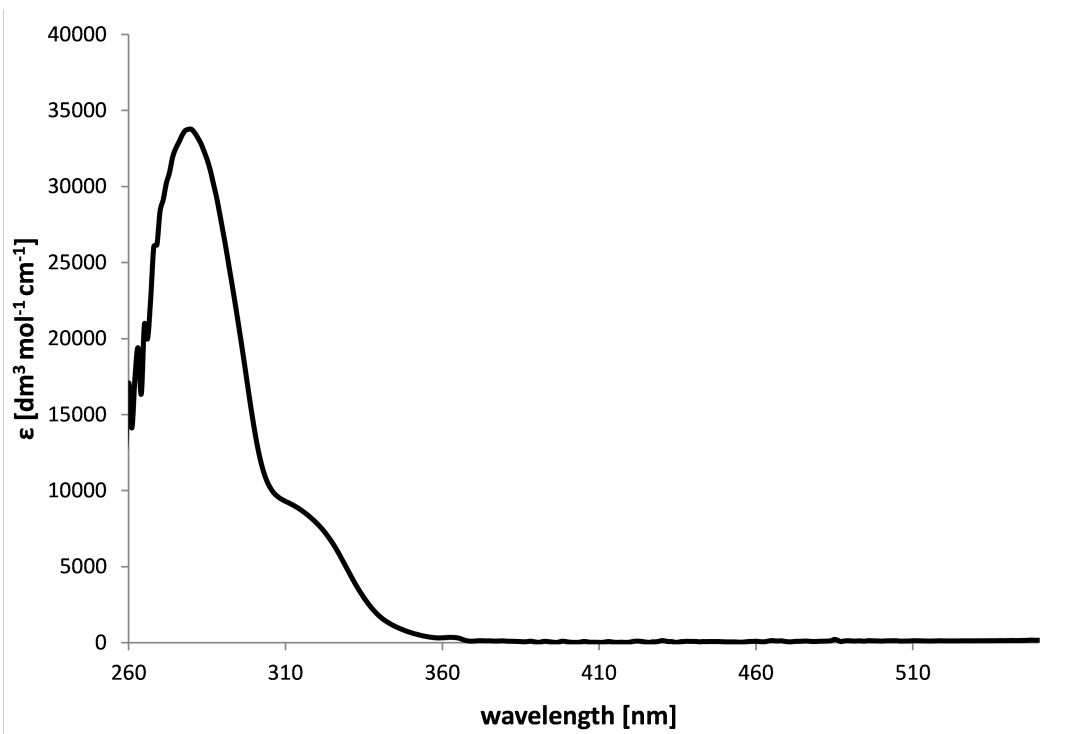

Figure 2.1: *UV-Vis spectrum of* ***L1*** *($CHCl_3$, $4.2 \cdot 10^{-5}$ M).*

Ligand L2

The absorption spectra of **L2-SAc**, **-CMe**, **-PEt** and **MeO-tpy** are shown in *Fig. 2.2.* All four compounds show an intense band at 287 nm. This absorption arises from π* ← π transitions. No difference between the various anchoring groups can be observed. Also the extinction coefficients are in the same range with ε ≈ 34000 $dm^3\,mol^{-1}\,cm^{-1}$.

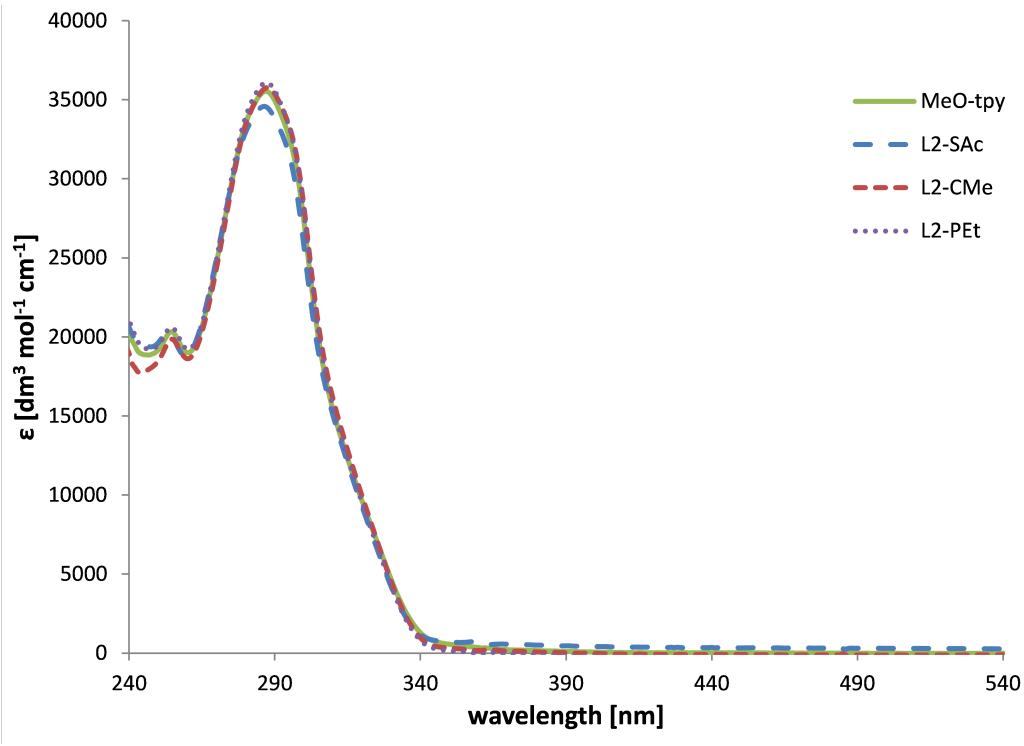

Figure 2.2: *UV-Vis spectra of the **L2** ligands ($CHCl_3$, $1 \cdot 10^{-5}$ M).*

Ligand L3

The ligand **L3** shows two main bands in the UV-Vis absorption spectrum. The first maximum is at a wavelength of 243 nm with an extinction coefficient of 16200 $dm^3\,mol^{-1}\,cm^{-1}$. The second band is at 301 nm with ε =11500 $dm^3\,mol^{-1}\,cm^{-1}$. Both bands arise from π* ← π transitions.

Ligand L4

In the solution absorption spectra, the ligand family **L4** shows different maxima, depending on the anchoring group (*Fig. 2.3*). Whereas **MeO-bpy** and **L4-CMe** have absorption maxima at 259 nm, **L4-PEt** and **L4-SAc** are blue-shifted with maxima at 255 nm and 240 nm respectively. All absorption bands arise from π*←π transitions.

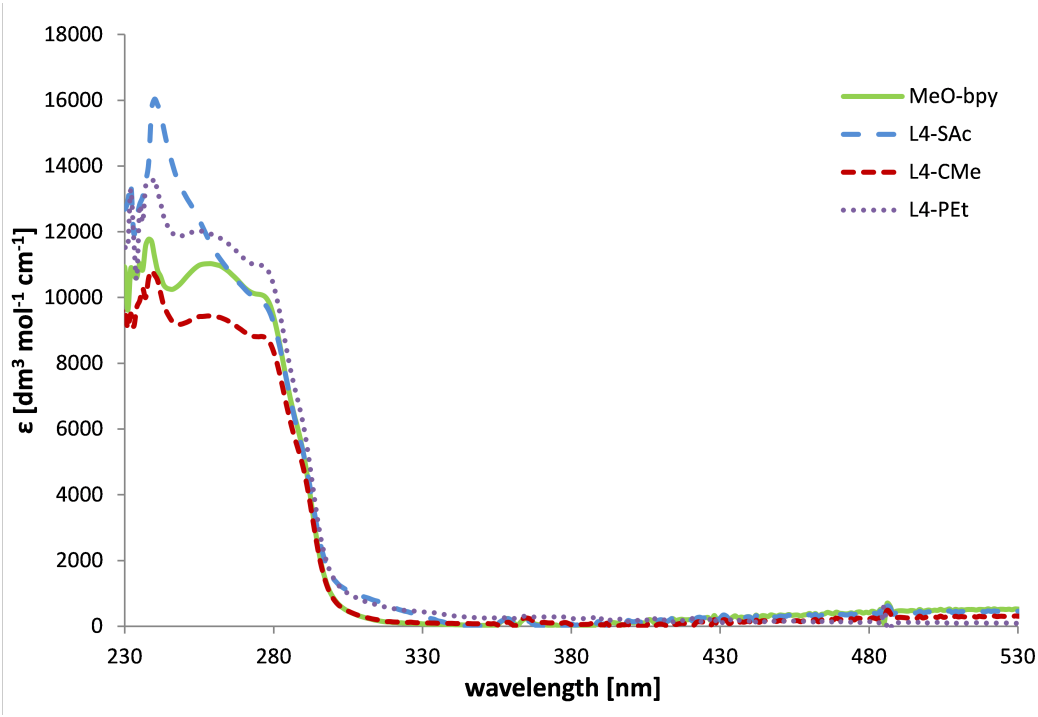

Figure 2.3: *UV-Vis spectra of the* ***L4*** *family (*$CHCl_3$*,* $1 \cdot 10^{-5}$ *M).*

2.3.2 Photoluminescene

Ligand L1

The emission and excitation spectra of **L1** are shown in *Fig. 2.4*. The excitation spectrum was recorded at λ_{em} = 360 nm and shows a maximum at 285 nm. This is in in accordance with the observations from the absorption spectroscopy, where the maximum was found at 280 nm. In the emission spectrum with an excitation wavelength of 280 nm, two maxima at 342 nm and 356 nm are found.

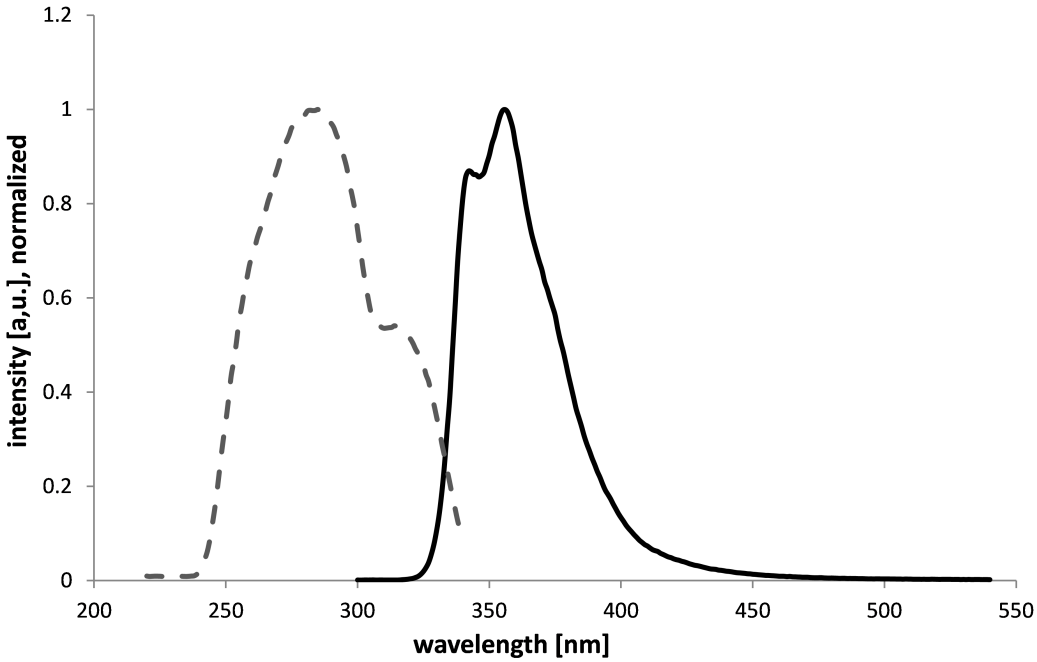

Figure 2.4: *Solution emission (solid line) and excitation (dashed line) spectra of $CHCl_3$ solutions of **L1**, λ_{exc} = 280 nm, λ_{em} = 360 nm, normalized.*

Ligand L2

The emission spectra were recorded with λ_{exc} = 290 nm. At 287 nm, the absorption maximum is located. All ligands of the **L2** family show emission with maximum at 359 nm (*Fig. 2.5*). As described above in the absorption spectra, no difference between the spectra for the various ether chains is observed.

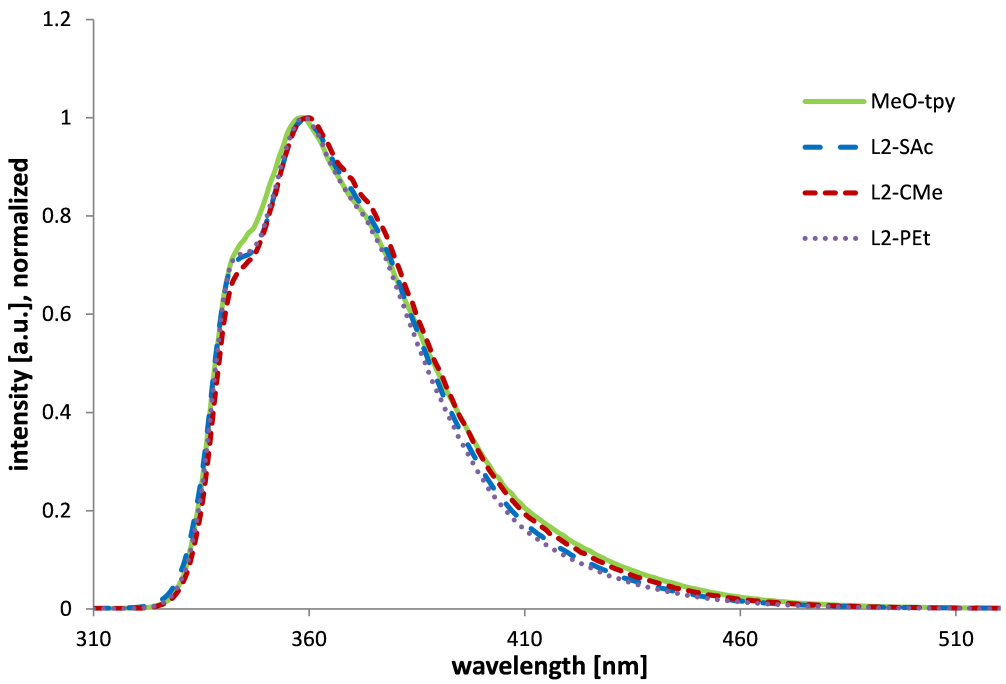

Figure 2.5: *Solution emission spectra of $CHCl_3$ solutions of ligands* ***MeO-tpy*** *and* ***L2***, λ_{exc} = *290 nm, normalized.*

Ligand L3

The solution emission and excitation spectra for **L3** are shown in *Fig. 2.6*. Upon excitation at 300 nm, where the maximum of the second absorption band is located, the ligand shows two emission maxima at 350 nm and 365 nm. In the excitation spectrum for 360 nm, the maximum is found at 287 nm.

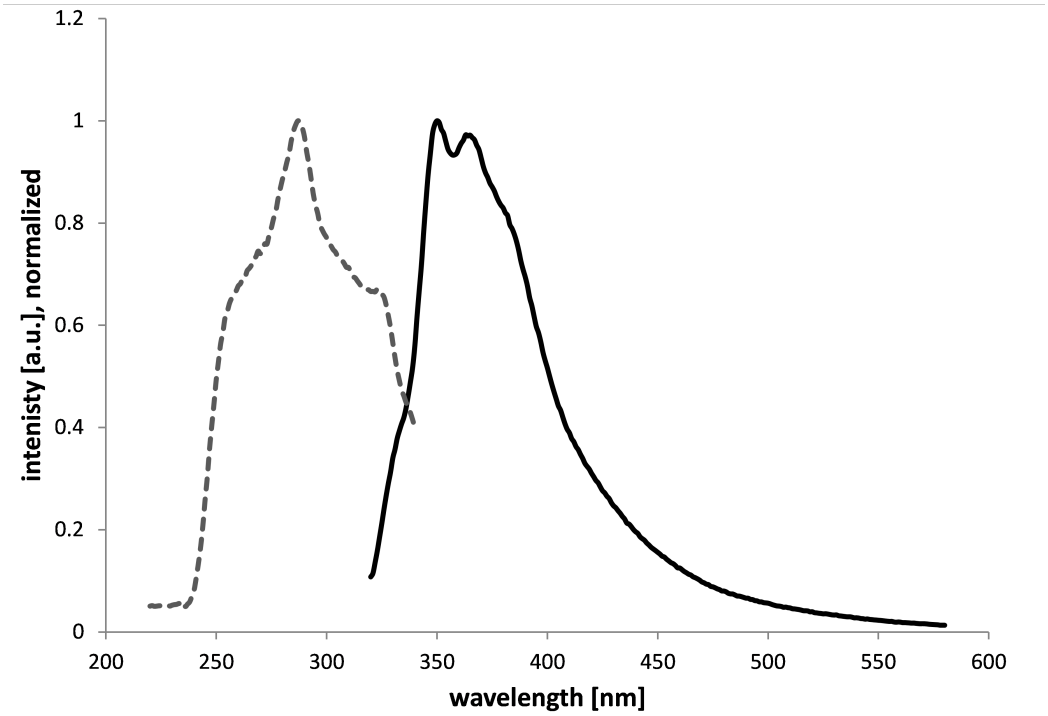

Figure 2.6: *Solution emission (solid line) and excitation (dashed line) spectra of $CHCl_3$ solutions of* ***L3****, λ_{exc} = 300 nm, λ_{em} = 360 nm, normalized.*

Ligand L4

Two different excitation wavelengths, 250 nm and 320 nm, were used to record emission spectra of **L4**. The first, 250 nm, was chosen due to the position of the absorption maxima, whereas the second, 320 nm, was found as a maximum in the excitation spectra. With λ_{exc} = 250 nm, **MeO-bpy** and **L4-PEt** show maxima at 316 nm with a shoulder at 382 nm, **L4-CMe** shows a maximum at 382 nm with a shoulder at 316 nm. **L4-SAc** shows also a shoulder at 382 nm and a red-shifted maximum at 443 nm. Excitation at 320 nm gives for **MeO-bpy**, **L4-CMe** and **L4-PEt** maxima at 386 nm whereas **L4-SAc** shows a red-shifted maximum at 443 nm. As observed in the electronic absorption spectroscopy, there is a dependence on the substituent present in the ligand.

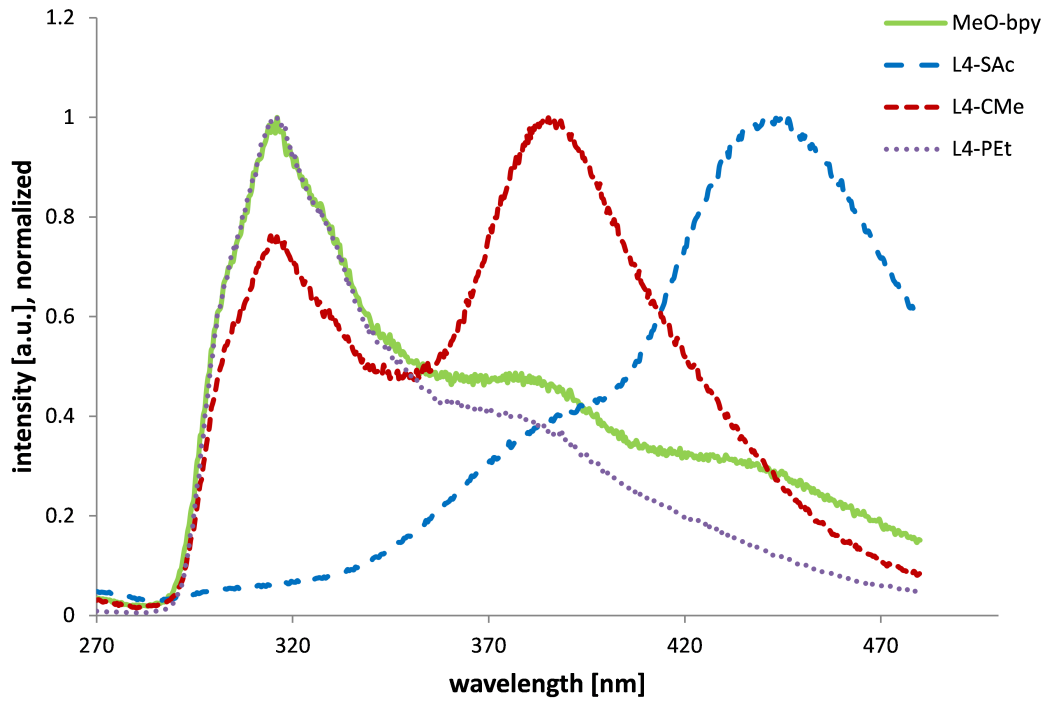

Figure 2.7: *Solution emission spectra of the* ***L4*** *family (CHCl*$_3$*,* $\lambda_{exc.}$ *= 250 nm), normalized.*

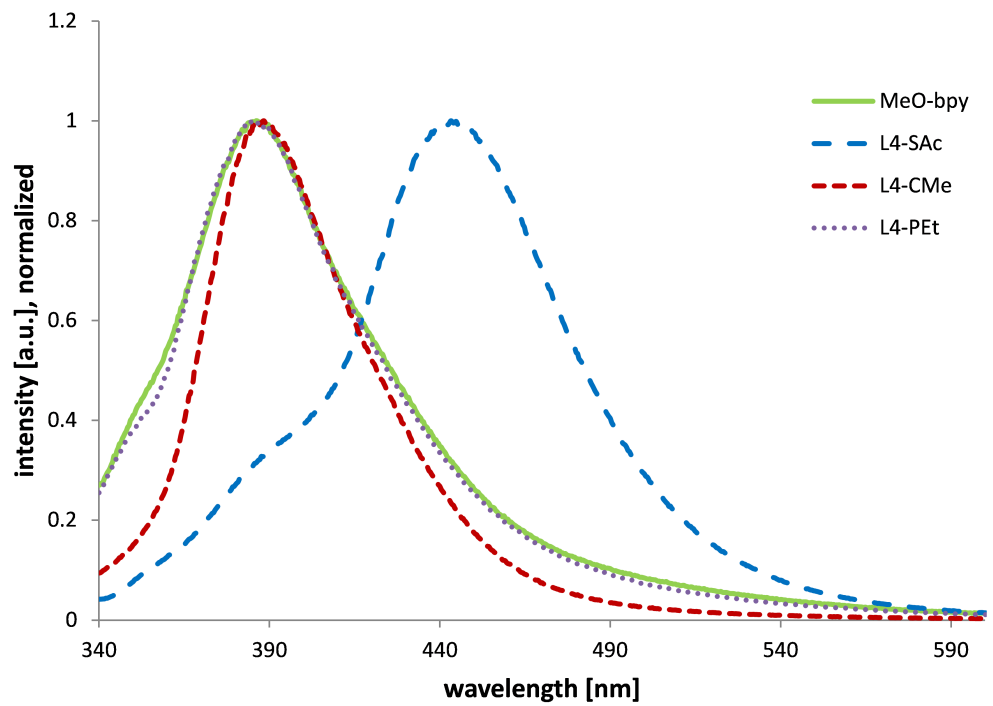

Figure 2.8: *Solution emission spectra of the* ***L4*** *family (CHCl*$_3$*,* $\lambda_{exc.}$*= 320 nm), normalized.*

2.4 XRD

2.4.1 L4-CMe

Crystallographic grade crystals of **L4-CMe** were grown by slow evaporation from acetone.

Crystallographic data

formula moiety	$C_{20}H_{24}N_2O_6$		μ(Cu-Kα) [mm^{-1}]	0.848
formula weight [g mol^{-1}]	388.41		T [K]	123
crystal colour and habit	colourless block		refln. collected	7934
crystal sytem	triclinic		unique refln.	1668
space group	P-1		refln. for refinement	1573
a,b,c [Å]	6.7491(4), 7.1363(5), 10.5428(7)		parameters	128
α, β,γ [°]	77.923(3), 73.076(3), 78.520(3)		threshold	$I > 2\sigma$
U [$Å^3$]	469.83(5)		R_1 (R_1 all data)	0.0363 (0.0377)
D_c [Mg m^{-3}]	1.373		wR_2 (wR_2 all data)	0.0960 (0.0971)
Z	1		goodness of fit	1.075

L4-CMe (*Fig. 2.9*) crystallizes in the space group P-1 with the bpy unit planar by symmetry in a trans conformation. The molecules arrange as layered sheets in the crystal. In one plane hydrogen bonds between the pyridine nitrogen (N1) and a hydrogen of the methyl group (H10B) are formed as well as between the ether oxygen (O1) and the hydrogen of the pyridine ring on the 4-position (H4A). Additional hydrogen bonding occurs between the carbonyl oxygen (O2) of one layer and a hydrogen of a CH_2 group (H6B) in the upper sheet (*Fig. 2.10*). The interplane distance between two pyridine rings is too large to enable π-stacking.

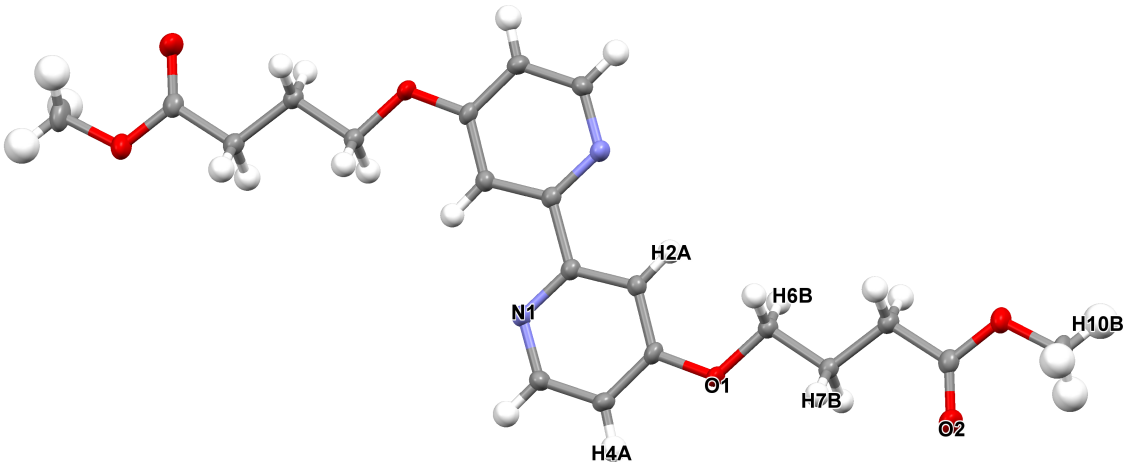

Figure 2.9: *Structure of* ***L4-CMe*** *with ellipsoids plotted at 50 % probability.*

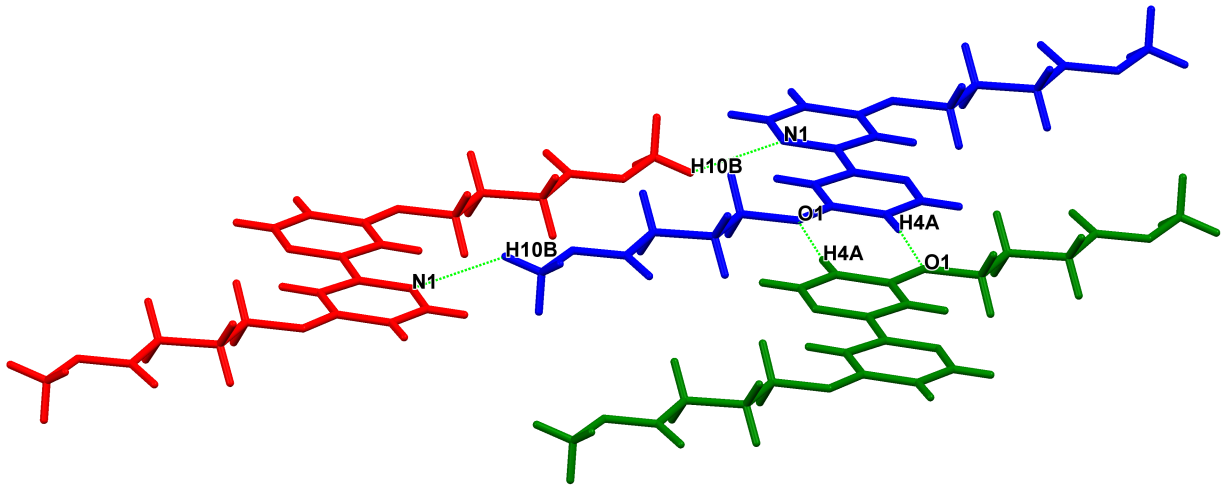

Figure 2.10: *Hydrogen bonding between the* ***L4-CMe*** *molecules in the crystal.* ***Distances:*** *N1-H10B = 2.675 Å; O1-H4A = 2.479 Å; O2-H6B (upper sheet) = 2.686 Å, interplane distance = 3.510 Å, interplane centroid-centroid distance = 5.071 Å.*

2.5 Concluding remarks

2.5.1 Ligand L1

The terpyridine-based anchoring ligand **L1** contains a disulfide group as the anchoring moiety. This group can be used for anchoring on gold surfaces and nanoparticles (NPs), but also applied for other materials like CdSe. For gold, functionalization with the ligand can be done directly[79] whereas for CdSe, reduction of the disulfide to the thiols is necessary.[80] The amide linkage between the tpy and the anchoring chain provides a very stable connection. Even under harsh conditions such as high temperatures or low pH values no cleavage was observed. A phenyl-substituted terpyridine acts as coordination site. With this, complexation with most transition metals is possible. Additionally the phenyl-substituent leads to the extension of the conjugated π system and a resultant photoluminescent emission near the visible region.
The synthetic route involves five steps with acceptable to good yields. All synthetic procedures and most intermediates are known in the literature. **L1** was used as anchoring ligand in complex **C1** (*chapter 3*).

2.5.2 Ligand L3

Anchoring ligand **L3** contains bipyridine as coordination site and acetate protected thiols as anchoring groups. These can be applied for functionalization of the same materials like **L1**. A flexible hexyl chain acts as spacer and an ester group as linkage between the anchor and the coordination site. The ester should yield a robust connection but problems concerning the stability were observed. It is known that esters are prone to hydrolysis under basic or acidic conditions. But we observed transesterification with different alcohols as solvent under elevated temperatures (*section 3.2.2*).
The synthesis of the ligand is straightforward and contains only three steps with good yields. **L3** was used as anchoring ligand in complex **C2** (*chapter 3*).

2.5.3 Ligands L2 and L4

L2 and **L4** were obtained following a similar synthetic strategy. Both ligand families were synthesized with each three anchoring groups. With carboxylic and phosphonic acids functionalization of metal oxides like TiO_2 or SiO_2 is possible. With thiols the same materials as described for **L1** and **L3** are accessible. This variety of materials offers a broad range of possible applications. The conncetion via an ether-bridge shows high stability under different conditions. Neither extreme pH values nor high temperatures or high pressure caused cleavage of the side chain. The bridging oxygen also expands the π-system of the ligands and leads to luminescence enhancement and for **L4** also to a red-shift of the emission maxima.
The synthetic approach starts from readily accessible materials and contains no more than five steps. Altering of the chain length as well as introduction of other anchoring groups is possible with this

strategy. **L2** and **L4** were used for surface functionalization (*chapter 4*). **L4-SAc** was applied as anchoring ligand in complex **C3** (*chapter 3*).

3 Complexes for ion detection

3.1 Abstract

In this chapter the synthesis, characterization and photophysical properties of six Ru(II) complexes are described. Also the sensing properties are examined and discussed. The complexes contain a sensor ligand and one or two anchoring ligands, described in *chapter 2*. The anchoring ligands should yield strong binding to a surface to give a metal complex functionalized material with detection properties. **C1** with its accessible pyridine nitrogen was tested for pH-sensing. **C2,** its model compound **C2***, and **C3** bear the phen-based ligand **L5** which is known to interact with F^- ions.[81, 82] These complexes were used as fluoride sensing agents. **C4** and **C5** contain 1,10-phenanthroline-4,7-dicarbaldehyde (**PDA**) as the detection ligand and should act as cyanide detectors, like other ruthenium-based PDA complexes from the literature.[83]

3.2 Synthetic strategy and synthesis

3.2.1 Complex C1

Complex **C1** (*Scheme 3.1*) was synthesized in a straightforward manner. Reaction of pytpy with $RuCl_3$ in refluxing EtOH gives the intermediate Ru(pytpy)Cl_3,[84] which was used directly for the next step. The complexation with **L1** under reflux yields the desired compound. As solvent and reducing agent, ethylene glycol was used.

3.2.2 Complexes C2 and C2*

In *Scheme 3.2*, the synthesis for the complex **C2** is shown. Reaction of the starting material $RuCl_3$ with 1,5-cyclooctadiene (cod) results in the intermediate $RuCl_2$(cod). Here cod acts as an η^4-ligand for the Ru(II) metal center.[85] In the next step, cod is substituted by two anchoring ligands **L3** to yield Ru(L3)$_2$Cl$_2$. The phen-based ligand **L5** was synthesized by *Dr. Iain A. Wright.* The precursor 1,10-phenanthroline-5,6-dione was synthesized as described in literature.[86] Reaction of this precursor with commercial 2,4-dinitrophenylhydrazine under acidic conditions yielded the desired compound. **L5** has a low solubility in many common solvents. Thus complexation was performed in the microwave reactor to allow higher temperatures and pressures in the closed vials. The solvents THF, DMF, *tert*-butyl alcohol and water were tested but none yielded the desired complex. When alcohols such as ethylene glycol and EtOH were used, the complexation proceeded, but partial transesterification of the anchoring ligands was observed. Lowering the reaction temperature to avoid this side reaction was unsuccessful. MeOH as solvent showed promising results although transesterification was also observed. Several test reactions were made to optimize the reaction parameters. No complexation at temperatures below 110 °C occured. Shorter reaction times showed slightly lower transesterification but also lower yields. Finally, a temperature of 115 °C and a reaction time of 23 min. showed the best results with respect to yield and transesterification.

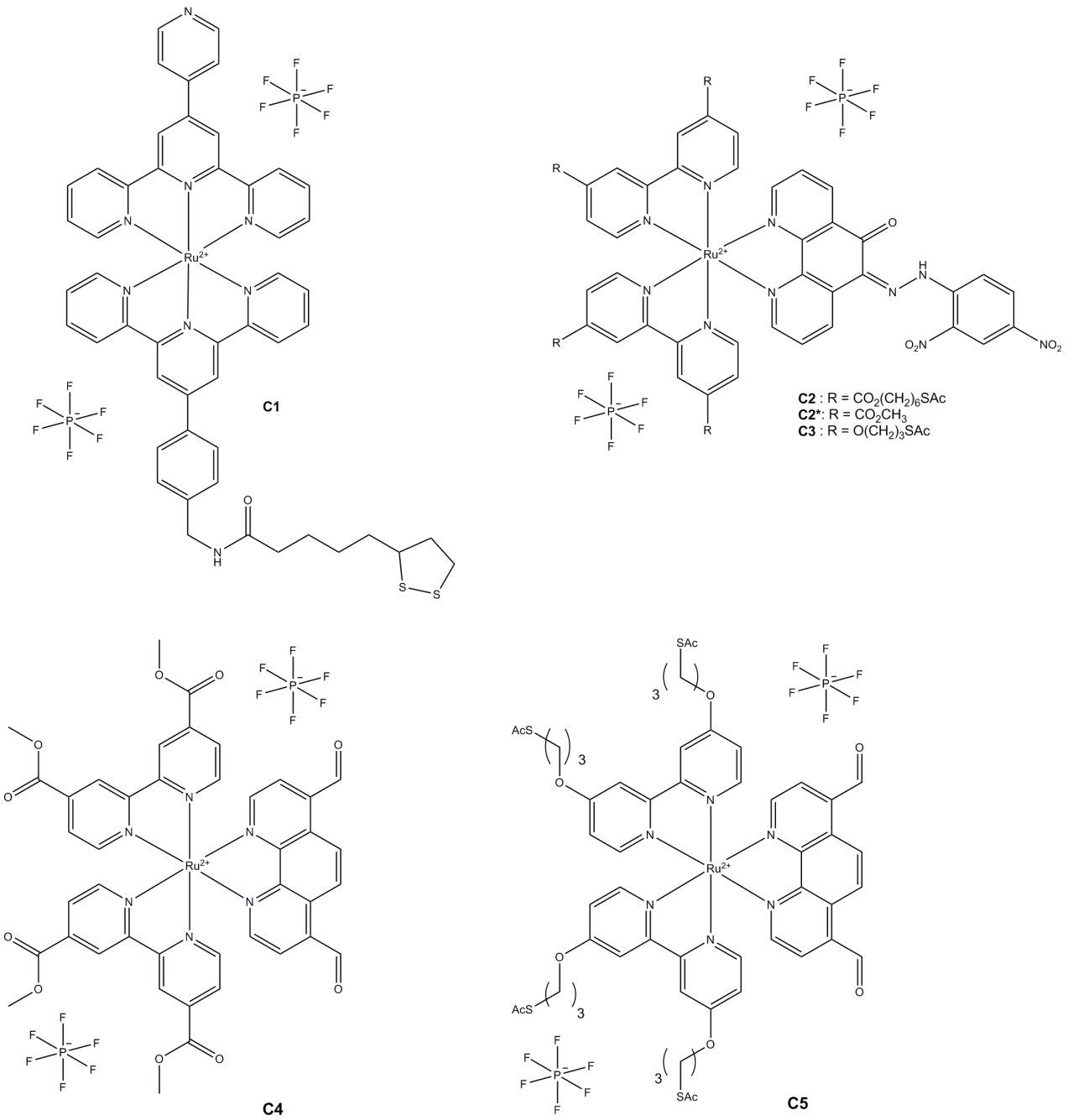

Scheme 3.1: *Complexes **C1-C5** for detection.*

Approaches to introduce the **L5**-precursor 1,10-phenanthroline-5,6-dione for subsequent reaction to the hydrazone did not work either.

Due to the rather demanding synthesis of **C2**, the model compound **C2*** was synthesized. In this complex, the anchoring ligand **L3** was substituted by dimethyl [2,2′-bipyridine]-4,4′-dicarboxylate (**dmcbpy**). It was supposed that the methyl ester would provide the same environment as the

substituted hexyl ester of **L3** and would have no influence on the detection properties of the complex. Thus, all further experiments were conducted with the model complex **C2***. As shown in *Scheme 3.2*, the **dmcbpy-**ligand was reacted with the $RuCl_3$, yielding cis-Ru(dmcbpy)$_2$Cl$_2$ as intermediate.[87] For the complexation with **L5**, higher temperatures and longer reaction times could be used because transesterification caused no problems.

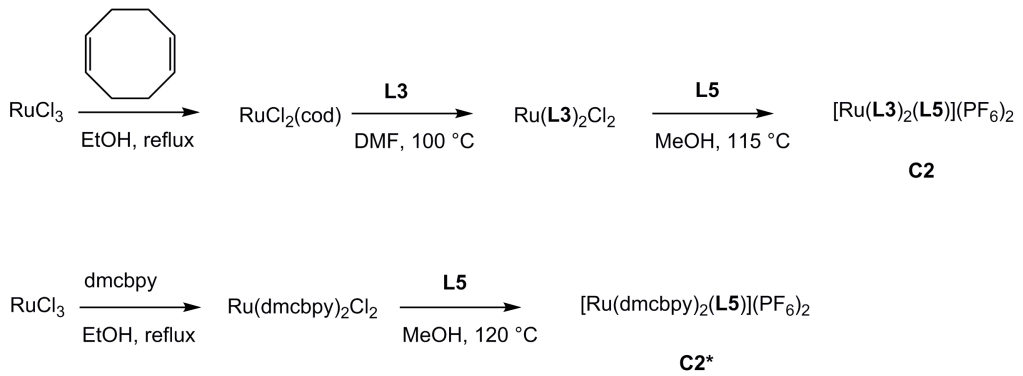

Scheme 3.2: *The synthetic routes to the complexes **C2** and **C2****.

3.2.3 Complex C3

The complex **C3** was made as an alternative to **C2**. It also contains the ligand **L5** for F^- detection, but as anchoring ligand **L4-SAc** was used instead of **L3**. For synthesis, the same procedure was applied as for **C2** (*Scheme 3.2*). First, two anchoring ligands were coordinated to the $RuCl_2$(cod) precursor. Then, **L5** was introduced, using MeOH as solvent in the microwave reactor. With **L4-SAc** as anchoring ligand, even at higher temperatures no stability problems were observed.

3.2.4 Complexes C4 and C5

The complexes contain a 1,10-phenanthroline ligand with two aldehyde groups (**PDA**) as detection unit. **C4** bears **dmcbpy**-ligands which should act as a model compound for the ligand **L3**, similar to **C2** and **C2***. The synthesis follows the same procedure as for **C2***. The complex is obtained from reaction of Ru(dmcbpy)$_2$Cl$_2$ and **PDA** in the microwave reactor. **C5** is yielded by the complexation of **PDA** to the cis-Ru(**L4-SAc**)$_2$Cl$_2$ precursor under reflux conditions in aqueous EtOH.

3.3 Photophysical properties

3.3.1 Absorption spectra

Complex C1

The heteroleptic complex **C1** shows three maxima in the absorption spectrum (*Fig. 3.1*). The two bands in the UV region at 280 nm ($\varepsilon = 68600\ dm^3\ mol^{-1}\ cm^{-1}$) and 312 nm ($\varepsilon = 65800\ dm^3\ mol^{-1}\ cm^{-1}$) arise from ligand based $\pi^* \leftarrow \pi$ transitions. The maximum at 490 nm with an extinction coefficient of 27500 $dm^3\ mol^{-1}\ cm^{-1}$ is caused by an MLCT transition. These maxima are comparable with the values obtained for the homoleptic complex $[Ru(pytpy)_2][PF_6]_2$.[88]

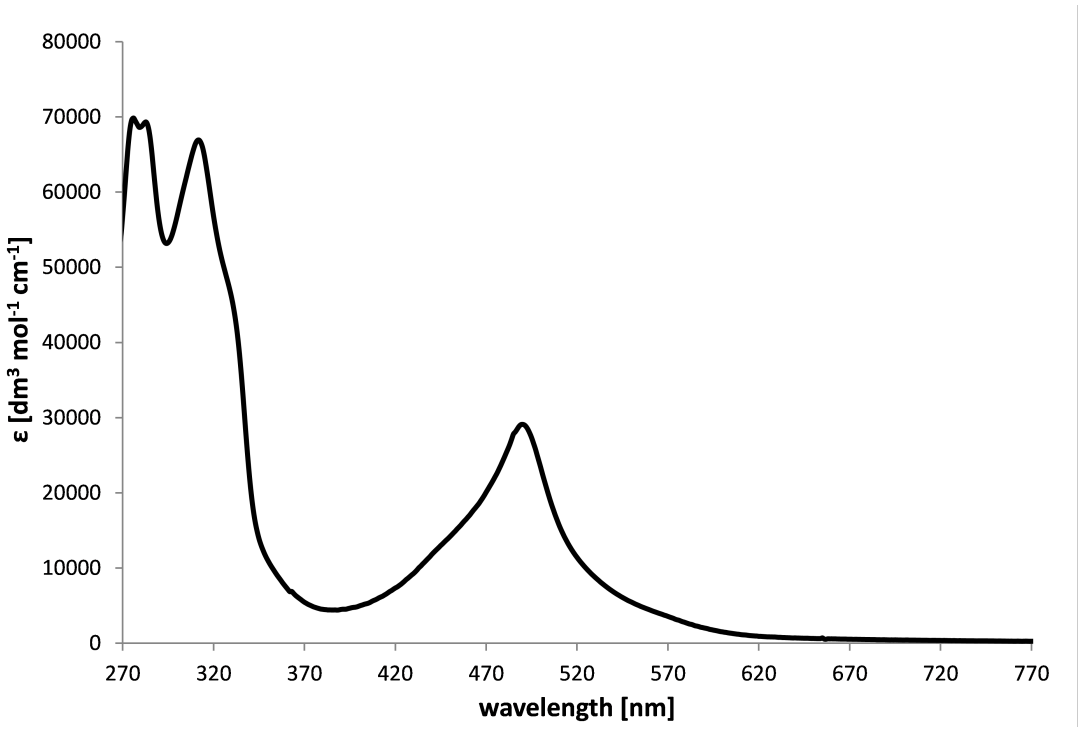

Figure 3.1: *Solution absorption spectrum of* ***C1*** *(MeCN, 1·10^{-5}M).*

Upon addition of H^+, the maximum of the MLCT is red-shifted due to protonation of the free nitrogen in the pendant pyridine ring (*Fig. 3.2*). This can be examined by titration with an acid. The results of the titration with HCl are shown in *Tab.3.1.* The first shift occurs after the addition of 2 eq. H^+ and levels off after about 4.5 eq. with a red-shift of 9 nm. This shift is in accordance with the values obtained for the mono-protonated homoleptic pyridyl-terpyridine complex.[89]

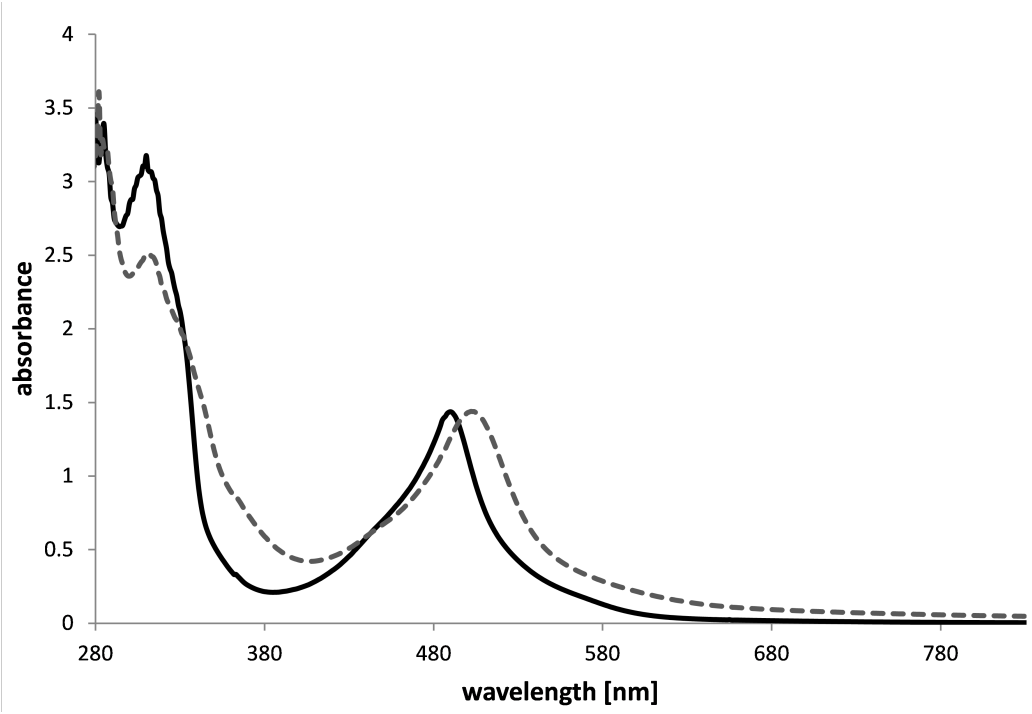

Figure 3.2: *Absorption spectrum of* ***C1*** *before (solid line) and after addition (dashed line) of an excess HCl (MeCN, 5·10^{-5}M).*

Eq. of HCl	*Absorption maximum [nm]*		*Eq. of HCl*	*Absorption maximum [nm]*
0	490		4.0	498
0.5	490		4.5	499
1.0	490		5.0	498
1.5	490		5.5	499
2.0	492		6.0	499
2.5	493		6.5	499
3.0	496		7.0	499

Table 3.1: *Titration of* ***C1*** *with HCl, correlation between absorption maximum and H^+ concentration.*

Complex C2*

Three maxima can be observed in the electronic absorption spectrum of the complex **C2***. The band at 309 nm (ε = 77000 $dm^3\,mol^{-1}\,cm^{-1}$) arises from ligand based $\pi^* \leftarrow \pi$ transitions. The second maximum at a wavelength of 474nm (ε = 53400 $dm^3\,mol^{-1}\,cm^{-1}$) is caused by a charge transfer centred on the **L5**-ligand[81] and the maximum of the MLCT transition is at 576 nm with an extinction coefficient of 18800 $dm^3\,mol^{-1}\,cm^{-1}$.

To examine the interaction between the complex and different halide ions, excess of the particular TBA salt was added and absorption spectra were recorded, as seen in *Fig. 3.3*. As expected the presence of fluoride ions causes a red-shift in the MLCT band by 7 nm and a strong enhancement to an extinction coefficient of 49700 $dm^3\,mol^{-1}\,cm^{-1}$(*Fig. 3.4*). This can also be observed by naked-eye with a colour change from red to purple. With other halides, no colour change is observed.

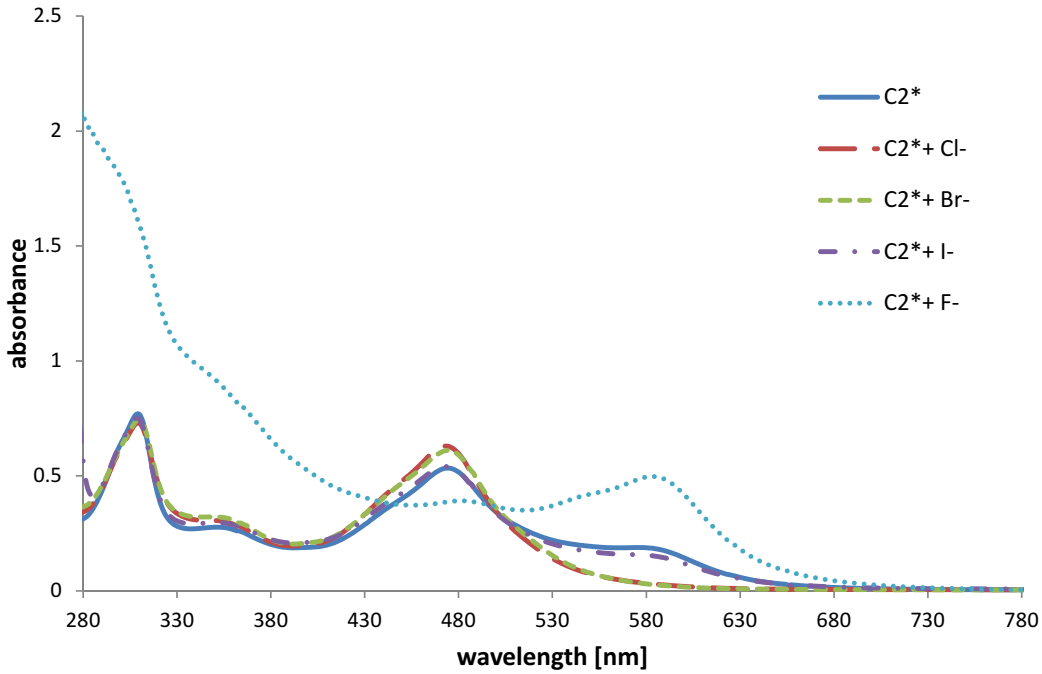

Figure 3.3: *Absorption spectra of* ***C2**** *with excess of TBA halide salts (MeCN, 1·10^{-5}M).*

Titrations of the complex **C2*** with TBA-F solutions were performed and monitored by absorption spectroscopy. As solvents, MeCN and CH_2Cl_2 were used. The spectra of the titration in MeCN are shown in *Fig. 3.4*. Based on the obtained values dissociation constants K_d were calculated by *Dr. Colin J. Martin* using WinEQNMR2 (version 2.00 by *Michael J. Hynes*[90]). The equilibrium constant was calculated according to *K.Hirose*[91] for a logarithmic fitting process. The output of this fit was used as input for a linear fit to determine the equilibrium constant for the reaction shown in *equation 2*.

For the measurements values of log K_d = 6.49 ± 0.05 (MeCN) and log K_d = 7.42 ± 1.15 (CH_2Cl_2) were obtained.

$$C2^* + F^- \rightleftarrows [C2^* \cdots F]^- \tag{2}$$

A colour change of the **C2*** solution was also observed upon addition of acetate and hydroxide anions. Hence titrations with TBA-Ac were performed, also using MeCN and CH_2Cl_2 as solvents. The titration was again monitored by absorption spectroscopy and the spectra of the MeCN titration are shown in *Fig. 3.5.* For acetate ions (*equation 3*), log K_d values of 7.58 ± 0.24 (MeCN) and 7.42 ± 0.34 (CH_2Cl_2) were calculated.

$$C2^* + AcO^- \rightleftarrows [C2^* \cdots AcO]^- \tag{3}$$

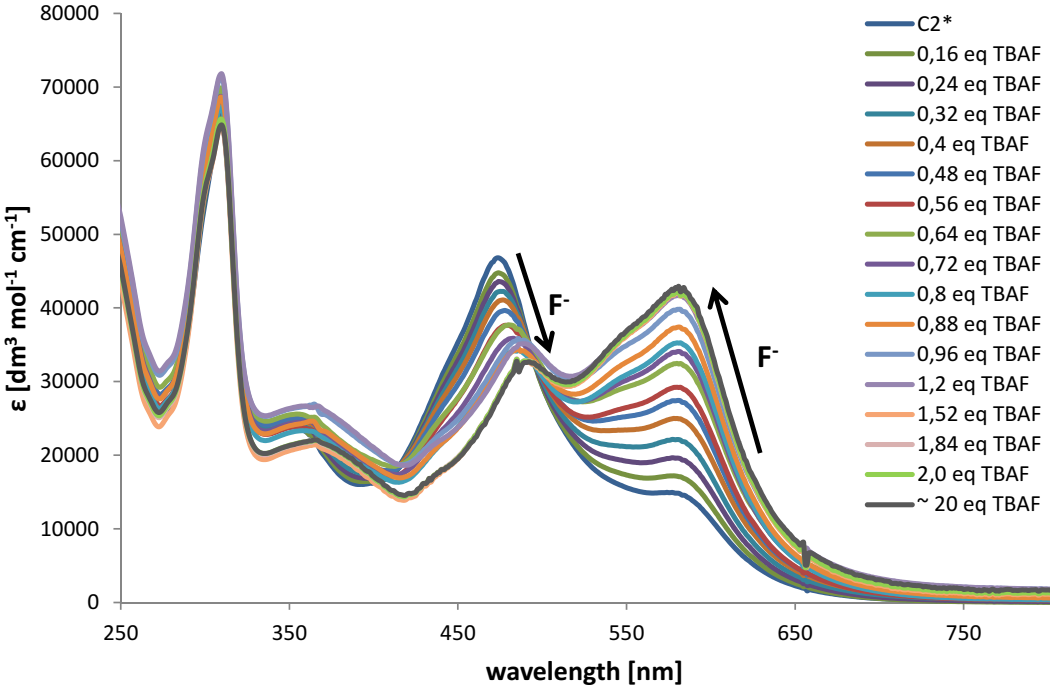

Figure 3.4: *Titration of* ***C2**** *with TBA-F in MeCN (2.5·10^{-5} M).*

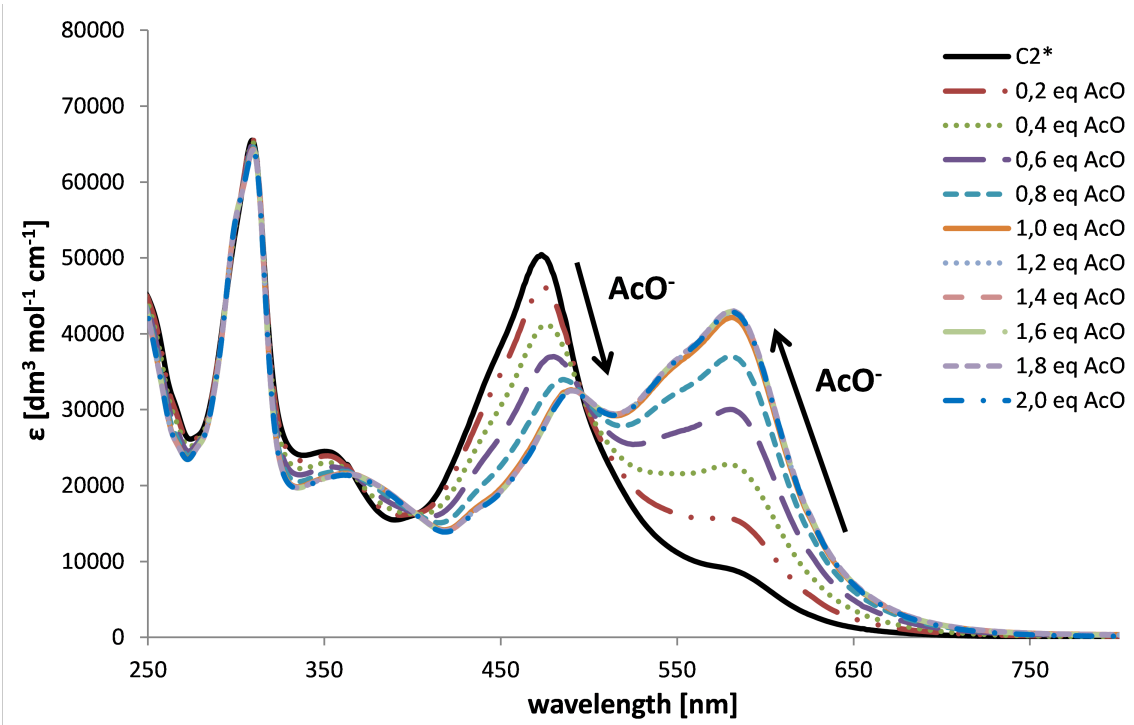

Figure 3.5: *Titration of* ***C2**** *with TBA-Ac in MeCN (2.5·10^{-5} M).*

Complex C4

In solution, the complex **C4** shows in the absorption spectrum a ligand-based maximum at 309 nm ($\varepsilon = 36200\ dm^3\,mol^{-1}\,cm^{-1}$) and a shoulder at 362 nm with $\varepsilon = 9600\ dm^3\,mol^{-1}\,cm^{-1}$. Both bands arise from $\pi^* \leftarrow \pi$ transitions. In between 420 nm and 500 nm, a broad MLCT transition can be observed. The maximum is at 473 nm ($\varepsilon = 13500\ dm^3\,mol^{-1}\,cm^{-1}$) with a shoulder at 440 nm ($\varepsilon = 11400\ dm^3\,mol^{-1}\,cm^{-1}$).

The complex was titrated with TBA-CN solution and the process was followed with absorption spectroscopy (*Fig. 3.7*). Only small changes were noticed during the addition of the cyanide salt. The maximum at 473 nm shows a decrease of the extinction from 13500 $dm^3\,mol^{-1}\,cm^{-1}$ to 11700 $dm^3\ mol^{-1}\ cm^{-1}$ whereas the maximum at 362 nm is red-shifted to 371 nm combined with an extinction coefficent increase from 9600 $dm^3\,mol^{-1}\,cm^{-1}$ to 11300 $dm^3\,mol^{-1}\,cm^{-1}$.

The addition of TBA-salts with Br^-, I^-, NO_2^- and HSO_4^- anions to **C4** caused no changes in the absorption spectrum. Upon addition of fluoride, acetate and hydroxide anions a different absorption behaviour was observed, as seen in *Fig. 3.8*. The maximum at 362 nm is red-shifted to 375 nm with an increase of the extinction (F^- : 11200 $dm^3\,mol^{-1}\,cm^{-1}$; AcO^-: 11600 $dm^3\,mol^{-1}\,cm^{-1}$; OH^-: 11400 $dm^3\,mol^{-1}\,cm^{-1}$). The MLCT at 473 experiences a blue-shift of almost 40 nm to 343 nm with an extinction of 13200 $dm^3\,mol^{-1}\,cm^{-1}$ (F^-) and 13100 $dm^3\,mol^{-1}\,cm^{-1}$ (AcO^-/OH^-).

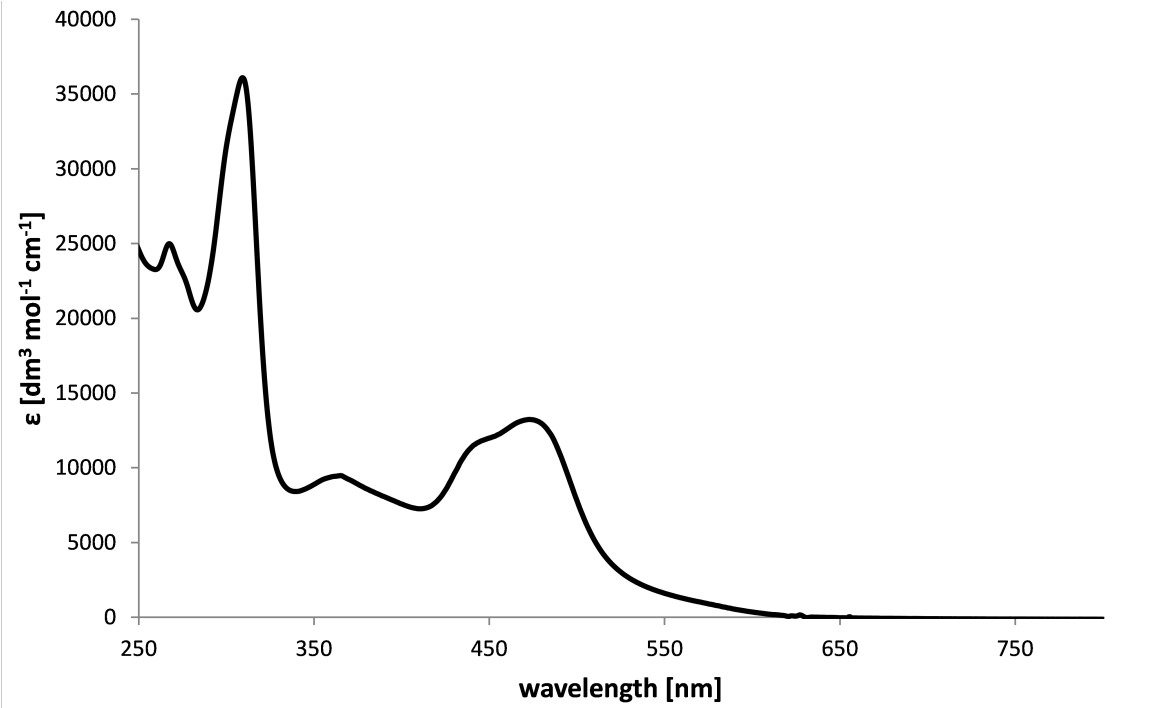

Figure 3.6: *Solution absorption spectrum of* ***C4*** *(MeCN, 2·10^{-5}M).*

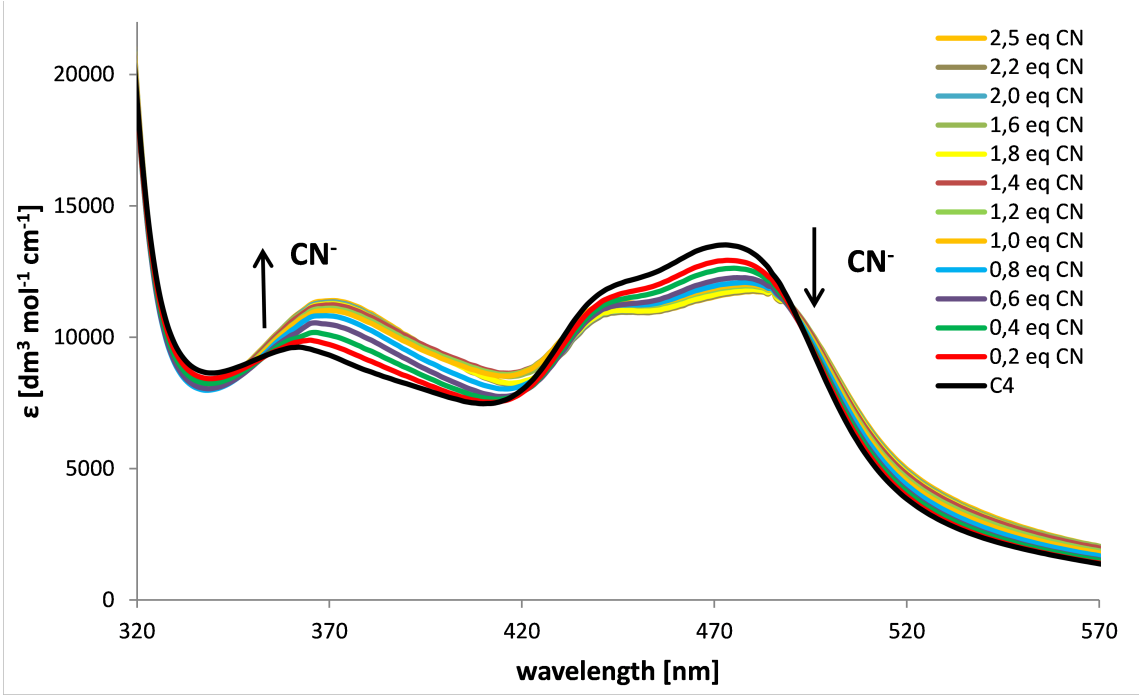

Figure 3.7: *Titration of* ***C4*** *with TBA-CN in MeCN (MeCN, 2·10^{-5}M).*

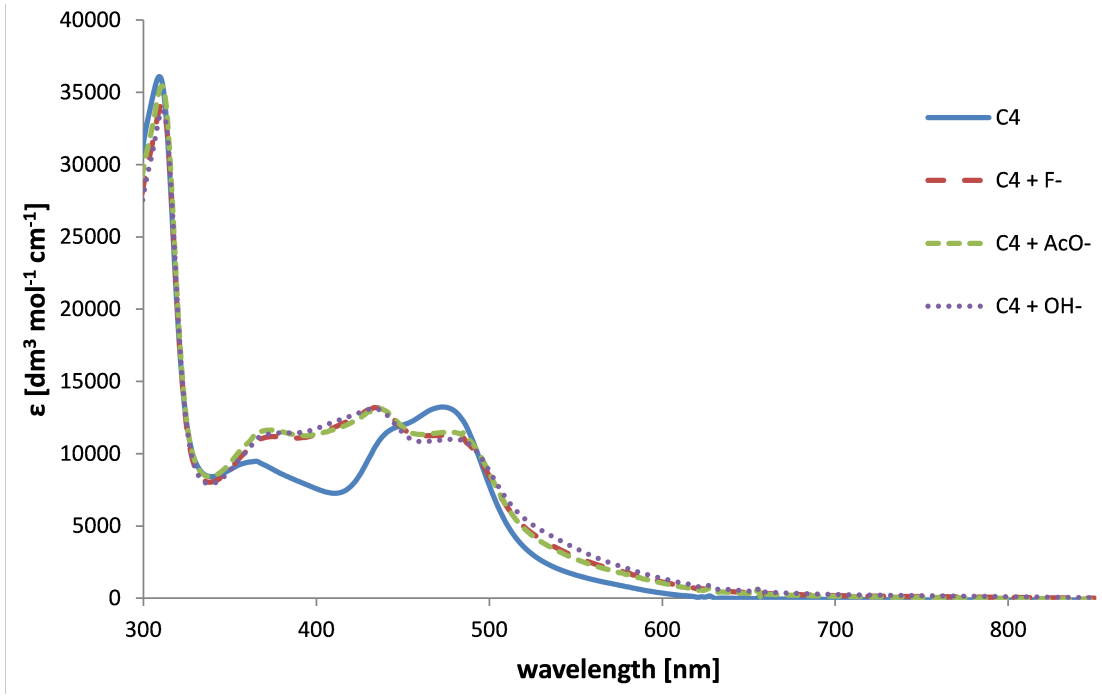

Figure 3.8: *Absorption spectra of* ***C4*** *with several TBA-salts (MeCN, $2 \cdot 10^{-5}$M).*

3.3.2 Photoluminescence

Complex C1

Solution emission spectra of **C1** with excitation wavelengths of 490 nm, 540 nm and 590 nm were recorded (*Fig. 3.9*). Excitation at 490 nm gives an emission maximum at 658 nm and a shoulder at 703 nm. With 540 nm as the excitation wavelength, a maximum at 707 nm and a smaller band at 653 nm are observed, whereas λ_{exc} = 590 nm gives only a maximum at 709 nm. For the homoleptic complexes $[Ru(pytpy)_2][PF_6]_2$ and $[Ru(phtpy)_2][PF_6]_2$, emission maxima at 655 nm,[89] and at 715 nm[92] respectively, were found in the literature. This suggests that the emission spectrum of **C1** is a superposition of two emissions, based on the different ligands.

Addition of HCl to a solution of **C1** leads to a red-shift of the maximum to 723 nm and a strong increase in the intensity (*Fig. 3.10*). This is in agreement with the literature, where an increase in intensity and an emission maximum of the mono-protonated complex $[Ru(pytpy)(Hpytpy)]^{3+}$ at 723 nm is reported.[89] Titrations with NaCl-solution were conducted to prove that the chloride anions have no influence on the results. Upon addition of up to 1.2 equivalents of NaCl, no changes of the maximum were observed. Reversibility of the protonation was proven by addition of solid K_2CO_3 after the addition of acid. The maximum and the intensity returned to their initial values.

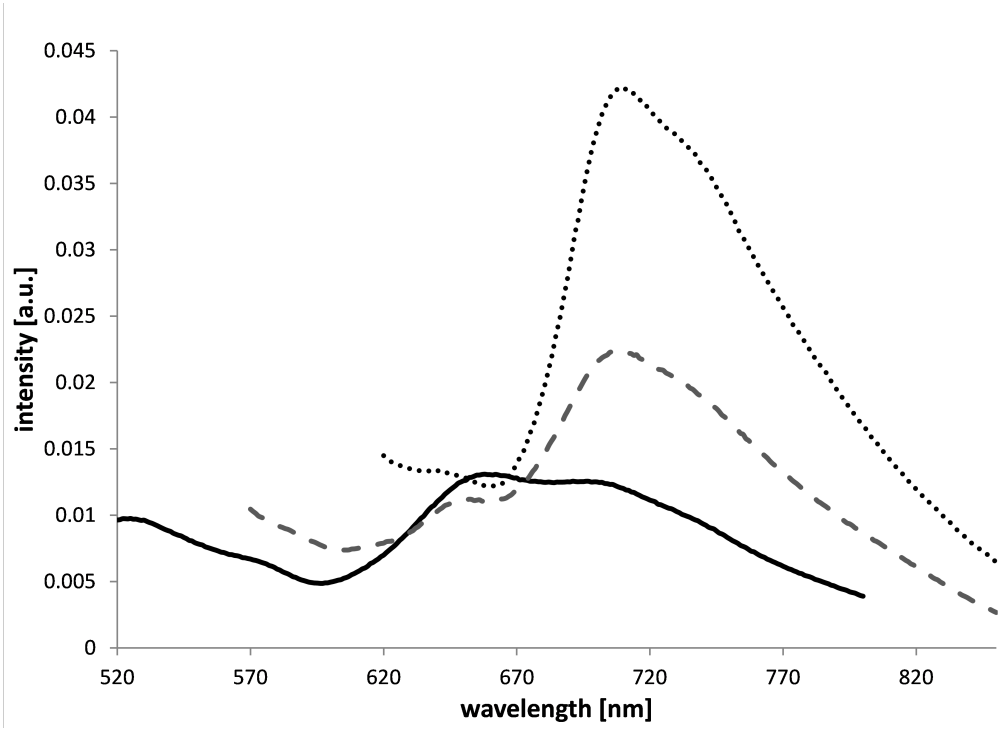

Figure 3.9: *Solution emission spectra of* ***C1*** *in MeCN with* λ_{exc} *= 490 nm (solid line),* λ_{exc} *= 540 nm (dashed line),* λ_{exc} *= 590 nm (dotted line).*

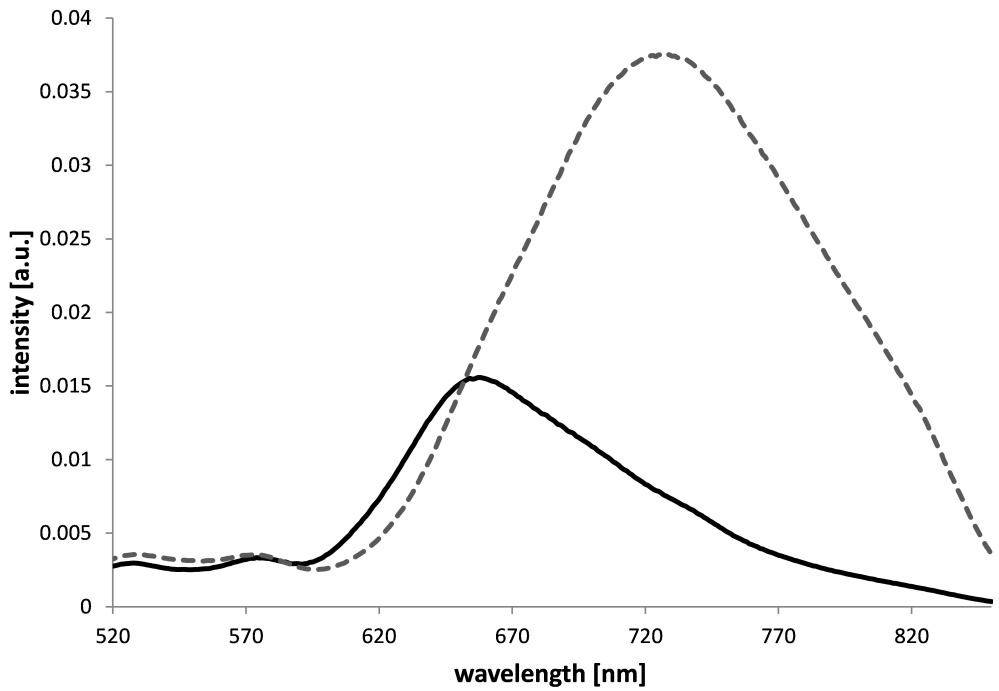

Figure 3.10: *Solution emission spectra of* ***C1*** *before (solid line) and after (dotted line) addition of HCl (MeCN, λ_{exc} = 490 nm).*

Complex C2*

The solution emission spectra of **C2*** were recorded at three different excitation wavelengths (*Fig. 3.11*). With λ_{exc} = 309 nm, the maximum was found at 630 nm. Excitation with 474 nm and 575 nm showed maxima at 643 nm and 648 nm, respectively. Titrations with TBA-F were performed to examine the effects of fluoride anions on the photoluminescent properties of the complex **C2***. The emission spectra were recorded with the excitation wavelengths as mentioned before. Emission enhancement upon addition of F^- was observed, independent of the excitation wavelength. With λ_{exc} = 474 nm, also a continuous shift of the maximum towards longer wavelengths was observed. The emission maximum for **C2*** with 2.6 eq. TBA-F is found at 657 nm, a red-shift of 13 nm. The spectra of this titration are shown in *Fig. 3.12*. Up to 2.6 equivalents of fluoride, no saturation of the emission intensity was observed. Only after addition of a huge excess of 22 equivalents, an intensity decrease was observed, presumably due to quenching. The increase of the emission intensity is linear. This is shown by plotting the maximum intensity vs. equivalents of F^- (*Fig. 3.13*). The R^2 value displays how good the linear regression fits to the experimental data. For λ_{exc} = 474 nm, a pseudo-linear increase with a R^2 value of 0.9922 (*Fig. 3.13*) was obtained, whereas λ_{exc} = 309 nm yielded an R^2 value of 0.95.

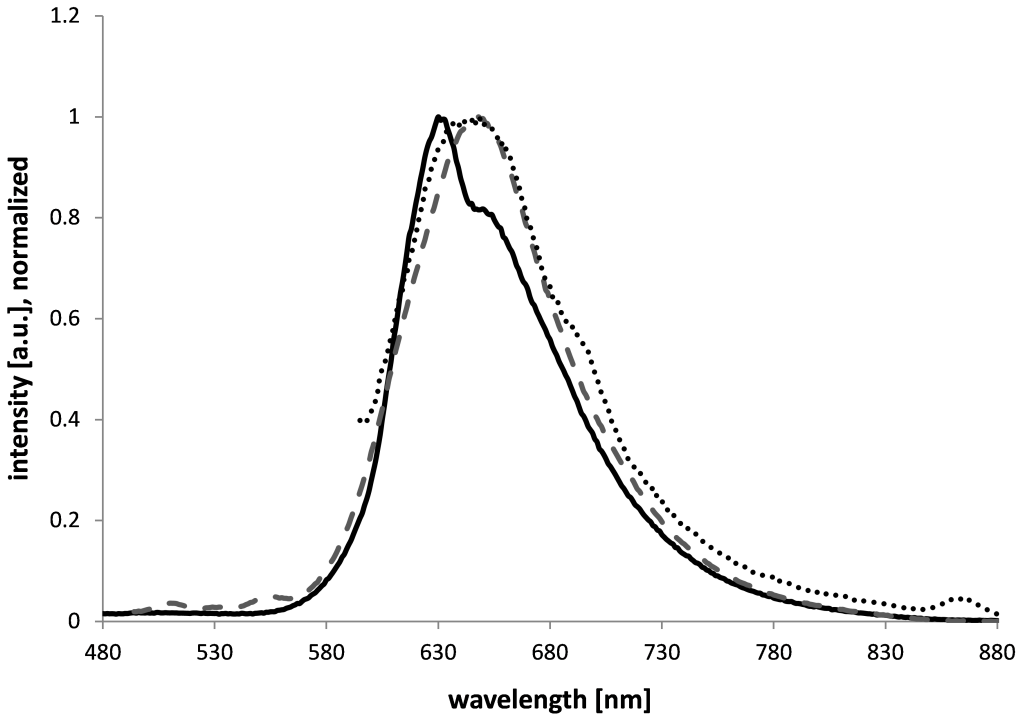

Figure 3.11: *Emission spectra of* ***C2**** *(MeCN), excited at different wavelengths,* λ_{exc}*= 309 nm (solid line),* λ_{exc}*= 474 nm (dashed line),* λ_{exc}*= 575 nm (dotted line).*

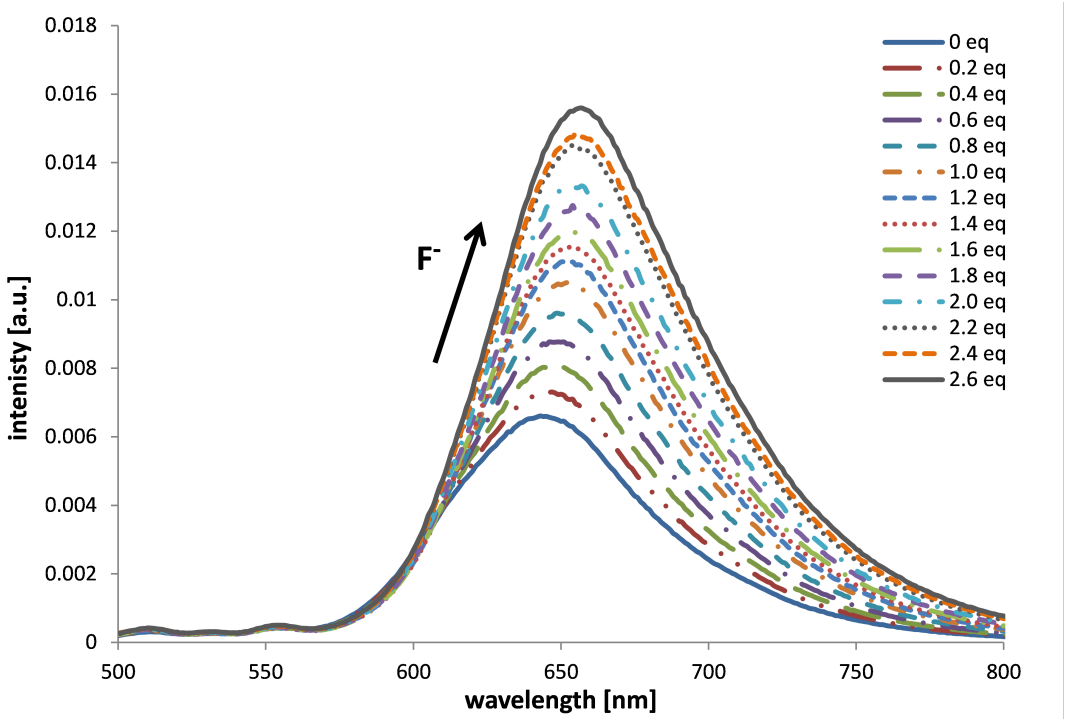

Figure 3.12: *Titration of* ***C2**** *with TBA-F in MeCN* (λ_{exc} *= 474 nm).*

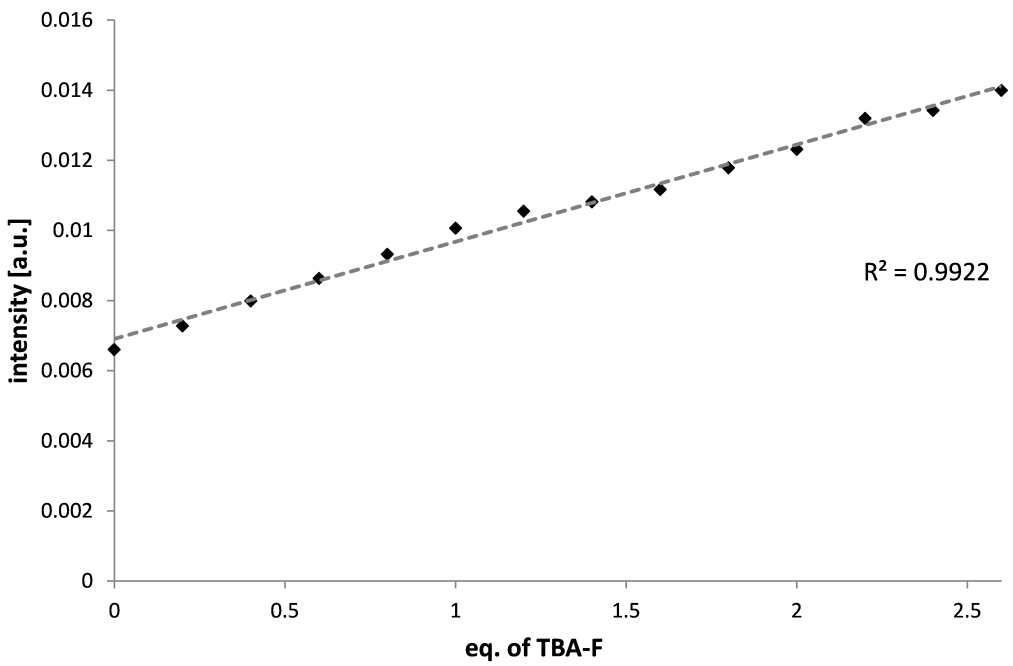

Figure 3.13: *Increase of emission intensity of* ***C2**** *during TBA-F addition (* λ_{exc} *= 474 nm).*

Complex C4

Emission spectra with two different excitation wavelengths (λ_{exc} = 280 nm and 485 nm) were recorded for the complex **C4**. With both wavelengths the same emission maximum at 652 nm was obtained. The influence of different anions on the photoluminescence properties of the complex were investigated by adding four equivalents of the TBA-salt to a solution of **C4** (MeCN, $2{\cdot}10^{-5}$ M) and emission spectra with an excitation wavelength of 485 nm were meassured (*Fig. 3.14*). No significant effects were observed, aside from an intensity decrease for some anions. When cyanide is added to a solution of the complex, small changes in intensity and a slight red-shift of 3 nm during the addition of TBA-CN were observed (*Fig. 3.15*). As these changes show no consistency, no clear conclusion can be drawn if these changes are real, just dilution effects or measuring errors.

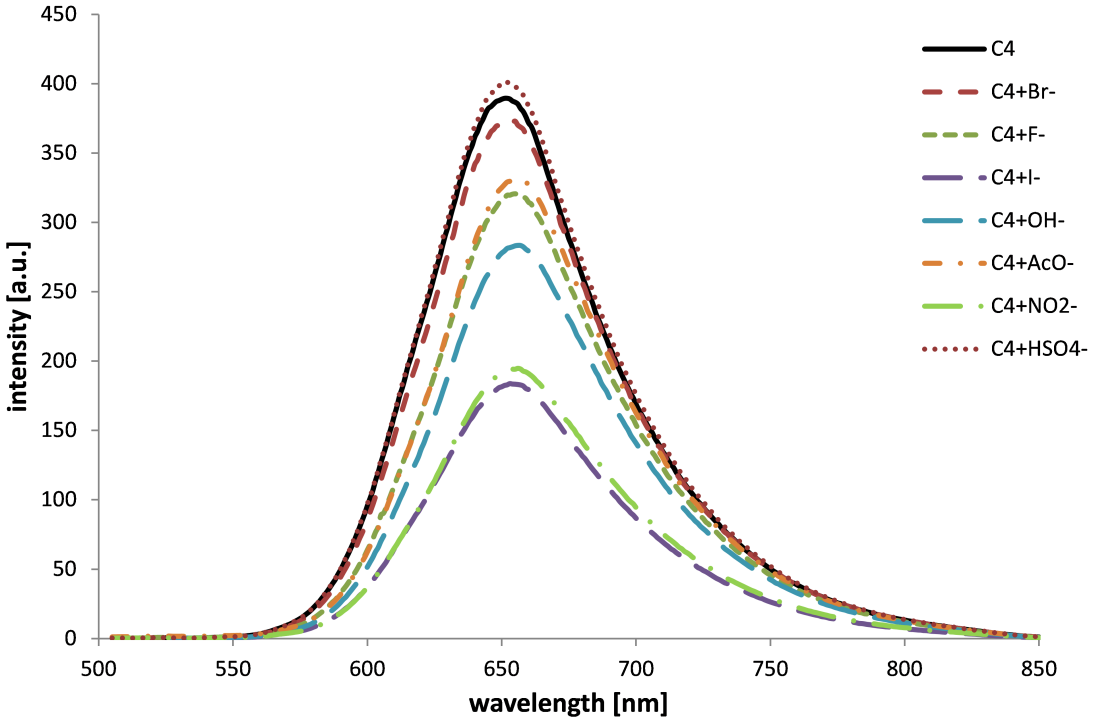

Figure 3.14: *Emission spectra of* ***C4*** *with 4.0 eq. of different TBA salts (λ_{exc} = 485 nm, MeCN, $2{\cdot}10^{-5}$ M).*

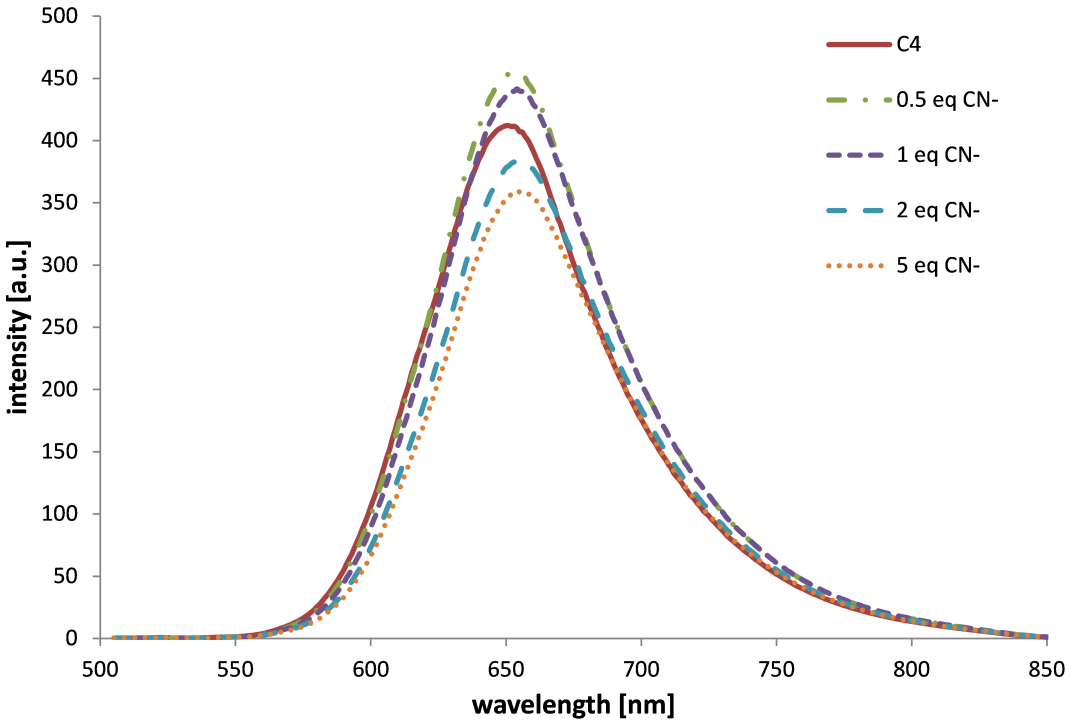

Figure 3.15: *Emission spectra of* ***C4*** *upon additon of TBA-CN (MeCN,* λ_{exc} *= 485 nm).*

Complex C5

Photoluminescence spectra of the complex **C5** are presented in *Fig. 3.16*. The emission spectrum with an excitation wavelength of 485 nm shows a maximum at 660 nm. The same results were obtained with λ_{exc}= 500 nm. The excitation spectrum was measured with λ_{em}= 660 nm. The main contributions to this emission were found at 274 nm and 484 nm with a smaller contribution at 574 nm. The effects of cyanide anions on the complex **C5** and its emission properties were examined (*Fig. 3.17*). Addition of TBA-CN causes a small blue-shift of 3 nm combined with an intensity decrease.

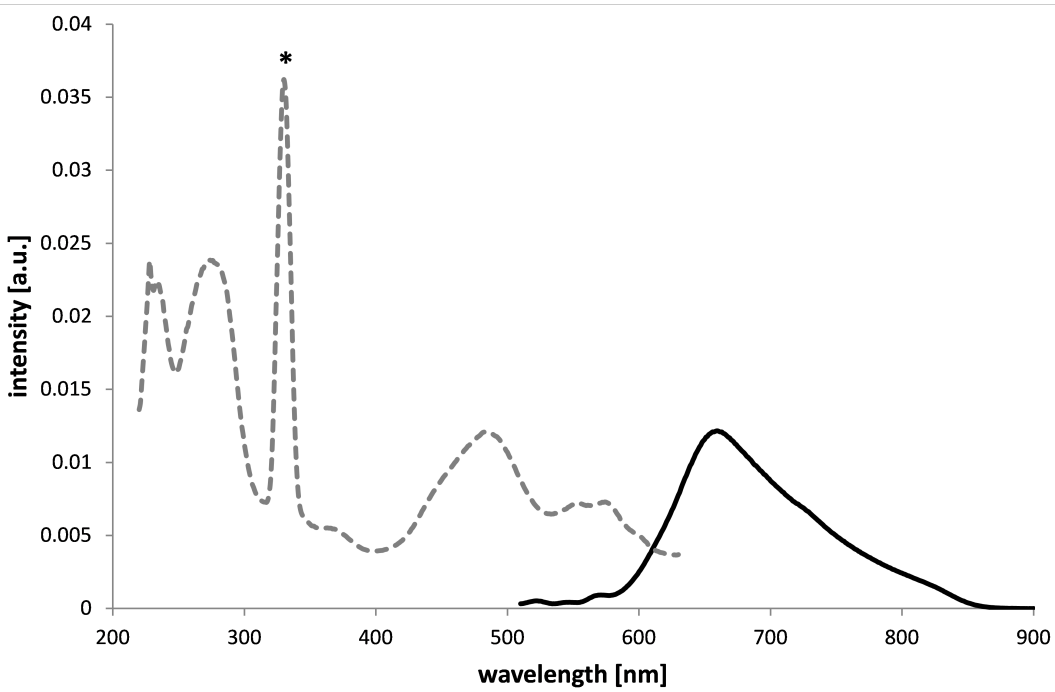

Figure 3.16: *Solution emission and excitation spectra of* ***C5*** *(MeCN, λ_{exc} = 485 nm, λ_{em} = 660 nm, * = secondary).*

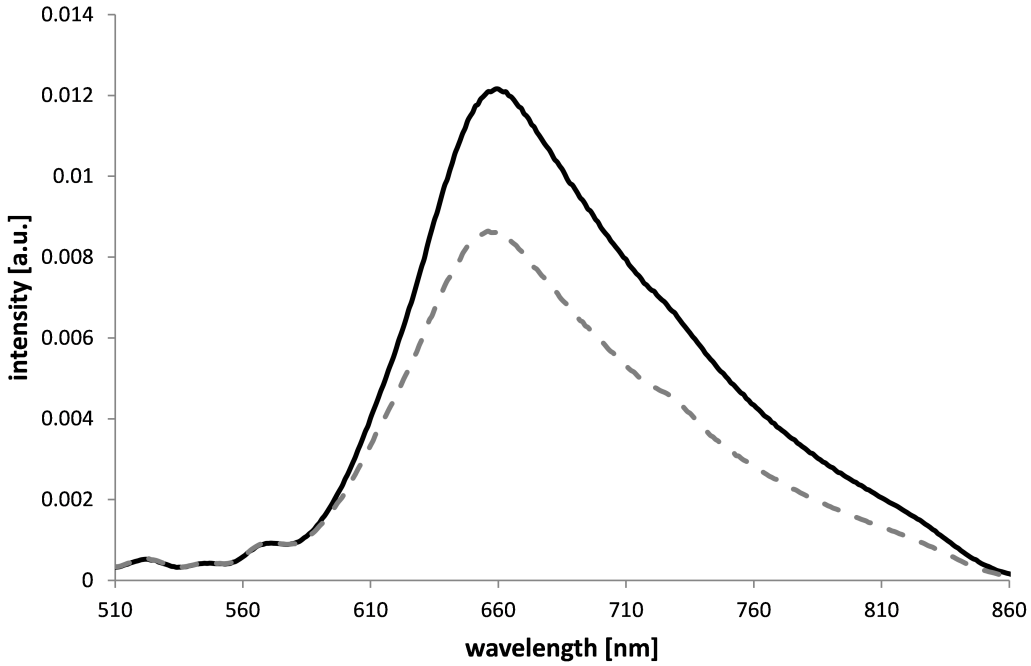

Figure 3.17: *Emission spectra of* ***C5*** *before (solid line) and after addition (dashed line) of TBA-CN (MeCN, λ_{exc} = 485 nm).*

3.4 Concluding remarks

3.4.1 Complex C1

The complex **C1** was tested towards its properties as a proton sensor. In the electronic absorption spectra, a clear difference between before and after addition of excess H^+ to the complex can be observed (*Fig. 3.2*). But the first shift of the maximum occurs after 2 equivalents of acid and in the further course the shift is not proportional to the concentration of H^+. So, absorption spectroscopy is not a suitable method for monitoring the H^+-concentration with **C1**.
In the photoluminescence spectra the addition of protons causes an intensity increase and a red-shift of the maximum to 723 nm, which is in good accordance with the literature.[89] The intensity enhancement and the red-shift could be observed for both excitation wavelengths 490 nm and 540 nm. Intensity saturation was observed at approximately 3 equivalents. The protonation is reversible, which was shown by the addition of excess K_2CO_3. **C1** shows a quite sensitive response to protons in photoluminescence spectroscopy. This could be a method for monitoring proton concentration using **C1** as detector.

3.4.2 Complex C2*

The complex **C2*** was synthesized as a model compound without anchoring groups. It is supposed that all results are transferable to the detection complexes **C2** and **C3** with anchoring moieties.
When halide salts were added to a solution of this compound, the absorption spectra showed only significant changes for fluoride. The intensity of the band at 474 nm decreases and the intensity of the MLCT band is strongly increased, causing a colour change from red to purple. These observations are consistent with the published data about this ligand.[82] *Bai et al.* also report that no changes were observed for the other halides or anions including HSO_4^-, NO_3^- and $H_2PO_4^-$. The proposed binding mode of F^- to the detection ligand **L5** is shown in *Scheme 3.3*. Without anions, the ligand can be seen as a quinonehydrazone, in which the keto oxygen and the N-H hydrogen undergo hydrogen bonding thus forming a six-membered ring. If fluoride is added, a partial proton transfer to the fluoride occurs which leads to a bond rearrangement. It is assumed that the band at 576 nm is caused by a charge transfer of the newly formed azophenol-ligand.[81]

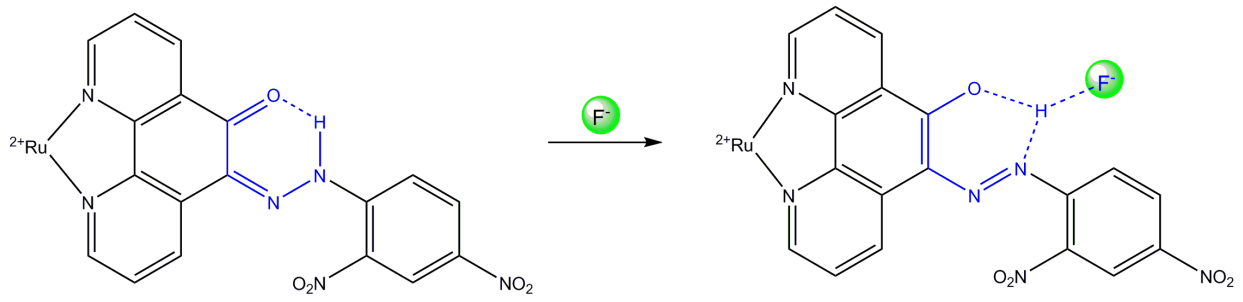

Scheme 3.3: *Proposed mode of anion binding of L5.*[81]

In the UV-Vis titration experiments, saturation was observed at 1.0 equivalent. This indicates that one detection ligand interacts with only one anion. To prove this 1:1 stoichiometry, several measurements were performed and presented as a *Job's plot*[93] (*Fig. 3.18*). The fact, that there are two different lines with a angular point at a molar fraction of 0.5 is a strong argument for the proposed 1:1 stoichiometry. Comparable results were obtained by *Lin et al.*[82] Also the calculated stability constants in MeCN with log$K$ being 6.23 ± 0.03[81] are of the same magnitude as the values we obtained (log K_d = 6.49 ± 0.05). Additional measurements were carried out using CH_2Cl_2 as solvent. This was done to gain an insight into the influence of the solvent. No significant changes in the shape of the curves were observed. But stability issues of the salts were noticed, thus only freshly prepared solutions could be used. It is assumed that this degradation, caused by the acidity of the solvent, led to the big error in the calculated dissociation constant (log K_d = 7.42 ± 1.15).

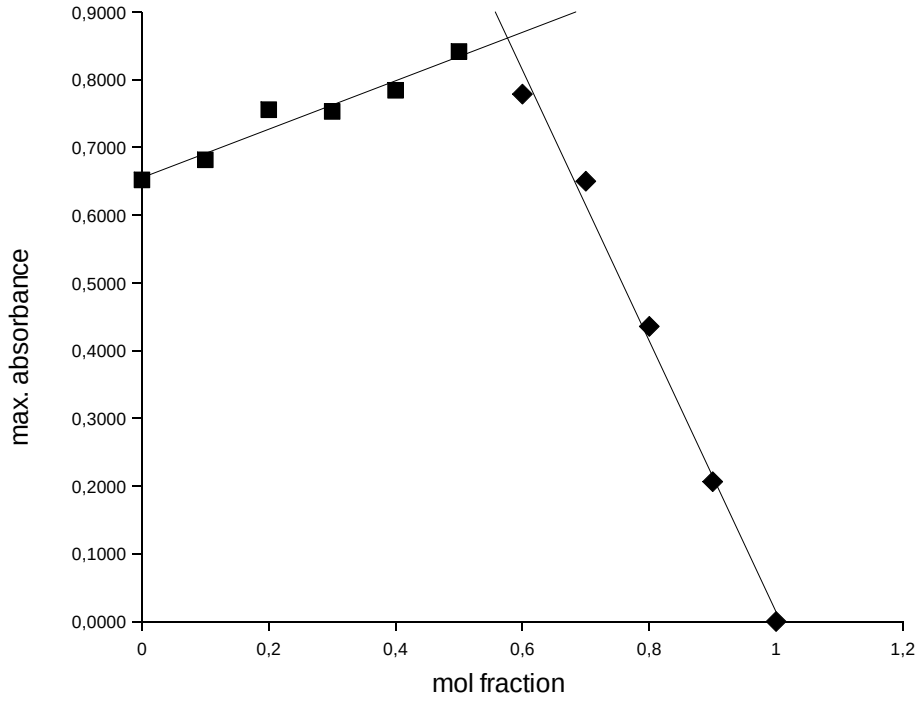

Figure 3.18: *Job's plot for the titration of* ***C2**** *with TBA-F in MeCN, data for maximum at 575 nm.*

In the emission spectrum, the addition of fluoride anions causes an increase in the intensity and leads to red-shifting of the maximum. This intensity gain seems to be linear, at least up to the tested 2.6 equivalents. The measurements were performed with two different excitation wavelengths (λ_{exc} = 309 nm and 474 nm) and comparable results were obtained. It is supposed that the presence of F^- ions enhances the rigidity of the complex and thus energy loss through non-radiative decay is

reduced. A second reason for the luminescent enhancement could be attributed to the deprotonation of the N–H group under the influence of the fluoride ion. This can weaken the luminescence quenching processes intensifying the luminescene.[82]

For related 2,4-dinitrophenyl-hydrazone-based molecules not only sensitivity with fluoride, but also with other anions have been reported.[94] For the compound, shown in *Fig. 3.19*, significant changes in the absorption spectra were observed upon addition of AcO^-, $H_2PO_4^-$ and F^-. Affinity constants were calculated for the anions and the highest affinity was found for AcO^-.

For the complex **C2*** similar results were obtained. The titrations with TBA-Ac showed the same changes of the absorption spectra as with TBA-F and here also a 1:1 stoichiometry can be assumed from the obtained data. This is in accordance with the results from *Shao et al.*[94] **C2*** shows also a higher affinity to acetate than to fluoride, indicated by the higher log K_d values of 7.58 ± 0.24.

The titration experiments also showed a colour change during the addition of hydroxide anions. It can be assumed, that this is caused by the same reasons as for fluoride. Hydroxide is a small ion with a high charge density, like fluoride. So it is reasonable that it can interact in the same way with the ligand.

In summary, **C2*** was synthesized, characterized and several measurements were performed. As reported, the ligand **L5** acted as a detector for fluoride and acetate and the results were in good agreement with the literature.[81, 82, 94] No significant differences were noticed between the performance of **C2*** and the complex with 2,2′-bipyridine as ancillary ligands, reported by *Lin et. al.*[81] So it was assumed that the ancillary ligands have no influence on the sensing properties of the complex and further investigations with the complexes **C2** and **C3** were omitted.

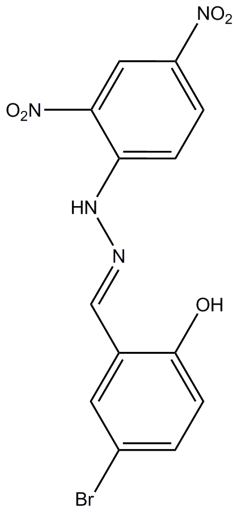

Figure 3.19: *A 2,4-dinitrophenyl-hydrazone-based compound with strong interaction with acetate ions.*[94]

3.4.3 Complex C4

The complex **C4** was synthesized as a detector for cyanide ions. It is reported that the aldehyde groups on the phenanthroline ligand interact with the CN^- ions and cyanohydrins are formed.[83] This should eliminate the interference with other reactive ions like fluoride, acetate or hydroxide. Titration of **C4** with TBA-CN showed in the absorption spectra similar changes to those reported for the complex with two 2,2′-bipyridine ancillary ligands. Other anions like F^-, AcO^- and OH^- induced a change in the UV-Vis spectra, which contrasts with the results reported by *Schmittel et al.*[83] For complex **1** and **2** (*Fig. 3.20*), no interaction with other ions was observed.

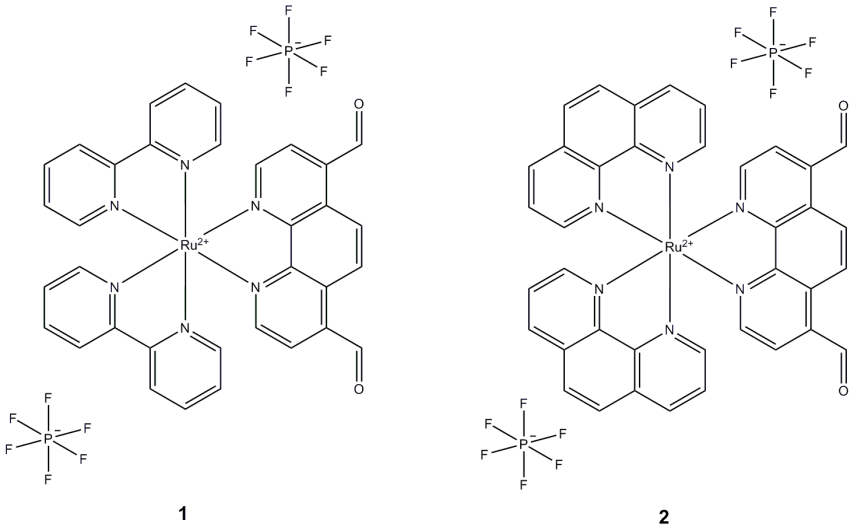

Figure 3.20: *Cyanide detection complexes **1** and **2**, reported by Schmittel et al.*[83]

In the emission spectra no significant changes were noticed upon addition of different anions. Adding TBA-CN to a solution of **C4** gave no strong enhancement, which is again in contrast to the report by *Schmittel et al.*[83] for their complexes. An explanation for this could be found in the calculated MO compositions (*Fig. 3.21*). For the complex **1** with bpy as ancillary ligand (*Fig. 3.20*), the LUMO and LUMO+1 are almost completely located on the PDA ligand. If the aldehyde is converted into the cyanohydrin, the orbital distribution changes and large parts of the MOs are located on the ancillary ligands. The HOMO is based for both complexes on the metal center (*Fig. 3.21*). It is assumed that the observed strong blue shift for compounds **1** and **2** is caused by an MLCT switch from Ru(II) → PDA to Ru(II) → bpy/phen upon addition of cyanide.[83] The complexes **1** and **2** show emission at 732 nm, whereas the emission maxima of the cyanohydrine complexes is at 624 nm and 614 nm, respectively. These values are comparable with the emission maxima of the homoleptic complexes at 615 nm[95] and 596 nm.[96]

The introduction of EWGs to the ancillary ligand can have a strong influence on the distribution and energy levels of the MOs. We assume that this is the reason for the different behaviour of

C4 compared to the complexes reported by *Schmittel et al.*[83] If the LUMO is already located on the anchoring ligand, the addition of cyanide ions may not necessarily cause a redistribution of the composition of the MOs and thus no MLCT switch can occur and no changes in the emission spectra are observed.

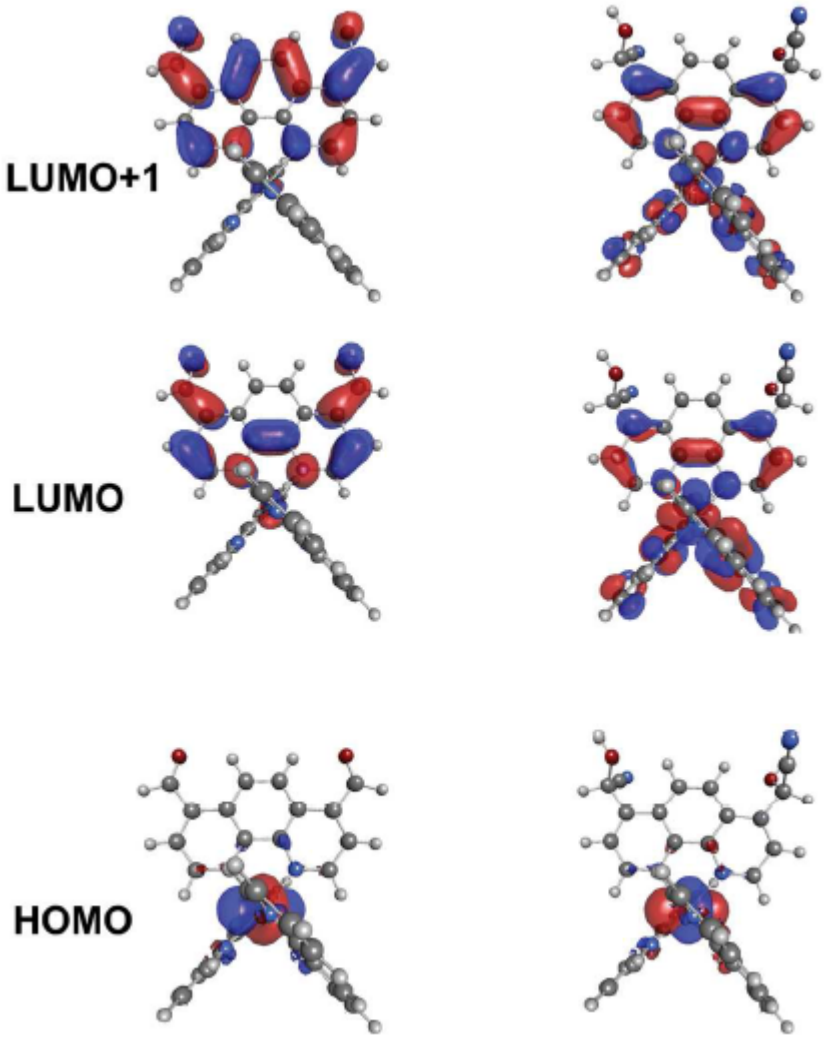

Figure 3.21: *Calculated MOs for [Ru(bpy)$_2$(PDA)][PF$_6$]$_2$ (left) and [Ru(bpy)$_2$(PDA-CN$_2$)][PF$_6$]$_2$ (right); DFT calculations with B3LYP/ 6-31G(d) for C, H, N and LANL2DZ for Ru as exchange correlation functional.*[83]

3.4.4 Complex C5

Complex **C5** shows similar properties as **C4** in the photoluminescence spectra. Addition of TBA-CN to a solution of the complex causes only a small blue-shift and a decrease in intensity. This indicates that here again the MO distribution on the complex with anchoring ligands is different to the one on **1** and **2** with unsubstituted ancillary ligands (*Fig. 3.20*). The ether bridge shows a weaker inductive (*-I*) and a stronger mesomeric (*+M)* effect, compared to the ester. But presumably the influence of this substituent is still too strong, so that the energy of the bpy-based MOs is lowered and the LUMO is located on the anchoring ligands and not, like in the complexes **1** and **2**, on the PDA-ligand (*Fig. 3.21*). With this MO composition, upon addition of CN^- no MLCT switch can occur, as described before (*section 3.4.3*).

3.5 Summary

In summary, six ruthenium complexes have been synthesized, characterized and tested towards their detection properties. Information read-out was investigated by absorption and photoluminescence spectroscopy. All tested sensing compounds were derivatives of known substances from the literature. Complex **C1** showed sensitivity towards protons, but the monitoring with photoluminescene spectroscopy cannot be done straightforward. Complex **C2***, bearing a fluoride-sensitive ligand, showed similar detection properties as reported in the literature.[81, 82] For monitoring the analyte concentration, both spectroscopic methods are suitable. Although the complex is quite selective towards F^-, comparable responses with two other anions were observed. The complexes **C2** and **C3** bear the same detector ligand as **C2***. Based on the obtained results, similar behaviour of these compounds as for **C2*** can be assumed. **C4** and **C5** are derived from a cyanide-sensitive compound from the literature.[83] Both complexes showed only slight changes upon addition of CN^-, unlike as reported. But a possible explanation for the different behaviour could be found. The structural changes from the literature complex **1** (*Fig. 3.20*) to **C4** and **C5** showed a bigger influence than expected.

4 Surface functionalization

4.1 Abstract

In this chapter several applications for the previously described anchoring ligands **L2** and **L4** (*Scheme 4.1*) are shown. Here the functionalization of TiO_2 surfaces with the ligands is described as well as the photophysical characterization of these surfaces (*section 4.2*). Possible applications of the terpyridine-based ligand as a detector for transition metal ions were investigated (*section 4.3*). Furthermore, gold nanoparticles (Au-NP) were synthesized, functionalized with **L2-S** and **L4-S** and examined by absorption and photoluminescence spectroscopy (*section 4.4*). **L2** was also used as ancillary ligand for three cyclometalated Ir(III) complexes (*section 4.5*).

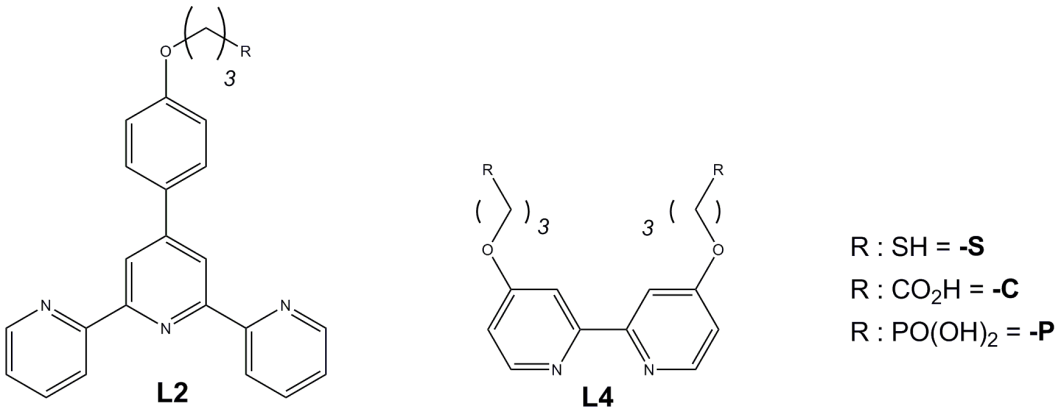

Scheme 4.1: *The anchoring ligands **L2** and **L4**.*

4.2 TiO_2

4.2.1 Preparation and functionalization of TiO_2 surfaces

TiO_2-coated FTO glass slides were prepared as previously described.[97] One layer of TiO_2-paste (DSL 90-T) was screenprinted onto FTO-glass, dried at 120 °C, sintered at 450 °C and had an area of approx. 0.28 cm^2. Functionalization of the TiO_2 surfaces was performed by dipping methods. Solutions of the ligands **L2-P**, **L2-C**, **L4-P** and **L4-C** (2.5 mM) in aqueous NaOH (pH 11) were prepared and for each, two TiO_2-coated FTO glass samples were immersed for a certain period of time. The slides were removed from the solutions and were washed with water, 0.1 M aqueous NaOH and again with water before drying in an air stream.
The ligand-functionalized TiO_2-samples were used for further complexation with transition metal ions. Aqueous solutions of $FeCl_2$ or $CoCl_2$ (10 mM) were dropped onto **L2**-functionalized samples, which led to an immediate colour change (Fe, purple; Co, yellow) of the initially colourless slides. Afterwards the samples were washed with water and dried.
L4-functionalized samples were treated first with a 10 mM aqueous $FeCl_2$ solution for 5 minutes and washed with water. The slides were then immersed in an acetone solution (10 mM) of either bpy or phen for 5 minutes, then removed and washed with acetone and dried. Persistence of a red colour indicated complex formation.

4.2.2 Photophysical properties

The solid state absorption spectroscopy was carried out in transmission mode. The samples were put in the light beam during the measurements. As a blank, a non-functionalized TiO_2 sample was used.

TiO_2 with ligand

Solid state absorption spectra of **L2** and **L4** functionalized TiO_2 surfaces were recorded. Absorption in the UV region was observed for all samples, but due to the background absorption of the TiO_2, no reliable results could be obtained.
In their solid state photoluminescence spectra, **L2-P** functionalized samples show an emission maximum at 359 nm upon excitation at 280 nm (*Fig. 4.1*). This is identical with the maximum obtained in solution (*section 2.3.2*). So there is no difference between emission of the free ligand in solution and bound on TiO_2. At the 366 nm-wavelength of a common laboratory UV-lamp the luminescence of the ligand can be seen by eye. So the coverage of the surface with the ligand after functionalization can be checked easily.
As the bypridine-based ligands **L4** are only weakly emissive, no solid state photoluminescence of the functionalized samples could be detected.

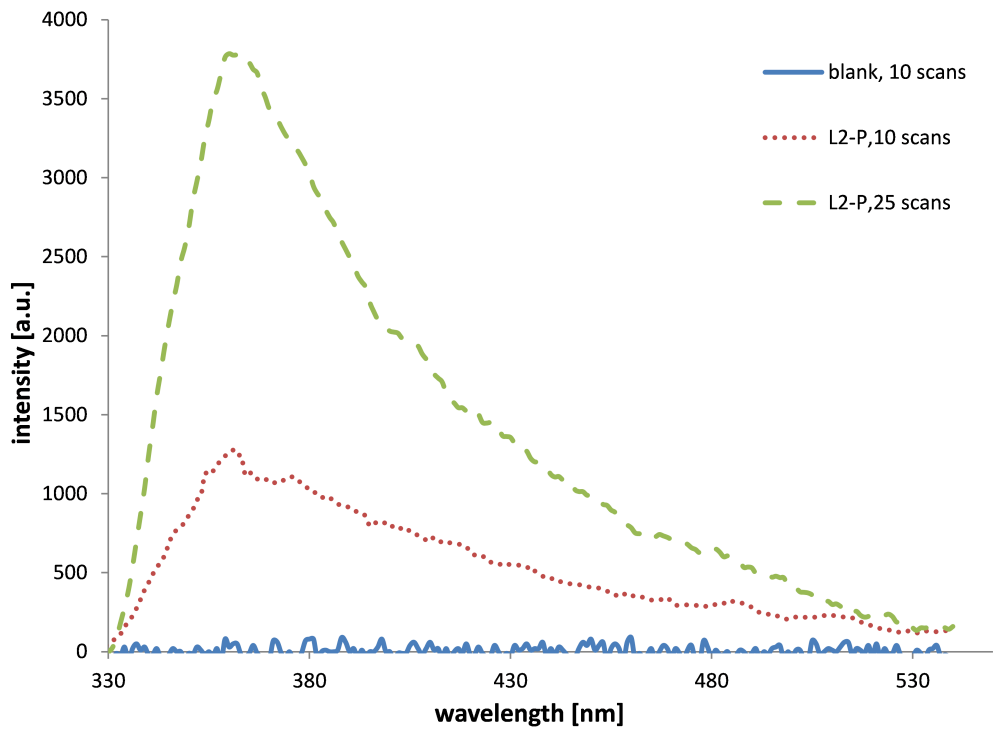

Figure 4.1: *Solid state emission of untreated and treated TiO_2, excitation at 280 nm.*

TiO_2 with metal complex

Fe(II) and Co(II) were used as metal ions because they yield coordination complexes with absorption in the visible region. Addition of aqueous $FeCl_2$ to the **L2**-functionalized samples caused an immediate colour change. Depending on the ligand used, a different colour was obtained. *Fig. 4.2* shows a picture of the samples. Solid state absorption spectroscopy showed an MLCT maximum at 577 nm for **L2-P** and at 594 nm for **L2-C**. For comparison, the homoleptic iron(II) complexes with the ligands **L2-PEt**, **L2-CMe** and **L2-C** were synthesized following the previous reported general procedure.[98] Purity was confirmed by ^{1}H-NMR spectroscopy. The solution absorption spectra of these complexes are displayed in *Fig. 4.3*. The maximum of the MLCT transition band for the three complexes is at 570 nm, demonstrating that the MLCT transition bands of the surface-bound complexes are red-shifted by 7 nm and 24 nm respectively.

Upon addition of $CoCl_2$ to a **L2**-functionalized sample, a colour change from colourless to yellow was observed. This indicates the formation of a complex.

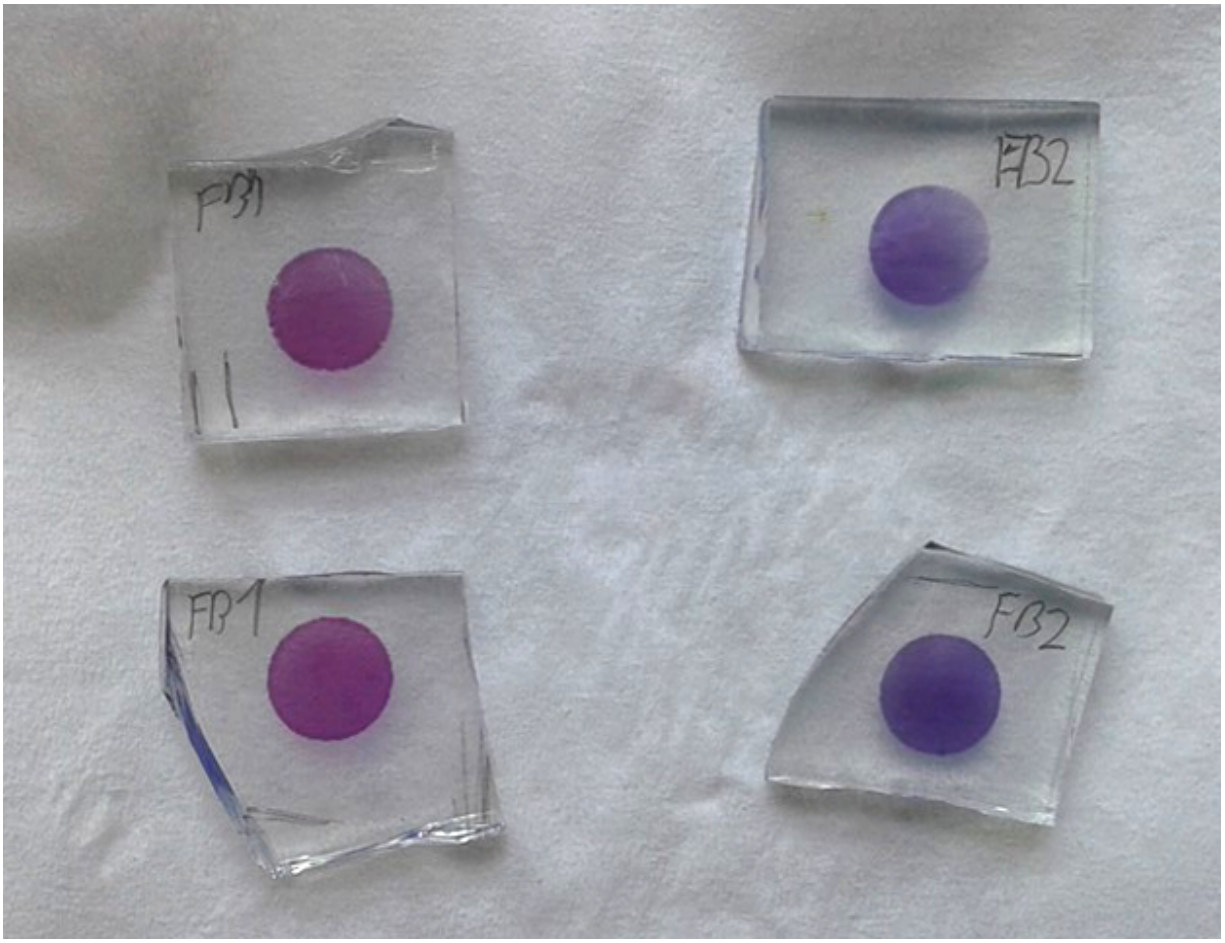

Figure 4.2: *Picture of TiO_2 samples functionalized with **L2-P** (left) and **L2-C** (right), after addition of $FeCl_2$.*

L4-functionalized samples show no colour change when aqueous $FeCl_2$ solution is applied. Only after the addition of another ligand, a change from colourless to red can be observed. From this, the formation of a heteroleptic complex on the surface can be assumed (*Scheme 4.2*). As capping units, different bidentate ligands such as **bpy, MeO-bpy** and **phen** were used. In the absorption spectra (*Fig. 4.4*) no significant differences between the ancillary ligands can be observed. All spectra show a broad absorption in the UV-region up to 360 nm which tails off into the visible range. The MLCT transitions are not observed due to their low extinction coefficients.

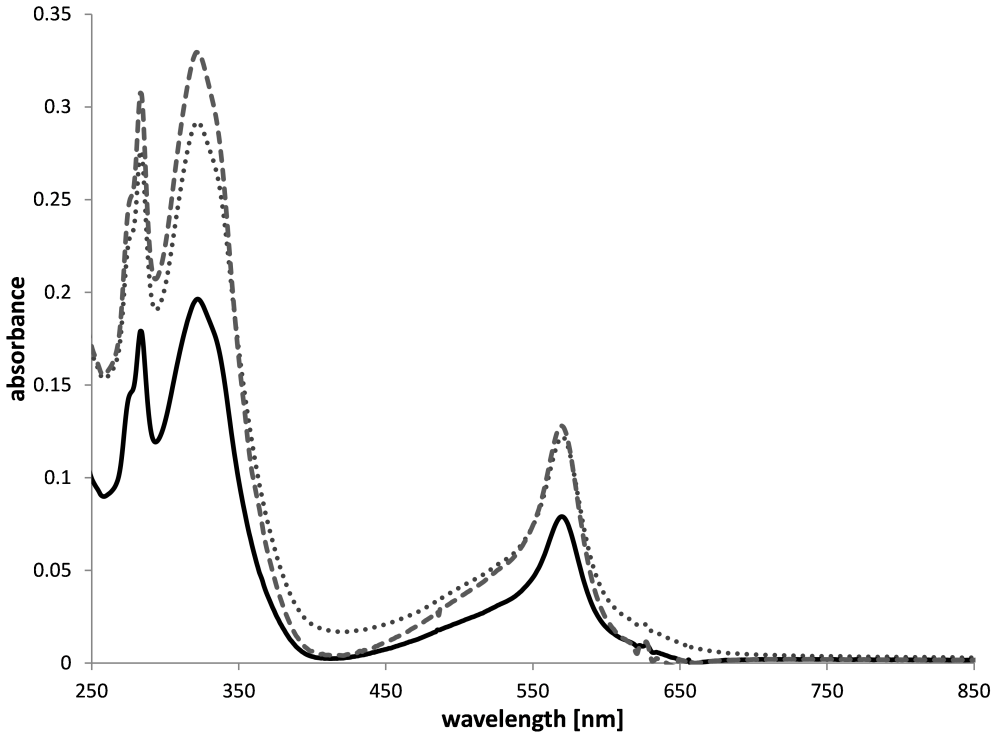

Figure 4.3: *Solution absorption spectra of the homoleptic complexes* ***[Fe(L2-PEt)$_2$][PF$_6$]$_2$*** *(solid line),* ***[Fe(L2-CMe)$_2$][PF$_6$]$_2$*** *(dashed line) and* ***[Fe(L2-C)$_2$][PF$_6$]$_2$*** *(dotted line) (MeCN).*

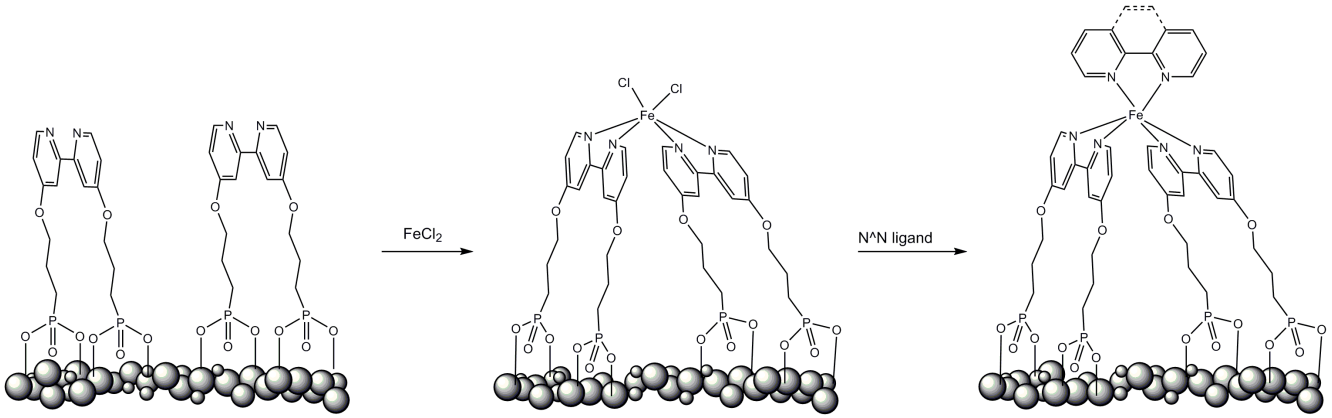

Scheme 4.2: *Scheme of the proposed processes on the TiO_2 surface upon addition of Fe(II) ions followed by addition of capping ligands.*

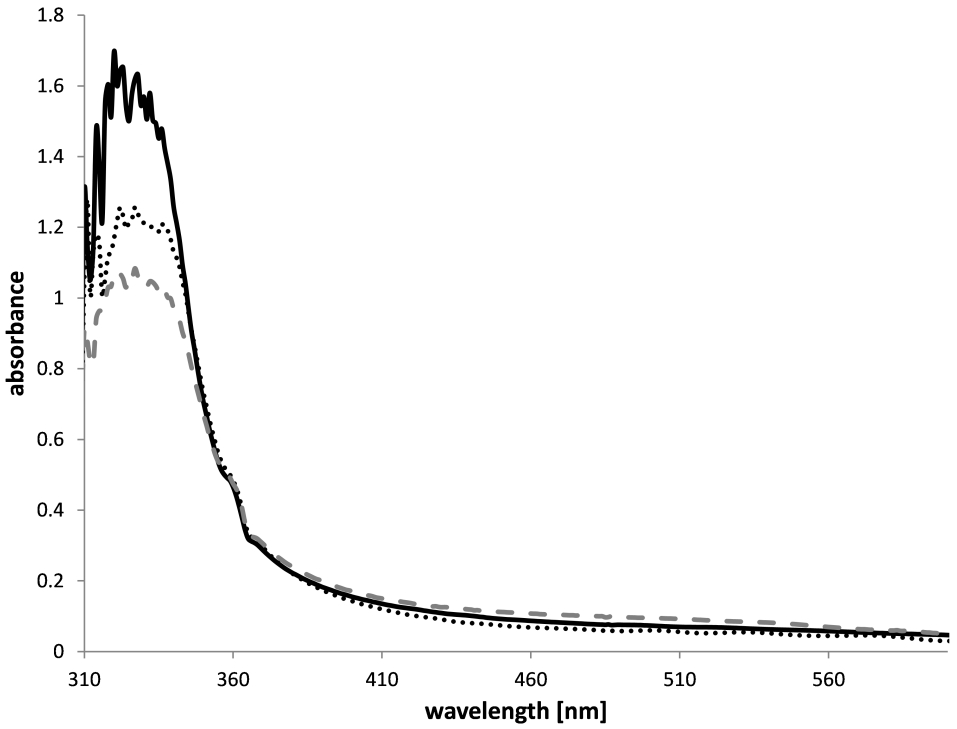

Figure 4.4: *Solid state absorption spectra of* ***L4-P*** *functionalized* TiO_2 *after addition of* $FeCl_2$*-solution and* ***bpy*** *(solid line),* ***MeO-bpy*** *(dotted line) and* ***phen*** *(dashed line) as ancillary ligand.*

4.2.3 Time dependence

The influence of the dipping time on the ligand loading on the surface was investigated for **L2**. Two samples were left in the dipping solution for one day, two days and three days. After addition of $FeCl_2$ solution, absorption spectra were recorded and the absorbance was compared. For **L2-P**, no significant difference between the dipping times can be observed (*Fig. 4.5*). Therefore it can be assumed that even after one day, the maximum ligand loading on the surface is obtained. Although for **L2-C** the measurements were performed several times, no consistent results have been obtained due to a broad background absorption over the whole spectrum (*Fig. 4.6*). Hence for this ligand no conclusion about the influence of the dipping time on the ligand loading can be made.

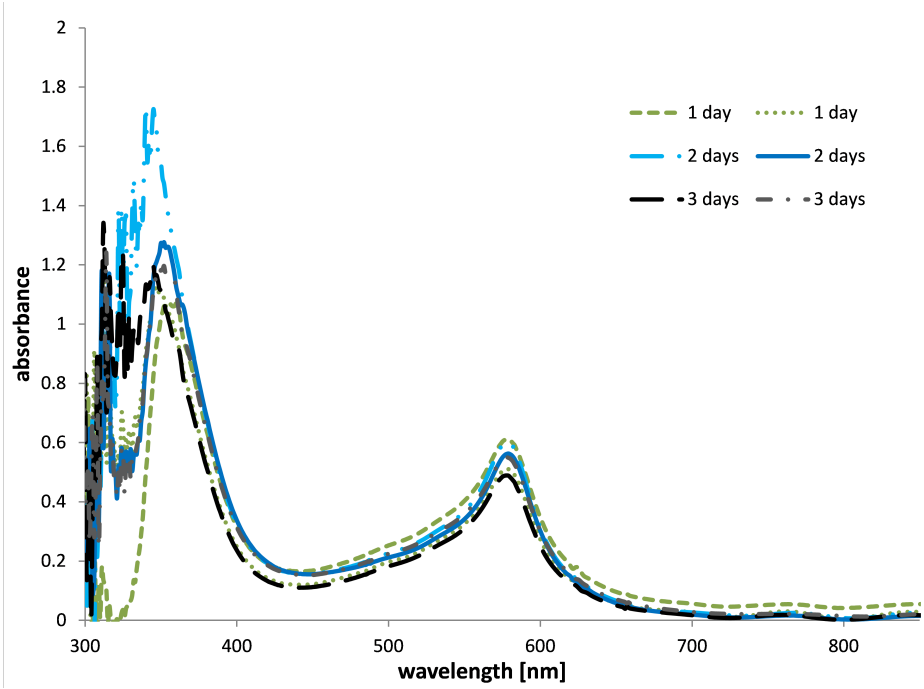

Figure 4.5: *Solid state absorption spectra of the* ***L2-P*** *functionalized and* $FeCl_2$*-treated* TiO_2 *samples with different dipping times.*

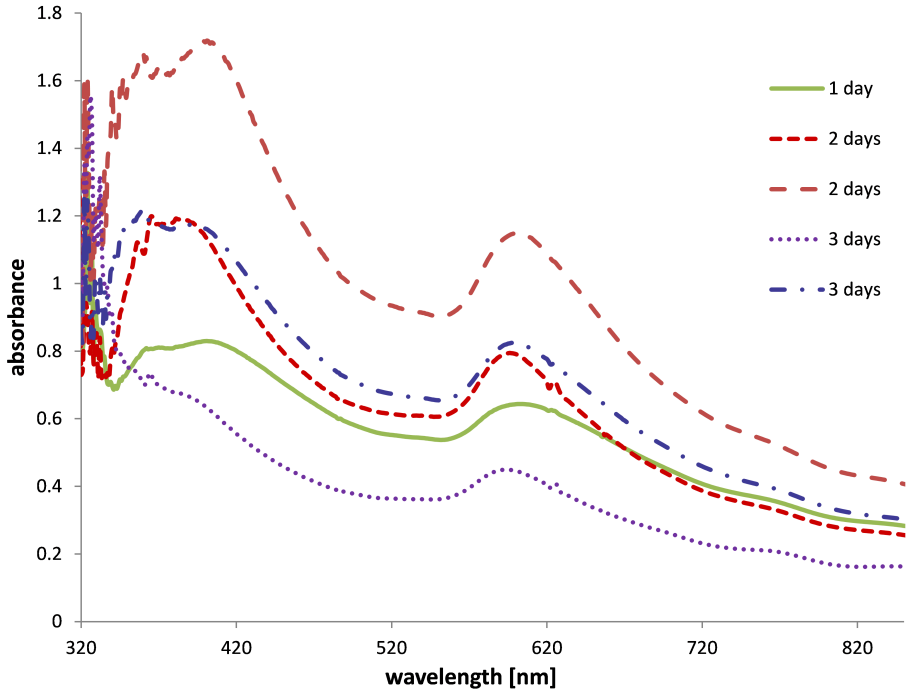

Figure 4.6: *Solid state absorption spectra of the* ***L2-C*** *functionalized and* $FeCl_2$*-treated* TiO_2 *samples with different dipping times.*

4.3 Metal ion sensing with MeO-tpy

Preliminary studies for a potential application as metal ion detector of the **L2**- functionalized TiO_2-samples, described in *section 4.2*, were performed. Homoleptic transition metal complexes with the model ligand 4′-(4-methoxyphenyl)-2,2′:6′,2″-terpyridine (MeO-tpy) were synthesized and characterized by absorption and photoluminescence spectroscopy. The metal ions Cd^{2+}, Co^{2+}, Cu^{2+}, Fe^{2+}, Mn^{2+}, Ni^{2+} and Zn^{2+} were used as chloride salts.

4.3.1 Complex synthesis

All complexes were synthesized following the same procedure. A 1 mM solution of MeO-tpy in MeOH was prepared. 10 ml of the ligand solution (10 µmol) and a metal salt solution (5 µmol in 5 ml water) were combined and stirred at room temperature for 30 min. NH_4PF_6 was added and the precipitate that formed was separated by centrifugation. The solid was suspended in water and separated by centrifugation. After drying in an airstream the complex was obtained as a solid.

4.3.2 Photophysical properties

The absorption and photoluminescence spectra were recorded in MeCN. In *Tab. 4.1*, the maxima for the different metal complexes are displayed. All complexes show two absorption bands in the UV-region. Both bands are ligand based and arise from $\pi^* \leftarrow \pi$ transitions. Only the complexes with Fe^{2+} and Co^{2+} show an MLCT transition in the visible region. The emission spectra were recorded with λ_{exc}= 290 nm (*Fig. 4.7*) and λ_{exc}= 330 nm (*Fig. 4.8*). With cadmium and zinc a strong blue emission at 460 nm was obtained at both excitation wavelengths. The Fe^{2+} complex showed an emission in the red region at 752 nm. The metal contribution to this emission is confirmed by the observation of a band at 588 nm in the excitation spectrum (*Fig. 4.9*). Attempts to measure the lifetime and quantum yield of this emission failed due to its weak intensity.

Metal ion	Max. absorbance	Max. emission (λ_{exc}= 290 nm)	Max. emission (λ_{exc}= 330 nm)
Cd^{2+}	283 nm / 330 nm	461 nm	460 nm
Co^{2+}	283 nm / 326 nm / 517 nm	399 nm	440 nm
Cu^{2+}	288 nm / 317 nm	427 nm	437 nm
Fe^{2+}	283 nm / 322 nm / 569 nm	389 nm / 752 nm	443 nm
Mn^{2+}	286 nm / 341 nm	390 nm	458 nm
Ni^{2+}	280 nm / 342 nm	420 nm	430 nm
Zn^{2+}	283 nm / 340 nm	462 nm	463 nm

Table 4.1: *Absorption and emission maxima of the homoleptic [M(MeO-tpy)$_2$][PF$_6$]$_2$ complexes.*

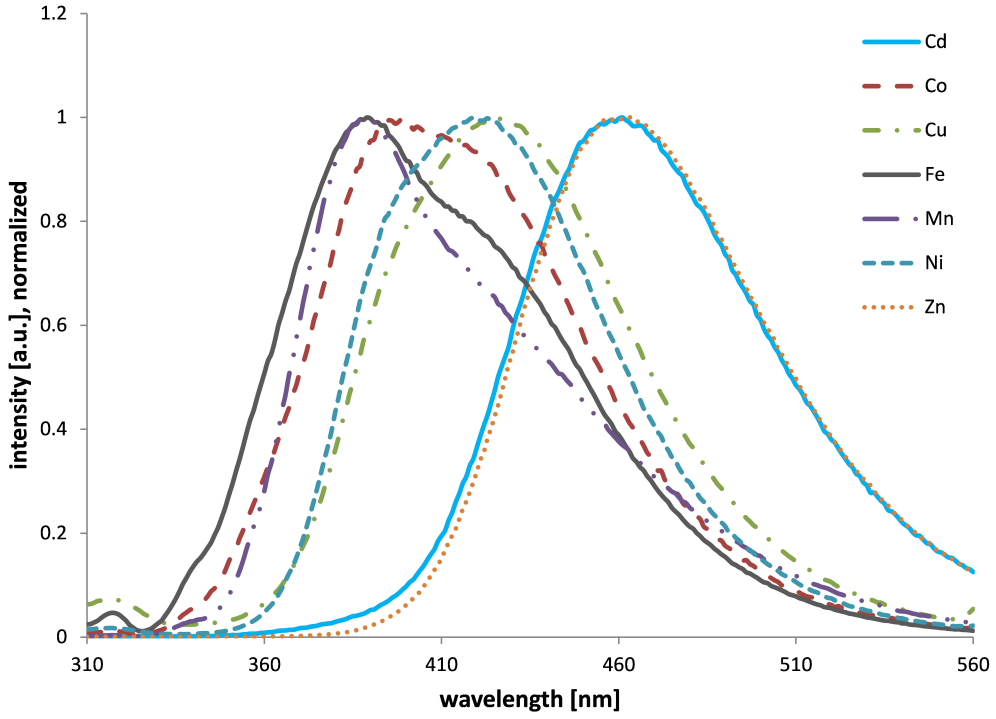

Figure 4.7: *Solution emission spectra of the homoleptic [M(MeO-tpy)$_2$][PF$_6$]$_2$ complexes. (MeCN, λ_{exc}= 290 nm).*

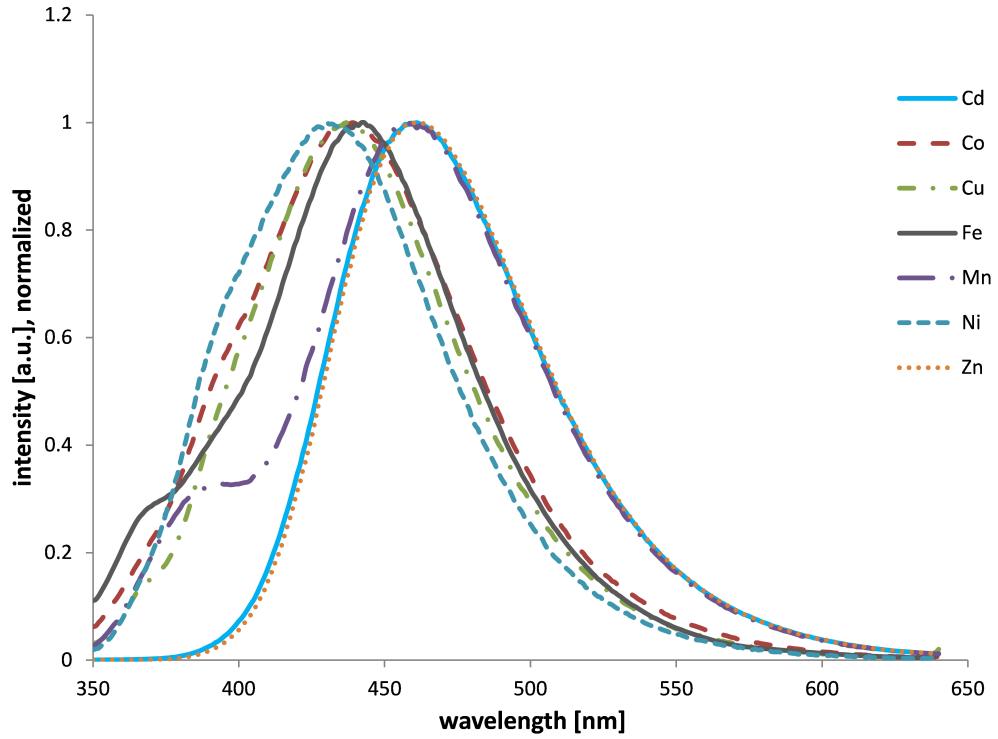

Figure 4.8: *Solution emission spectra of the homoleptic [M(MeO-tpy)$_2$][PF$_6$]$_2$ complexes (MeCN, λ_{exc}= 330 nm).*

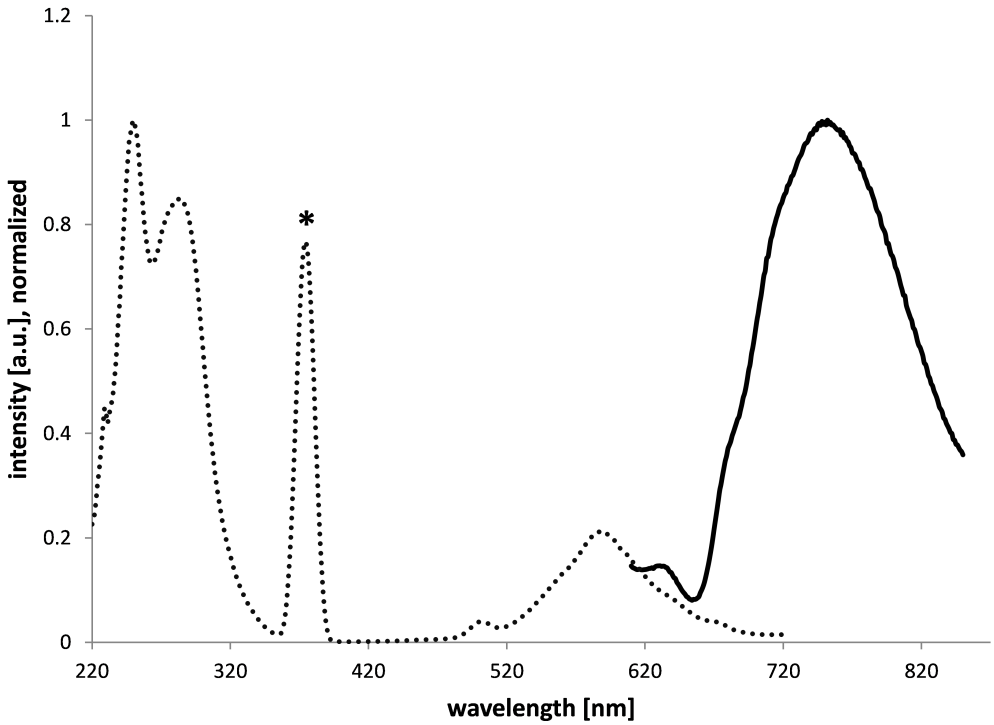

Figure 4.9: *Photoluminescence spectra of* $\mathbf{[Fe(MeO\text{-}tpy)_2][PF_2]_2}$*, emission (*$\lambda_{exc}$*= 290 nm, solid line) and excitation (*λ_{em}*= 750 nm, dotted line); MeCN, * = secondary.*

4.4 Gold nanoparticles

4.4.1 Synthesis and functionalization

Two nanoparticle solutions (*A* and *B*) were synthesized according to a literature procedure.[99] A solution of 1% aqueous $HAuCl_4$-solution (*A*: 1 ml, *B*: 2 ml), water (100 ml) and 1% aqueous sodium citrate-solution (2 ml) was heated to reflux for 1.5 h. During this time the colourless solution turned red. After cooling to room temperature, 0.1 M aqueous K_2CO_3-solution (0.5 ml) was added. The solutions were stored in the dark.

Functionalization of both particle solutions *A* and *B* was performed with ligands **L2-S** and **L4-S**. The ligands were deprotected as described earlier (*section 2.2.4*). The solutions with an approximate concentration of **L2-S**: 1.5 mM and **L4-S**: 1.0 mM were used directly for functionalization. The nanoparticle solution (10 ml) and ligand solution (1 ml) were mixed and stirred at room temperature for 1.5 h. For **L2-S**, the excess ligand was floating on top of the solution and was removed by filtering with a syringe filter (0.20 µm).

The obtained solutions *A*-**L2**, *B*-**L2**, *A*-**L4** and *B*-**L4** were mixed with 10 mM $FeCl_2$-solution (100 μl). This caused a colour change from red to purple of solutions *A*-**L2** and *B*-**L2**. A small amount of each solution was taken and NH_4PF_6 was added. As no precipitation was observed it can be assumed that essentially no complex is unbound in solution.

Filtering of the solutions *A* and *B* with a 0.20 µm syringe filter had no effect on the solutions. No precipitate in the filter was visible. Also no change in the absorption spectrum before and after filtering was observed. After filtration of the solutions *A*-**L2** and *B*-**L2** no change in colour or intensity could be detected by eye. This observation was proven by absorption spectroscopy. Similar results were obtained for *A*-**L4** and *B*-**L4.** Filtration of the solutions after addition of iron(II) yielded colourless liquids and purple particles in the filter. This can also be seen as an indication for almost no free complex in solution.

4.4.2 Photophysical properties

Absorption spectra

In the electronic absorption spectra of the nanoparticle solutions *A* and *B*, surface plasmon resonance (SPR) bands at 522 nm and 519 nm, respectively were observed (*Fig. 4.10*). According to the literature, from this wavelength a particle size of 15-20 nm[100, 101, 102, 103] and a concentration of 0.15 nM for *A* and 0.27 nM for *B* can be approximated.[103, 104]

The **L2-S** functionalized particles show a ligand-based absorption band at 290 nm. The SPR band is red-shifted to 541 nm (*Fig. 4.11*). Functionalization with **L4-S** leads to a red-shift of the SPR band to 540 nm (*A*-**L4**) and 524 nm (*B*-**L4**) (*Fig. 4.12*). It is presumed that these shifts are attributed to the increased size of the functionalized particles. The addition of $FeCl_2$ to *A*-**L2** and *B*-**L2** again

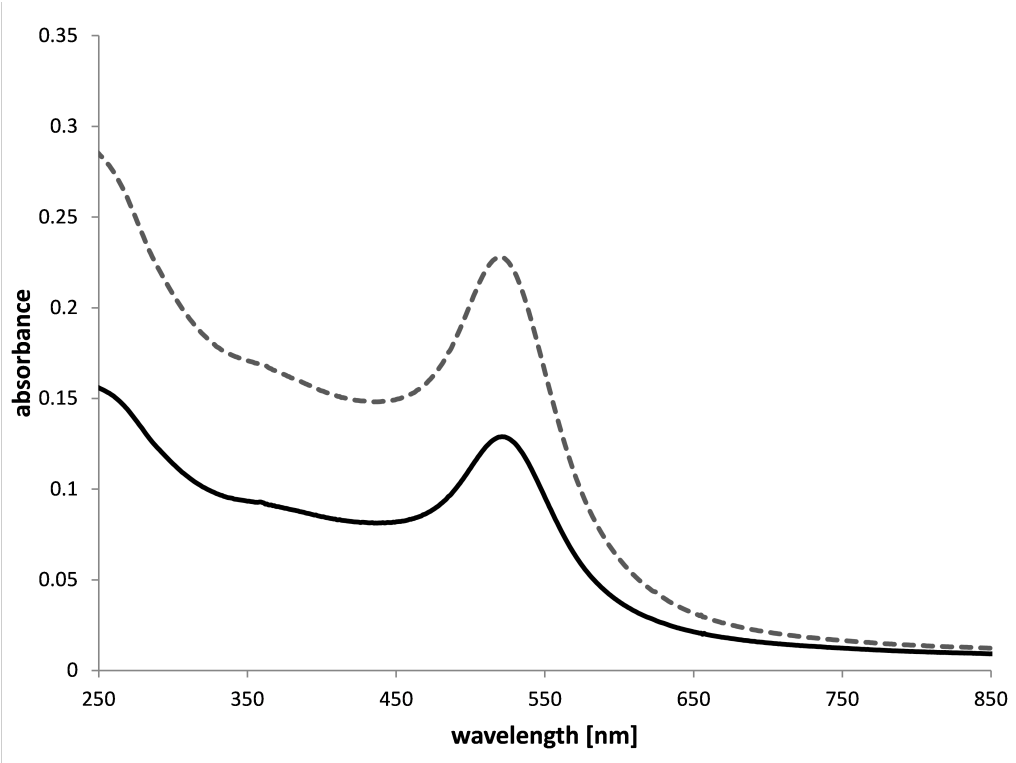

Figure 4.10: *Absorption spectra of the gold nanoparticle solutions A (solid line) and B (dotted line).*

causes a change in the absorption spectra (*Fig. 4.11*). With maxima at 283 nm, 319 nm and 571 nm the spectra are similar to the ones obtained from the homoleptic complexes **[Fe(MeO-tpy)$_2$][PF$_6$]$_2$** (*section 4.3.2*), **[Fe(L2-PEt)$_2$][PF$_6$]$_2$**, **[Fe(L2-CMe)$_2$][PF$_6$]$_2$** and **[Fe(L2-C)$_2$][PF$_6$]$_2$** (*section 4.2.2*). This gives rise to the assumption that the homoleptic complex is formed on the surface of the nanoparticles.

The presence of iron(II) in solutions *A*-**L4** and *B*-**L4** causes a further red-shift of the SPR to 548 nm and 542 nm respectively (*Fig. 4.12*). This is consistent with another particle size increase. The maximum of the MLCT transition of the homoleptic complex **[Fe(L4-SAc)$_3$][PF$_6$]$_2$** is at 538 nm. This gives rise to the assumption that the species present is not the homoleptic coordination complex. These results are congruent with the observations on TiO_2 (*section 4.2*).

A second batch of **L2-S** functionalized particles *A*-**L4**$'$ and *B*-**L4**$'$ were prepared. For these samples absorption maxima of 532 nm and 543 nm were obtained. The samples were measured again after one week. Both maxima were red-shifted to 540 nm and 547 nm respectively. Addition of Fe(II) to the solution caused no further change. A reason for the observed shift could be aggregation processes. The unfunctionalized particle solutions *A* and *B* showed no change in the absorption spectra after 3 weeks.

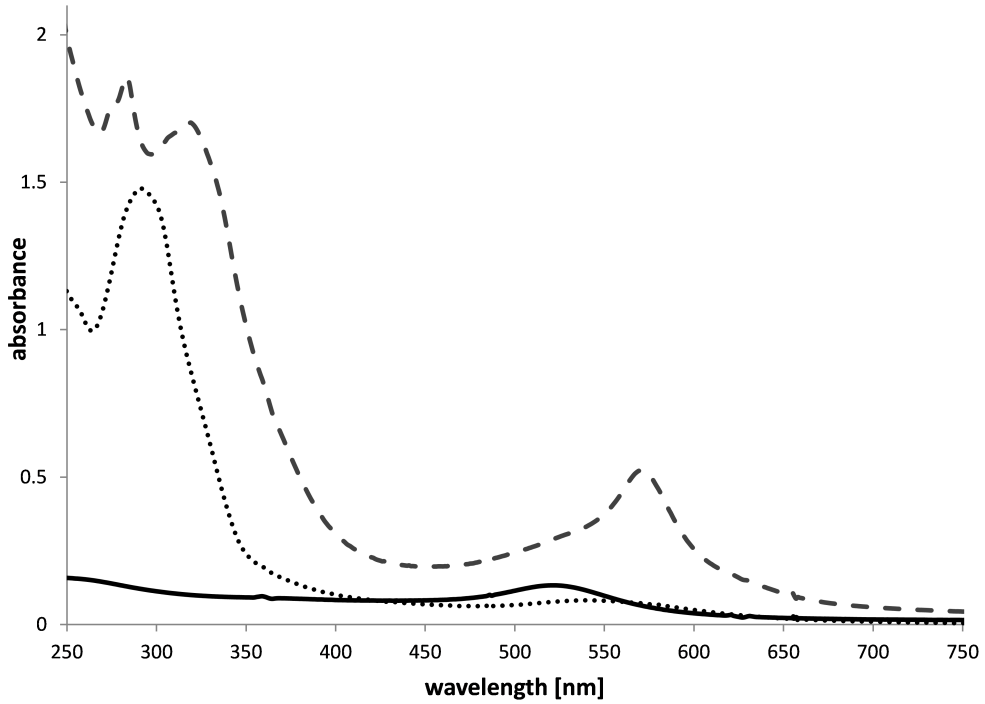

Figure 4.11: *Absorption spectra of A (solid line), A-**L2** (dotted line) and A-**L2+Fe** (dashed line).*

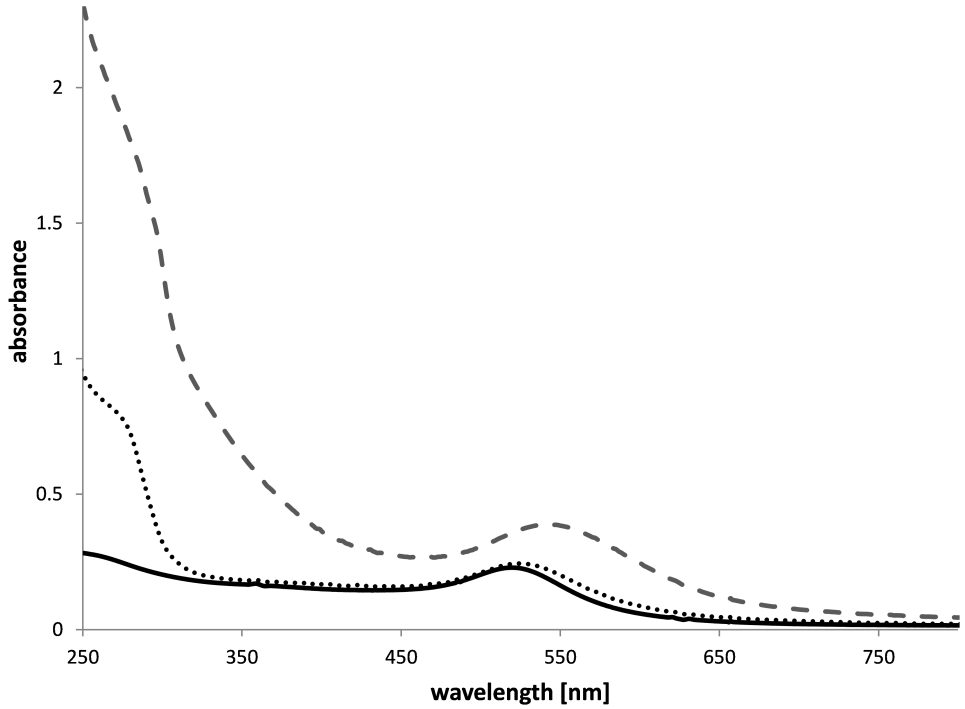

Figure 4.12: *Absorption spectra of B (solid line), B-**L4** (dotted line) and B-**L4+Fe** (dashed line).*

Photoluminescence

Both particle solutions *A* and *B* were excited at 520 nm and showed emission maxima at 571 nm, 632 nm and 781 nm. After functionalization, *A*-**L2** and *B*-**L2** show an intensity increase for the emission at 781 nm. After the addition of iron(II) to the solution, the emission is quenched and returns to the initial values (*Fig. 4.13*).
For *A*-**L4** and *B*-**L4**, comparable results as for the **L2-S** functionalized particles were obtained. Upon excitation at 520 nm, an increased intensity for the emission at 783 nm was observed. The addition of $FeCl_2$ leads to a decreased intensity of that emission.

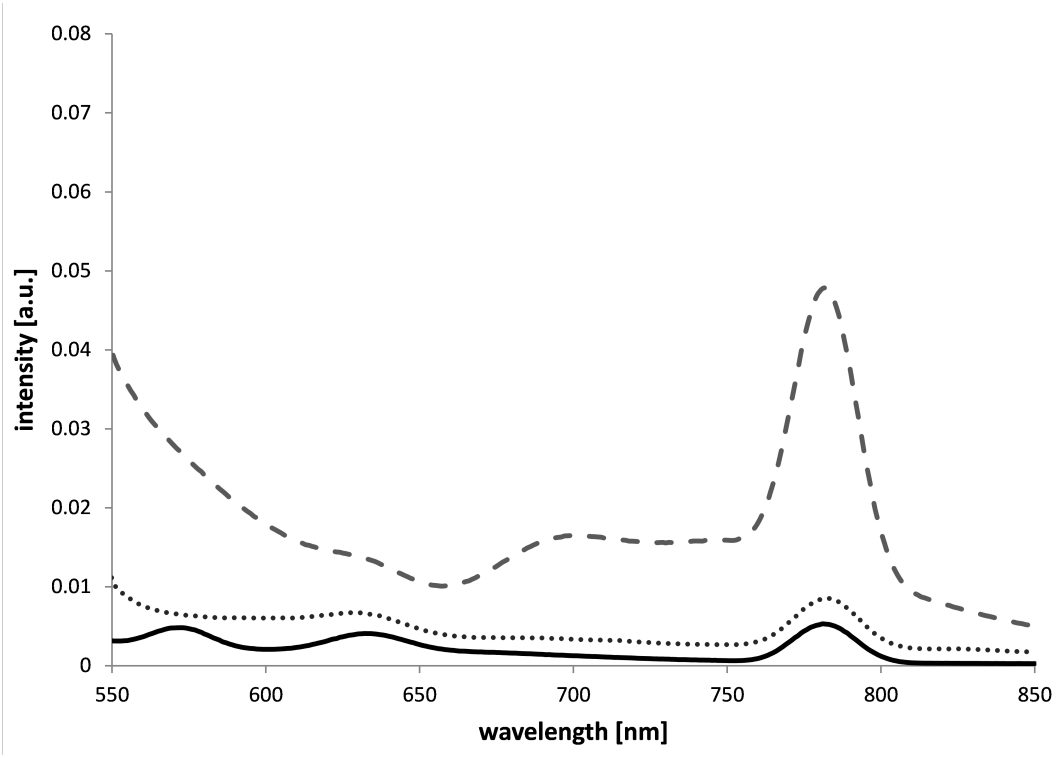

Figure 4.13: *Solution emission spectra of B (solid line), B-**L2** (dashed line) and B-**L2**+Fe (dotted line) (λ_{exc}= 520 nm).*

4.5 Iridium(III) complexes

4.5.1 Synthetic strategy and synthesis

The Ir(III) complexes **C6**, **C7** and **C8** were synthesized following a common strategy. $IrCl_3$ and cyclometalating ligands H(C^N) were reacted to yield a chloride-bridged dimer $Ir_2(C^N)_4Cl_2$. Ligands 2-phenylpyridine (Hppy), 2-(4-fluorophenyl)pyridine (Hfppy) and 2-(2,4-difluorophenyl)pyridine (Hdfppy) were used. In the next step, an ancillary ligand (N^N) was introduced to obtain the mononuclear complex $[Ir(C^N)_2(N^N)][PF_6]$.[105] For all three complexes **L4-SAc** was used as ancillary ligand. Complex **C6** was first synthesized and partially characterized by *Dr. Iain A. Wright*.

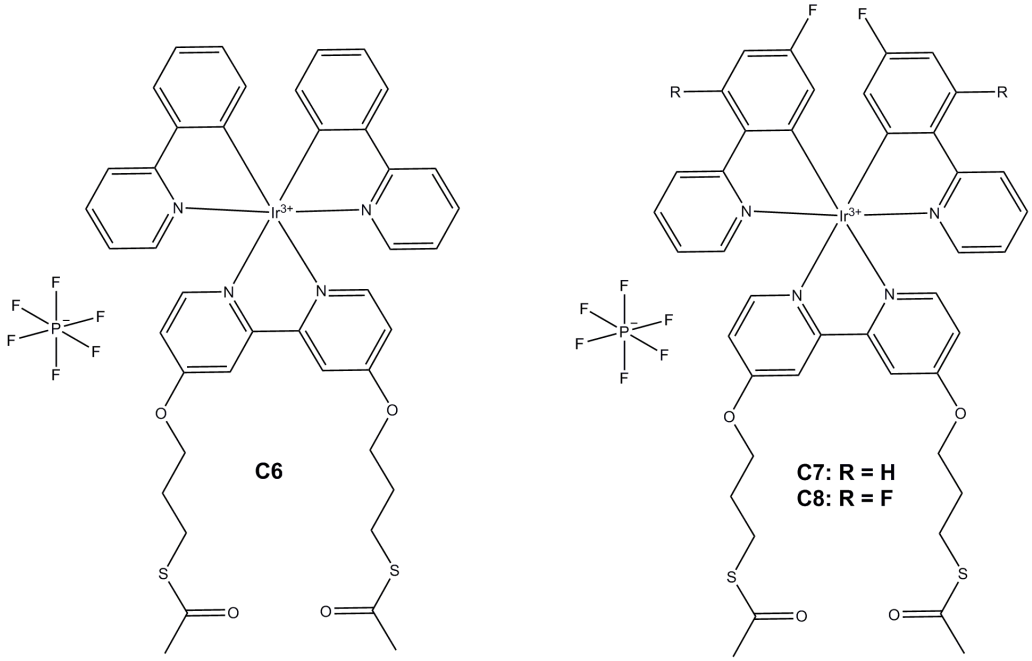

Scheme 4.3: *The cyclometalated Ir(III) complexes* ***C6***, ***C7*** *and* ***C8***.

4.5.2 Photophysical properties

In the electronic absorption spectrum of **C6**, a maximum at 256 nm is observed. Complex **C7** shows two bands in its solution absorption spectrum in the UV region at 227 nm and 251 nm. **C8** shows a shoulder at 232 nm and a maximum at 247 nm. The absorption of the three complexes tails off into in the visible region up to approximately 460 nm (**C6**, **C7**) and to 420 nm (**C8**) (*Fig. 4.14*).

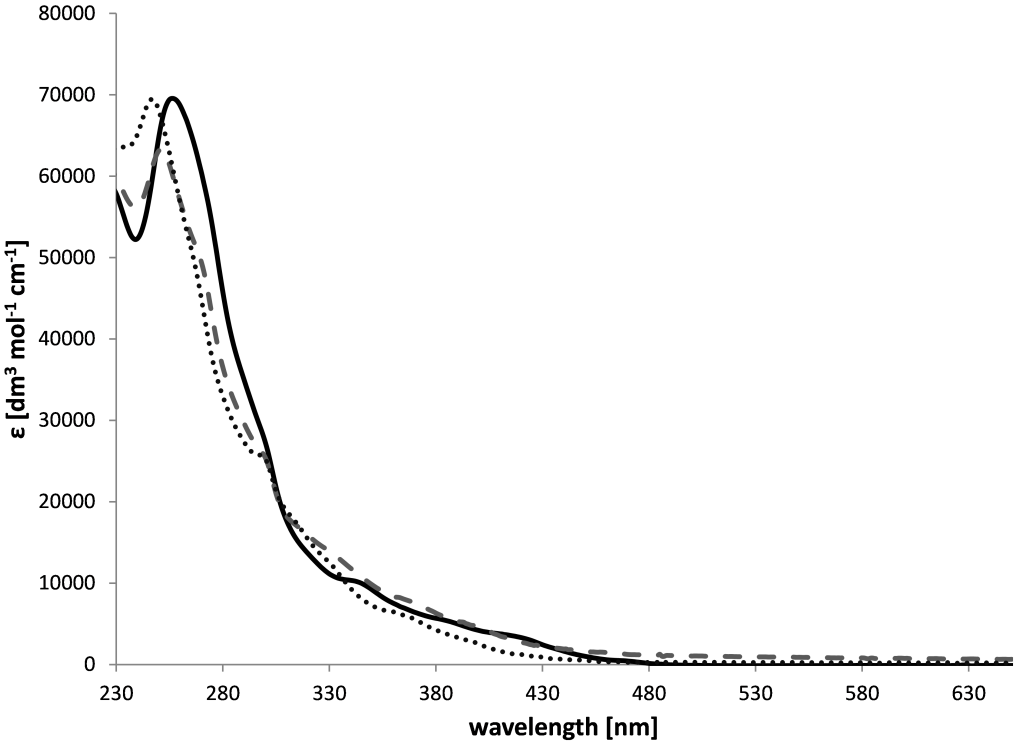

Figure 4.14: *Solution absorption spectra of* ***C6*** *(solid line),* ***C7*** *(dashed line) and* ***C8*** *(dotted line) (MeCN, 2·10^{-5} M).*

The wavelength of the emission maximum depends on the substituents of the phenylpyridine ligand. The fluoro-substituents cause a blue-shift of the emission wavelength. The different coloured emissions can be seen by eye under UV radiation at 366 nm. The photoluminescence spectra of **C7** and **C8** are shown in *Fig. 4.15*. The several photoluminescence emissions of the complexes **C6**, **C7** and **C8** are displayed in *Tab. 4.2*.

Complex	Emission [nm]	Emission [nm]	Colour of emission at λ_{exc}= 366 nm
C6	574, 638_{sh} (λ_{exc}= 260 nm)	358 (λ_{exc}= 292 nm)	orange
C7	360, 542 (λ_{exc}= 290 nm)	542 (λ_{exc}= 340 nm)	yellow
C8	360, 512 (λ_{exc}= 280 nm)	512 (λ_{exc}= 360 nm)	green

Table 4.2: *Emission maxima and colour of the complexes **C6**, **C7** and **C8** (MeCN, $1 \cdot 10^{-5}$ M).*

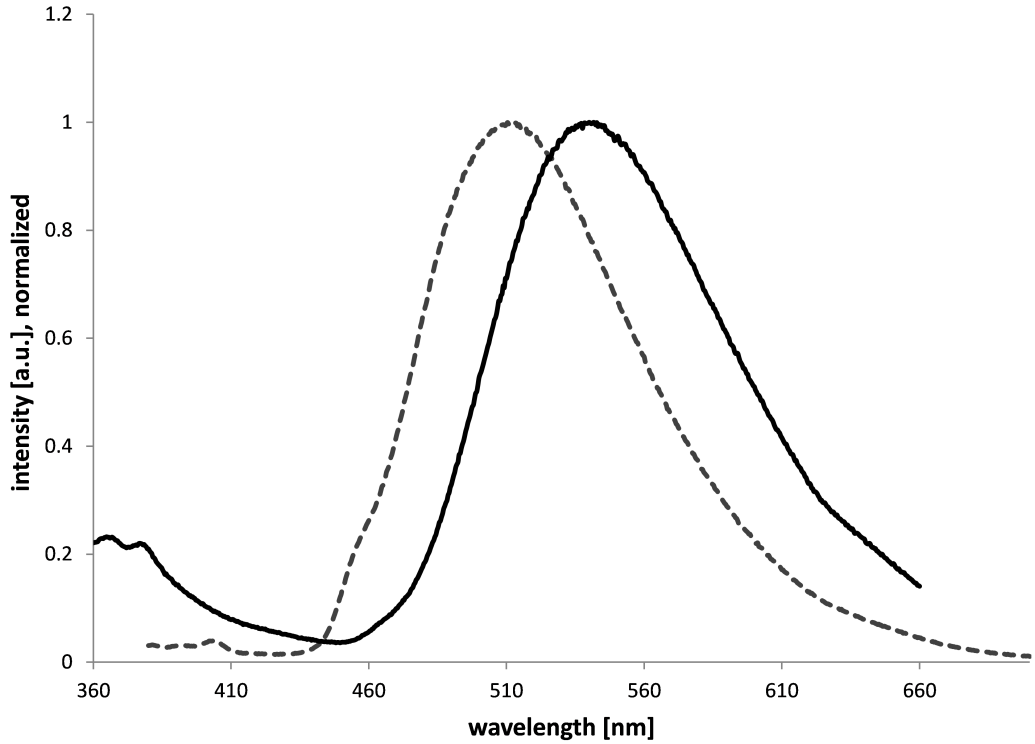

Figure 4.15: *Solution emission spectra of **C7** (solid line,λ_{exc}= 340 nm) and **C8** (dotted line, λ_{exc} = 360 nm) (MeCN, $1 \cdot 10^{-5}$ M).*

The ether chains on the bipyridine also influence the photoluminescence properties. This can be seen by comparing the emission wavelengths and the corresponding quantum yields Φ with the analogous unsubstituted bpy-complexes (*Tab. 4.3*). The emission maxima of **C6**, **C7** and **C8** are blue-shifted and the quantum yields of the complexes **C7** and **C8** are increased. The value of **C6** is not comparable as the measurement was performed with a non-degassed solution. The presence of oxygen in the solution has a strong effect on the quantum yield.

Complex	λ_{em}^{max} [nm]	Φ [%]		Complex	λ_{em}^{max} [nm]	Φ [%]
C6	574	3.9		$[Ir(ppy)_2(bpy)](PF_6)$[106]	590	4.5
C7	542	50.8		$[Ir(fppy)_2(bpy)](PF_6)$[105]	557	36
C8	512	83		$[Ir(dfppy)_2(bpy)](PF_6)$[107]	537	40

Table 4.3: *Emission wavelengths and corresponding quantum yields for Ir(III)complexes (MeCN-solutions, degassed except for* ***C6****).*

4.6 Concluding remarks

4.6.1 TiO_2

TiO_2-samples have been prepared and were functionalized with the four ligands **L2-P**, **L2-C**, **L4-P** and **L4-C**. Characterization of the functionalized surfaces was performed by absorption and photoluminescence spectroscopy. The **L2-P** functionalized surfaces showed in the photoluminescence spectrum a similar emission maximum as the ligand in solution. Treatment of the functionalized surfaces with aqueous $FeCl_2$-solution resulted for **L2-P** and **L2-C** in an immediate colour change to purple. From this observation, the formation of the homoleptic complex on the surface can be assumed. This is possible due to the ligand structure with one flexible linker chain and an ether bridge. A difference in colour was observed between the complexes of **L2-P** and **L2-C**. This was confirmed by solid state absorption spectroscopy. Compared to the complexes in solution, both surface-bound compounds showed a red-shifted MLCT maximum of 7 nm (**L2-P**) and 24 nm (**L2-C**). Similar effects were also reported for ruthenium based DSC dyes upon adsorption on TiO_2.[108] An immediate colour change from colourless to yellow and thus complex formation was observed upon addition of $CoCl_2$.

For **L2**, the dipping time of the TiO_2 samples in the ligand solution was varied between one and three days to investigate the time influence on the ligand loading. Analysis was performed by solid state absorption spectroscopy after adding aqueous $FeCl_2$-solution. With **L2-P**, the results obtained indicated that even after one day, the maximum ligand loading was reached. The measurements with **L2-C** yielded no unambiguous results.

L4-P functionalized samples show no immediate colour change when aqueous $FeCl_2$-solution is added. Only upon addition of another bidentate ligand like **bpy** or **phen** a colour change from colourless to red can be observed. This indicates that a surface-bound heteroleptic Fe(II) complex is formed. The capping ligand is necessary due to the structure of the anchoring ligand. With its two binding sites the ligand is too rigid to form a homoleptic complex. Furthermore, due to the bidenticity of **L4**, three ligands would be required to form the octahedral complex. This is not possible with only surface-bound ligands.

In the absorption spectra, no significant differences between the diverse complexes were observed. Due to the low extinction coefficient, no MLCT transition was measurable. Only absorption in the UV-region was observed, but the TiO_2 also absorbs in this area.

4.6.2 Metal ion sensing with MeO-tpy

Homoleptic complexes of Cd^{2+}, Co^{2+}, Cu^{2+}, Fe^{2+}, Mn^{2+}, Ni^{2+} and Zn^{2+} with MeO-tpy as ligand were synthesized and examined by electronic absorption and photoluminescence spectroscopy. In the solution absorption spectra, all complexes show two absorption bands in the UV-region with slightly shifted maxima. Only the iron(II) and cobalt(II) complexes show absorption in the visible region. All complexes show emission in the range between 390 nm to 460 nm with excitation wavelengths of

290 nm and 330 nm. Only the iron complex shows an additional emission at 752 nm. The complexes with Cd(II) and Zn(II) show at both excitation wavelengths a strong blue emission with maxima at approximately 460 nm.
Differences between the various coordination complexes were observed in the absorption as well as in the photoluminescence spectra. Using both spectroscopy methods, in principle it should be possible to distinguish between the different metals. For metals like iron with its characteristic absorption in the visible region or zinc with its strong emission, detection of the metal ion should be feasible. But as seen in *section 4.2.2*, binding to a surface can influence the photophysical properties of the metal complex. Thus, further investigation is required to see if this would be an appropriate method for metal ion detection.

4.6.3 Gold nanoparticles

Two gold nanoparticle solutions (A, B) were prepared, functionalized with **L2-S** and **L4-S** and treated with $FeCl_2$-solution. Characterization of all samples was performed by absorption and photoluminescence spectroscopy. Functionalization with the ligands led to a red-shifted maximum of the SPR band in the absorption spectra. This shift can be attributed to a size increase of the particles due to the attached ligands as the SPR absorption maximum is depending on the particle size. After addition of iron(II) ions, the absorption spectra of the **L2** functionalized particles showed the characteristics of the homoleptic complex in solution. For the solutions A-**L4** and B-**L4** a further red-shift was observed upon addition of $FeCl_2$. This is consistent with a further size increase.
The nanoparticle solutions show a maximum at 781 nm in the emission spectra at λ_{exc}= 520 nm. Functionalization with **L2-S** and **L4-S** caused an increased intensity of this emission. When Fe(II) ions are added, the emission is quenched and returns almost to its initial values. To gain a more accurate insight into this phenomenon, more experiments have to be performed.

4.6.4 Iridium(III) complexes

A series of three different luminescent Ir(III) complexes bearing the anchoring ligand **L4-SAc** were successfully synthesized and charaterized. The complexes emit light of different wavelengths with λ_{exc} = 366 nm. Comparison with the analogous unsubstituted bpy-complexes show blue-shifted emission maxima and for **C7** and **C8** increased quantum yields. This enhancement can be attributed to the ether substituents.

5 Diverse ligands

5.1 Abstract

In this chapter, the synthetic route to several different ligands is described. Attempts to an improved synthetic pathway to the DSSC anchoring ligand **ALP** are shown as well as the synthesis of the new anchoring ligand **ALP2**. Furthermore the preparation of the compounds **TA-TEG** and **TA-PEG** is shown. Also the synthesis of a new detection ligand **L6** is described.

5.2 DSSC anchoring ligands

5.2.1 ALP

For DSSCs with copper(I) dyes, different ligands are needed compared to those optimized for ruthenium. If a bpy-based ligand is used, the molecule bears sterically demanding groups like phenyl or alkyl chains on the 6,6′-positions. These substituents are required to stabilize the tetraheadral geometry of the Cu(I) complex and prevent oxidation of the metal to Cu(II), which prefers a square planar coordination environment.[42] Two common anchoring ligands are 6,6′-dimethyl-[2,2′-bipyridine]-4,4′-dicarboxylic acid (**ALC**) and (6,6′-dimethyl-[2,2′-bipyridine]-4,4′-diyl)bis(phosphonic acid) (**ALP**), shown in *Fig. 5.1.* DSSCs with **ALP** as anchoring ligand showed better results compared to **ALC**. [44] But the synthetic route to this ligand implies in total 7 steps, including several with low yields. The synthesis of the compound **P16** (*Scheme 5.1*), starting from 2,2′-bipyridine, has an overall yield of 1 % for this 5-step synthesis. From this precursor, the phosphonate ester **ALPE** is obtained by a palladium-catalyzed coupling reaction and the ligand **ALP** by hydrolysis of the ester under acidic conditions.[43] Due to the very low yield of the precursor **P16**, an improved synthetic route was investigated.

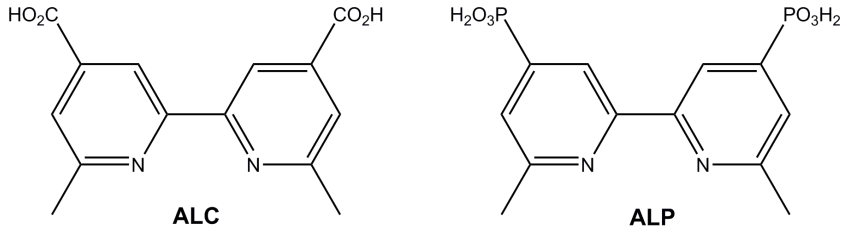

Figure 5.1: *Anchoring ligands **ALC** and **ALP** for copper(I) dyes.*

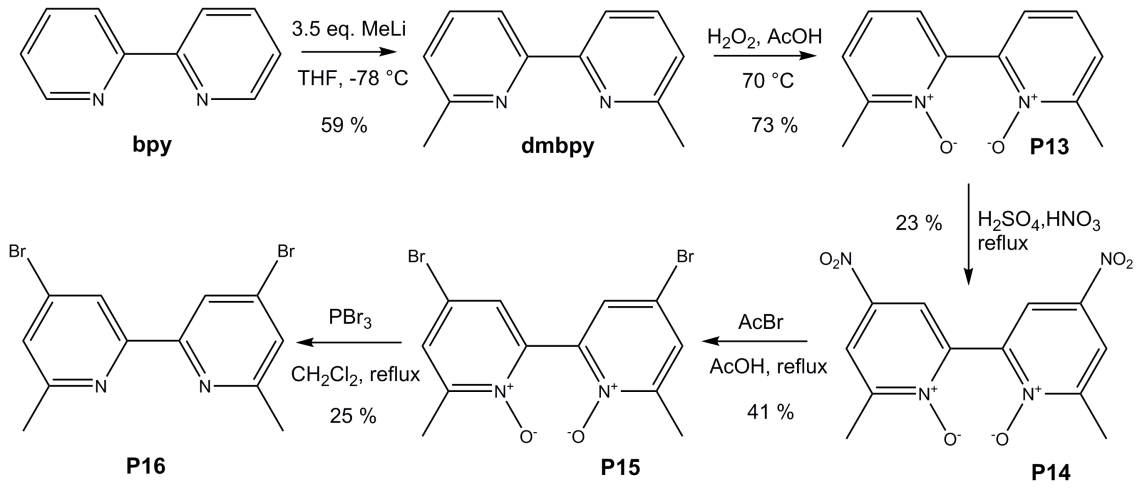

Scheme 5.1: *The synthetic route to the* ***ALP*** *precursor* ***P16***.

Synthetic strategy and synthesis

A different route to the precursor **P16** was sought. The new approach follows the same route as the current way (*Scheme 5.1*), but instead of starting with bpy the functionalizations are done on a pyridine-ring (*Scheme 5.2*). Then, a crosscoupling should yield the precursor **P16** or its chloro-derivative **P21**. The chloro-substituent on the 4-position was planned to prevent the formation of unwanted side products during the crosscpoupling reaction and should allow the reaction to the phosphonate ester in the next step. This route was expected to deliver higher yields and probably also allows other substitution patterns or the preparation of asymmetric ligands. Starting from commercially available 2-bromo-6-methylpyridine, the N-oxide **P17** was obtained by reaction with mCPBA. Treatment of this compound with sulfuric and nitric acids under reflux conditions yielded the nitro-compound **P18** in good yields for this type of reaction. The substitution of the nitro-group by a chloride to obtain compound **P19** was tried several times, but never succeeded. Neither did the reaction with acetyl chloride in acetic acid nor with $POCl_3$ in CH_2Cl_2 yield the desired product. The bromination with acetyl bromide to obtain compound **P20** and the subsequent oxygen removal with PBr_3 should work as reported for similar substances.[109] From this intermediate, bipyridine **P16** should be obtained by a homo-coupling. In the literature, some examples are known where nickel-based catalysts were used for this type of coupling reaction.[110, 111] By choosing the ideal reaction conditions, the formation of the substituted bpy should be possible. The nitrogen can probably coordinate to the metal and thus form the desired bidentate ligand. Unfortunately, the best conditions for these reactions still have to be found.

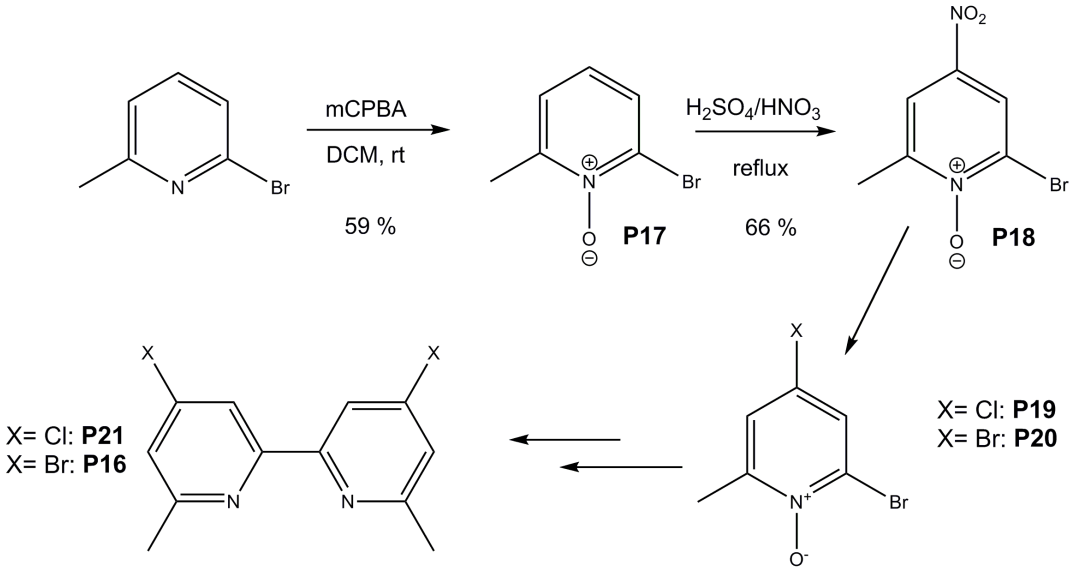

Scheme 5.2: *The planned new synthetic route to the* ***ALP*** *precursor.*

5.2.2 ALP2

To improve the performance of DSSCs, different modifications were made to the anchoring ligands. The introduction of a phenyl-spacer between the coordinating and the anchoring part of the ligand yielded the anchoring ligands **ALC1** and **ALP1** (*Fig. 5.2*). Solar cells, built with these ligands, showed improved efficiencies compared to the ligands **ALC** and **ALP**.[44, 43] So the next step was the introduction of a biphenyl spacer to obtain the next generation ligand **ALP2** (*Fig. 5.2*).

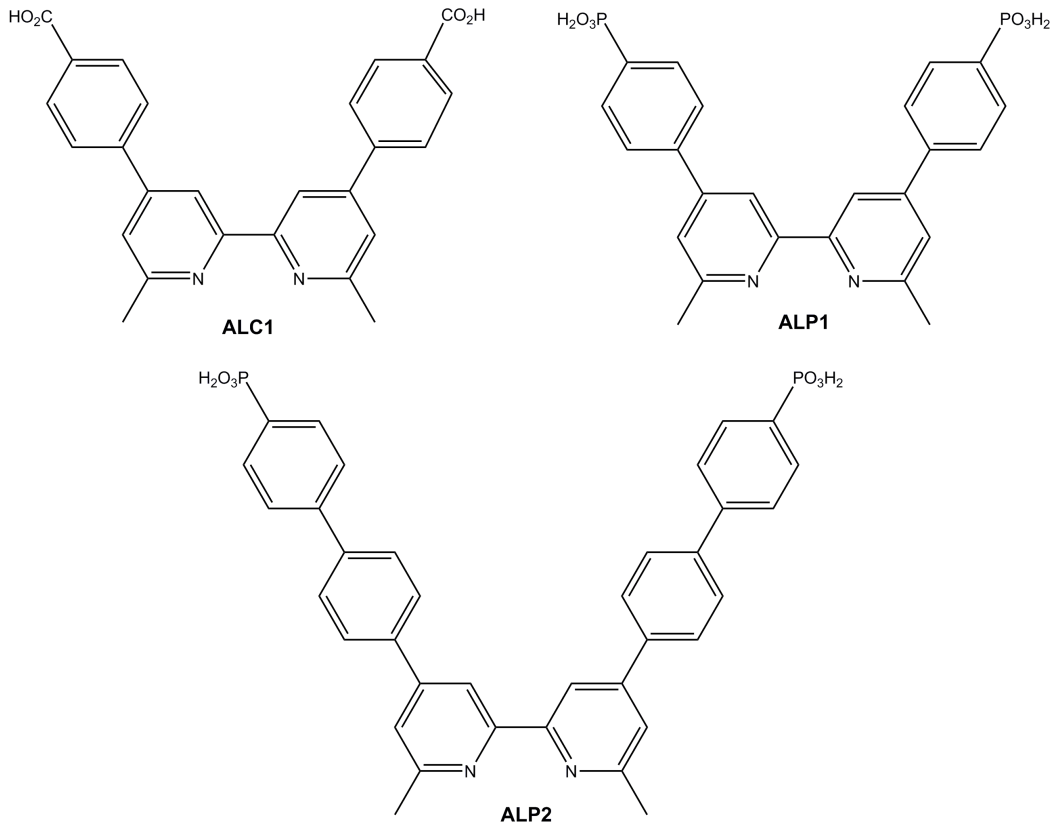

Figure 5.2: *Anchoring ligands **ALC1**, **ALP1** and **ALP2** for copper(I) dyes.*

A synthetic route to this ligand (*Scheme 5.3*) was developed and the reactions partly done by *Dr. Iain A. Wright*. As the first step, commercially available 4,4′-dibromo-1,1′-biphenyl was converted into the mono-aldehyde **P22**.[112] Then, the substituted bipyridine **P24** was synthesized following the *Kröhnke*-strategy.[19] From this intermediate, the phosphonate ester **ALPE2** was obtained by a palladium-catalyzed coupling reaction, similar to the procedure used for the syntheses of **ALPE** and **ALPE1**.[43] Transformation of this ester to the ligand **ALP2** was tried by acidic hydrolysis, following the procedure for **ALP1**,[43] but the reaction did not succeed. Attempts to hydrolyze the ester by reaction with bromotrimethylsilane in CH_2Cl_2 under inert atmosphere also did not work, although this common method works for many other compounds.[113, 114, 115]

Due to the low solubility in any common solvent, the intermediates **P23** and **P24** were only characterized by MALDI-MS. For **ALPE2**, a micro-TXI probe was used to record $^{1}H\{^{31}P\}$, ^{13}C, $^{31}P\{^{1}H\}$, HMQC$\{^{31}P\}$, HMBC$\{^{31}P\}$ and ^{13}C-^{31}P correlation NMR spectra.

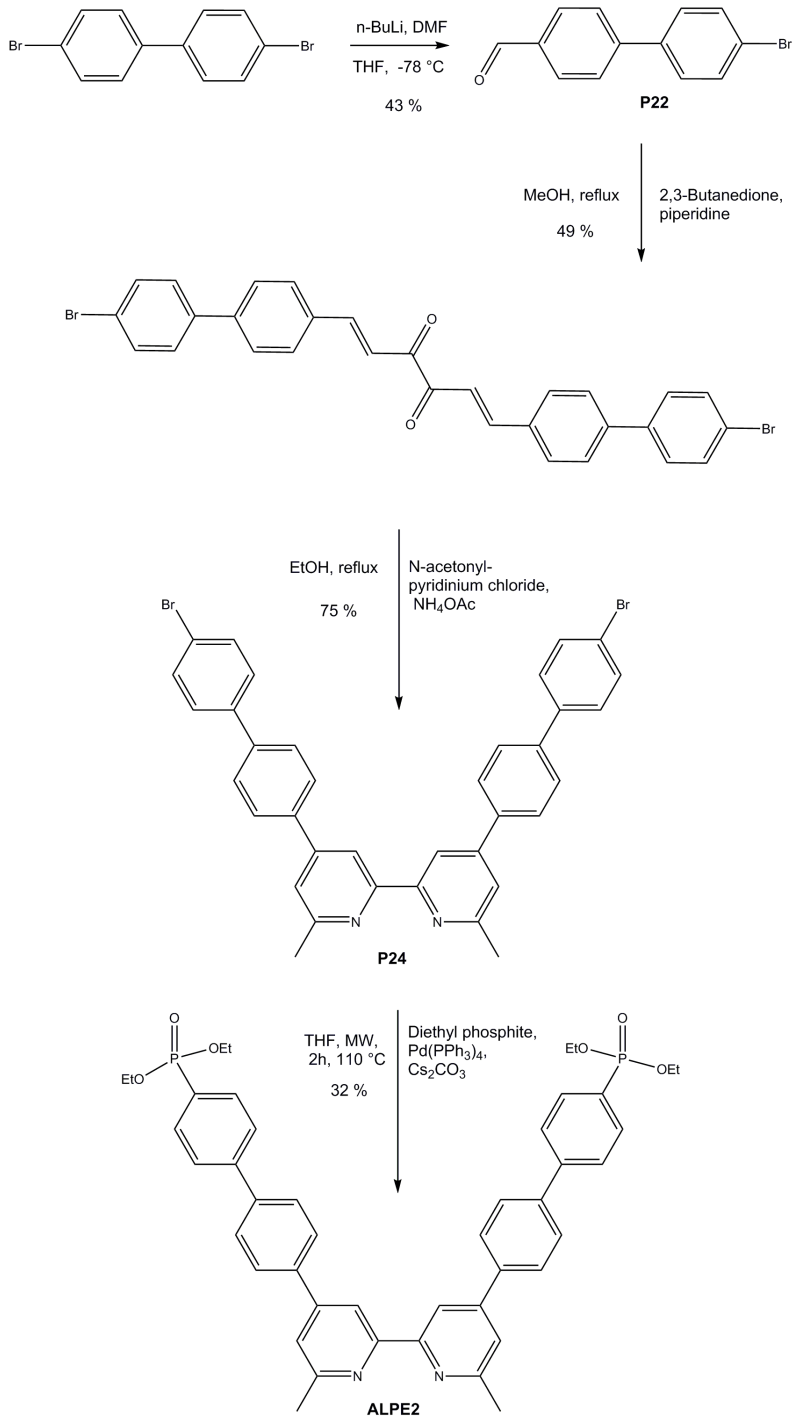

Scheme 5.3: *Synthesis of the* ***ALP2*** *precursor* ***ALPE2***.

5.3 TA-PEG, TA-TEG

Semiconductor nanocrystals, so-called quantum dots (QDs), offer unique electronic and optical properties and are promising candidates for molecular fluorophores with many different applications.[80] For bioimaging, QDs made of CdSe and CdTe show high potential.[116] Common methods for the synthesis of these QDs are carried out in organic solvents, but especially bioimaging applications require solubility in aqueous media. One way to modulate the solubility of the QDs is the exchange of the hydrophobic surface ligands, which are needed during synthesis to obtain the desired size and properties. Common ligands for replacement are the hydrophilic compounds thioctic acid (TA) or its reduced form dihydrothioctic acid (DHTA).[80] The hydrophilicity can be even increased if derivatives of TA with poly(ethylene glycol) (PEG) chains of different lengths are used. With these ligands, water-soluble and biocompatible QDs can be obtained.[116]
Two TA-based ligands containing either a tetraethylene glycol (**TA-TEG**) or a PEG400 (**TA-PEG**) chain (Fig. 5.3) have been prepared on a multigram scale . The synthesis followed the route described by *Mattoussi et al.*[116] Reaction of the particular ethylene glycol with racemic TA under *Steglich* conditions[75] yielded the desired ligand. The compounds were delivered to the group of *Prof. A. Credi*, University of Bologna for further investigations.

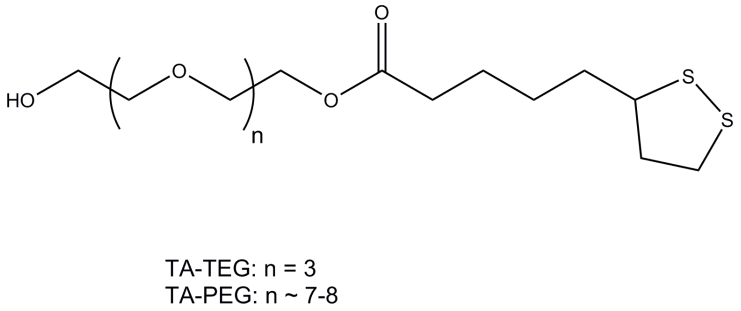

Figure 5.3: *Structure of the ligands* ***TA-TEG*** *and* ***TA-PEG***.

5.4 Detector ligand L6

The detection of anions and transition metal cations in aqueous media is of great interest. Of special interest is so-called "naked-eye" detection with chromogenic receptors which offer easy read-out without complicated instruments. Compound **3a** (*Fig. 5.4*) is reported in the literature as a detector for Hg^{2+} ions[117] and **3b**, as its metal complex, as anion sensor.[118] The ligands consist of an azathia macrocycle, which can coordinate to transition metal ions, and *p*-nitroazobenzene as chromophore. Upon addition of a range of metal nitrate salts, compound **3a** shows only a colour change with the mercury(II) salt.[117] Neither the addition of several group 1 and 2 metals as perchlorate salts nor different anions as TBA salts to a solution of **3b** caused a change. Also with diverse transition metal ions like Ni^{2+}, Zn^{2+}, Cd^{2+}, Pb^{2+}, Fe^{2+} and Ag^{+} no significant effect was observed. Only with Cu^{2+}, Hg^{2+} and Fe^{3+} changes in the absorption spectrum were observed. The mercury(II) and iron(III) complexes of **3b** also showed selective response to some anions such as nitrate or iodide.[118] To use the specific detection properties of this type of compound and probably also improve them, the nitro-group was substituted by a tpy-ligand. This led to an enlarged conjugated π-system and also offered the possibility for further coordination.

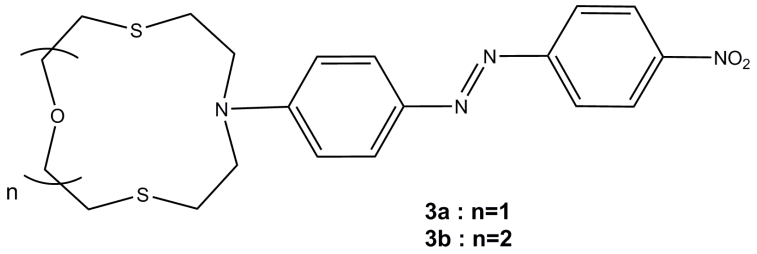

Figure 5.4: *Structure of the detector ligand 3.*

Synthetic strategy and synthesis

The synthetic route to **L6** (*Scheme 5.4*) followed the strategy reported by *Kou et al.*[117] with some modifications. Reaction of *N*-phenyldiethanolamine with methanesulfonyl chloride under basic conditions yielded compound **P25**. The macrocyclic compound **P26** was obtained by the reaction with 3,6-dioxa-1,8-octanedithiol in the presence of potassium carbonate. 4-([2,2′:6′,2″-Terpyridin]-4′-yl)aniline was first converted into the diazonium salt and then reacted with **P26** to the ligand **L6**.[119] Unfortunately, this last step was not reproducible. Although several attempts were made to reproduce it, none of them was successful. Changing the order of the reactions yielded intermediates, but never succeeded to the final compound. Because of this, no ion sensing experiments were performed. **L6** was characterized by ^{1}H and ^{13}C NMR spectroscopy and mass spectrometric methods.

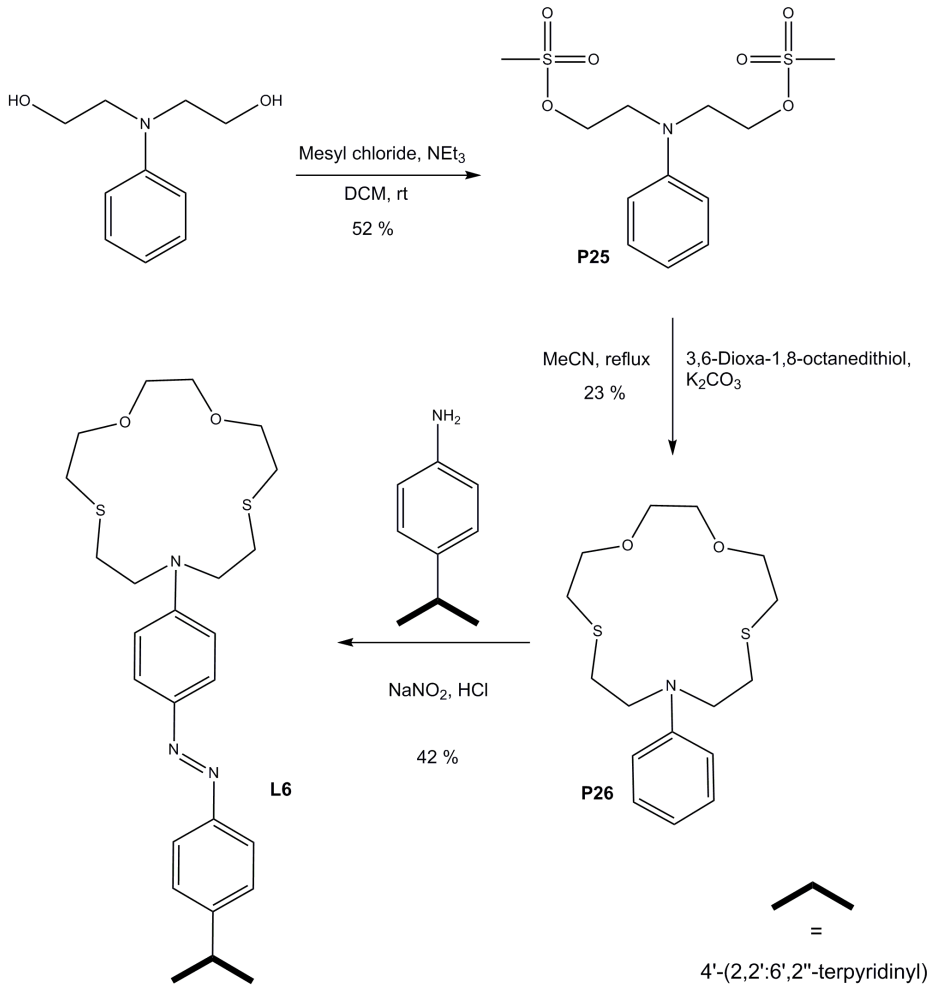

Scheme 5.4: *Synthetic route to ligand* ***L6***.

5.5 Concluding remarks

5.5.1 ALP

The already established synthesis to **ALPE** was performed and slightly improved. A novel route to intermediate **P16** (*Scheme 5.2*) was developed in theory and parts of it performed experimentally. This new approach should improve the very low yields of the currently used method. To obtain the desired compound in good yields and high purity, further investgations are necessary.

5.5.2 ALP2

The synthetic pathway to the phosphonate ester **ALPE2** has been developed further and the intermediate compounds have been characterized by mass spectrometry. Full ^{1}H and ^{13}C NMR assignment of **ALPE2** was performed with NMR spectroscopic methods. Different ways for the hydrolysis of the ester to the acid have been tried, but none was successful. This last step has to be part of further investigations to obtain the new anchoring ligand **ALP2**.

5.5.3 TA-PEG, TA-TEG

The two compounds **TA-TEG** and **TA-PEG** were successfully synthesized on a multigram scale and delivered to the partner-group at the University of Bologna. There, the materials were used for the modulation of the solubility of QDs.

5.5.4 Detector ligand L6

The new ligand **L6** was synthesized once and characterized by standard methods. Unfortunately, the resynthesis was not possible and also other synthetic approaches did not succeed. As no reliable synthesis for this ligand was established, further investigations of the targetted ion sensing experiments were not performed.

6 Summary

In this thesis, the synthesis and characterization of a series of polypyridine anchoring ligands have been presented. A part of these anchoring ligands have been used for the preparation of coordination complexes for detection applications. The transition metal complexes have been characterized and their sensing abilities have been examined. Futhermore, the anchoring ligands have been used for the functionalization of different kinds of surfaces. Additionally, some other ligands have been prepared for different types of applications.

In Chapter 2, several bpy and tpy-based ligands have been synthesized and fully characterized by ^{1}H and ^{13}C NMR spectroscopy, mass spectrometry, IR spectroscopy, melting point and absorption and photoluminescene spectroscopy. The ligand families of **L2** and **L4** have been prepared by a straightforward synthetic procedure. This strategy allows also variation in the linker chain length and the use of other anchoring groups.

In Chapter 3, a series of different Ru(II) complexes for detection applications are discussed. The complexes have been synthesized and characterized by standard analytical methods. Sensing tests have been performed and investigated by absorption and photoluminescence spectroscopy. Complex **C2*** performed well as detection compound for fluoride anions, but also showed sensitivity towards acetate and hydroxide ions. Complexes **C4** and **C5** showed only little potential as cyanide detector compounds.

In Chapter 4, simple protocols have been established for the functionalization of different materials with the anchoring ligands **L2** and **L4.** For TiO_2 surfaces, phosphonic and carboxylic acids have been used as anchoring groups, whereas thiols have been applied for gold nanoparticle. The functionalized surfaces have been characterized by absorption and photoluminescence spectroscopy. Post-treatment of these materials with transition metal salts were performed and evidence for the formation of coordination complexes on the surface was obtained. Furthermore, three luminescent Ir(III) complexes with **L4-SAc** as ancillary ligand have been synthesized and characterized. Comparison of the photoluminescent properties with the analogous unsubstituted bpy-complexes showed for **C6**, **C7** and **C8** blue-shifted emission maxima. For **C7** and **C8**, the quantum yield was increased. These changes can be attributed to the substituents on the bpy-ligand.

In Chapter 5, a new synthetic strategy to the DSSC anchoring ligand **ALP** was presented as well as to a new compound **ALP2**. For **ALP**, the improved synthesis should give higher yields than the one currently used. The preparation of the desired compound was not performed successfully, but the obtained intermediates showed promising results. For **ALP2**, the synthesis of the precursor **ALPE2** was performed and improved. Different methods for the hydrolysis of the phosphonate ester

were tried but did not work. Additionally, a possible new detection ligand **L6** has been synthesized and characterized by ^{1}H and ^{13}C NMR spectroscopy, IR spectroscopy and mass spectrometric methods. Due to synthetic problems, only a small amount of **L6** was obtained and no further sensing experiments were performed.

7 Experimental

7.1 General

^{1}H, ^{13}C, ^{19}F and ^{31}P NMR spectra were recorded using a Bruker Avance III-250, Avance III-400 and Avance III-500 NMR spectrometer. For full assignment additional COSY, HMBC and HMQC spetra were recorded on the Bruker Avance III-500. The chemical shifts δ were referenced to residual solvent peaks (chloroform: ^{1}H : 7.26 ppm, ^{13}C : 77.16 ppm, acetonitrile: ^{1}H : 1.94 ppm, ^{13}C : 118.26 ppm, DMSO: ^{1}H : 2.50 ppm, ^{13}C : 39.52 ppm, trifluoroacetic acid: ^{1}H : 11.50 ppm).
Infrared spectra were recorded on a Shimadzu FTIR 8400 S Fourier-transform spectrophotometer with Golden Gate accessory for solid samples.
Solid state and solution absorption spectra were recorded on an Agilent 8453 spectrophotometer, for solution photo luminescence a Shimadzu RF-5301PC spectrofluorometer was used. Solid state emission spectra were measured using a Hamamatsu Compact Fluorescence lifetime Spectrometer C11367-11 Quantaurus-Tau. Quantum yields were measured with a Hamamatsu absolute PL quantum yield spectrometer C11347 Quantaurus-QY.
Electron impact spectrometry was performed on a Finnigan MAT 95 spectrometer by *Dr. P. Nadig*. Electrospray ionization (ESI) and MALDI-TOF mass spectra were recorded on Bruker esquire 3000 plus and Bruker Daltonics Microflex mass spectrometers, respectively. LC-ESI-MS was measured on a Shimadzu Prominence UFLC and a Bruker amaZon X instrument. The microanalyses were performed with a Vario Micro Cube microanalyser by *Sylvie Mittelheisser*.
Microwave reactions were carried out in a Biotage Initiator^{TM} 8 reactor.
X-ray diffraction data were collected on a Bruker-Nonius KappaAPEX diffractometer with data reduction, solution and refinement using the programs *APEX2*[120] and *SHELXL97*.[121]

7.2 Synthesis of ligands

4′-(p-Tolyl)-2,2′:6′,2″-terpyridine (ttpy)

SM21

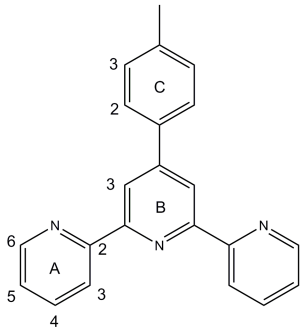

2-Acetylpyridine (4.5 ml, 40 mmol, 2 eq.), *p*-tolualdehyde (2.37 ml, 20 mmol, 1.0 eq.), KOH (3.1 g) and ammonia (aq., 32 wt%, 60 ml) were mixed with EtOH (100 ml) and the mixture was stirred at 34 °C for 8 h. The precipitated solid was filtered off and washed several times with cold EtOH. The crude product was recrystallized from EtOH. **Ttpy** was obtained as colourless needles (2.3 g, 7.11 mmol, 35 %). [21]

^{1}**H-NMR** (500 MHz, $CDCl_3$) δ/ppm: 8.73 (m, 4H, B3,H^{A6}), 8.67 (dt, J = 8.0, 1.0 Hz, 2H, H^{A3}), 7.88 (m, 2H, H^{A4}), 7.83 (d, J = 8.2 Hz,2H, H^{C2}), 7.35 (ddd, J = 7.5, 4.8, 1.2 Hz, 2H, H^{A5}), 7.32 (d, J = 8.4 Hz, 2H, H^{C3}), 2.43 (s, 3H, H^{Me}). ^{13}**C-NMR** (101 MHz, $CDCl_3$) δ/ppm: 156.5 ($C^{A2/B2}$), 156.0 ($C^{A2/B2}$), 150.3 (C^{B4}), 149.3 (C^{A6}), 139.2 (C^{C4}), 137.0 (C^{A4}), 135.6 (C^{C1}), 129.8 (C^{C3}), 127.3 (C^{C2}), 123.9 (C^{A5}), 121.5 (C^{A3}), 118.8 (C^{B3}), 21.4 (C^{Me}). The ^{1}H NMR spectroscopic data are in accord with the literature.[122]

4′-(4-(Bromomethyl)phenyl)-2,2′:6′,2″-terpyridine (P1)

SM22

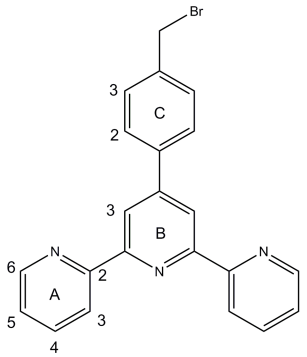

A solution of ttpy (1.0 g, 3.1 mmol, 1.0 eq.), N-bromosuccinimide (663 mg, 3.72 mmol, 1.2 eq.), AIBN (61 mg, 372 µmol, 0.12 eq.) in CCl_4(15 ml) was refluxed for 2 h. The precipitated solid was removed by filtration of the warm solution. After removal of the solvent, the crude product was recrystallized from EtOH/$CHCl_3$. **P1** was obtained as an off-white solid (1.04 g, 2.6 mmol, 83 %).

^{1}**H-NMR** (400 MHz, $CDCl_3$) δ/ppm:(Lit. 2) 8.73 (m, 4H,$H^{A6,B2}$), 8.68 (d, J = 8.0 Hz, 2H, H^{A3}), 7.89 (m, 4H, A4, H^{C2}), 7.54 (d, J = 8.3 Hz, 2H, H^{C3}), 7.36 (ddd, J = 7.5, 4.8, 1.2 Hz, 2H, H^{A5}), 4.57 (s, 2H, H^{CH_2}). ^{13}**C-NMR** (101 MHz, $CDCl_3$) δ/ppm: 156.3, 156.2, 149.7, 149.3, 138.8, 137.0, 129.8, 127.9, 127.3, 124.0, 121.5, 118.9, 33.1. The ^{1}H NMR spectroscopic data are in accord with the literature.[122]

2-(4-([2,2′:6′,2″-Terpyridin]-4′-yl)benzyl)isoindoline-1,3-dione (P2)

SM24

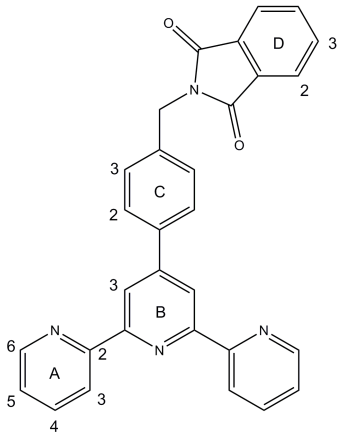

A microwave flask was charged with **P1** (403 mg, 1.0 mmol, 1.0 eq.), potassium phthalimide (195 mg, 1.05 mmol, 1.05 eq.) and DMF (15 ml) and heated for 30 min to 180 °C in a MW reactor. After the reaction was finished, water was added, the resulting solid filtered off and washed several times with water and Et_2O. **P2** was yielded as an off-white solid (300 mg, 640 µmol, 64 %).

^{1}**H-NMR** (500 MHz, $CDCl_3$) δ/ppm: 8.71 (ddd, J = 4.8, 1.8, 0.9 Hz, 2H, H^{A6}), 8.69 (s, 2H, H^{B3}), 8.65 (dt, J = 7.9, 1.0 Hz, 2H, H^{A3}), 7.87 (m, 6H, $H^{A2,C2,D2}$), 7.72 (dd, J = 5.5, 3.0 Hz, 2H, H^{D3}), 7.58 (d, J = 8.4 Hz, 2H, H^{C3}), 7.34 (ddd, J = 7.5, 4.8, 1.2 Hz, 2H, H^{A5}), 4.93 (s, 2H, H^{C5}). The ^{1}H NMR spectroscopic data are in accord with the literature. [64]

(4-([2,2′:6′,2″-Terpyridin]-4′-yl)phenyl)methanamine (P3)

SM27

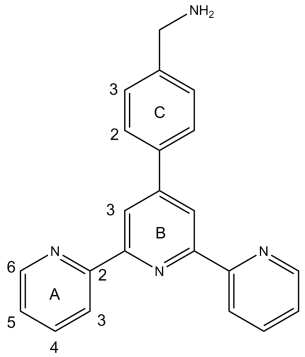

P2 (223 mg, 475 µmol, 1 eq.) was dissolved in anhydrous EtOH (7.5 ml) and $CHCl_3$ (5 ml) under nitrogen atmosphere. Hydrazine hydrate (64 % solution, 0.121 ml, 2.5 mmol, 5.26 eq.) was added and the mixture was refluxed for 4 h. $CHCl_3$ (12 ml) was added to the cooled solution and the white precipitate was filtered off. The resulting yellow solution was washed with water, 1 M aq. NaOH, a second time with water and dried over $MgSO_4$. After removal of the solvent **P3** was obtained as a yellow solid (143 mg, 423 µmol, 89 %).

^{1}**H-NMR** (400 MHz, $CDCl_3$) δ/ppm: 8.73 (m, 4H, $H^{A6,B3}$), 8.68 (d, J = 8.0 Hz, 2H, H^{A3}), 7.95 – 7.85 (m, 4H, $H^{A4,C2}$), 7.46 (d, J = 8.3 Hz, 2H, H^{C3}), 7.37 (ddd, J = 7.4, 4.8, 1.2 Hz, 2H, H^{A5}), 3.96 (s, 2H, H^{CH_2}). ^{13}**C-NMR** (101 MHz, $CDCl_3$) δ/ppm: 156.5 ($C^{A2/B2}$), 156.1 ($C^{A2/B2}$), 150.1 (C^{B4}), 149.3 (C^{A6}), 137.0 (C^{A4}), 127.7 ($C^{C2/C3}$), 127.6 ($C^{C2/C3}$), 124.0 (C^{A5}), 121.5 (C^{A3}), 118.9 (C^{B3}), 46.4 ($\mathbf{C}^{CH_2}$). **MS** (EI, m/z)**:** 338.1 $[M]^+$ (calc. 338.1). The ^{1}H NMR spectroscopic data are in accord with the literature. [64]

N-(4-([2,2′:6′,2″-Terpyridin]-4′-yl)benzyl)-5-(1,2-dithiolan-3-yl)pentanamide (L1)

SM28

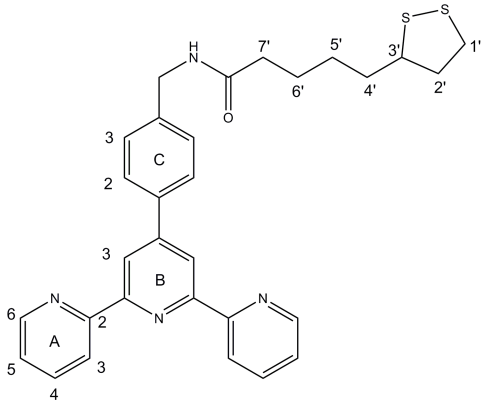

P3 (200 mg, 591 µmol, 1 eq.), DL- thioctic acid (158 mg, 768 µmol, 1.3 eq.), *N*,*N*′-dicyclohexylcarbodiimide (158 mg, 768 µmol, 1.3 eq.) and anhydrous CH_2Cl_2(50 ml) were mixed and stirred under nitrogen atmosphere for 48 h. The solvent was removed partially and the reduced solution was cooled. The precipitate was filtered off and the solvent was removed completely. The crude product was purified chromatographically (Al_2O_3, cyclohexane/ethyl acetate, 2:1 => 1: 5, R_f (1:1) = 0.48). **L1** was obtained as a yellow solid (155 mg, 295 µmol, 50 %)

^{1}**H-NMR** (500 MHz, $CDCl_3$) δ/ppm:8.72 (ddd, J = 4.8, 1.8, 0.9 Hz, 2H, H^{A6}), 8.71 (s, 2H, H^{B3}), 8.67 (dt, J = 7.9, 1.0 Hz, 2H, H^{A3}), 7.88 (m, 4H, A4, H^{C2}), 7.41 (d, J = 8.3 Hz, 2H, H^{C3}), 7.35 (ddd, J = 7.5, 4.8, 1.2 Hz, 2H, H^{A5}), 5.89 (t, J = 5.4 Hz, 1H, H^{NH}), 4.52 (d, J = 5.8 Hz, 2H, H^{C5}), 3.57 (dq, J = 12.6, 6.4 Hz, 1H, $H^{3'}$), 3.14 (m, 2H, $H^{1'}$), 2.45 (dtd, J = 12.0, 6.6, 5.4 Hz, 1H, $H^{2'}$), 2.26 (td, J = 7.4, 2.0 Hz, 2H, $H^{7'}$),1.90 (dq, J = 12.8, 7.0 Hz, 1H, $H^{2'}$),1.79– 1.65 (m, 4H, $H^{4',6'}$),1.55 – 1.43 (m, 2H, $H^{5'}$). ^{13}**C-NMR** (126 MHz, $CDCl_3$) δ/ppm: 172.7 ($C^{C=O}$), 156.3 ($C^{A2/B2}$), 156.1 ($C^{A2/B2}$), 149.8 (C^{B4}), 149.3 (C^{A6}), 139.5 (C^{C4}), 137.8 (C^{C1}), 137.0 (C^{A4}), 128.5 (C^{C3}), 127.8 (C^{C2}), 124.0 (C^{A5}), 121.5 (C^{A3}), 118.9 (C^{B3}), 56.5 ($C^{3'}$), 43.4 (C^{CH_2}), 40.4 ($C^{2'}$), 38.6 ($C^{1'}$), 36.6 ($C^{7'}$), 34.8 ($C^{4'}$), 29.0 ($C^{5'}$), 25.6 ($C^{6'}$). **MP**: 149 °C. **IR** (solid, ν/cm^{-1}): 681 (m), 731 (s), 787 (s), 887 (w), 989 (w), 1036 (w), 1261 (w), 1385 (m), 1466 (m), 1537 (s), 1583 (m), 1636 (s), 2355 (w), 2851 (w), 2922 (w), 3273 (w). **MS** (EI, m/z): 526.2 $[M]^+$ (calc. 526.2). **EA:** Found C 66.29 %, H 5.86 %, N 10.05 %, $C_{30}H_{30}N_4OS_2{\cdot}H_2O$ requires C 66.15 %, H 5.92 %, N 10.29 %.

S-(6-Hydroxyhexyl) ethanethioate (SC1)

SM44

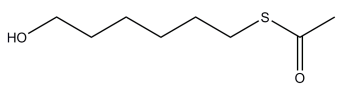

6-Bromo-1-hexanol (2.5 g, 13.8 mmol, 1.0 eq.) and potassium thioacetate (3.16 g, 27.7 mmol, 2.0 eq.) were added to DMF (20 ml) and molecular sieves (4 Å). The mixture was stirred at rt for 48 h, filtered and diluted with water and Et_2O. The organic phase was separated, the aqueous phase extracted 4 times with Et_2O and the combined organic phases were dried over $MgSO_4$. The solvent was removed and the brown oil was purified chromatographically (SiO_2, cyclohexane/ethyl acetate, 1:1 => 1:3, R_f (1:1) = 0.34). **SC1** was obtained as a brown oil (2.24 g, 12.7 mmol, 92 %).

^{1}**H-NMR** (250 MHz, $CDCl_3$) δ/ppm: 3.61 (t, J = 6.5 Hz, 2H), 2.85 (t, J = 7.5 Hz 2H), 2.31 (s, 3H), 1.55 (m, 4H), 1.36 (m, 4H). The ^{1}H NMR spectroscopic data are in accord with the literature.[66]

[2,2′-Bipyridine]-4,4′-dicarboxylic acid (dcbpy)

SM50

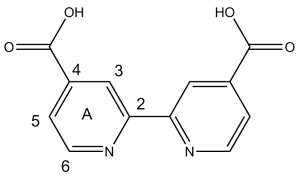

A microwave vial was charged with 4,4′-dimethyl-2,2′-bipyridine (200 mg, 1.08 mmol, 1.0 eq.), $KMnO_4$ (0.95 g, 6.0 mmol, 5.5 eq.) and water (16 ml) and heated in a MW reactor for 1 h at 130 °C. The formed MnO_2 was filtered off and the solution was acidified with concentrated HCl. The precipitate was filtered off, washed with water, ethyl acetate and Et_2O. After drying, **dcbpy** was obtained as a colourless solid (140 mg, 573 µmol, 50 %).

^{1}**H NMR** (250 MHz, DMSO-d_6) δ/ppm: 13.82 (s, 2H, H^{OH}), 8.92 (d, J = 5.5 Hz, 2H, H^{A6}), 8.85 (s, 2H, H^{A3}), 7.92 (dd, J = 4.9, 1.6 Hz, 2H, H^{A5}). The ^{1}H NMR spectroscopic data are in accord with the literature.[123]

Bis(6-(acetylthio)hexyl) [2,2′-bipyridine]-4,4′-dicarboxylate (L3)

SM51

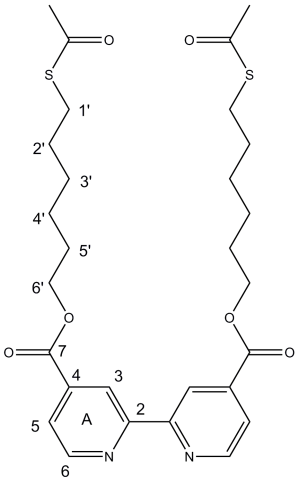

Dcbpy (0.5 g, 2.05 mmol, 1.0 eq.) was added to thionyl chloride (5 ml) and refluxed under N_2-atmosphere for 1.5 h until the solution was clear. The remaining thionyl chloride was removed under vacuum. Anhydrous toluene (16 ml), anhydrous triethyl amine (1.15 ml, 8.19 mmol, 4.0 eq.) and **SC1** (0.76 g, 4.3 mmol, 2.1 eq.) were added to the solid and the mixture was refluxed for 3 h. $CHCl_3$ (25 ml) and cold aq. $NaHCO_3$-solution (25 ml) were added, the organic phase was separated, dried over $MgSO_4$ and the solvent was removed. The crude material was purified by recrystallization (MeOH/EtOH/n-hexane). **L3** was obtained as an off-white solid (0.75 g, 1.34 mmol, 65 %).

^{1}**H NMR** (500 MHz, $CDCl_3$) δ/ppm: 8.94 (dd, J = 1.6, 0.9 Hz, 2H, H^{A3}), 8.87 (dd, J = 5.0, 0.8 Hz, 2H, H^{A6}), 7.90 (dd, J = 5.0, 1.6 Hz, 2H, H^{A5}), 4.39 (t, J = 6.7 Hz, 4H, $H^{6'}$), 2.88 (t, J = 7.3, 4H, $H^{1'}$), 2.32 (s, 6H, H^{Me}), 1.82 (m, 4H, $H^{5'}$), 1.61 (m, 4H, $H^{2'}$), 1.46 (m, 8H, $H^{3',4'}$).

^{13}**C NMR** (126 MHz, $CDCl_3$) δ/ppm: 196.1 ($C^{C=O,Ac}$), 165.3 ($C^{C=O}$), 156.7 (C^{A2}), 150.2 (C^{A6}), 139.0 (C^{A4}), 123.4 (C^{A5}), 120.7 (C^{A3}), 66.0 ($C^{6'}$), 30.8 (C^{Me}), 29.5 ($C^{2'}$), 29.1 ($C^{1'}$), 28.6 ($C^{5'}$), 28.5 ($C^{3'}$), 25.6 ($C^{4'}$). **MP**: 101 °C. **IR** (solid, ν/cm^{-1}): 507 (s), 513 (s), 522 (s), 549 (m), 561 (m), 571 (m), 582 (m), 628 (s), 665 (m), 697 (s), 722 (s), 744 (m), 764 (s), 832 (m), 866 (m), 890 (m), 921 (m), 960 (s), 1008 (m), 1064 (m), 1091 (m), 1109 (m), 1137 (s), 1240 (s), 1260 (m), 1292 (s), 1358 (m), 1395 (w), 1425 (m), 1458 (m), 1467 (m), 1560 (m), 1592 (m), 1688 (s), 1720 (s), 2855 (m), 2898 (w), 2926 (m), 2961 (w). **MS** (ESI, m/z): 561.2 $[M+H]^+$ (calc. 561.2), 583.2 $[M+Na]^+$ (calc. 583.2). **EA**: Found C 60.07 %, H 6.64 %, N 5.35 %, $C_{28}H_{36}N_2O_6S_2$ requires C 59.98 %, H 6.47 %, N 5.00 %.

[2,2′-Bipyridine]-4,4′-diol (OH-bpy)

SM109

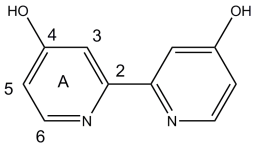

4,4′-Dimethoxy-2,2′-bipyridine (1.51 g, 7.0 mmol, 1.0 eq.) was dissolved in acetic acid (80 ml) and HBr (48 wt% sol. in water, 7.97 ml, 70.0 mmol, 10 eq.) was added. After refluxing for 24 h and cooling to rt the formed precipitate was filtered off and disolved in water. Neutralisation of the solution with aqueous ammonia yielded precipitate which was filtered off, washed with water and dried. OH-bpy was obtained as a colourless solid (1.07 g, 5.68 mmol, 81 %).

^{1}**H NMR** (250 MHz, D_2O + NaOH) δ/ ppm: 8.04 (d, J = 6.3 Hz, 2H, H^{A6}), 6.99 (d, J = 2.5 Hz, 2H, H^{A3}), 6.58 (dd, J = 6.3, 2.5 Hz, 2H, H^{A5}). The ^{1}H NMR spectroscopic data are in accord with the literature.[124]

4′-(4-Methoxyphenyl)-2,2′:6′,2″-terpyridine (MeO-tpy)

SM173

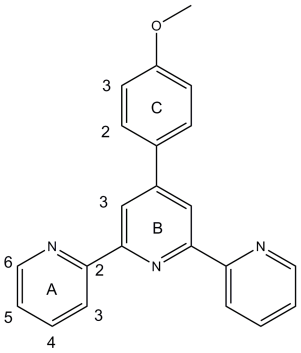

4-Methoxybenzaldehyde (2.43 ml, 20 mmol, 1.0 eq.), 2-acetylpyridine (4.5 ml, 40 mmol, 2.0 eq.) and KOH (3.14 g, 56 mmol, 2.8 eq.) were mixed with ammonia (aq., 30 wt%, 60 ml) and EtOH (100 ml) and the solution was stirred at rt for 24 h. The formed precipitate was filtered off, washed with cold EtOH and dried. Purification was performed by recrystallization (ethyl acetate/n-hexane). **MeO-tpy** was obtained as small colourless needles (2.4 g, 7.07 mmol, 35 %).

^{1}**H NMR** (400 MHz, $CDCl_3$) δ/ppm: 8.73 (ddd, J = 4.8, 1.8, 0.9 Hz, 2H), 8.71 (s, 2H), 8.67 (dt, J = 8.0, 1.0 Hz, 2H), 7.93 – 7.83 (m, 4H), 7.35 (ddd, J = 7.5, 4.8, 1.2 Hz, 2H), 7.04 (m, 2H), 3.89 (s, 3H). The ^{1}H NMR spectroscopic data are in accord with the literature.[125]

4-([2,2′:6′,2″-Terpyridin]-4′-yl)phenol (OH-tpy)

SM185

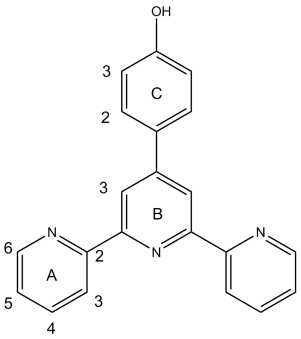

A 2-5 ml MW-vial was charged with MeO-Phtpy (0.8 g, 2.36 mmol, 1.0 eq.) and pyridine hydrochloride (1.3 g, 11.2 mmol, 4.7 eq.) and heated in the MW reactor at 200 °C for 1 h. Water was added to the reaction mixture and the formed solid was filtered off, washed with water and dried. The washing water was filtered again and the obtained solid was washed with water and dried. **OH-tpy** was obtained as a colourless solid (650 mg, 2.0 mmol, 84 %).

^{1}**H NMR** (400 MHz, DMSO-d_6) δ/ppm: 9.94 (s, 1H), 8.76 (ddd, J = 4.8, 1.8, 0.9 Hz, 2H), 8.68 (m, 4H), 8.05 (td, J = 7.7, 1.8 Hz, 2H), 7.80 (d, J = 8.6 Hz, 2H), 7.54 (ddd, J = 7.5, 4.8, 1.2 Hz, 2H), 6.97 (d, J = 8.6 Hz, 2H). The ^{1}H NMR spectroscopic data are in accord with the literature.[59]

S-(3-Bromopropyl) ethanethioate (SC2)

SM107

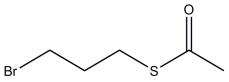

Potassium thioacetate (2.1 g, 18 mmol, 1.0 eq.) and 1,3-dibromopropane (2.02 ml, 19.8 mmol, 1.1 eq.) were refluxed in THF (100 ml) for 2.5 h. After cooling, the mixture was stirred at rt for 3 h followed by removal of the solvent under reduced pressure. The residue was dissolved in CH_2Cl_2, filtered over celite and the solvent was removed in vacuo. **SC2** was obtained after distillation (65 °C at $1{\cdot}10^{-1}$mbar) as colourless oil (1.73 g, mmol, 8.78 mmol, 48 %).

^{1}**H NMR** (400 MHz, $CDCl_3$) δ/ppm: 3.44 (t, J = 6.5 Hz, 2H), 3.00 (t, J = 7.0 Hz, 2H), 2.33 (s, 3H, Me), 2.11 (m, 2H). The ^{1}H NMR spectroscopic data are in accord with the literature.[126]

Diethyl (3-bromopropyl)phosphonate (SC3)

SM180

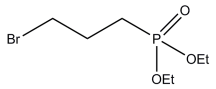

Triethyl phosphite (2.58 ml, 15 mmol, 1.0 eq.) and 1,3-dibromopropane (6.12 ml, 60 mmol, 4.0 eq.) were heated for 2 h at 160 °C. The during the reaction produced bromoethane was distilled off with a distillation bridge. **SC3** was obtained after distillation (100 °C at $5{\cdot}10^{-2}$mbar) as colourless oil (2.02 g, 7.80 mmol, 52 %).

^{1}H{^{31}P} NMR (400 MHz, $CDCl_3$) δ/ppm: 4.10 (m, 4H), 3.47 (t, J = 6.5 Hz, 2H), 2.15 (m, 2H), 1.89 (m, 2H), 1.33 (t, J = 7.1 Hz, 6H). **^{31}P NMR** (162 MHz, $CDCl_3$) δ/ppm: 30.53. The ^{1}H NMR spectroscopic data are in accord with the literature.[72]

S-(3-(4-([2,2′:6′,2″-Terpyridin]-4′-yl)phenoxy)propyl) ethanethioate (L2-SAc)

SM154

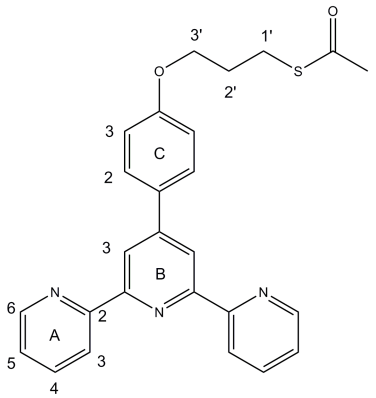

OH-tpy (415 mg, 1.28 mmol, 1.0 eq.) and potassium carbonate (670 mg, 4.84 mmol, 3.8 eq.) were added to a solution of **SC2** (300 mg, 1.52 mmol, 1.2 eq.) in DMF (15 ml). The suspension was stirred at 80 °C for 5.5 h. The solvent was removed under reduced pressure and the resulting solid was suspended in water and extracted three times with CH_2Cl_2. The combined organic fractions were dried over $MgSO_4$ and the solvent was removed under reduced pressure. The product was purified by colunm chromatography (Al_2O_3, Ethyl acetate/cyclohexane 1:1, R_f = 0.74). **L2-SAc** was obtained as a colourless solid (300 mg, 679 µmol, 53 %).

^{1}H NMR (500 MHz, $CDCl_3$) δ/ppm: 8.73 (m, 2H, H^{A6}), 8.70 (s, 2H, H^{B3}), 8.67 (dt, J = 8.0, 1.1 Hz, 2H, H^{A3}), 7.88 (m, 4H, $H^{A4,C2}$), 7.35 (ddd, J = 7.5, 4.8, 1.2 Hz, 2H, H^{A5}), 7.02 (d, J = 8.7 Hz, 2H, H^{C3}), 4.09 (t, J = 6.0 Hz, 2H, $H^{3'}$), 3.10 (t, J = 7.1 Hz, 2H, $H^{1'}$), 2.36 (s, 3H, H^{Me}), 2.12 (m, 2H, $H^{2'}$).**^{13}C NMR** (126MHz, $CDCl_3$) δ/ppm: 195.9 (C^{d}), 159.8 (C^{C4}), 156.5 (C^{A2}), 155.9 (C^{B2}), 149.8 (C^{B4}), 149.2 (C^{A6}), 137.0 (C^{A4}), 131.0 (C^{C1}), 128.7 (C^{C2}), 123.1 (C^{A5}), 121.5 (C^{A3}), 118.4 (C^{B3}), 115.0 (C^{C3}), 66.4 ($C^{3'}$), 30.8 (C^{Me}), 29.4 ($C^{2'}$), 26.0 ($C^{1'}$). **MP**: 161 °C. **IR** (solid, ν/cm^{-1}): 520 (s), 533 (m), 566 (s), 577 (s), 603 (s), 619 (s), 659 (m), 675 (m), 687 (m), 733 (s), 745 (m), 791 (s), 834 (s), 872 (m), 890 (s), 922 (m), 944 (m), 968 (m), 988 (m), 1000 (m), 1009 (m), 1024 (m), 1036 (m), 1054 (w), 1075 (m), 1091 (m), 1097 (m), 1115 (m), 1131 (m), 1187 (s), 1227 (m), 1257 (m), 1287 (m), 1350 (m), 1391 (m), 1421 (m), 1441 (m), 1464 (s), 1514 (s), 1546 (m), 1566 (m),

1581 (s), 1598 (m), 1644 (m), 1651 (m), 1678 (s), 2867 (w), 2931 (w), 3053 (w). **MS** (MALDI-TOF, m/z)**:** 442.1 $[M+H]^+$ (calc. 442.2). **EA**: Found C 70.24 %, H 5.32 %, N 9.29 %, $C_{26}H_{23}N_3O_2S$ requires C 70.73 %, H 5.25 %, N 9.52 %.

3-(4-([2,2′:6′,2″-Terpyridin]-4′-yl)phenoxy)propane-1-thiol (L2-S)

SM204

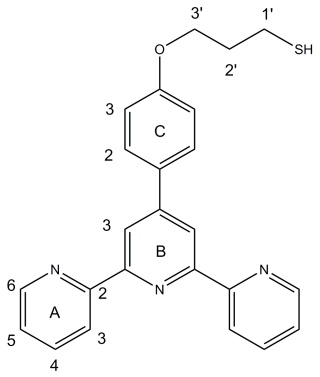

L2-SAc (40 mg, 90.6 µmol, 1.0 eq.) and NaOMe (6 mg, 111 µmol, 1.2 eq.) were stirred in anhydrous MeOH (15 ml) under an inert nitrogen atmosphere at room temperature for 2 h. Dowex 50WX4 ion changer resin was added, the mixture was stirred for 5 min. then filtered and the resin washed with MeOH. After removal of the solvent from the filtrate, **L2-S** was obtained as a colourless solid.

^{1}**H NMR** (500 MHz, $CDCl_3$) δ/ppm: 8.74 (ddd, J = 4.8, 1.8, 0.9 Hz, 2H, H^{A6}), 8.71 (s, 2H, H^{B3}), 8.67 (m, 2H, H^{A3}), 7.88 (m, 4H, $H^{A4,C2}$), 7.36 (ddd, J = 7.5, 4.8, 1.2 Hz, 2H, H^{A5}), 7.02 (m, 2H, H^{C3}), 4.15 (t, J = 5.9 Hz, 2H, $H^{3'}$), 2.77 (m, 2H, $H^{1'}$), 2.12 (m, 2H, $H^{2'}$), 1.43 (t, J = 8.1 Hz, 1H, H^{SH}). ^{13}**C NMR** (126 MHz, $CDCl_3$) δ/ppm: 159.9 (C^{C4}), 156.4 (C^{A2}), 155.8 (C^{B2}), 149.9 (C^{B4}), 149.1 (C^{A6}), 137.2 (C^{A4}), 130.9 (C^{C1}), 128.7 (C^{C2}), 123.9 (C^{A5}), 121.6 (C^{A3}), 118.5 (C^{B3}), 115.0 (C^{C3}), 65.9 ($C^{3'}$), 33.5 ($C^{2'}$), 21.4 ($C^{1'}$). **IR** (solid, ν/cm^{-1}): 504 (s), 566 (m), 781 (s), 837 (m), 1032 (m), 1185 (m), 1238 (m), 1295 (m), 1357 (w), 1416 (w), 1521 (s), 1586 (s), 3054 (m), 3358 (m). **MS** (MALDI-TOF, m/z): 400.1 $[M+H]^+$ (calc. 400.1).

Diethyl (3-(4-([2,2′:6′,2″-terpyridin]-4′-yl)phenoxy)propyl)phosphonate (L2-PEt)

SM181

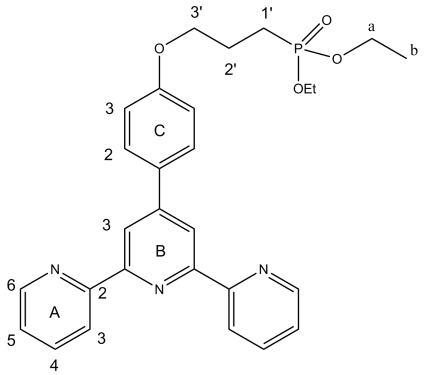

OH-tpy (200 mg, 615 µmol, 1.0 eq.) and potassium carbonate (297 mg, 2.15 mmol, 3.5 eq.) were added to a solution of **SC3** (191 mg, 738 µmol, 1.2 eq.) in DMF (15 ml) and stirred for 4 h at 80 °C. After removal of the solvent, the residue was suspended in water and extracted three times with CH_2Cl_2. The combined organic fractions were dried over $MgSO_4$ and then solvent was removed. The crude product was purified by recrystallization (n-hexane/ethyl acetate). **L2-PEt** was obtained as a colourless solid (280 mg, 556 µmol, 90%).

^{1}H{^{31}P} NMR (500 MHz, $CDCl_3$) δ/ppm: 8.73 (d, J = 3.4 Hz, 2H, H^{A6}), 8.70 (s, 2H, H^{B3}), 8.67 (d, J = 8.0 Hz, 2H, H^{A3}), 7.88 (m, 4H, $H^{A4,C2}$), 7.35 (dd, J = 7.4, 4.7 Hz, 2H, H^{A5}), 7.01 (m, 2H, H^{C3}), 4.12 (m, 6H, $H^{3',a}$), 2.13 (m, 2H, $H^{2'}$), 1.98 (m, 2H, $H^{1'}$), 1.34 (t, J = 7.1 Hz, 6H, H^{b}). **^{13}C NMR** (126 MHz, $CDCl_3$) δ/ppm: 159.8 (C^{C1}) , 156.5 (C^{A2}) , 156.0 (C^{B2}) , 149.8 (C^{B4}) , 149.2 (C^{A6}) , 137.0 (C^{A4}) , 131.0 (C^{C4}) , 128.7 (C^{C2}), 123.9 (C^{A5}) , 121.5 (C^{A3}) , 118.4 (C^{B3}), 114.9 (C^{C3}) , 67.6 (d, J = 16.0 Hz, $C^{3'}$), 61.8 (d, J = 6.5 Hz, C^{a}), 22.8 (d, J = 4.8 Hz, $C^{2'}$), 22.5 (d, J = 142.7 Hz, $C^{1'}$), 16.6 (d, J = 6.0 Hz, C^{b}). **^{31}P{^{1}H} NMR** (162 MHz, $CDCl_3$) δ/ppm: 31.6. **MP**: 136 °C. **IR** (solid, ν/cm^{-1}): 506 (s), 517 (s), 533 (m), 603 (m), 736 (m), 789 (s), 831 (m), 893 (m), 953 (m), 989 (m), 1015 (s), 1052 (m), 1183 (m), 1212 (m), 1230 (m), 1391 (m), 1440 (m), 1467 (m), 1514 (m), 1565 (m), 1582 (m), 1602 (w), 2980 (w), 3051 (w), 3446 (w). **MS** (MALDI-TOF, m/z): 504.3 $[M+H]^+$ (calc. 504.2), 526.3 $[M+Na]^+$ (calc. 526.2), 542.4 $[M+K]^+$ (calc. 542.2). **EA**: Found C 65.92 %, H 6.10 %, N 8.56 %, $C_{28}H_{30}N_3O_4P{\cdot}0.5H_2O$ requires C 65.62 %, H 6.10 %, N 8.20 %.

(3-(4-([2,2′:6′,2″-Terpyridin]-4′-yl)phenoxy)propyl)phosphonic acid (L2-P)

SM186

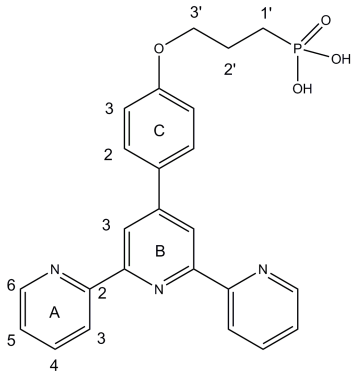

A solution of **L2-PEt** (60 mg, 119 µmol, 1.0 eq.) and bromotrimethylsilane (0.13 ml, 0.95 mmol, 8.0 eq.) in CH_2Cl_2 (20 ml) was stirred at room temperature for 16 h. The reaction was quenched by addition of water and the pH was brought to the basic range by addition of conc. aqueous NH_3. The formed solid was separated by filtration, washed with water followed by acetone and Et_2O, and dried. **L2-P** was isolated as a yellow solid (36 mg, 80.5 µmol, 68%).

^{1}H{^{13}P} NMR (500 MHz, DMSO-d_6) δ/ppm: 8.91 (d, J = 8.0 Hz, 2H, H^{A3}), 8.87 (d, J = 4.6 Hz, 2H. H^{A6}), 8.81 (s, 2H, H^{B3}), 8.30 (t, J = 7.7 Hz, 2H, H^{A4}), 8.00 (d, J = 8.6 Hz, 2H, H^{C2}), 7.75 (t, J = 6.4 Hz, 2H, H^{A5}), 7.17 (d, J = 8.6 Hz, 2H, H^{C3}), 4.14 (t, J = 6.5 Hz, 2H, $H^{3'}$), 1.97 (m, 2H, $H^{2'}$), 1.70 (m, 2H, $H^{1'}$). **^{13}C NMR** (126 MHz, DMSO-d_6) δ/ppm: 160.6 (C^{C4}), 152.9 (C^{A2}), 150.2 (C^{B4}), 147.2 (C^{A6}), 140.1 (C^{A4}), 129.1 (C^{C1}), 128.3 (C^{C2}), 125.3 (C^{A5}), 122.2 (C^{A3}), 118.4 (C^{B3}), 115.1 (C^{C3}), 67.5 ($C^{3'}$), 23.7 (d, J = 141.4 Hz, $C^{1'}$), 22.7 ($C^{2'}$). **^{31}P{^{1}H} NMR** (202 MHz, DMSO-d_6) δ/ppm: 25.8. **MP**: Dec. > 265 °C. **IR** (solid, ν/cm^{-1}): 527 (m), 536 (m), 545 (m), 571 (m), 599 (m), 741 (w), 782 (m), 833 (w), 1184 (w), 1239 (w), 1516 (m), 1591 (m). **MS** (MALDI-TOF, m/z): 448.2 $[M+H]^+$ (calc. 448.14), 470.3 $[M+Na]^+$ (calc. 470.1).

Methyl 4-(4-([2,2′:6′,2″-terpyridin]-4′-yl)phenoxy)butanoate (L2-CMe)

SM168

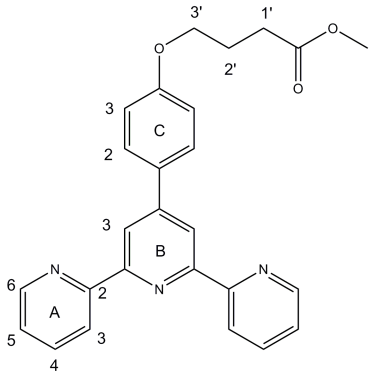

OH-tpy (240 mg, 738 µmol, 1.0 eq.) and potassium carbonate (357 mg, 2.58 mmol, 3.5 eq.) were added to a solution of 4-bromobutanoate (160 mg, 0.11 ml, 885 µmol, 1.2 eq.) in DMF (15 ml) and the mixture was stirred for 6 h at 80 °C. After cooling and removal of the solvent, the residue was suspended in water and extracted three times with CH_2Cl_2. The combined organic fractions were dried over $MgSO_4$ and the solvent was then removed. The product was purified by recrystallization (n-hexane/ethyl acetate). **L2-CMe** was obtained as a colourless solid (300 mg, 705 µmol, 95%).

^{1}**H NMR** (500 MHz, $CDCl_3$) δ/ppm: 8.72 (ddd, J = 4.8, 1.8, 0.9 Hz, 2H, H^{A6}), 8.70 (s, 2H, H^{B3}), 8.66 (dt, J = 8.0, 1.1 Hz, 2H, HA3), 7.86 (m, 4H, $H^{A4,C2}$), 7.34 (ddd, J = 7.5, 4.8, 1.2 Hz, 2H, H^{A5}), 7.01 (m, 2H, H^{C3}), 4.07 (t, J = 6.1 Hz, 2H, $H^{3'}$), 3.70 (s, 3H, H^{Me}), 2.57 (t, J = 7.3 Hz, 2H, $H^{1'}$), 2.16 (m, 2H, $H^{2'}$). ^{13}**C NMR** (126 MHz, $CDCl_3$) δ/ppm: 173.8 ($C^{C=O}$), 159.9 (C^{C4}), 156.5 (C^{A2}), 155.9 (C^{B2}), 149.8 (C^{B4}), 149.2 (C^{A6}), 137.0 (C^{A4}), 130.9(C^{C1}), 128.6 (C^{C2}), 123.9 (C^{A5}), 121.5 (C^{A3}), 118.4 (C^{B3}), 114.9 (C^{C3}), 66.9 ($C^{3'}$), 51.8 (C^{Me}), 30.6 ($C^{1'}$), 24.7 ($C^{2'}$). **MP**: 141 °C. **IR** (solid, ν/cm^{-1}): 512 (s), 578 (m), 607 (s), 659 (w), 739 (s), 791 (s), 833 (s), 886 (m), 987 (m), 1018 (m), 1036 (w), 1081 (w), 1114 (w), 1184 (s), 1229 (m), 1266 (s), 1366 (m), 1388 (m), 1418 (m), 1439 (m), 1470 (m), 1514 (s), 1549 (m), 1562 (m), 1582 (m), 1602 (m), 1732 (s), 2947 (w), 3053 (w). **MS** (MALDI-TOF, m/z): 426.5 $[M+H]^+$ (calc. 426.2), 448.6 $[M+Na]^+$ (calc. 448.2). **EA**: Found C 72.75, H 5.57, N 9.88% , $C_{26}H_{23}N_3O_3$ requires C 73.39 %, H 5.45 %, N 9.88 %.

4-(4-([2,2′:6′,2″-Terpyridin]-4′-yl)phenoxy)butanoic acid (L2-C)

SM170

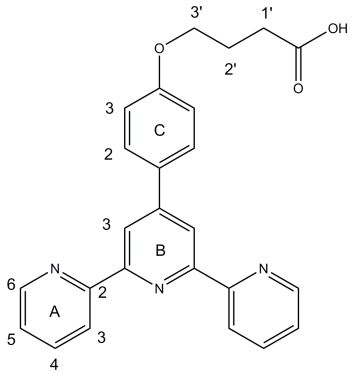

L2-CMe (80 mg, 188 µmol, 1.0 eq.) and potassium carbonate (260 mg, 1.88 mmol, 10 eq.) were stirred in MeOH/water (15ml/10ml) at 80 °C for 1 h. After cooling and removal of the organic solvent, the aqueous phase was diluted with water, neutralized with 1M HCl and extracted three times with CH_2Cl_2. The combined organic fractions were dried over $MgSO_4$ and the solvent was removed. **L2-C** was isolated as a colourless solid (54 mg, 131 µmol, 70%).

^{1}**H NMR** (500 MHz, DMSO-d$_6$) δ/ppm: 12.16 (s, 1H, H^{OH}), 8.76 (ddd, J = 4.8, 1.8, 0.8 Hz, 2H, H^{A6}), 8.68 (s, 2H, H^{B3}), 8.67 (dt, J = 8.0, 1.1 Hz, 2H, H^{A3}), 8.04 (td, J = 7.7, 1.8 Hz, 2H, H^{A4}), 7.89 (d, J = 8.8 Hz, 2H, H^{C2}), 7.53 (ddd, J = 7.5, 4.8, 1.2 Hz, 2H, H^{A5}), 7.14 (d, J = 8.8 Hz, 2H, H^{C3}), 4.08 (t, J = 6.4 Hz, 2H, H$^{3'}$), 2.43 (t, J = 7.3 Hz, 2H, H$^{1'}$), 1.99 (m, 2H, H$^{2'}$). ^{13}**C NMR** (126 MHz, DMSO-d$_6$) δ/ppm: 174.1 (C$^{C=O}$), 159.7 (C^{C4}), 155.6 (C^{B2}), 155.1 (C^{A2}), 149.3 (C^{A6}), 149.0 (C^{B4}), 137.5 (C^{A4}), 129.5 (C^{C1}), 128.2 (C^{C2}), 124.5 (C^{A5}), 120.9 (C^{A3}), 117.3 (C^{B3}), 115.3 (C^{C3}), 66.8 (C$^{3'}$), 30.1 (C$^{1'}$), 24.2 (C$^{2'}$). **MP**: 253 °C. **IR** (solid, ν/cm^{-1}): 518 (m), 610 (m), 629 (m), 725 (m), 744 (m), 768 (m), 787 (s), 838 (s), 987 (m), 1036 (m), 1190 (s), 1227 (m), 1249 (m), 1267 (m), 1287 (m), 1393 (m), 1441 (w), 1466 (m), 1518 (m), 1564 (m), 1584 (s), 1605 (m), 1693 (m), 1700 (m), 2478 (w), 2871 (w), 3063 (w). **MS** (MALDI-TOF, m/z): 412.4 [M+H]$^+$ (calc. 412.2), 368.3 [M-CO$_2$]$^+$ (calc. 368.2). **EA**: Found C 68.26 %, H 5.01 %, N 9.33 %, $C_{25}H_{21}N_3O_3 \cdot 1.5H_2O$ requires C 68.48 %, H 5.52 %, N 9.58 %.

S,*S*′-(([2,2′-Bipyridine]-4,4′-diylbis(oxy))bis(propane-3,1-diyl)) diethanethioate (L4-SAc)

SM111

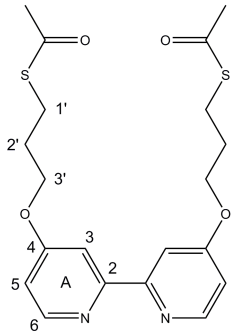

OH-bpy (226 mg, 1.2 mmol, 1.0 eq.) and K2CO3 (1.0 g, 7.24 mmol, 6.0 eq.) were added to a solution of **SC2** (500 mg, 2.54 mmol, 2.1 eq.) in DMF (15 ml) and the reaction mixture was stirred for 6 h at 80 °C. After cooling and removal of the solvent, the residue was suspended in water and extracted three times with CH_2Cl_2. The combined organic fractions were dried over $MgSO_4$ and the solvent was removed. The crude product was purified by column chromatography (SiO_2, cyclohexane/ethyl acetate 1:6, Rf = 0.2). **L4-SAc** was isolated as a colourless solid (0.43 g, 1.02 mmol, 85%).

^{1}**H NMR** (400 MHz, $CDCl_3$) δ/ppm: 8.46 (d, J = 5.7 Hz, 2H, H^{A6}), 7.95 (d, J = 2.5 Hz, 2H, H^{A3}), 6.83 (dd, J = 5.7, 2.6 Hz, 2H, H^{A5}), 4.18 (t, J = 6.0 Hz, 4H, $H^{3'}$), 3.07 (t, J = 7.1 Hz, 4H, $H^{1'}$), 2.34 (s, 6H, H^{Me}), 2.11 (m, 4H, $H^{2'}$). ^{13}**C NMR** (126 MHz, $CDCl_3$) δ/ppm: 195.8 ($C^{C=O}$, 166.0 (C^{A4}), 158.0 (C^{A2}), 150.3 (C^{A6}), 111.4 (C^{A5}), 106.8 (C^{A3}), 66.3 ($C^{3'}$), 30.8 (C^{Me}), 29.1 ($C^{2'}$), 25.9 ($C^{1'}$). **MP**: 134 °C. **IR** (solid, ν/cm^{-1}): 509 (m), 537 (m), 577 (m), 625 (s), 753 (m), 827 (s), 857 (m), 928 (m), 953 (m), 987 (m), 1026 (m), 1065 (m), 1105 (m), 1134 (s), 1181 (m), 1223 (m), 1243 (s), 1294 (s), 1348 (m), 1384 (m), 1408 (m), 1438 (m), 1454 (m), 1507 (m), 1538 (m), 1560 (s), 1581 (s), 1630 (m), 1687 (s), 2930 (w). **MS** (ESI, m/z): 421.2 $[M+H]^+$ (calc. 421.1). **EA**: Found C 57.19 %, H 5.83 %, N 6.55 %, $C_{20}H_{24}N_2O_4S_2$ requires C 57.12 %, H 5.75 %, N 6.66 %.

3,3′-([2,2′-Bipyridine]-4,4′-diylbis(oxy))bis(propane-1-thiol) (L4-S)

SM203

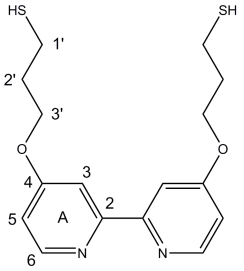

L4-SAc (30 mg, 71.3 µmol, 1.0 eq.) and NaOMe (6.5 mg, 114 µmol, 1.6 eq.) were stirred in anhydrous MeOH (5 ml) under an inert atmosphere at room temperature for 2 h. Dowex 50WX4 ion changer resin was added, stirred for 5 min., then removed by filtration and washed with MeOH. After removal of solvent from the filtrate, **L4-S** was isolated as a colourless solid (yield not determined).

^{1}**H NMR** (500 MHz, $CDCl_3$) δ/ppm: 8.46 (d, J = 5.5 Hz, 2H, H^{A6}), 7.96 (d, J = 2.6 Hz, 2H, H^{A3}), 6.83 (dd, J = 5.6, 2.6 Hz, 2H, H^{A5}), 4.26 (t, J = 5.9 Hz, 4H, $H^{3'}$), 2.75 (m, 4H, $H^{1'}$), 2.13 (m, 4H. $H^{2'}$), 1.41 (t, J = 8.1 Hz, 2H, H^{SH}). ^{13}**C NMR** (126 MHz, $CDCl_3$) δ/ppm: 166.0 (C^{A4}), 157.9 (C^{A2}), 150.3 (C^{A6}), 111.4 (C^{A5}), 106.9 (C^{A3}), 65.8 ($C^{3'}$), 33.1 ($C^{2'}$), 21.2 ($C^{1'}$). **IR** (solid, ν/cm^{-1}): 516 (m), 549 (m), 567 (m), 727 (w), 822 (m), 849 (m), 860 (w), 1019 (s), 1177 (m), 1208 (m), 1231 (m), 1255 (m), 1294 (m), 1313 (m), 1442 (m), 1458 (m), 1494 (m), 1558 (s), 1584 (s), 1607 (m), 2937 (w). **MS** (MALDI-TOF, m/z): 337.1 $[M+H]^+$ (calc. 337.1), 359.0 $[M+Na]^+$ (calc. 359.1), 375.0 $[M+K]^+$ (calc. 375.1).

Tetraethyl (([2,2′-bipyridine]-4,4′-diylbis(oxy))bis(propane-3,1-diyl))bis(phosphonate) (L4-PEt)

SM182

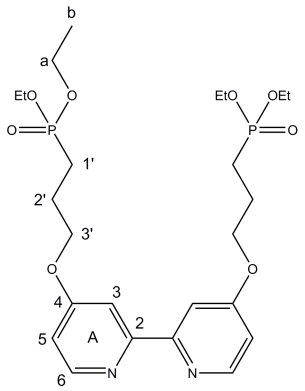

OH-bpy (150 mg, 797 µmol, 1.0 eq.) and potassium carbonate (0.55 g, 4.0 mmol, 5.0 eq.) were added to a solution of **SC3** (454 mg, 1.75 mmol, 2.2 eq.) in DMF (15 ml) and the reaction mixture was stirred for 5 h at 80 °C. After removal of the solvent, the residue was suspended in water and extracted three times with CH_2Cl_2. The combined organic fractions were dried over $MgSO_4$ and the solvent was then removed. The product was recrystallized from n-hexane/ethyl acetate, and **L4-PEt** was isolated as a colourless solid (280 mg, 514 µmol, 65%).

^{1}H{^{31}P} NMR (500 MHz, $CDCl_3$) δ/ppm: 8.45 (d, J = 5.6 Hz, 2H, H^{A6}), 7.94 (d, J = 2.5 Hz, 2H, H^{A3}), 6.81 (dd, J = 5.6, 2.6 Hz, 2H, H^{A5}), 4.18 (t, J = 6.1 Hz, 4H, $H^{3'}$), 4.10 (m, 8H, H^a), 2.13 (m, 4H, $H^{2'}$), 1.93 (m, 4H, $H^{1'}$), 1.32 (t, J = 7.1 Hz, 12H, H^b). **^{13}C NMR** (126 MHz, $CDCl_3$) δ/ppm: 165.9 (C^{A4}), 157.9 (C^{A2}), 150.3 (C^{A6}), 111.3 (C^{A5}), 106.9 (C^{A3}), 67.5 (d, J = 16.6 Hz, $C^{3'}$), 61.8 (d, J = 6.5 Hz, C^a), 22.6 (d, J = 4.8 Hz, $C^{2'}$), 22.4 (d, J = 143.1 Hz, $C^{1'}$), 16.6 (d, J = 6.0 Hz, C^b). **^{31}P{^{1}H} NMR** (162 MHz, $CDCl_3$) δ/ppm: 31.2. **MP**: 54 °C. **IR** (solid, ν/cm^{-1}): 518 (w), 550 (m), 749 (m), 783 (m), 824 (s), 850 (s), 865 (m), 959 (s), 1012 (s), 1217 (s), 1233 (s), 1304 (s), 1393 (w), 1460 (m), 1561 (m), 1582 (s), 2977 (w). **MS** (MALDI-TOF, m/z): 545.5 $[M+H]^+$ (calc. 545.2), 567.5 $[M+Na]^+$ (calc. 567.2), 583.5 $[M+K]^+$ (calc. 583.2). **EA**: Found C 52.38 %, H 7.05 %, N 5.34 % , $C_{24}H_{38}N_2O_8P_2$ requires C 52.94 %, H 7.03 %, N 5.14 %.

(([2,2′-Bipyridine]-4,4′-diylbis(oxy))bis(propane-3,1-diyl))bis(phosphonic acid) (L4-P)

SM188

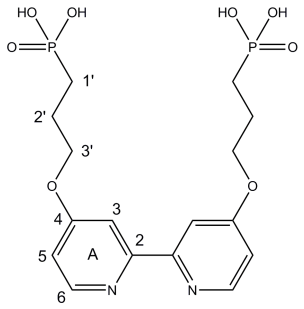

A solution of **L4-PEt** (50 mg, 92 µmol, 1.0 eq.) and bromotrimethylsilane (0.18 ml, 1.38 mmol, 15 eq.) in CH_2Cl_2 (20 ml) was stirred at room temperature for 19 h. The reaction was quenched by addition of water and the phases were separated. After neutralization of the aqueous phase with aqueous NH_3, the solvent was removed in vacuo to yield **L4-P** as a colourless solid (34 mg, 79 µmol, 86%).

^{1}**H{^{31}P} NMR** (500 MHz, D_2O) δ/ppm: 8.61 (d, J = 6.7 Hz, 2H, H^{A6}), 7.80 (s, 2H, H^{A3}), 7.38 (d, J = 6.7 Hz, 2H, H^{A5}), 4.41 (t, J = 6.3 Hz, 4H, $H^{3'}$), 2.12 (m, 4H, $H^{2'}$), 1.83 (m, 4H, $H^{1'}$). ^{13}**C NMR** (126 MHz, D_2O) δ/ppm: 169.4 (C^{A4}), 149.0 (C^{A2}), 147.0 (C^{A6}), 112.7 (C^{A5}), 110.3 (C^{A3}), 70.4 ($C^{3'}$), 24.1 (d, J = 134.6 Hz, $C^{1'}$), 22.8 (d, J = 3.9 Hz, $C^{2'}$). ^{31}**P{^{1}H} NMR** (202 MHz, D_2O) δ/ppm: 25.1. **IR** (solid, ν/cm^{-1}): 521 (s), 548 (s), 554 (s), 582 (s), 638 (s), 1017 (w), 1052 (w), 1117 (w), 1287 (m), 1337 (m), 1389 (s), 1586 (m), 1629 (m), 1688 (w), 2792 (m), 3010 (s), 3096 (m). **MS** (MALDI-TOF, m/z): 449.0 $[M+NH_3]^+$ (calc. 449.1), 433.2 $[M+H]^+$ (calc. 433.1).

Dimethyl 4,4′-([2,2′-bipyridine]-4,4′-diylbis(oxy))dibutyrate (L4-CMe)

SM175

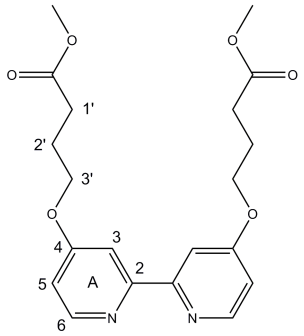

OH-bpy (250 mg, 1.33 mmol, 1.0 eq.) and potassium carbonate (0.92 g, 6.64 mmol, 5.0 eq.) were added to a solution of methyl 4-bromobutanoate (529 mg, 0.37 ml, 2.92 mmol, 2.2 eq.) in DMF (15 ml) and the mixture was stirred for 5 h at 80 °C. After removal of the solvent the residue was suspended in water and extracted three times with CH_2Cl_2. The combined organic fractions were dried over $MgSO_4$ and the solvent was removed. The crude product was purified by recrystallization (n-hexane/ethyl acetate). **L4-CMe** was obtained as a colourless solid (480 mg, 1.23 mmol, 93%).

^{1}**H NMR** (500 MHz, $CDCl_3$) δ/ppm: 8.45 (d, J = 5.6 Hz, 2H, H^{A6}), 7.94 (d, J = 2.5 Hz, 2H, H^{A3}), 6.82 (dd, J = 5.6, 2.6 Hz, 2H, H^{A5}), 4.18 (t, J = 6.1 Hz, 4H, $H^{3'}$), 3.69 (s, 6H, H^{Me}), 2.54 (t, J = 7.2 Hz, 4H, $H^{1'}$), 2.16 (m, 4H, $H^{2'}$). ^{13}**C NMR** (126 MHz, $CDCl_3$) δ/ppm: 173.5 ($C^{C=O}$), 166.0 (C^{A4}), 158.0 (C^{A2}), 150.3 (C^{A6}), 111.4 (C^{A5}), 106.8 (C^{A3}), 66.9 ($C^{3'}$), 51.9 (C^{Me}), 30.5 ($C^{1'}$), 24.5 ($C^{2'}$). **MP**: 144 °C.

IR (solid, ν/cm^{-1}): 579 (m), 766 (m), 846 (s), 881 (m), 976 (m), 1022 (s), 1087 (m), 1167 (s), 1190 (m), 1242 (m), 1277 (m), 1303 (m), 1369 (m), 1400 (m), 1436 (m), 1465 (m), 1560 (s), 1580 (s), 1729 (s), 2887 (w), 2957 (m), 3084 (w). **MS** (MALDI-TOF, m/z): 389.4 $[M+H]^+$ (calc. 389.2), 411.4 $[M+Na]^+$ (calc. 411.2), 427.4 $[M+K]^+$ (calc. 427.1). **EA**: Found C 61.54 %, H 6.34 %, N 7.16 % , $C_{20}H_{24}N_2O_6$ requires C 61.85 %, H 6.23 %, N 7.21 %.

4,4′-([2,2′-Bipyridine]-4,4′-diylbis(oxy))dibutyric acid (L4-C)

SM196

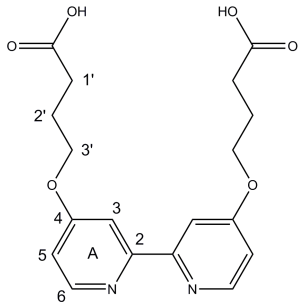

L4-CMe (80 mg, 206 µmol, 1.0 eq.) and NaOH (20.6 mg, 515 µmol, 2.5 eq.) were added to water (20 ml) and heated at reflux for 2 h. After filtering, the solution was neutralized with 1M HCl and a colourless precipitate formed that was separated by filtration and dried. **L4-C** was isolated as a colourless solid (65 mg, 180 µmol, 87.5%).

^{1}**H NMR** (500 MHz, DMSO-d_6) δ/ppm: 12.18 (s, 2H, H^{OH}), 8.48 (d, J = 5.6 Hz, 2H, H^{A6}), 7.91 (d, J = 2.6 Hz, 2H, H^{A3}), 7.03 (dd, J = 5.7, 2.6 Hz, 2H, H^{A5}), 4.16 (t, J = 6.4 Hz, 4H, $H^{3'}$), 2.41 (t, J = 7.3 Hz, 4H, $H^{1'}$), 1.99 (m, 4H, $H^{2'}$). ^{13}**C NMR** (126 MHz, DMSO-d_6) δ/ppm: 174.0 ($C^{C=O}$, 165.4 (C^{A4}), 156.7 (C^{A2}), 150.2 (C^{A6}), 110.7 (C^{A5}), 106.1 (C^{A3}), 66.8 ($C^{3'}$), 29.8 ($C^{1'}$), 23.7 ($C^{2'}$). **MP**: 229 °C. **IR** (solid, ν/cm^{-1}): 655 (m), 673 (m), 769 (m), 845 (s), 856 (s), 868 (m), 1021 (s), 1192 (s), 1247 (s), 1266 (s), 1280 (s), 1304 (m), 1391 (m), 1403 (m), 1457 (m), 1467 (s), 1559 (m), 1592 (s), 1712 (m), 2973 (w). **MS** (MALDI-TOF, m/z): 361.3 $[M+H]^+$ (calc. 361.1). **EA**: Found C 59.06 %, H 5.71 %, N 7.96 %, $C_{18}H_{20}N_2O_6 \cdot 0.5H_2O$ requires . C 58.53 %, H 5.73 %, N 7.58 %.

Methyl 2-chloroisonicotinate (P4)

SM41

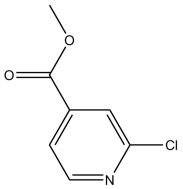

A solution of 2-chloroisonicotinic acid (0.5 g, 3.17 mmol, 1.0 eq.) and 4-dimethylaminopyridine (0.12 g, 0.95 mmol, 0.3 eq.) in CH_2Cl_2(30 ml) and MeOH (5 ml) was degassed with nitrogen for 10 min. *N*,*N′*-dicyclohexylcarbodiimide (0.85 g, 4.13 mmol, 1.3 eq.) was dissolved in CH_2Cl_2 (5 ml), degassed with nitrogen for 5 min. and added to the solution. After stirring for 3 h at rt, the solvent was removed and the residue was suspended in CH_2Cl_2. The suspension was cooled, filtered and the solvent was removed. This was repeated three times. The crude product was purified by column chromatography (SiO_2, ethyl acetate/cyclohexane 1:3, R_f = 0.21). **P4** was obtained as a colourless solid (0.4 g, 2.33 mmol, 73.5 %).

^{1}**H NMR** (400 MHz, $CDCl_3$) δ/ppm: 8.55 (dd, J = 5.0, 0.6 Hz, 1H), 7.89 (s, 1H), 7.77 (dd, J = 5.1, 1.3 Hz, 1H), 3.97 (s, 3H). The ^{1}H NMR spectroscopic data are in accord with the literature.[127]

Methyl [2,2′-bipyridine]-4-carboxylate (P5)

SM43

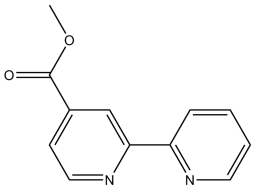

A microwave vial was charged with **P4** (0.4 g, 2.33 mmol, 1.0 eq.) and $Pd(PPh_3)_4$ (135 mg, 0.12 mmol, 0.05 eq.). The substances were dried under high vacuum for 10 min. Under nitrogen atmosphere, 2-pyridylzinc bromide (0.5M in THF, 7.0 ml, 3.5 mmol, 1.5 eq.) and anhydrous THF (5 ml) were added and the mixture was heated in a microwave reactor for 2 h at 115 °C. The resulting brown solution was diluted with saturated aq. $NaHCO_3$-solution (30 ml) and extracted four times with ethyl acetate. The combined organic fractions were dried over $MgSO_4$ and the solvent was removed. The obtained brown oil was diluted with CH_2Cl_2, filtered over a plug of SiO_2 and the solvent was removed. The crude product was purified by recrystallization from n-hexane. P5 was obtained as a colourless solid (0.27 g, 1.28 mmol, 55 %).

^{1}**H NMR** (250 MHz, $CDCl_3$) δ/ppm: 8.94 (dd, J = 1.5, 0.9 Hz, 1H), 8.83 (dd, J = 5.0, 0.8 Hz, 1H), 8.73 (ddd, J = 4.8, 1.7, 0.9 Hz, 1H), 8.43 (dt, J = 8.0, 1.0 Hz, 1H), 7.85 (m, 2H), 7.35 (ddd, J = 7.5, 4.8, 1.2 Hz, 1H), 3.99 (s, 4H). The ^{1}H NMR spectroscopic data are in accord with the literature.[128]

[2,2′-Bipyridine]-4-carboxylic acid (P6)

SM45

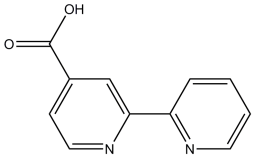

P5 (74 mg, 345 µmol) was refluxed for 2 h in a mixture of MeOH (5 ml) and aq. 1 M NaOH (2.5 ml). The organic solvent was removed and 0.5 M HCl was added to adjust pH to 2.5 - 3. The aqueous phase was extracted three times with ethyl acetate, the combined organic fractions were dried over $MgSO_4$ and the solvent was removed. **P6** was obtained as a colourless solid (40 mg, 200 µmol, 58 %).

^{1}**H NMR** (250 MHz, DMSO-d_6) δ/ppm: 8.87 (d, J = 4.9 Hz, 1H), 8.83 (s, 1H), 8.73 (dd, J = 4.7, 0.7 Hz, 1H), 8.42 (d, J = 7.9 Hz, 1H), 7.98 (td, J = 7.8, 1.8 Hz, 1H), 7.87 (dd, J = 4.9, 1.6 Hz, 1H), 7.50 (ddd, J = 7.5, 4.8, 1.1 Hz, 1H). The ^{1}H NMR spectroscopic data are in accord with the literature.[129]

6-(Acetylthio)hexyl [2,2′-bipyridine]-4-carboxylate (S1)

SM46

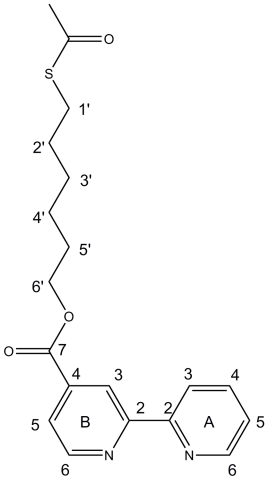

A solution of **P6** (76 mg, 379 µmol, 1.0 eq.), **SC1** (74 mg, 417 µmol, 1.1 eq.) and 4-dimethylaminopyridine (20 mg, 164 µmol, 0.4 eq.) in CH_2Cl_2 (50 ml) was degassed with nitrogen for 10 min. *N*,*N*′-dicyclohexylcarbodiimide (102 mg, 582 µmol, 1.5 eq.) was dissolved in CH_2Cl_2 (5 ml), degassed with nitrogen for 5 min. and added to the solution. After stirring for 20 h at rt, the solvent was removed and the residue was suspended in CH_2Cl_2. The suspension was cooled, filtered and the solvent was removed. This was repeated twice. The crude product was purified by column chromatography (SiO_2, ethyl acetate/cyclohexane 2:1 + 2 % MeOH, R_f = 0.61). **S1** was obtained as a colourless solid (86 mg, 240 µmol, 63 %).

^{1}**H NMR** (500 MHz, $CDCl_3$) δ/ppm: 8.90 (dd, J = 1.6, 0.9 Hz, 1H, H^{B3}), 8.80 (dd, J = 5.0, 0.9 Hz, 1H, H^{B6}6), 8.71 (ddd, J = 4.8, 1.8, 0.9 Hz, 1H, H^{A6}), 8.39 (dt, J = 8.0, 1.0 Hz, 1H, H^{A3}), 7.85 (dd, J = 5.0, 1.6 Hz, 1H, H^{B5}), 7.82 (td, J = 7.8 , 1.8 Hz, 1H, H^{A4}), 7.33 (ddd, J = 7.5, 4.8, 1.2 Hz, 1H, H^{A5}), 4.36 (t, J = 6.7 Hz, 2H, $H^{6'}$), 2.86 (t, J = 7.3, 2H, $H^{1'}$), 2.30 (s, 3H, H^{Me}), 1.79 (m, 2H, $H^{5'}$), 1.59 (m, 2H, $H^{2'}$), 1.45 (m, 4H, $H^{3',4'}$).

^{13}**C NMR** (126 MHz, $CDCl_3$) δ/ppm: 196.0 ($C^{C=O,Ac}$), 165.4 ($C^{C=O,B7}$), 157.4 (C^{B2}), 155.5 (C^{A2}), 150.0 (C^{B6}), 149.5(C^{A6}), 138.9 (C^{B4}), 137.1 (C^{A4}), 124.2 (C^{A5}), 122.9 (C^{B5}), 121.3 (C^{A3}), 120.5 (C^{B3}), 65.8 ($C^{6'}$), 30.7 (C^{Me}), 29.5 ($C^{2'}$), 29.0 ($C^{1'}$), 28.6 ($C^{3'}$), 28.5 ($C^{5'}$), 25.6 ($C^{4'}$).

[2,2′-Bipyridine] 1-oxide (P7)

SM228

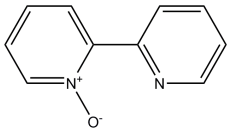

2,2′-Bipyridine (2.6 g, 16.6 mmol, 1.0 eq.) was dissolved in TFA (15 ml) and H_2O_2 (30 %, 2.6 ml, 25.5 mmol, 1.5 eq) was added. the mixture was stirred at rt for 4 h, neutralized with 3 M aq. NaOH-solution and extracted four times with CH_2Cl_2. The combined organic fractions were washed with sat. NaCl-solution, dried over $MgSO_4$ and the solvent was removed. **P7** was obtained as orange oil which solidified over night (1.72 g, 10.0 mmol, 60 %).

^{1}**H NMR** (250 MHz, $CDCl_3$) δ/ppm: 8.88 (d, J = 8.1 Hz, 1H), 8.71 (m, 1H), 8.31 (m, 1H), 8.17 (dd, J = 7.7, 1.8 Hz, 1H), 7.82 (m, 1H), 7.33 (m, 2H). The ^{1}H NMR spectroscopic data are in accord with the literature.[77]

4-Nitro-[2,2′-bipyridine] 1-oxide (P8)

SM229

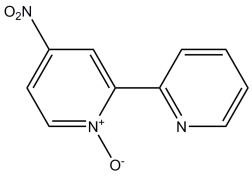

P7 (1.5 g, 8.71 mmol) was dissolved in conc. H_2SO_4 (8 ml) and cooled. A mixture of conc. H_2SO_4 (8 ml) and HNO_3 (68 %, 10 ml) was added slowly and the solution was stirred at 100 °C for 7.5 h. The reaction mixture was poured on ice and was made alkaline with 30% aq. NaOH-solution. The formed precipitate was filtered off, washed with water and diethyl ether and dried. **P8** was yielded as an off-white solid (0.95 g, 4.37 mmol, 50 %).

^{1}**H NMR** (250 MHz, $CDCl_3$) δ/ppm: 9.16 (d, J = 3.2 Hz, 1H), 8.89 (d, J = 8.1 Hz, 1H), 8.79 (d, J = 4.2 Hz, 1H), 8.36 (d, J = 7.2 Hz, 1H), 8.06 (dd, J = 7.2, 3.3 Hz, 1H), 7.88 (td, J = 7.9, 1.7 Hz, 1H), 7.43 (dd, J = 6.9, 5.0 Hz, 1H). The ^{1}H NMR spectroscopic data are in accord with the literature.[77]

4-Methoxy-[2,2′-bipyridine] 1-oxide (P9)

SM230

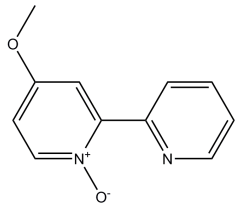

A solution of **P8** (300 mg, 1. 38 mmol, 1.0 eq.) and sodium methoxide (164 mg, 3.04 mmol, 2.2 eq.) in anhydrous MeOH (15 ml) was stirred at 60 °C under nitrogen atmosphere for 4.5 h. The solution was neutralized with 4 M HCl and the solvent was removed. The residue was suspended in water and extracted three times with CH_2Cl_2. The combined organic fractions were dried over $MgSO_4$ and the solvent was removed. **P9** was yielded as an off-white solid (191 mg, 945 µmol, 68 %).

^{1}**H NMR** (250 MHz, $CDCl_3$) δ/ppm: 9.04 (dt, J = 8.1, 1.1 Hz, 1H), 8.72 (ddd, J = 4.8, 1.8, 0.9 Hz, 1H), 8.21 (d, J = 7.3 Hz, 1H), 7.84 (ddd, J = 8.1, 7.6, 1.8 Hz, 1H), 7.74 (d, J = 3.6 Hz, 1H), 7.36 (ddd, J = 7.6, 4.8, 1.2 Hz, 1H), 6.84 (dd, J = 7.3, 3.6 Hz, 1H), 3.93 (s, 3H). The ^{1}H NMR spectroscopic data are in accord with the literature.[130]

4-Methoxy-2,2′-bipyridine (P10)

SM232

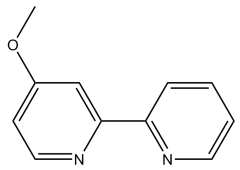

PBr_3 (0.21 ml, 2.23 mmol, 3.0 eq.) was added to a solution of **P9** (150 mg, 742 µmol, 1.0 eq.) in ethyl acetate (15 ml). The mixture was stirred at 75 °C for 2 h, poured on ice and was neutralized with 3 M aq. NaOH-solution. The aqueous phase was extracted three times with CH_2Cl_2 and the combined organic fractions were dried over $MgSO_4$. The solvent was removed and an oil was obtained which solidified upon cooling. **P10** was yielded as a brown solid (124 mg, 666 µmol, 90 %).

^{1}**H NMR** (250 MHz, $CDCl_3$) δ/ppm: 8.67 (ddd, J = 4.8, 1.8, 0.9 Hz, 1H), 8.49 (d, J = 5.7 Hz, 1H), 8.40 (dt, J = 8.0, 1.0 Hz, 1H), 7.98 (d, J = 2.5 Hz, 1H), 7.81 (td, J = 7.8, 1.8 Hz, 1H), 7.31 (ddd, J = 7.5, 4.8, 1.2 Hz, 1H), 6.85 (dd, J = 5.7, 2.6 Hz, 1H), 3.95 (s, 3H). The ^{1}H NMR spectroscopic data are in accord with the literature.[130]

[2,2′-Bipyridin]-4-ol (P11)

SM236

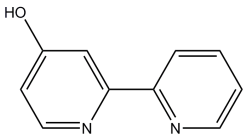

A solution of **P10** (0.55 g, 2.95 mmol, 1.0 eq.) and HBr (48 %, 2.0 ml, 17.7 mmol, 6.0 eq.) in glacial acetic acid (45 ml) was stirred under reflux for 21 h. The formed solid was filtered off, dissolved in H_2O and the solution was neutralized with aq. NH_3-solution. The aqueous phase was extracted four times with CH_2Cl_2, the combined organic fractions were dried over $MgSO_4$ and the solvent was removed. **P11** was obtained as a colourless solid (0.26 g, 1.51 mmol, 51 %).

^{1}**H NMR** (250 MHz, $CDCl_3$) δ/ppm: 8.65 (dt, J = 4.9, 1.5 Hz, 1H), 7.90 (m, 2H), 7.65 (d, J = 7.3 Hz, 1H), 7.42 (ddd, J = 6.4, 4.8, 2.4 Hz, 1H), 7.20 (d, J = 2.4 Hz, 1H), 6.56 (dd, J = 7.3, 2.4 Hz, 1H).

10-Bromodecan-1-ol (P12)

SM213

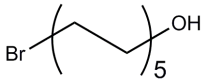

To a suspension of 1,10-decandiol (5.0 g, 28.7 mmol, 1.0 eq.) in toluene (50 ml) was added HBr (48 %, 3.8 ml, 33.4 mmol, 1.1 eq.) and the mixture was stirred under reflux for 64 h. H_2O (15 ml) was added to the yellow solution and the phases were separated. The organic phase was diluted with diethyl ether (25 ml) and washed with 1 M aq. NaOH-solution and saturated NaCl-solution. After drying over $MgSO_4$ the solvent was removed. The obtained dark-yellow liquid was purified by column chromatography (SiO_2, cyclohexane/ethyl acetate 2:1, $KMnO_4$, R_f = 0.32). **P12** was obtained as a pale-yellow liquid (5.13 g, 21.6 mmol, 75 %).

^{1}**H NMR** (250 MHz, $CDCl_3$) δ/ppm: 3.64 (t, J = 6.6 Hz, 2H), 3.40 (t, J = 6.9 Hz, 2H), 1.95 – 1.75 (m, 2H), 1.63 – 1.47 (m, 4H), 1.37 – 1.25 (m, 10H). The ^{1}H NMR spectroscopic data are in accord with the literature.[76]

10-([2,2′-Bipyridin]-4-yloxy)decan-1-ol (S5)

SM237

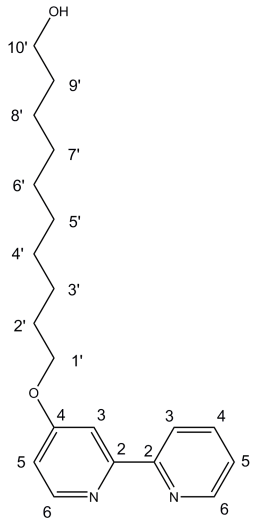

A mixture of **P11** (120 mg, 697 µmol, 1.0 eq.), **P12** (182 mg, 767 µmol, 1.1 eq.) and potassium carbonate (337 mg, 2.44 mmol, 3.5 eq.) in DMF (15 ml) was stirred at 80 °C for 5.5 h. The solvent was removed and the residue suspended in water. The aqueous phase was extracted three times with CH_2Cl_2, the combined organic fractions were dried over $MgSO_4$ and the solvent was removed. The crude product was purified by recrystallization from n-hexane. **S5** was obtained as a colourless solid (118 mg, 359 µmol, 51 %).

^{1}**H NMR** (500 MHz, $CDCl_3$) δ/ppm: 8.67 (ddd, J = 4.8, 1.8, 0.9 Hz, 1H, H^{A6}), 8.47 (d, J = 5.6 Hz, 1H, H^{B6}), 8.39 (dt, J = 8.0, 1.0 Hz, 1H, H^{A3}), 7.94 (d, J = 2.5 Hz, 1H, H^{B3}), 7.81 (ddd, J = 8.0, 7.5, 1.8 Hz,1H, H^{A4}), 7.31 (ddd, J = 7.5, 4.8, 1.2 Hz, 1H,H^{A5}), 6.83 (dd, J = 5.7, 2.5 Hz, 1H, H^{B5}), 4.13 (t, J = 6.5 Hz, 2H,$H^{1'}$), 3.64 (t, J = 6.8 Hz, 2H, $H^{10'}$), 1.82 (m, 2H, $H^{2'}$), 1.56 (m, 2H, $H^{9'}$), 1.47 (m, 2H, $H^{3'}$), 1.37 – 1.27 (m, 10H, $H^{4'-8'}$). ^{13}**C NMR** (126 MHz, $CDCl_3$) δ/ppm: 166.37 (C^{B4}), 158.03(C^{B2}), 156.20 (C^{A2}), 150.39 (C^{B6}), 149.17 (C^{A6}), 137.07 (C^{A4}), 123.94 (C^{A5}), 121.42 (C^{A3}), 111.31 (C^{B5}), 106.77 (C^{B3}), 68.19 ($C^{1'}$),63.19 ($C^{10'}$), 32.92 ($C^{9'}$), 29.60 (CH_2,$C^{4'-8'}$), 29.55 (CH_2,$C^{4'-8'}$), 29.49(CH_2,$C^{4'-8'}$), 29.37 (CH_2,$C^{4'-8'}$, 29.07 ($C^{2'}$), 26.04 ($C^{3'}$),25.85 (CH_2,$C^{4'-8'}$). **MS** (ESI, m/z): 329.4 $[M+H]^+$ (calc. 329.2). **EA**: Found C 72.15 %, H 8.56 %, N 8.05 % , $C_{20}H_{28}N_2O_2$ requires C 73.14 %, H 8.59 %, N 8.53 %.

10,10′-([2,2′-Bipyridine]-4,4′-diylbis(oxy))bis(decan-1-ol) (S6)

SM218

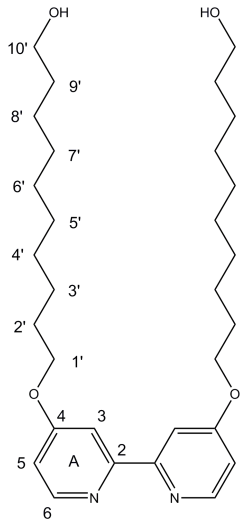

A mixture of **OH-bpy** (150 mg, 797 µmol, 1.0 eq.), **P12** (410 mg, 170 mmol, 2.1 eq.) and potassium carbonate (550 mg, 3.99 mmol, 5.0 eq.) in DMF (20 ml) was stirred at 85 °C for 5.5 h. The solvent was removed and the residue suspended in water. The aqueous phase was extracted four times with a mixture of ethyl acetate/CH_2Cl_2 (1:1), the combined organic fractions were dried over $MgSO_4$ and the solvent was removed. Purification was performed by suspending the crude product in boiling n-hexane prior to cooling and filtration. **S5** was obtained as a colourless solid (181 mg, 361 µmol, 45 %).

^{1}**H NMR** (500 MHz, $CDCl_3$) δ/ppm: 8.45 (d, J = 5.7 Hz, 2H, H^{A6}), 7.94 (d, J = 2.5 Hz, 2H, H^{A3}), 6.83 (dd, J = 5.7, 2.5 Hz, 2H, H^{A5}), 4.13 (t, J = 6.5 Hz, 4H, $H^{1'}$),3.64 (t, J = 6.6 Hz, 4H, $H^{10'}$),1.82 (m, 4H, $H^{2'}$), 1.56 (m, 4H,$H^{9'}$), 1.46 (m, 4H, $H^{3'}$), 1.38 - 1.28 (m, 20H, $H^{4'-8'}$).^{13}**C NMR** (126 MHz, $CDCl_3$) δ/ppm: 166.4 (C^{A4}), 157.7 (C^{A2}), 150.2 (C^{A6}), 111.5 (C^{A5}), 106.9 (C^{A3}), 68.2 ($C^{1'}$), 63.2 ($C^{10'}$), 32.9 ($C^{9'}$), 29.6 (CH_2, $C^{4'-8'}$), 29.5 (CH_2, $C^{4'-8'}$), 29.5 (CH_2, $C^{4'-8'}$), 29.3 (CH_2, $C^{4'-8'}$), 29.0 ($C^{2'}$), 26.0 ($C^{3'}$), 25.8 (CH_2, $C^{4'-8'}$). **MS** (ESI, m/z): 501.6 $[M+H]^+$ (calc 501.4). **EA**: Found C 70.34 %, H 9.63 %, N 5.95 %, $C_{30}H_{48}N_2O_4{\cdot}0.5H_2O$ requires C 70.69 %, H 9.69 %, N 5.50 %.

6-(2-(2,4-Dinitrophenyl)hydrazono)-1,10-phenanthrolin-5-one (L5)

IW43

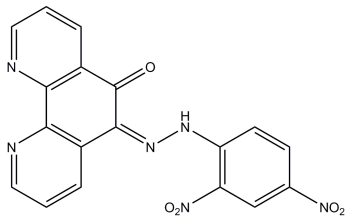

The precursor 1,10-phenanthroline-5,6-dione (phen-dione) was synthesized following the procedure reported by *Paw* and *Eisenberg*. [86] Phen-dione (1.0 g, 4.76 mmol, 1.0 eq.) was suspended in EtOH (15 ml) and conc. H_2SO_4 (3 ml) and added to a suspension of 2,4-dinitrophenylhydrazine (1.62 g, 5.71 mmol, 1.2 eq.) in EtOH (15 ml) and conc. H_2SO_4 (2 ml). The mixture was heated to reflux overnight. The formed orange precipitate was filtered off and washed with 5% aq. $NaHCO_3$-solution to remove residual acid, then washed with water. The solid was stirred as a suspension in hot EtOH/acetone to remove precursors. After filtering and drying the product **L5** was obtained as a bright orange solid (1.62 g, 4.1 mmol, 87 %).

^{1}**H NMR** (250 MHz, TFA-d) δ/ppm: 9.62 (dd, J = 8.4, 1.2 Hz, 1H), 9.40 (m, 2H), 9.25 (dd, J = 4.8, 1.5 Hz, 1H), 9.13 (m, 2H), 8.78 (d, J = 1.2 Hz, 2H), 8.33 (dd, J = 8.4, 5.6 Hz, 1H), 8.09 (dd, J = 8.1, 4.9 Hz, 1H).

Dimethyl [2,2′-bipyridine]-4,4′-dicarboxylate (dmcbpy)

SM64

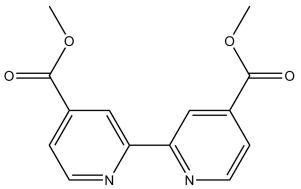

A mixture of **dcbpy** (372 mg, 1.52 mmol) and MeOH (60 ml) was cooled in an ice-bath and conc. H_2SO_4 (8 ml) was added. After refluxing for 15 h the clear solution was cooled to room temperature, added to 100 ml water and the pH was adjusted to 8 by addition of NaOH-solution. The aqueous phase was extracted twice with CH_2Cl_2, dried over $MgSO_4$ and the solvent was removed. **Dmcbpy** was obtained as a colorless solid (320 mg, 1.18 mmol, 77 %).

^{1}**H NMR** (400 MHz, $CDCl_3$, δ/ppm): 8.96 (dd, J = 1.6, 0.9 Hz, 2H), 8.86 (dd, J = 5.0, 0.8 Hz, 2H), 7.90 (dd, J = 5.0, 1.6 Hz, 2H), 4.00 (s, 6H). The ^{1}H NMR spectroscopic data are in accord with the literature.[131]

1,10-Phenanthroline-4,7-dicarbaldehyde (PDA)

SM73

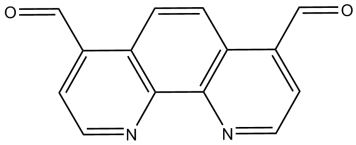

To a mixture of 4,7-dimethyl-1,10-phenanthroline (208 mg, 1.0 mmol, 1.0 eq.) and SeO_2 (464 mg, 4,18 mmol, 4.2 eq.) in 1,4-dioxane (25ml) were added 3 drops of water and the suspension was stirred under reflux for 3.5 h. The hot mixture was filtered over a plug of celite, the plug was washed with 1,4-dioxane and the resulting yellow solution was cooled. The formed precipitate was filtered off and dried. **PDA** was obtained as yellow needles (220 mg, 931 µmol, 93 %).

^{1} **H NMR** (400 MHz, $CDCl_3$) δ/ppm: 10.64 (s, 2H), 9.54 (d, J = 4.3 Hz, 2H), 9.23 (s, 2H), 8.10 (d, J = 4.3 Hz, 2H). The ^{1}H NMR spectroscopic data are in accord with the literature.[83]

7.3 Synthesis of complexes

Ru(pytpy)Cl_3

SM32

A solution 4′-(pyridin-4-yl)-2,2′:6′,2″-terpyridine (100 mg, 322 µmol) and $RuCl_3{\cdot}xH_2O$ (90 mg) in EtOH (20 ml) was refluxed for 3 h. The reaction mixture was filtered and the solid was dried. Ru(pytpy)Cl_3 was obtained as a black solid (132 mg, 255 µmol, 79%).

The product was used without further purification or chararterization

[Ru(pytpy)(L1)][PF_6]$_2$ (C1)

SM33

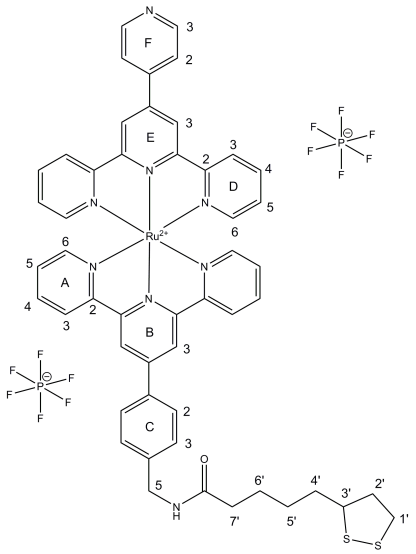

Ru(ptpy)Cl_3 (41 mg, 79 µmol, 1.04 eq.), **L1** (40 mg, 76 µmol, 1.0 eq.) and ethylene glycol (20 ml) were heated in a household microwave to reflux for 3 minutes. The red solution was cooled, diluted with water and aqueous NH_4PF_6-solution was added. The formed precipitate was filtered over Celite, washed with water and diethyl ether and dried in an airstream. The solid was dissolved in acetonitrile and the solvent was evaporated. **C1** was obtained as a red solid (67 mg, 54.6 µmol, 72 %).

^{1}**H-NMR** (500 MHz, CD_3CN) δ/ppm: 9.07 (s, 1H, H^{E3}), 9.06 (s, 1H, H^{E3}), 9.01 (s, 1H, H^{B3}), 9.00 (s, 1H, H^{B3}), 8.96 (m, 2H, H^{F3}), 8.66 (m, 4H, $H^{A3,D3}$), 8.15 (m, 4H, $H^{C2,F2}$), 7.96 (m, 4H, $H^{A4,D4}$), 7.65 (d, J = 8.2 Hz, 2H, H^{C3}), 7.44 (m, 4H, $H^{A6,D6}$), 7.20 (m, 4H,$H^{A5,D5}$), 7.03 (t, J = 6.0 Hz, 1H, H^{NH}), 4.52 (d, J = 6.1 Hz, 2H, H^{C5}), 3.62 (ddd, J = 12.3, 8.8, 6.4 Hz, 1H, $H^{3'}$), 3.19 (m, 1H, $H^{1'}$), 3.11 (m, 1H, $H^{1'}$), 2.46 (dt, J = 12.0, 6.5 Hz, 1H, $H^{2'}$), 2.27 (t, J = 7.3 Hz, 2H, $H^{7'}$), 1.90 (dd, J = 13.3, 6.4 Hz, 1H, $H^{2'}$), 1.75 (m, 1H, $H^{4'}$), 1.68 (m, 2H, $H^{6'}$), 1.62 (m, 1H, $H^{4'}$), 1.46 (m, 2H, $H^{5'}$). ^{13}**C-NMR** (126 MHz, CD_3CN) δ/ppm: 173.8 ($C^{C=O}$), 159.1 ($C^{A2/D2}$), 158.9 ($C^{A2/D2}$), 156.9 ($C^{B2/E2}$), 156.2 ($C^{B2/E2}$), 153.5 ($C^{A6/D6}$), 153.4 ($C^{A6/D6}$), 152.1 (C^{F3}), 139.1 ($C^{A4,D4}$), 129.5 (C^{C3}), 128.9 (C^{C2}), 128.6 ($C^{A5/D5}$), 128.4 ($C^{A5/D5}$), 125.7 ($C^{A3/D3}$), 125.5 ($C^{A3/D3}$), 122.9 (C^{F2}), 122.8 (C^{E3}), 122.7 (C^{E3}), 122.6 (C^{B3}), 57.5 ($C^{3'}$), 43.2 (C^{C5}), 41.1 ($C^{2'}$), 39.3 ($C^{1'}$), 36.6 ($C^{7'}$), 35.4 ($C^{4'}$), 29.6 ($C^{5'}$), 26.3 ($C^{6'}$). **IR** (solid, ν/cm^{-1}): 521 (s), 555 (s), 586 (m), 610 (m), 744 (m), 784 (m), 829 (s), 1025 (w), 1404 (m), 1468 (m), 1528 (m), 1601 (m),

1647 (m), 2925 (w), 3638 (w). **MS** (ESI, m/z): 469.1 $[M\text{-}2PF_6]^{2+}$ (calc. 469.1). **EA**: Found C 46.08 %, H 4.48 %, N 8.92 %, $C_{50}H_{44}F_{12}N_8OP_2RuS_2 \cdot 4H_2O$ requires C 46.19 %, H 4.03 %, N 8.62 %.

$[Ru(L1)_2][PF_6]_2$

SM35

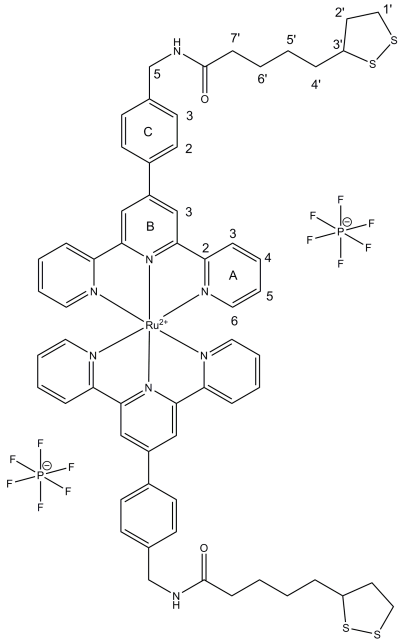

A solution of **L1** (150 mg, 285 µmol) and $RuCl_3 \cdot xH_2O$ (42 mg) in EtOH (15 ml) was heated in a microwave reactor at 130 °C for 2 h. The obtained red solution was cooled, diluted with water and aqueous NH_4PF_6-solution was added. The formed precipitate was filtered over Celite, washed with water and diethyl ether and dried in an airstream. The solid was dissolved in acetonitrile and the solvent was evaporated. $[Ru(L1)_2][PF_6]_2$ was obtained as a red solid (140 mg, 97 µmol, 68 %).

^{1}**H-NMR** (500 MHz, CD_3CN) δ/ppm: 9.00 (s, 4H, H^{B3}), 8.64 (d, J = 8.0 Hz, 4H, H^{A3}), 8.16 (d, J = 8.3 Hz, 4H, H^{C2}),7.94 (td, J = 8.0, 1.4 Hz, 4H, H^{A4}), 7.64 (d, J = 8.4 Hz, 4H, H^{C3}), 7.44 (dd, J = 4.9, 0.6 Hz, 4H, H^{A6}), 7.18 (m, 4H, H^{A5}), 7.07 (t, J = 6.2 Hz, 2H, H^{NH}), 4.52 (d, J = 6.1 Hz, 4H, H^{C5}), 3.61 (ddd, J = 12.2, 8.8, 6.4 Hz, 2H, $H^{3'}$), 3.18 (m, 2H, $H^{1'}$),3.10 (m, 2H, $H^{1'}$), 2.45 (tdd, J = 11.9, 6.5, 5.5 Hz, 2H, $H^{2'}$), 2.27 (t, J = 7.3 Hz, 4H, $H^{7'}$), 1.89 (dd, J = 12.8, 6.9 Hz, 2H, $H^{2'}$), 1.74 (m, 2H, $H^{4'}$), 1.66 (m, 4H, $H^{6'}$), 1.61 (m, 2H, $H^{4'}$), 1.44 (m, 4H, $H^{5'}$). ^{13}**C-NMR** (126 MHz, CD_3CN) δ/ppm: 174.0 ($C^{C=O}$), 159.2 (C^{A2}), 156.4 (C^{B2}), 153.4 (C^{A6}), 149.1 (C^{B4}), 143.4 (C^{C4}),139.0 (C^{A4}), 136.4 (C^{C1}), 129.5 (C^{C3}), 128.9 (C^{C2}), 128.5 (C^{A5}), 125.5 (C^{A3}), 122.5 (C^{B3}), 57.5 ($C^{3'}$), 43.3 (C^{C5}),41.1 ($C^{2'}$), 39.3 ($C^{1'}$), 36.6 ($C^{7'}$), 35.4 ($C^{4'}$), 29.6 ($C^{5'}$), 26.3 ($C^{6'}$). **MS** (ESI, m/z): 577.1 $[M\text{-}2PF_6]^{2+}$ (calc. 577.1).

$\mathbf{RuCl_2(cod)}$

SM54

A solution of 1,5-cyclooctadien (4.4 g, 5.0 ml, 40.7 mmol) and $RuCl_3 \cdot x\ H_2O$ (4 g, ∼ 14.5 mmol) in Ethanol (50 ml) was refluxed for 55 h. After cooling to room temperature the brown precipitate was filtered off, washed with Et_2O and dried. $\mathbf{RuCl_2(cod)}$ was obtained as a brown solid. (3.98 g, 14.2 mmol, 98 %).

$\mathbf{Ru(L3)_2Cl_2}$

SM55

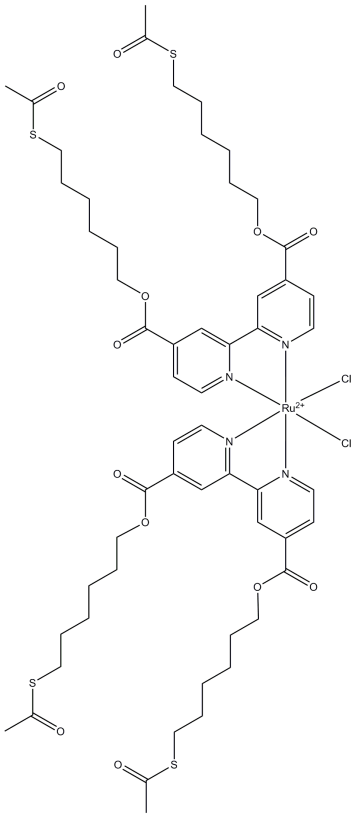

A microwave vial was charged with $\mathbf{RuCl_2(cod)}$ (50 mg, 178 µmol, 1.0 eq), **L3** (200 mg, 357 µmol, 2.0 eq) and DMF (12 ml) and heated in a microwave reactor for 1 h at 100 °C. The solvent was removed and $\mathbf{Ru(L3)_2Cl_2}$ was obtained as a dark green solid without further purification. (230 mg, quant. yield).

MS (MALDI-TOF, m/z): 1257.2 $[M\text{-}Cl]^+$(calc. 1257.3).

Ru[(L3)$_2$(L5)][PF$_6$]$_2$ (C2)

SM71

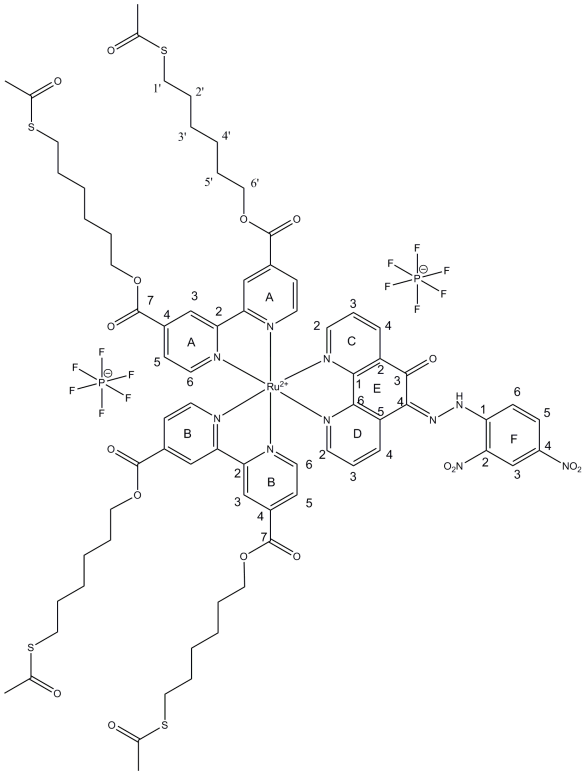

Ru(L3)$_2$Cl$_2$ (25mg, 19 µmol, 1.0 eq.) and **L5** (10 mg, 26 µmol, 1.3 eq.) were mixed with MeOH (4 ml), degassed with nitrogen for 5 min. and heated in a microwave reactor for 23 min. at 115 °C. The red solution was poured into water and aqueous NH_4PF_6-solution was added. The formed precipitate was filtered over Celite, washed with water and diethyl ether and dried in an airstream. The solid was dissolved in acetonitrile, the solvent was removed and the crude product was purified by recrystallization (EtOH/n-hexane) **C2** was obtained as a red solid (15 mg, 8 µmol, 41 %).

^{1}**H NMR** (500 MHz, CD_3CN) δ/ppm: 9.10 (d, J = 2.5 Hz, 1H, H^{F3}), 9.05 (d, J = 1.0 Hz, 4H, H^{A3,B3}), 8.97 (dd, J = 8.3, 1.0 Hz, 1H, H^{D4}), 8.85 (dd, J = 8.1, 1.3 Hz, 1H, H^{C4}), 8.69 (d, J = 9.4 Hz, 1H, H^{F6}), 8.59 (dd, J = 9.4, 2.5 Hz, 1H, H^{F5}), 8.00 (m, 1H, H^{C2}), 7.88 (d, J = 5.9 Hz, 4H, H^{A6,B6}), 7.83 (dd, J = 5.9, 1.7 Hz, 4H, H^{A5,B5}), 7.79 (dd, J = 5.4, 1.2 Hz, 1H, H^{D2}), 7.68 (dd, J = 8.1, 5.6 Hz, 1H, H^{C3}), 7.63 (dd, J = 8.4, 5.4 Hz, 1H, H^{D3}), 4.40 (t, J = 6.4 Hz, 8H, H$^{6'}$), 2.84 (m, 8H, H$^{1'}$), 2.25 (s, 12H, H^{Me}), 1.79 (m, 8H, H$^{5'}$), 1.55 (m, 8H, H$^{2'}$), 1.43 (m, 16H, H$^{3',4'}$). ^{13}**C NMR** (126 MHz, CD_3CN) δ/ppm: 196.6 (C$^{C=O}$), 178.4 (C^{E3}), 164.3 (C^{A7,B7}), 158.2 (C^{A2,B2}), 157.4 (C^{C2}), 155.8 (C^{E1}), 153.0 (C^{A6,B6}), 153.0 (C^{D2}), 148.5 (C^{E6}), 144.3 (C^{F4}), 143.3 (C^{F1}), 140.6 (C^{A4,B4}), 137.4 (C^{C4}), 136.1 (C^{F2}), 133.6 (C^{D4}), 133.1 (C^{E5}), 131.4 (C$^{E2/E4}$), 131.3 (C$^{E2/E4}$), 131.0 (C^{F5}), 129.0 (C^{D3}), 128.6 (C^{C3}), 127.7 (C^{A5,B5}), 125.0 (C^{A3,B3}), 123.4 (C^{F3}), 120.0 (C^{F6}), 67.5 (C$^{6'}$), 30.8 (C^{Me}), 30.2 (C$^{2'}$), 29.4 (C$^{1'}$), 28.9 (C$^{5'}$), 28.9 (C$^{3'}$), 26.0 (C$^{4'}$). **IR** (solid, ν/cm^{-1}): 510 (s), 515 (s), 527 (m), 555 (s), 621 (s), 726 (m), 740 (m), 824 (s), 953 (m), 1012 (m), 1029 (m), 1107 (m), 1134 (m), 1213 (m), 1246 (w), 1312 (m), 1336 (m), 1393 (w), 1442 (m), 1465 (m), 1485 (m), 1555 (m), 1609 (s), 1682 (s), 1973 (w), 2931 (w). **MS** (ESI, m/z): 1612.3 [M-2PF$_6$]$^+$ (calc. 1612.4), 806.2 [M-2PF$_6$]$^{2+}$(calc. 806.2). **EA**: Found C 46.74 %, H 4.86 %, N 6.74 %, $C_{74}H_{82}F_{12}N_{10}O_{17}P_2RuS_4$·EtOH requires C 46.84 %, H 4.55 %, N 7.19 %.

Ru(dmcbpy)$_2$Cl$_2$

SM65

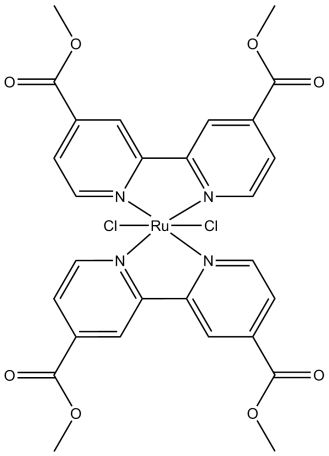

A solution of **dmcbpy** (200 mg, 735 µmol, 2.0 eq) and $RuCl_3 \cdot x\ H_2O$ (100 mg, 367 µmol, 1.0 eq) in ethanol (20 ml) was degassed with argon for 5 min and the mixture was refluxed under argon atmosphere for 5 h. The solvent was removed, the resulting solid was suspended in ethyl acetate, filtered, washed with ethyl acetate and dried. **Ru(dmcbpy)$_2$Cl$_2$** was obtained as a black solid (236 mg, 329 µmol, 90 %).

^{1}H NMR (250 MHz, $CDCl_3$) δ/ppm: 10.44 (d, J = 5.5 Hz, 2H), 8.84 (d, J = 1.3 Hz, 2H), 8.67 (d, J = 1.3 Hz, 2H), 8.16 (dd, J = 5.7, 1.4 Hz, 2H), 7.70 (d, J = 6.1 Hz, 2H), 7.49 (d, J = 5.8 Hz, 2H), 4.11 (s, 6H), 3.97 (s, 6H). The ^{1}H NMR spectroscopic data are in accord with the literature.[87]

[Ru(dmcbpy)$_2$(L5)] [PF$_6$]$_2$ (C2*)

SM69

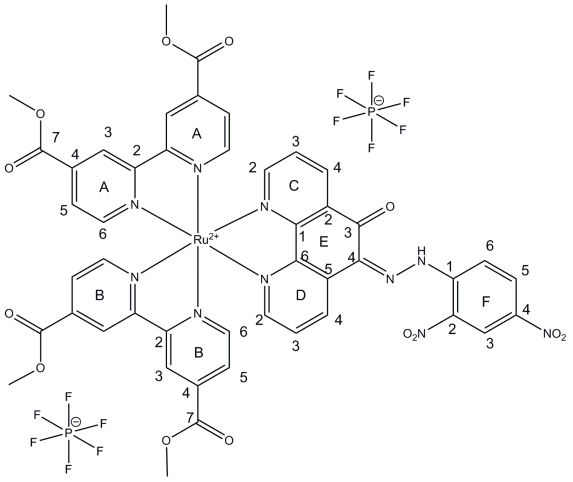

Ru(dmcbpy)$_2$Cl$_2$ (42 mg, 59 µmol, 1.0 eq.) and **L5** (23 mg, 59 µmol, 1.0 eq.) were mixed with MeOH (4 ml) and heated in a microwave reactor for 2.5 h at 120 °C. The red solution was poured into water and aqueous NH_4PF_6-solution was added. The formed precipitate was filtered over Celite, washed with water and diethyl ether and dried in an airstream. The solid was dissolved in acetonitrile, the solvent was removed and **C2*** was obtained as a red solid (54 mg, 41 µmol, 70 %).

^{1}**H NMR** (500 MHz, CD_3CN) δ/ppm: 9.09 (m, 4H, $H^{A3,B3}$), 9.06 (d, J = 2.5 H, 1H, H^{F3}), 8.97 (d, J = 7.5 Hz, 1H, H^{D4}), 8.84 (dd, J = 8.1, 1.3 Hz, 1H, H^{C4}), 8.69 (d, J = 9.4 Hz, 1H, H^{F6}), 8.58 (dd, J = 9.4, 2.5 Hz, 1H, H^{F5}), 8.02 (m, 2H, $H^{A6/B6}$) 8.01 (d, J = 5.6 Hz, 2H, ^{C2}) 7.96 (m, 2H. $H^{A6/B6}$), 7.85 (m, 4H, $H^{A5,B5}$), 7.79 (dd, J = 5.4, 1.0 Hz, 1H, H^{D2}), 7.68 (dd, J = 8.1, 5.5 Hz, 1H, H^{C3}), 7.63 (dd, J = 8.3, 5.4 Hz, 1H, H^{D3}), 4.01 (d, J = 1.9 Hz, 6H, H^{Me}), 3.99 (s, 6H, H^{Me}).^{13}**C NMR** (126 MHz, CD_3CN) δ/ppm: 178.5 (C^{E3}), 164.9 ($C^{A7,B7}$), 158.7 ($C^{A2/B2}$), 158.4 ($C^{A2/B2}$), 157.6 (C^{C2}), 155.9 (C^{E1}), 154.4 ($C^{A6/B6}$), 154.3 ($C^{A6/B6}$), 153.1 (C^{D2}), 148.6 (C^{E6}), 144.4 (C^{F4}), 143.4 (C^{F1}), 140.2 ($C^{A4,B4}$), 137.5 (C^{C4}), 136.1 (C^{F2}), 133.7 (C^{D4}), 133.2 (C^{E5}), 131.5 (C^{E4}), 131.3 (C^{E2}), 131.1 (C^{F5}), 129.1 (C^{D3}), 128.7 (C^{C3}), 127.6 ($C^{A5,B5}$), 124.9 ($C^{A3,B3}$), 123.4 (C^{F3}), 120.1 (C^{F6}), 54.1 (C^{Me})**. IR** (solid, ν/cm^{-1}): 517 (s), 539 (s), 551 (s), 555 (s), 615 (m), 697 (s), 831 (s), 980 (w), 1028 (w), 1074 (w), 1124 (m), 1256 (m), 1319 (m), 1487 (m), 1612 (w), 1722 (m), 3090 (w). **MS** (ESI, m/z): 1035.0 $[M\text{-}H,\text{-}2PF_6]^+$(calc. 1035.1), 518.1 $[M\text{-}2PF_6]^{2+}$ (calc. 518.1). **EA:** Found C 40.15 %, H 3.02 %, N 10.09 %, $C_{46}H_{34}F_{12}N_{10}O_{13}P_2Ru{\cdot}3H_2O$ requires C 40.04 %, H 2.92 %, N 10.15 %.

Ru(L4-SAc)$_2$Cl$_2$

SM113

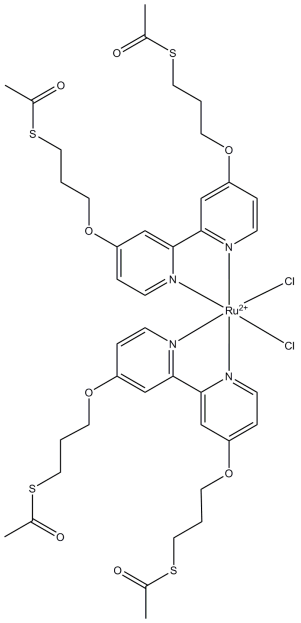

A microwave vial was charged with **RuCl$_2$(cod)** (60 mg, 214 µmol, 1.0 eq.), **L4-SAc** (180 mg, 428 µmol, 2.0 eq.) and DMF (15 ml) and heated in a microwave reactor for 1 h at 100 °C. The solvent was removed and **Ru(L4-SAc)$_2$Cl$_2$** was obtained as a dark red solid without further purification. (215 mg, quant. yield).

[Ru(L4-SAc)$_2$(L5)] [PF$_6$]$_2$ (C3)

SM114

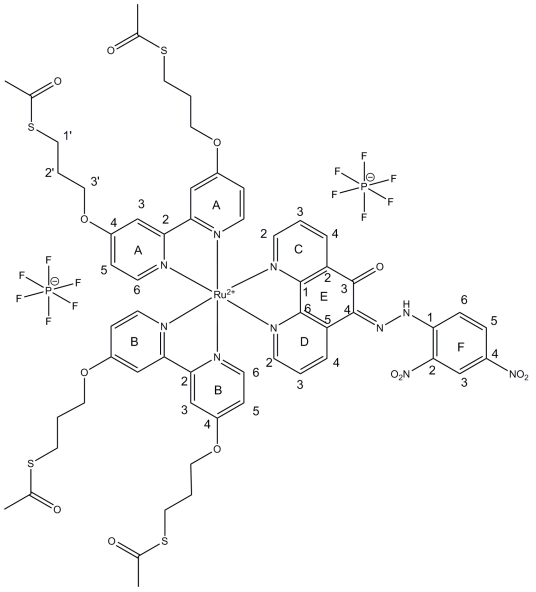

A mixture of **Ru(L4-SAc)$_2$Cl$_2$** (100 mg, 99 µmol, 1.0 eq.) and **L5** (46 mg, 118 µmol, 1.2 eq.) in MeOH (14 ml) was heated in a microwave reactor at 115 °C for 1.5 h. The resulting solution was poured into water and aqueous NH_4PF_6-solution was added. The formed precipitate was filtered over Celite, washed with water and diethyl ether and dried in an airstream. The solid was dissolved in acetonitrile, the solvent was removed, the red solid was dissolved in acetone (3 ml) and precipitated in petrol ether. Further purification was performed by recrystallization from EtOH. **C3** was obtained as a red solid. (90 mg, 55 µmol, 56 %).

^{1}**H NMR** (500 MHz, CD_3CN) δ/ppm: 9.10 (d, J = 2.5 Hz, 1H, H^{F3}), 8.87 (dd, J = 8.4, 1.2 Hz, 1H, H^{D4}), 8.76 (dd, J = 8.0, 1.4 Hz, 1H, H^{C4}), 8.69 (d, J = 9.6 Hz, 1H, H^{F6}), 8.59 (dd, J = 9.3, 2.6 Hz, 1H, H^{F5}), 8.14 (dd, J = 5.4, 1.4 Hz, 1H, H^{C2}), 7.96 (d, J = 2.6 Hz, 4H, H^{A3,B3}), 7.93 (m, 1H, H^{D2}), 7.65 (dd, J = 8.0, 5.5 Hz, 1H, H^{C3}), 7.61 (m, 1H, H^{D3}), 7.51 (d, J = 6.5 Hz, 4H, H^{A6,B6}), 6.91 (m, 4H, H^{A5,B5}), 4.24 (t, J = 6.1 Hz, 8H, H$^{3'}$), 3.02 (t, J = 7.1 Hz, 8H, H$^{1'}$), 2.30 (s, 12H, H^{Me}), 2.08 (m, 8H, H$^{2'}$). ^{13}**C NMR** (126 MHz, CD_3CN) δ/ppm: 196.3 (C$^{C=O}$), 179.0 (C^{E3}), 166.9 (C^{A4,B4}), 159.4 (C^{A2,B2}), 157.4 (C^{C2}), 157.0 (C^{E1}), 153.1 (C^{A6,B6}), 152.9 (C^{D2}) 149.8 (C^{E6}), 144.2 (C^{F4}), 143.5 (C^{F1}), 135.9 (C^{F2}), 135.5 (C^{C4}), 132.7 (C^{E5}), 131.8 (C^{E4}), 131.1 (C^{E2}), 131.0 (C^{F5}), 128.5 (C^{D3}) 128.1 (C^{C3}), 123.4 (C^{F3}), 119.9 (C^{F6}), 115.0 (C^{A5,B5}), 112.0 (C^{A3,B3}), 68.9 (C$^{3'}$), 30.8 (C^{Me}), 29.6 (C$^{2'}$), 26.0 (C$^{1'}$). **IR** (solid, ν/cm^{-1}): 557 (m), 585 (s), 613 (s), 825 (s), 955 (m), 1028 (s), 1131 (m), 1211 (m), 1333 (m), 1438 (m), 1484 (m), 1608 (s), 1682 (m), 1973 (w), 2928 (w), 3235 (w). **MS** (ESI, m/z): 666.1 [M-2PF$_6$]$^{2+}$(calc. 666.1), (MALDI-TOF, m/z) 1332.2 [M-2PF$_6$]$^+$(calc. 1332.2). **EA**: Found C 42.60 %, H 4.13 %, N 7.03 %, $C_{58}H_{58}F_{12}N_{10}O_{13}P_2RuS_4$·3$H_2O$ ·4EtOH requires C 42.60 %, H 4.77 %, N 7.53 %.

Ru[(dmcbpy)$_2$(PDA)][PF$_6$]$_2$ (C4)

SM74

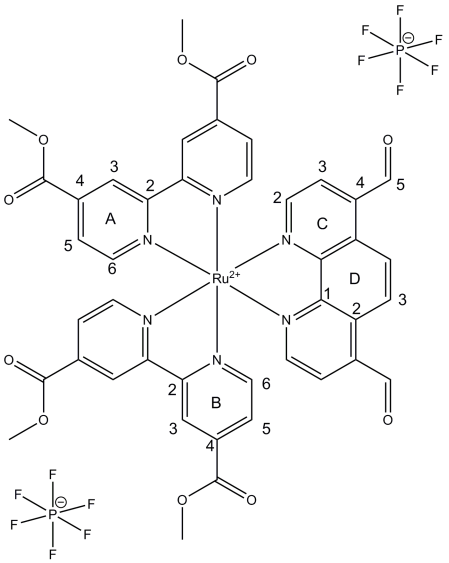

A mixture of **Ru(dmcbpy)$_2$Cl$_2$** (50 mg, 69.8 µmol, 1.0 eq.) and **PDA** (19 mg, 80.4 µmol, 1.1 eq.) in MeOH (4 ml) was heated in a microwave reactor at 115 °C for 30 min. The red solution was diluted with water and and aqueous NH_4PF_6-solution was added. The formed precipitate was filtered over Celite, washed with diethyl ether and dried in an airstream. The solid was dissolved in acetonitrile and the solvent was removed. The red solid was dissolved in hot ethyl acetate (5 ml) and n-hexane was added until a precipitate was formed. **C4** was obtained as a red solid (27 mg, 23 µmol, 33 %).

^{1}**H NMR** (500 MHz, CD_3CN) δ/ppm: 10.62 (s, 2H, H^{C5}), 9.35 (s, 2H, H^{D3}), 9.12 (m, 2H, H^{A3}), 9.08 (m, 2H, H^{B3}), 8.41 (d, J = 5.4 Hz, 2H, H^{C2}), 8.15 (d, J = 5.4 Hz, 2H, H^{C3}), 7.98 (dd, J = 5.8, 0.6 Hz, 2H, H^{A6}) 7.89 (dd, J = 5.8, 1.8 Hz, 2H, H^{A5}), 7.69 (m, 2H, H^{B6}) 7.67 (dd, J = 5.7, 1.7 Hz, 2H, H^{B5}), 4.02 (s, 6H, H^{Me}), 3.96 (s, 6H, H^{Me}). ^{13}**C NMR** (101 MHz, CD_3CN) δ/ppm: 192.9 (C^{C5}), 164.7 ($C^{C=O}$), 158.3 ($C^{A2,B2/A4,B4}$), 158.2 ($C^{A2,B2/A4,B4}$), 155.5 (C^{C2}), 154.2 ($C^{A6,B6}$) , 149.0 (C^{D1}), 137.9 (C^{C4}), 130.1 (C^{C3}3), 128.4 (C^{D2}), 127.8 (C^{D3}), 127.7 (C^{A5}), 127.6 (C^{B5}), 125.0 (C^{A3}), 124.9 (C^{B3}), 54.0 (C^{Me}). **MS** (MALDI-TOF, m/z): 1027.3 [M-PF$_6$]$^+$ (calc. 1027.1), 882.2 [M-2PF$_6$]$^+$ (calc. 882.1). **EA**: Found C 44.41 %, H 3.99 %, N 7.85 %, $C_{42}H_{32}F_{12}N_6O_{10}P_2Ru$·MeCN· EtOAc requires C 44.32 %, H 3.33 %, N 7.54 %.

Ru[(L4-SAc)$_2$(PDA)][PF$_6$]$_2$ (C5)

SM119

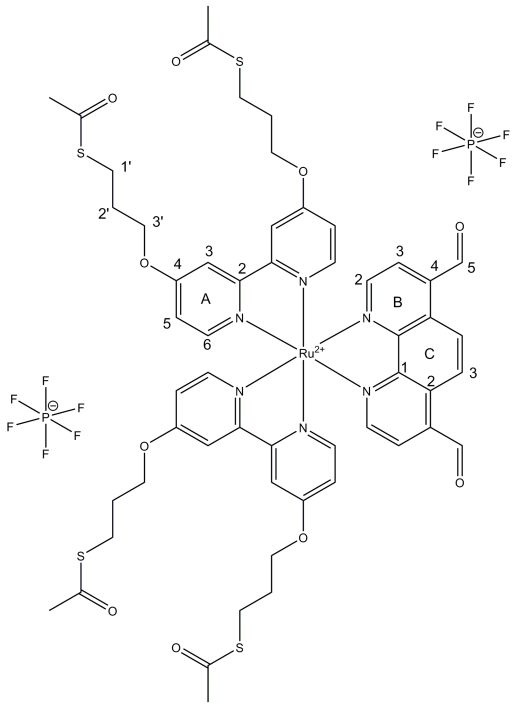

Ru(L4-SAc)$_2$Cl$_2$ (101 mg, 100 µmol, 1.0 eq.) and **PDA** (28 mg, 120 µmol, 1.2 eq.) were dissolved in aqueous EtOH (66 Vol%, 30 ml), degassed with argon for 20 min. and refluxed under inert atmosphere for 22 h. Aqueous NH_4PF_6-solution was added, the organic solvent was removed and the formed precipitate filtered off. The solid was washed with water, dissolved in CH_2Cl_2 and the solution was dried over $MgSO_4$. The solvent was removed and the crude product was purified by recrystallization from ethyl acetate/n-hexane. **C5** was obtained as a red solid (86 mg, 46 µmol, 46%).

^{1}**H NMR** (500 MHz, CD_3CN) δ/ppm: 10.61 (s, 2H, H^{B5}), 9.35 (s, 2H, H^{C3}), 8.56 (d, J = 5.4 Hz, 2H, H^{B2}), 8.12 (d, J = 5.4 Hz, 2H, H^{B3}), 7.96 (m, 4H, H^{A3}), 7.51 (m, 4H, H^{A6}), 6.91 (m, 4H, H^{A5}), 4.24 (t, J = 6.0 Hz, 8H, $H^{3'}$), 3.01 (m, 8H, $H^{1'}$), 2.30 (s, 12H, H^{Me}), 2.07 (m, 8H, $H^{2'}$). ^{13}**C NMR** (101 MHz, CD_3CN) δ/ppm: 196.4 ($C^{C=O}$), 192.9 (C^{B5}) 166.8 (C^{A4}), 159.3 (C^{A2}), 155.3 (C^{B2}), 153.3 (C^{A6}), 150.4 (C^{C1}), 136.6 (C^{B4}), 129.9 (C^{B3}), 128.1 (C^{C2}), 127.7 (C^{C3}), 115.1 (C^{A5}), 112.3 (C^{A3}), 69.0 ($C^{3'}$) 30.8 (C^{Me}), 29.6 ($C^{2'}$), 260.0 ($C^{1'}$). **IR** (solid, ν/cm^{-1}): 555 (s), 587 (s), 592 (s), 615 (s), 669 (m), 826 (s), 955 (m), 1031 (m), 1111 (w), 1130 (w), 1215 (m), 1254 (w), 1332 (w), 1440 (m), 1488 (w), 1555 (w), 1609 (m), 1685 (m), 2923 (w). **MS**: (LC-ESI, m/z): 589.0 [M-2PF$_6$]$^{2+}$ (calc. 589.1).

[Ir(ppy)$_2$(L4-SAc)][PF$_6$] (C6)

SM149/IW162

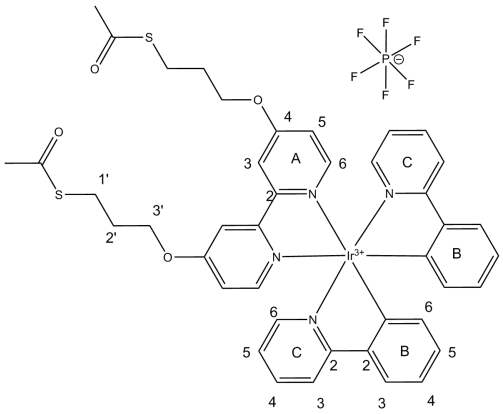

A solution of **L4-SAc** (50 mg, 118 µmol, 2.1 eq.) and the dimer **Ir$_2$(ppy)$_4$Cl$_2$**(60 mg, 56 µmol, 1.0 eq.) in MeOH (4 ml) was degassed with nitrogen for 5 min. and heated in a microwave reactor at 120 °C for 2 h. NH_4PF_6 (91 mg, 560 µmol, 10 eq.) was added to the cooled solution and after stirring for 30 min. at rt the solvent was removed. The residue was dissolved in CH_2Cl_2, filtered over celite and the solvent was removed. The crude product was purified by column chromatography (SiO_2, CH_2Cl_2, 2 % MeOH, $R_f = 0.23$). The obtained oil was dissolved in CH_2Cl_2 and precipitated with n-pentane. **C6** was yielded as a yellow solid (75 mg, 70 µmol, 63 %).

^{1}**H NMR** (500 MHz, CD_3CN) δ/ppm: 8.05 (d, J = 8.0 Hz, 2H, H^{C3}), 7.96 (d, J = 2.6 Hz, 2H, H^{A3}), 7.85 (m, 2H, H^{C4}), 7.78 (dd, J = 7.80, 1.1 Hz, 2H, H^{B3}), 7.71 (d, J = 6.4 Hz, 2H, H^{A6}), 7.65 (m, 2H, H^{C6}), 7.03 (m, 4H, H^{B4,C5}), 6.98 (dd, J = 6.4, 2.6 Hz, 2H, H^{A5}), 6.89 (td, J = 7.4, 1.3 Hz, 2H, H^{B5}), 6.27 (dd, J = 7.6, 0.8 Hz, 2H, H^{B6}), 4.25 (t, J = 6.1 Hz, 4H, H$^{3'}$), 3.01 (t, J = 7.2 Hz, 4H, H$^{1'}$), 2.30 (s, 6H, H^{Me}), 2.07 (p, J = 6.4 Hz, 4H, H$^{2'}$). ^{13}**C NMR** (126 MHz, CD_3CN) δ/ppm: 196.3 (C$^{C=O}$), 168.5 (C^{C2}), 167.9 (C^{A4}), 158.3 (C^{A2}), 152.3 (C^{A6}), 151.8 (C^{B1}), 149.9 (C^{C6}), 145.1 (C^{B2}), 139.3 (C^{C4}), 132.5 (C^{B6}) , 131.2 (C^{B5}), 125.7 (C^{B3}), 124.3 (C^{C5}), 123.2 (C^{B4}), 120.6 (C^{C3}), 115.3 (C^{A5}), 112.4 (C^{A3}), 69.0 (C$^{3'}$), 30.8 (C^{Me}), 29.5 (C$^{2'}$), 25.9 (C$^{1'}$). **IR** (solid, ν/cm^{-1}): 515 (m), 524 (m), 544 (m), 557 (s), 576 (w), 628 (m), 730 (s), 737 (s), 757 (s), 794 (w), 834 (s), 876 (m), 955 (m), 1031 (s), 1063 (w), 1134 (w), 1219 (m), 1249 (m), 1267 (w), 1314 (m), 1334 (m), 1419 (m), 1439 (m), 1477 (s), 1556 (m), 1582 (m), 1607 (s), 1683 (m), 1766 (w), 3055 (w). **MS** (LC-ESI, m/z): 921.3 [M-PF$_6$]$^+$ (calc. 921.2).

[Ir(fppy)$_2$(L4-SAc)][PF$_6$] (C7)

SM152

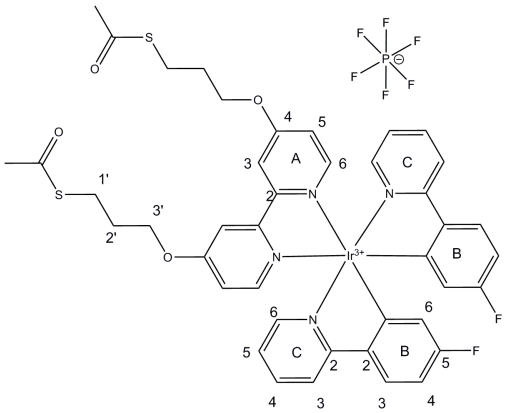

A solution of **L4-SAc** (48 mg, 115 µmol, 2.1 eq.) and the dimer **Ir$_2$(fppy)$_4$Cl$_2$** (60 mg, 53 µmol, 1.0 eq.) in MeOH (15 ml) was degassed with nitrogen for 5 min. and heated in a microwave reactor at 120 °C for 2 h. NH_4PF_6 (86 mg, 530 µmol, 10 eq.) was added to the cooled solution and after stirring for 30 min. at rt water was added until a precipitate was formed. The formed solid was filtered off, washed with aq. MeOH and diethyl ether and dried in an airstream. The crude product was purified by column chromatography (SiO_2, CH_2Cl_2, 2 % MeOH, R_f = 0.35). The obtained oil was dissolved in CH_2Cl_2 and precipitated with n-pentane. **C7** was yielded as a yellow solid (29 mg, 26 µmol, 25 %).

^{1}H NMR (500 MHz, CD_3CN) δ/ppm: 8.02 (ddd, J = 8.5, 1.4, 0.7 Hz, 2H, H^{C3}), 7.97 (d, J = 2.7 Hz, 2H, H^{A3}), 7.86 (m, 4H, H^{B3,C4}), 7.73 (d, J = 6.4 Hz, 2H, H^{A6}), 7.62 (ddd, J = 5.7, 1.6, 0.8 Hz, 2H, H^{C6}), 7.07 (ddd, J = 7.4, 5.8, 1.4Hz, 2H, H^{C5}), 6.99 (dd, J = 6.4, 2.6 Hz, 2H, H^{A5}), 6.80 (td, J = 9.0, 2.6 Hz, 2H, H^{B4}), 5.87 (dd, J = 9.6, 2.6 Hz, 2H, H^{B6}), 4.26 (t, J = 6.1 Hz, 4H, H$^{3'}$), 3.02 (t, J = 7.2 Hz, 4H, H$^{1'}$), 2.30 (s, 6H, H^{Me}), 2.07 (p, J = 6.3 Hz, 4H, H$^{2'}$). **^{13}C NMR** (126 MHz,)CD_3CN) δ/ppm: 196.3 (C$^{C=O}$), 168.1 (C^{A4}), 167.3 (C^{C2}) 165.60/163.59 (d,C B5), 158.2 (C^{A2}), 154.8 (C^{B1}), 152.5 (C^{A6}), 149.9 (C^{C6}), 141.5 (C^{B2}), 139.6 (C^{C4}), 128.0 (C^{B3}), 124.3 (C^{C5}), 120.9 (C^{C3}), 118.3 (C B6 unter Lsm), 115.4 (C^{A5}), 112.6 (C^{A3}), 110.3 (C^{B4}), 69.1 (C$^{3'}$), 30.8 (C^{Me}), 29.5 (C$^{2'}$), 25.9 (C$^{1'}$). **^{19}F NMR** (376 MHz, CD_3CN) δ/ppm: -111.25. **IR** (solid, ν/cm^{-1}): 556 (s), 625 (w), 752 (m), 774 (s), 834 (s), 956 (w), 1029 (m), 1133 (w), 1187 (m), 1224 (m), 1250 (m), 1315 (w), 1334 (m), 1433 (m), 1446 (m), 1481 (m), 1555 (m), 1594 (m), 1609 (s), 1685 (w), 3404 (w). **MS** (MALDI-TOF, m/z): 957.7 [M-PF$_6$]$^+$ (calc. 957.2). **EA**: Found C 44.87 %, H 3.50 %, N 5.35 %, $C_{42}H_{38}F_8IrN_4O_4PS_2{\cdot}H_2O$ requires C 45.04 %, H 3.60 %, N 5.00 %.

[Ir(dfppy)$_2$(L4-SAc)][PF$_6$] (C8)

SM151

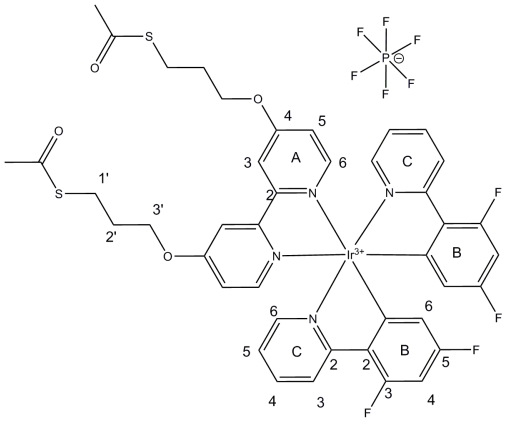

A solution of **L4-SAc** (54 mg, 127 µmol, 2.1 eq.) and the dimer **Ir$_2$(dfppy)$_4$Cl$_2$** (70 mg, 58 µmol, 1.0 eq.) in MeOH (15 ml) was degassed with nitrogen for5 min. and heated in a microwave reactor at 120 °C for 2 h. NH_4PF_6 (95 mg, 580 µmol, 10 eq.) was added to the cooled solution and after stirring for 30 min. at rt water was added until a precipitate was formed. The solid was filtered off, washed with aq. EtOH (70 %vol.) and diethyl ether and dried in an airstream. The crude product was purified by column chromatography (SiO_2, CH_2Cl_2, 2 % MeOH, $R_f = 0.28$). The obtained oil was dissolved in CH_2Cl_2 and precipitated with n-pentane. **C8** was yielded as a yellow solid (90 mg, 79 µmol, 69 %).

^{1}**H NMR** (400 MHz, CD_3CN) δ/ppm: 8.31 (dt, J = 8.6, 1.0 Hz, 2H, H^{C3}), 7.97 (d, J = 2.7 Hz, 2H, H^{A3}), 7.91 (m, 2H, H^{C4}), 7.74 (d, J = 6.4 Hz, 2H, H^{A6}), 7.67 (ddd, J = 5.7, 1.5, 0.7 Hz, 2H, H^{C6}), 7.11 (ddd, J = 7.4, 5.8,1.4 Hz, 2H, H^{C5}), 7.00 (dd, J = 6.4, 2.6 Hz, 2H, H^{A5}), 6.67 (ddd, J = 12.8, 9.4, 2.4 Hz, 2H, H^{B4}), 5.73 (dd, J = 8.6, 2.4 Hz, 2H, H^{B6}), 4.27 (t, J = 6.1 Hz, 4H , H$^{3'}$), 3.02 (t, J = 7.1 Hz, 4H, H$^{1'}$), 2.30 (s, 6H, H^{Me}), 2.08 (m, 4H, H$^{2'}$). ^{13}**C NMR** (126 MHz, CD_3CN) δ/ppm: 196.3 (C$^{C=O}$), 168.3 (C^{A4}), 164.7 (C^{C2}), 163.4 (C^{B5}),161.3 (C^{B3}), 158.0 (C^{A2}), 155.9 (C^{B1}), 152.6 (C^{A6}), 150.3 (C^{C6}), 140.3 (C^{C4}),129.0 (C^{B2}), 124.7 (C^{C5}), 124.5 (C^{C3}),115.5 (C^{A5}), 114.6 (C^{B6}), 112.7 (C^{A3}), 99.4 (C^{B4}), 69.1 (C$^{3'}$), 30.8 (C^{Me}), 29.5 (C$^{2'}$), 25.9 (C$^{1'}$). ^{19}**F NMR** (376 MHz, CD_3CN) δ/ppm: -108.48 (d, J = 10.4 Hz), -110.28 (d, J = 10.5 Hz). **IR** (solid, ν/cm^{-1}): 515 (s), 526 (s), 536 (s), 542 (s), 556 (s), 567 (s), 713 (m), 719 (m), 737 (m), 756 (m), 788 (m), 827 (s), 985 (s), 1030 (m), 1041 (m), 1104 (m), 1164 (w), 1224 (m), 1247 (m), 1265 (w), 1295 (m), 1318 (m), 1339 (m), 1404 (m), 1428 (m), 1448 (w), 1478 (m), 1491 (w), 1556 (s), 1573 (m), 1601 (s), 1687 (m), 3086 (w). **MS**: (LC-ESI, m/z): 993.2 [M-PF$_6$]$^+$ (calc. 993.2). **EA**: Found C 43.74 %, H 3.46 %, N 5.04 %, $C_{42}H_{36}F_{10}IrN_4O_4PS_2{\cdot}H_2O$ requires C 43.64 %, H 3.31 %, N 4.85 %.

[Fe(MeO-tpy)$_2$][PF$_6$]$_2$

SM167

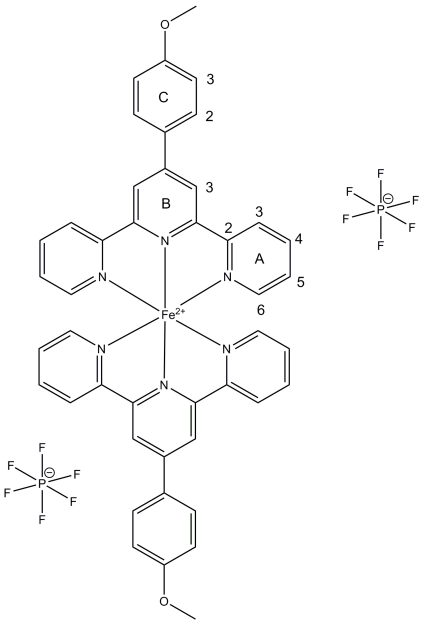

MeO-tpy (76 mg, 197 µmol, 1.7 eq.) was dissolved in hot MeOH (15 ml) and mixed with a solution of $FeCl_2$ (15 mg, 118 µmol,1.0 eq.) in water (5 ml). The resulting purple solution was stirred at rt for 20 min. and NH_4PF_6 was added. After stirring for another 20 min. the formed solid was filtered over Celite, washed with water and diethyl ether and dried in an airstream. The solid was dissolved in MeCN and the solvent was removed. The crude product was purified by recrystallization (EtOH/cyclohexane). **[Fe(MeO-tpy)$_2$][PF$_6$]$_2$** was obtained as a purple solid (79 mg, 77 µmol, 65 %).

^{1}**H NMR** (500 MHz, CD_3CN) δ/ppm: 9.15 (s, 4H, H^{B3}), 8.61 (d, J = 8.1 Hz, 4H, H^{A3}), 8.31 (d, J = 7.8 Hz, 4H, H^{C2}), 7.90 (t, J = 7.8 Hz, 4H, H^{A4}), 7.35 (m, 4H, H^{C3}), 7.20 (d, J = 5.6 Hz, 4H, H^{A6}), 7.08 (m, 4H, H^{A5}), 4.00 (s, 6H, H^{Me}). ^{13}**C NMR** (126 MHz, CD_3CN) δ/ppm: 163.0 (C^{C4}), 161.1 (C^{B2}), 159.1 (C^{A2}), 154.0(C^{A6}), 151.0 (C^{B4}), 139.6 (C^{A4}), 130.3 (C^{C2}), 129.7 (C^{C1}), 128.2 (C^{A5}), 124.7 (C^{A3}), 121.8 (C^{B3}), 116.1 (C^{C3}), 56.4 (C^{Me}). **IR** (solid, ν/cm^{-1}): 555 (s), 651 (w), 737 (m), 753 (s), 787 (s), 828 (s), 1031 (w), 1177 (m), 1242 (m), 1302 (w), 1411 (m), 1465 (w), 1517 (w), 1603 (m), 2010 (w), 2936 (w). **MS**: (ESI, m/z): 367.2 [M-2PF$_6$]$^{2+}$ (calc. 367.1). **EA**: Found C 50.86 %, H 3.49 %, N 8.51 %, $C_{44}H_{34}F_{12}FeN_6O2_4P_2{\cdot}H_2O$ requires C 50.69 %, H 3.48 %, N 8.06 %.

7.4 Diverse ligands

6,6′-Dimethyl-2,2′-bipyridine (dmbpy)

SM206

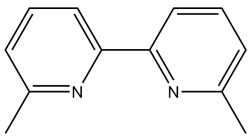

A mixture of 2,2′-bipyridine (7.0 g, 44.8 mmol, 1.0 eq.) and anhydrous THF (125 ml) was cooled to -78 °C under nitrogen atmosphere. Methyl lithium (1.6 M, 100 ml, 160 mmol, 3.6 eq.) was added which resulted in a color change of the solution from colourless to cherry red. The solution was stirred at -78 °C for 1-2 h followed by slow warming up to room temperature overnight. Then the mixture was refluxed for 4 h, cooled to room temperature and later cooled further in an ice bath. Ice-water (50-60 ml) was added slowly and the mixture was stirred for 10 min. The organic solvents were removed in vacuo and the resulting aqueous phase was extracted with CH_2Cl_2 (4 x 70 ml). After combining the organic phases and drying over $MgSO_4$, the volume was reduced to approx. 250 ml. The brown clear solution was cooled in a water-bath and activated MnO_2 (100 g) was added. After stirring for 1.5 h the mixture was filtered over celite and the solvent was removed in vacuo. The received solid was purified by recrysalisation from n-hexane. The product **dmbpy** (4.91 g, 26.6 mmol, 59 %) was obtained as a colourless solid.

^{1}**H NMR** (250 MHz, $CDCl_3$) δ/ppm: 8.18 (d, J = 7.8 Hz, 2H), 7.68 (t, J = 7.7 Hz, 2H), 7.15 (d, J = 7.6 Hz, 2H), 2.63 (s, 6H). The ^{1}H NMR spectroscopic data are in accord with the literature.[132]

6,6′-Dimethyl-[2,2′-bipyridine] 1,1′-dioxide (P13)

SM126

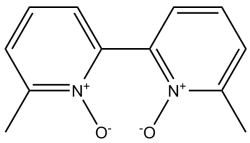

A mixture of dmbpy (1.7 g, 9.23 mmol, 1.0 eq.), H_2O_2 (35 %, 10 ml, 145 mmol, 15.7 eq.) and glacial acetic acid (20 ml) was stirred at 70 °C for 23 h. After evaporation of the solvent, **P13** was obtained as a yellow solid (1.45 g, 6.74 mmol, 73 %) and used without further purification.

^{1}**H NMR** (400 MHz, DMSO-d_6) δ/ppm: 7.58 (m, 2H), 7.45 (m, 2H), 7.31 (t, J = 7.8 Hz, 2H), 2.38 (s, 6H).

6,6′-Dimethyl-4,4′-dinitro-[2,2′-bipyridine] 1,1′-dioxide (P14)

SM127

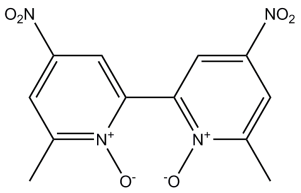

P13 (1.45 g, 6.74 mmol) was cooled in an icebath while a mixture of sulfuric acid (95 %, 8 ml, 143 mmol) and nitric acid (68 %, 14 ml, 212 mmol) was added dropwise. The resulting solution was refluxed for 22 h, cooled to room temperature and poured on ice. The mixture was stirred for 30 min. while a precipitate was formed. The solid was filtered off, washed with water, EtOH and diethyl ether and dried. **P14** was obtained as a yellow solid (474 mg, 1.55 mmol, 23 %)

^{1}**H NMR** (400 MHz, DMSO-d$_6$) δ/ppm: 8.61 (d, J = 3.2 Hz, 2H), 8.53 (d, J = 3.2 Hz, 2H), 2.48 (s, 6H). The ^{1}H NMR spectroscopic data are in accord with the literature.[133]

4,4′-Dibromo-6,6′-dimethyl-[2,2′-bipyridine] 1,1′-dioxide (P15)

SM128

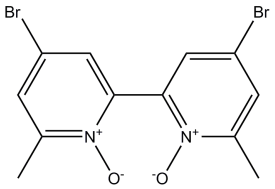

A mixture of glacial acetic acid (30 ml) and **P14** (0.5 g, 1.63 mmol, 1.0 eq.) was warmed to 60 °C and acetyl bromide (3.63 ml, 49 mmol, 30 eq.) was added. The mixture was stirred under reflux for 4 h, cooled to room temperature and poured on ice. The solution was neutralized with saturated aq. Na_2CO_3-solution and the formed precipitate was filtered off. After washing with water, EtOH and diethyl ether **P15** was obtained as a yellow solid (176 mg, 470 µmol, 29 %). The compound was used without further characterization.

4,4′-Dibromo-6,6′-dimethyl-2,2′-bipyridine (P16)

SM129

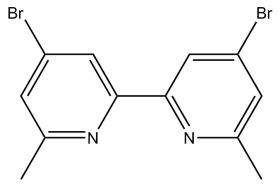

P15 (240 mg, 642 µmol, 1.0 eq.) and anhydr. CH_2Cl_2 (15 ml) were mixed and cooled in an icebath. Tribromophospane (1 ml, 10.4 mmol, 16.2 eq.) was added and the mixture was stirred under reflux for 5 h. The solution was cooled to room temperature, poured on ice and saturated aq. Na_2CO_3 was added. The phases were separated and the aqueous phase was extracted twice with CH_2Cl_2. The combined organic fractions were dried over $MgSO_4$ and the solvent was evaporated. The resulting brown solid was purified by column chromatography (Al_2O_3, cyclohexane / CH_2Cl_2 2:1, R_f = 0.63). **P16** was obtained as a colourless solid (55 mg, 160 µmol, 25 %).

^{1}**H NMR** (250 MHz, $CDCl_3$) δ/ppm: 8.40 (d, J = 1.5 Hz, 2H), 7.36 (d, J = 1.5 Hz, 2H), 2.60 (s, 6H). The ^{1}H NMR spectroscopic data are in accord with the literature.[133]

ALPE

SM138

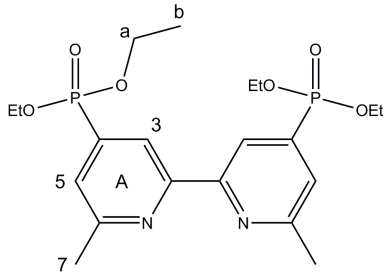

A Microwave flask was charged under nitrogen amosphere with **dmbpy** (130 mg, 380 µmol, 1.0 eq.), Cs_2CO_3(272 mg, 836 µmol, 2.2 eq.), $Pd(PPh_3)_4$ (44 mg, 38 µmol, 0.1 eq.), anhydr. THF (15 ml) and diethyl phosphite (190 µl, 1.52 mmol, 4.0 eq.). The mixture was heated for 2 h to 110 °C in a MW reactor. After cooling, the mixture was filtered and the solvent was removed. The crude product was purified by column chromatography (SiO_2, ethyl acetate, R_f = 0.14). **ALPE** was obtained as a colourless solid (115 mg, 252 µmol, 66 %).

^{1}**H{31P} NMR**(400 MHz, $CDCl_3$) δ/ppm: 8.57 (s, 2H, H^{A3}), 7.56 (s, 2H, H^{A5}), 4.17 (m, 8H, H^a), 2.69 (s, 6H, H^{A7}), 1.37 (t, J = 7.1 Hz, 12H, H^b). ^{31}**P{1H} NMR** (162 MHz, $CDCl_3$) δ/ppm: 15.75
.

2-Bromo-6-methylpyridine 1-oxide (P17)

SM139

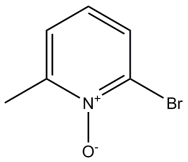

A mixture of 2-bromo-6-methylpyridine (1.14 ml, 10 mmol, 1.0 eq.) and mCPBA (2.59 g, 15 mmol, 1.5 eq.) in CH_2Cl_2 (25 ml) was stirred at rt for 19 h. The solution was neutralized with saturated aq. Na_2CO_3-solution and extracted twice with CH_2Cl_2. The combined organic fractions were dried over $MgSO_4$, the solvent was removed and the obtained orange oil was purified by column chromatography (SiO_2, cyclohexane/ethyl acetate 1:2 , R_f = 0.1). **P17** was obtained as a colourless solid (1.1 g, 5.85 mmol, 59 %).

^{1}**H NMR** (400 MHz, $CDCl_3$) δ/ppm: 7.55 (d, J = 8.1 Hz, 1H), 7.22 (d, J = 7.9 Hz, 1H), 6.99 (t, J = 8.0, 1H), 2.58 (s, 3H). The ^{1}H NMR spectroscopic data are in accord with the literature.[134]
MS (LC-ESI, m/z): 187.9 $[M+H]^+$ (calc. 188.0).

2-Bromo-6-methyl-4-nitropyridine 1-oxide (P18)

SM140

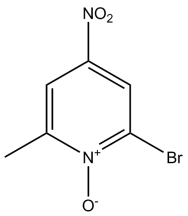

P17 (1.1 g, 5.85 mmol) was dissolved in conc. H_2SO_4 (10 ml) and heated to 90 °C. A mixture of conc. H_2SO_4 (10 ml) and fuming HNO_3 (5 ml) was added dropwise to the reaction mixture and the solution was stirred at 95 °C for 3.5 h. After cooling to rt, the mixture was poured on ice and aq. Na_2CO_3-solution was added until the mixture was alkaline. The formed precipitate was filtered, washed with water and dried in an airstream. **P18** was obtained as a green solid (0.9 g, 3.86 mmol, 66 %).

^{1}**H NMR** (400 MHz, $CDCl_3$) δ/ppm: 8.42 (d, J = 3.1 Hz, 1H), 8.10 (d, J = 3.0 Hz, 1H), 2.64 (s, 3H). The ^{1}H NMR spectroscopic data are in accord with the literature.[134]

4′-Bromo-[1,1′-biphenyl]-4-carbaldehyde (P22)

SM156

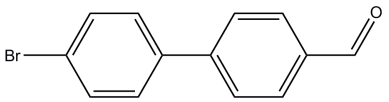

An oven-dried flask was charged with 4,4′-dibromo-1,1′-biphenyl (4.0 g, 12.8 mmol, 1.0 eq.) and anhydr. THF (37 ml) under nitrogen atmosphere. The mixture was cooled to -78 °C and n-BuLi (1.6 M, 8.0 ml, 12.8 mmol, 1.0 eq.) was added during 5 min. After stirring for 5 min., anhydr. DMF (0.99 ml, 12.8 mmol, 1.0 eq.) was added and the mixture was slowly warmed to rt. After quenching with water, the yellow solution was extracted twice with diethyl ether and the combined organic fractions were dried over $MgSO_4$. The solvent was removed and the yellow solid was purified by column chromatography (SiO_2, cyclohexane/CH_2Cl_2 1:1, $R_f = 0.34$).. **P22** was obtained as a colourless solid (1.45 g, 5.55 mmol, 43 %).

^{1}**H NMR** (400 MHz, $CDCl_3$) δ/ppm: 10.06 (s, 1H), 7.96 (d, J = 8.3 Hz, 2H), 7.72 (d, J = 8.2 Hz, 2H), 7.61 (d, J = 8.5 Hz, 2H), 7.50 (d, J = 8.6 Hz, 2H). The ^{1}H NMR spectroscopic data are in accord with the literature.[112]

1,6-Bis(4'-bromo-[1,1'-biphenyl]-4-yl)hexa-1,5-diene-3,4-dione (P23)

SM158

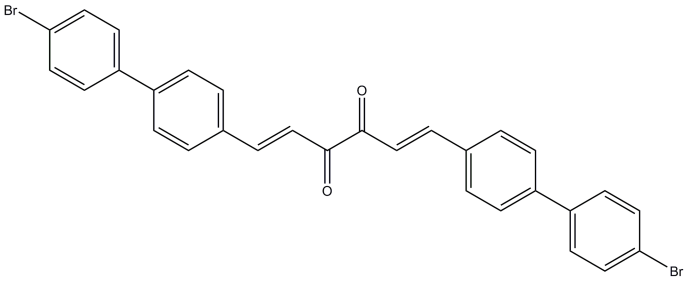

2,3-Butanedione (0.29 ml, 3.33 mmol, 1.0 eq.) in MeOH (50 ml) was added dropwise to a mixture of **P22** (1.74 g, 6.66 mmol, 2.0 eq.) and piperidine (80 µl, 0.81 mmol, 0.25 eq.) in MeOH (50 ml). The mixture was stirred under reflux for 69 h. After cooling, the formed solid was filtered, washed with MeOH and diethyl ether and dried. **P23** was obtained as a brown solid (0.94 g, 1.65 mmol, 49 %).

MS (MALDI-TOF, m/z): 284.8 $[M/2]^+$ (calc. 285.0).

1,6-Bis(4'-bromo-[1,1'-biphenyl]-4-yl)hexa-1,5-diene-3,4-dione (P24)

SM159

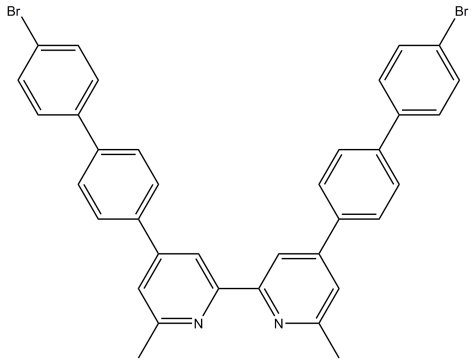

A mixture of **P23** (0.5 g, 874 µmol, 1.0 eq.), *N*-acetonylpyridinium chloride (0.9 g, 5.24 mmol, 6.0 eq.) and ammonium acetate (2.1 g, 26.2 mmol, 30 eq.) in EtOH (50 ml) was stirred under reflux for 70 h. After cooling, the reaction mixture was filtered, the solid was washed with EtOH and diethyl ether and dried. **P24** was obtained as a grey solid (428 mg, 662 µmol, 75 %).

MS (MALDI-TOF, m/z): 647.0 $[M+H]^+$ (calc. 647.9).

ALPE2

SM157

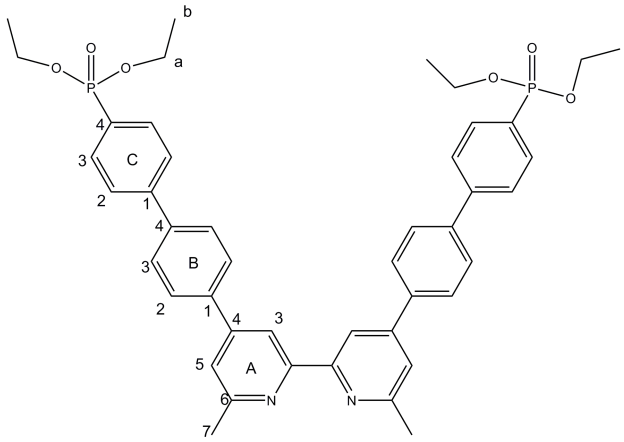

A Microwave flask was charged under nitrogen amosphere with **P24** (170 mg, 263 µmol, 1.0 eq.), Cs_2CO_3 (189 mg, 579 µmol, 2.2 eq.), $Pd(PPh_3)_4$ (61 mg, 52 µmol, 0.2 eq.), anhydr. THF (15 ml) and diethyl phosphite (135 µl, 1.05 mmol, 4.0 eq.). The mixture was heated for 2 h to 115 °C in a MW reactor. After cooling, the mixture was filtered and the solvent was removed. The obtained solid was dissolved in CH_2Cl_2 (20 ml), stirred with activated charcoal for 15 min., filtered over celite and the solvent was removed. The crude product was purified by column chromatography (SiO_2, ethyl acetate, 3 % MeOH, R_f = 0.15) or by recrystallization from ethyl acetate. **ALPE2** was obtained as a pale-yellow solid (68 mg, 84 µmol, 32 %).

^{1}H {^{31}P} NMR (600 MHz, $CDCl_3$) δ/ppm: 8.47 (d, J = 1.7 Hz, 2H, H^{A3}), 7.83 (d, E = 7.8 Hz, 4H, H^{C3}), 7.77 (d, J = 7.9 Hz, 4H, H^{B2}), 7.64 (m, 8H, $H^{B3,C2}$),7.35 (d, J = 1.8 Hz, 2H, H^{A5}), 4.10 (m, 4H, H^a), 4.04 (m, 4H, H^a), 2.64 (s, 6H, H^{A7}), 1.26 (t, J = 7.1 Hz, 12H, H^b).

^{13}**C NMR** (151 MHz, $CDCl_3$) δ/ppm:158.6 (C^{A6}), 156.5 (C^{A2}), 148.8 (C^{A4}), 144.4 (d, J = 3.4 Hz, C^{C1}), 140.4 (C^{B4}), 138.5 (C^{B1}), 132.4 (d, J = 10.2 Hz, C^{C3}), 127.8 (C^{B2}) , 127.8 (C^{B3}), 127.1 (d, J = 15.3 Hz, C^{C2}), 121.0 (C^{A5}), 116.6 (C^{A3}), 62.3 (d, J = 5.4 Hz, C^{a}), 24.8 (C^{A7}), 16.4 (d, J = 6.5 Hz, C^{b}). ^{31}**P{^{1}H} NMR** (243 MHz, $CDCl_3$) δ/ppm: 18.8. **MS** (MALDI-TOF, m/z): 783.8 $[M+Na]^+$ (calc. 783.3), 761.8 $[M+H]^+$ (calc. 761.3).

TA-TEG

SM37

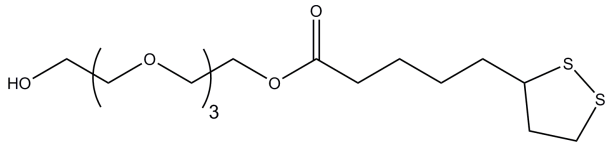

DL-thioctic acid (2.06 g, 10 mmol, 1.0 eq.), tetraethylene glycol (17.3 ml, 100 mmol, 10 eq.) and 4-dimethylaminopyridine (0.367 g, 3.0 mmol, 0.3 eq.) were mixed in CH_2Cl_2 (150 ml) and degassed with nitrogen for 20 min. The solution was cooled in an ice-bath and a nitrogen degassed solution of N,N'-dicyclohexylcarbodiimide (2.5 g, 12.1 mmol, 1.2 eq.) in CH_2Cl_2 (15 ml) was added dropwise. The solution was stirred under nitrogen atmosphere for 2 h in the ice-bath and for 18 h at rt. The mixture was filtered over celite and the volume of the solvent was reduced to ∼15 ml. After cooling and filtering, the solvent was removed, the residue suspended in saturated $NaHCO_3$-solution (150 ml) and extracted with ethyl acetate (5 x 70 ml). The organic fractions were combined, the volume of the solvent was reduced and the formed solid was filtered off. After drying over $MgSO_4$, the solvent was removed. The crude product was purified by column chromatography (SiO_2, ethyl acetate/MeOH 95:5, $R_f = 0.35$). **TA-TEG** was obtained as a yellow oil (2.62 g, 6.86 mmol, 69 %).

^{1}**H NMR** (400 MHz, $CDCl_3$) δ/ppm: 4.23 (m, 2H), 3.67 (m, 12H), 3.61 (m, 2H), 3.15 (m, 2H), 2.45 (m, 1H), 2.35 (t, J = 7.4 Hz, 2H), 1.91 (m, 1H), 1.82 (s, 1H), 1.67 (m, 4H), 1.46 (m, 2H).^{13}**C NMR** (101 MHz, $CDCl_3$) δ/ppm: 173.6, 72.6, 70.8, 70.6, 70.4, 69.3, 63.5, 61.9, 56.5, 40.3, 38.6, 34.7, 34.0, 28.8, 24.7. The ^{1}H and ^{13}C NMR spectroscopic data are in accord with the literature.[116]

TA-PEG

SM38

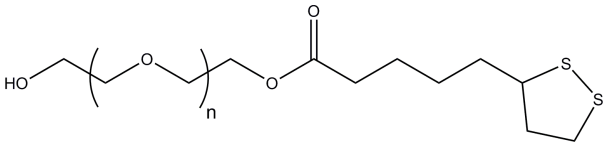

DL-thioctic acid (2.06 g, 10 mmol, 1.0 eq.), polyethylene glycol 400 (37 ml, 100 mmol, 10 eq.) and 4-dimethylaminopyridine (0.367 g, 3.0 mmol, 0.3 eq.) were mixed in CH_2Cl_2 (150 ml) and degassed with nitrogen for 20 min. The solution was cooled in an ice-bath and a nitrogen degassed solution of *N*,*N'*-dicyclohexylcarbodiimide (2.5 g, 12.1 mmol, 1.2 eq.) in CH_2Cl_2 (15 ml) was added dropwise. The solution was stirred under nitrogen atmosphere for 2 h in the ice-bath and for 18 h at rt. The mixture was filtered over celite, the solvent was removed and the obtained yellow oil was filtered again. The residue was suspended in saturated $NaHCO_3$-solution (150 ml) and extracted with ethyl acetate (3 x 70 ml). The combined organic fractions were dried over $MgSO_4$ and the solvent was removed. After filtering, the oil was diluted with ethyl acetate to avoid gelation. The crude product was purified by column chromatography (SiO_2, ethyl acetate/cyclohexane/EtOH 4:3:2 + 2 % MeOH). **TA-PEG** was obtained as a yellow oil (3.5 g, 5.8 mmol, 58 %).

^{1}**H NMR** (400 MHz, $CDCl_3$) δ/ppm: 4.22 (t, J = 4.8 Hz, 2H), 3.65 (m, 36H), 3.13 (m, 2H), 2.78 (d, J = 6.2 Hz, 1H), 2.45 (m, 1H), 2.35 (t, J = 7.4 Hz, 2H), 1.99 (m, 1H), 1.91 (m, 1H), 1.67 (m, 4H), 1.47 (m, 2H). The ^{1}H NMR spectroscopic data are in accord with the literature.[116]

(Phenylazanediyl)bis(ethane-2,1-diyl) dimethanesulfonate (P25)

SM76

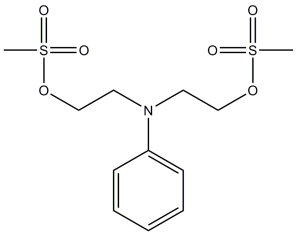

To a cooled solution of *N*-phenyldiethanolamine (10.0 g, 55 mmol, 1.0 eq.) and NEt_3 (23 ml, 166 mmol, 3.0 eq.) in CH_2Cl_2 (200 ml) was added dropwise methanesulfonyl chloride (9.0 ml, 116 mmol, 2.1 eq.). After stirring for 45 min. in an ice-bath, the mixture was stirred for 1.5 h at rt. After filtering, the solution was poured into an acidic ice-water mixture. The organic phase was separated, washed with water (2 x 50 ml). and saturated NaCl-solution (3 x 50 ml) and dried over $MgSO_4$. The solvent was removed and the crude product was recrystallized (CH_2Cl_2/cyclohexane). **P25** was obtained as a yellow oil (9.56 g, 28.3 mmol, 52 %).

^{1}**H NMR** (400 MHz, $CDCl_3$) δ/ppm: δ7.27 (m, 2H), 6.80 (t, J = 7.3 Hz, 1H), 6.74 (dd, J = 8.8, 0.8 Hz, 2H), 4.36 (t, J = 5.9 Hz, 4H), 3.77 (t, J = 5.9 Hz, 4H), 2.97 (s, 6H). The ^{1}H NMR spectroscopic data are in accord with the literature.[135]

10-Phenyl-1,4-dioxa-7,13-dithia-10-azacyclopentadecane (P26)

SM77

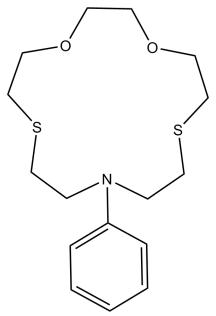

A mixture of 3,6-dioxa-1,8-octanedithiol (1.2 g, 6.6 mmol, 1.0 eq.) and K_2CO_2 (3.65 g, 26.4 mmol, 4.0 eq.) in anhydr. MeCN (150 ml) was stirred for 1 h under reflux. **P25** (2.23 g, 6.6 mmol, 1.0 eq.) was dissolved in anhydr. MeCN (20 ml) and and added slowly the the reaction mixture. After refluxing for 18 h, the mixture was filtered and the solvent was removed. The obtained yellow oil was purified by column chromatography (SiO_2, CH_2Cl_2/ethyl acetate 10:1, R_f = 0.55). **P26** was obtained as an off-white solid (0.5 g, 1.53 mmol, 23 %).

^{1}**H NMR** (500 MHz, $CDCl_3$) δ/ppm: 7.22 (dd, J = 8.7, 7.4 Hz, 2H), 6.69 (t, J = 7.2Hz,1H) 6.65 (m, 2H), 3.81 (t, J = 5.1 Hz, 4H), 3.65 (s, 4H), 3.62 (m, 4H), 2.90 (t, J = 8.0 Hz, 4H), 2.76 (t, J = 5.1 Hz, 4H). ^{13}**C NMR** (126 MHz, $CDCl_3$) δ/ppm: 146.9, 129.6, 116.2, 111.8, 74.4, 70.8, 51.9, 31.2, 29.6. The ^{1}H and ^{13}C NMR spectroscopic data are in accord with the literature.[136] **MS**: (EI, m/z): 327.1 $[M]^+$ (calc. 327.1).

L6

SM78

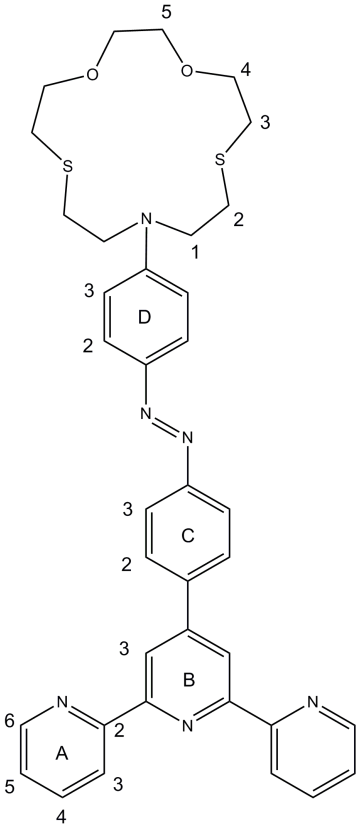

4-([2,2′:6′,2″-terpyridin]-4′-yl)aniline (90 mg, 277 µmol, 1.0 eq.) was dissolved in HCl (16 %, 10 ml), and the orange solution was cooled to -4 °C. A solution of $NaNO_2$ (20 mg, 290 µmol, 1.05 eq.) in water (0.4 ml) was added dropwise. After 5 min. stirring, the solution was tested to free nitrous acid with potassium iodide starch paper and the excess of acid was quenched with sulfamic acid. This mixture was added to a solution of **P26** (0.1 g, 305 µmol, 1.1 eq.) in HCl (1 M, 10 ml) at 7 °C and stirred for 1 h. NaOAc-solution (4 M, 25 ml) and saturated Na_2CO_3-solution (30 ml) were added until the mixture was neutral and the formed solid was filtered off. After washing with water and diethyl ether, the solid was dried. **L6** was otained as an orange solid (78 mg, 117 µmol, 42 %).

^{1}**H NMR** (500 MHz, $CDCl_3$) δ/ppm: 8.79 (s, 2H, H^{B3}), 8.73 (m, 2H, H^{A6}), 8.68 (m, 2H, H^{A3}), 8.03 (d, J = 8.5 Hz, 2H, H^{C2}), 7.97 (d, J = 8.6 Hz, 2H, H^{C3}), 7.88 (m, 2H, H^{A4}), 7.36 (ddd, J = 7.5, 4.8, 1.0 Hz, 2H, H^{A5}), 7.21 (m, 2H, H^{D2}), 6.66 (m, 2H, H^{D3}), 3.80 (m, 4H, H^4), 3.74 (m, 4H, H^1), 3.64 (s, 4H, H^5), 2.95 (m, 4H, H^2), 2.76 (m, 6H, H^3). ^{13}**C NMR** (126 MHz, $CDCl_3$) δ/ppm: 156.3 (C^{A2}), 156.0 (C^{B2}), 153.6 (C^{C4}), 149.7 (C^{B4}), 149.2 (C^{A6}), 146.8 (C^{D4}) 144.0 (C^{D1}), 139.2 (C^{C1}), 137.1 (C^{A4}), 129.6 (C^{D2}), 128.1 (C^{C2}), 124.0 (C^{A5}), 122.9 (C^{C3}), 121.5 (C^{A3}), 118.9 (C^{B3}), 111.6 (C^{D3}), 74.5 (C^4), 70.8 (C^5), 51.9 (C^1), 31.4 (C^3), 29.7 (C^2). **MS**: (ESI, m/z): 701.5 $[M+K]^+$ (calc. 701.2); 663.3 $[M+H]^+$ (calc. 663.3).

References

[1] A. F. Holleman, E. Wiberg and N. Wiberg, *Lehrbuch der Anorganische Chemie*, Walter de Gruyter, 101. edition, **1995**.

[2] G. A. Lawrance, *Introduction to Coordination Chemistry*, John Wiley & Sons, Ltd, Chichester, UK, 1st edition, **2010**.

[3] C. E. Housecroft and A. G. Sharpe, *Anorganische Chemie*, Pearson Studium, Mï¿œnchen, 2. edition, **2006**.

[4] K. Kalyanasundaram and M. Grätzel, *Coord. Chem. Rev.*, **1998**, *77*, 347.

[5] G. C. Vougioukalakis, A. I. Philippopoulos, T. Stergiopoulos and P. Falaras, *Coord. Chem. Rev.*, **2011**, *255*, 2602.

[6] D. Tordera, A. M. Bünzli, A. Pertegás, J. M. Junquera-Hernández, E. C. Constable, J. A. Zampese, C. E. Housecroft, E. Ortí and H. J. Bolink, *Chem. Eur. J.*, **2013**, *19*, 8597.

[7] E. C. Constable, C. E. Housecroft, G. E. Schneider, J. A. Zampese, H. J. Bolink, A. Pertegás and C. Roldan-Carmona, *Dalton Trans.*, **2014**, *43*, 4653.

[8] U. S. Schubert, A. Winter and G. R. Newkome, *Terpyridine-based Materials*, Wiley-VCH, Weinheim,Germany, 1st. edition, **2011**.

[9] B. Happ, A. Winter, M. D. Hager and U. S. Schubert, *Chem. Soc. Rev.*, **2012**, *41*, 2222.

[10] F. Wu, Y. Feng and C. W. Jones, *ACS Catalysis*, **2014**, *4*, 1365.

[11] A. C. Gomes, M. Pillinger, P. Nunes, I. S. Gonçalves and M. Abrantes, *J. Organomet. Chem.*, **2014**, *760*, 42.

[12] P. Liu, C.-Y. Zhou, S. Xiang and C.-M. Che, *Chem. Commun.*, **2010**, *46*, 2739.

[13] E. C. Constable, *Adv. Inorg. Chem.*, **1989**, *34*, 1.

[14] D. Wenkert and R. B. Woodward, *J. Org. Chem.*, **1983**, *48*, 283.

[15] S. Hug, M. E. Tauchert, S. Li, U. E. Pachmayr and B. V. Lotsch, *J. Mater. Chem.*, **2012**, *22*, 13956.

[16] H. Shimada, T. Sakurai, Y. Kitamura, H. Matsuura and T. Ihara, *Dalton Trans.*, **2013**, *42*, 16006.

[17] T. N. Y. Hoang, M. Humbert-Droz, T. Dutronc, L. Guénée, C. Besnard and C. Piguet, *Inorg. Chem.*, **2013**, *52*, 5570.

[18] J. S. Dhau, A. Singh, Y. Kasetti, S. Bhatia, P. V. Bharatam, P. Brandão, V. Félix and K. N. Singh, *Tetrahedron*, **2013**, *69*, 10284.

[19] F. Kröhnke, *Synthesis*, **1976**, 1.

[20] I. Eryazici, C. N. Moorefield, S. Durmus and G. R. Newkome, *J. Org. Chem.*, **2006**, *71*, 1009.

[21] J. Wang and G. S. Hanan, *Synlett*, **2005**, 1251.

[22] E. C. Constable, *Adv. Inorg. Radiochem.*, **1986**, *30*, 69.

[23] C. Kaes, A. Katz and M. W. Hosseini, *Chem. Rev.*, **2000**, *100*, 3553.

[24] E. C. Constable, K. Harris, C. E. Housecroft, M. Neuburger and J. A. Zampese, *Dalton Trans.*, **2011**, *40*, 11441.

[25] B. Brisig, E. C. Constable and C. E. Housecroft, *New J. Chem.*, **2007**, *31*, 1437.

[26] P. A. Anderson, G. B. Deacon, K. H. Haarmann, F. R. Keene, T. J. Meyer et al., *Inorg. Chem.*, **1995**, *34*, 6145.

[27] E. Z. Jandrasics and F. R. Keene, *J. Chem. Soc., Dalt. Trans.*, **1997**, *2*, 153.

[28] C. M. Kepert, A. M. Bond, G. B. Deacon, L. Spiccia et al., *Dalton Trans.*, **2004**, 1766.

[29] M. Myahkostupov and F. N. Castellano, *Inorg. Chem.*, **2011**, *50*, 9714.

[30] N. S. Lewis and D. G. Nocera, *PNAS*, **2006**, *103*, 15729.

[31] G. Steinhauser, A. Brandl and T. E. Johnson, *The Science of the total environment*, **2014**, *470-471*, 800.

[32] M. Graetzel, *Nature*, **2001**, *414*, 338.

[33] E. Barraud, *Chimia*, **2013**, *67*, 181.

[34] A. Hagfeldt, G. Boschloo, L. Sun, L. Kloo and H. Pettersson, *Chem. Rev.*, **2010**, *110*, 6595.

[35] A. Mishra, M. K. R. Fischer and P. Bäuerle, *Angew. Chem.*, **2009**, *48*, 2474.

[36] E. Galoppini, *Coord. Chem. Rev.*, **2004**, *248*, 1283.

[37] http://www.dyesol.com, **19.08.2014**.

[38] http://www.solaronix.com, **19.08.2014**.

[39] http://www.gcell.com, **19.08.2014**.

[40] http://www.infomine.com, **18.08.2014**.

[41] K. H. Wedepohl, *Geochim. Cosmochim. Acta*, **1995**, *59*, 1217.

[42] M. Mara, K. A. Fransted and L. Chen, *Coord. Chem. Rev.*, **2014**, *doi 10.1016/j.ccr.2014.06.013*.

[43] B. Bozic-Weber, S. Y. Brauchli, E. C. Constable, S. O. Fürer, C. E. Housecroft, F. J. Malzner, I. A. Wright and J. A. Zampese, *Dalton Trans.*, **2013**, *42*, 12293.

[44] B. Bozic-Weber, S. Y. Brauchli, E. C. Constable, S. O. Fürer, C. E. Housecroft and I. A. Wright, *Phys. Chem. Chem. Phys.*, **2013**, *15*, 4500.

[45] S. Ito, T. N. Murakami, P. Comte, P. Liska, C. Grätzel, M. K. Nazeeruddin and M. Grätzel, *Thin Solid Films*, **2008**, *516*, 4613.

[46] F. J. Malzner, S. Y. Brauchli, E. C. Constable, C. E. Housecroft and M. Neuburger, *RSC Adv.*, **2014**, *4*, 48712.

[47] T. Hu, L. He, L. Duan and Y. Qiu, *J. Mater. Chem.*, **2012**, *22*, 4206.

[48] R. D. Costa, E. Ortí, H. J. Bolink, F. Monti, G. Accorsi and N. Armaroli, *Angew. Chem.*, **2012**, *51*, 8178.

[49] E. Holder, B. M. W. Langeveld and U. S. Schubert, *Adv. Mater.*, **2005**, *17*, 1109.

[50] B. Valeur and I. Leray, *Coord. Chem. Rev.*, **2000**, *205*, 3.

[51] R. Martínez-Máñez and F. Sancenón, *Chem.Rev.*, **2003**, *103*, 4419.

[52] J. Ma, J. Wu, W. Liu, P. Wang and Z. Fan, *Spectrochimica Acta Part A*, **2012**, *94*, 340.

[53] P. D. Beer and J. Cadman, *Coord. Chem. Rev.*, **2000**, *205*, 131.

[54] J. J. Concepcion, J. W. Jurss, M. K. Brennaman, P. G. Hoertz, A. O. T. Patrocinio, N. Y. Murakami Iha, J. L. Templeton and T. J. Meyer, *Acc. Chem. Res.*, **2009**, *42*, 1954.

[55] F. Puntoriero, A. Sartorel, M. Orlandi, G. La Ganga, S. Serroni, M. Bonchio, F. Scandola and S. Campagna, *Coord. Chem. Rev.*, **2011**, *255*, 2594.

[56] W. J. Youngblood, S.-H. A. Lee, K. Maeda and T. E. Mallouk, *Acc. Chem. Res.*, **2009**, *42*, 1966.

[57] T. Ishiyama and N. Miyaura, *Pure Appl. Chem.*, **2006**, *78*, 1369.

[58] G. D. Jones, J. L. Martin, C. McFarland, O. R. Allen, R. E. Hall, A. D. Haley, R. J. Brandon, T. Konovalova, P. J. Desrochers, P. Pulay and D. A. Vicic, *J. Am. Chem. Soc.*, **2006**, *128*, 13175.

[59] D.-W. Yoo, S.-K. Yoo, C. Kim and J.-K. Lee, *J. Chem. Soc., Dalton Trans.*, **2002**, 3931.

[60] U. S. Schubert and C. Eschbaumer, *Angew. Chem.*, **2002**, *41*, 2892.

[61] G. G. Talanova, L. Zhong and R. A. Bartsch, *J. Appl. Polym. Sci.*, **1999**, *74*, 849.

[62] J. Clayden, N. Greeves, S. Warren and P. Wothers, *Organic Chemistry*, Oxford University Press, 1st edition, **2001**.

[63] R. Brückner, *Reaktionsmechanismen*, Elsevier, 3rd edition, **2004**.

[64] O. Johansson, M. Borgström, R. Lomoth, M. Palmblad, J. Bergquist, L. Hammarström, L. Sun and B. Akermark, *Inorg. Chem.*, **2003**, *42*, 2908.

[65] D. P. Cormode, A. J. Evans, J. J. Davis and P. D. Beer, *Dalton Trans.*, **2010**, *39*, 6532.

[66] M. Wijtmans, S. J. Rosenthal, B. Zwanenburg and N. A. Porter, *J. Am. Chem. Soc.*, **2006**, *128*, 11720.

[67] G. Wu, P. Verwilst, J. Xu, H. Xu, R. Wang, M. Smet, W. Dehaen, C. F. J. Faul, Z. Wang and X. Zhang, *Langmuir*, **2012**, *28*, 5023.

[68] G.-J. Brink, I. W. C. E. Arends, M. Hoogenraad, G. Verspui and R. A. Sheldon, *Adv. Synth. Catal.*, **2003**, *345*, 497.

[69] Y.-R. Hong and C. B. Gorman, *J. Org. Chem.*, **2003**, *8204*, 9019.

[70] E. C. Constable, R. Frantz, C. E. Housecroft, J. Lacour and A. Mahmood, *Inorg. Chem.*, **2004**, *43*, 4817.

[71] H. J. Jung, H. Min, H. Yu, T. G. Lee and T. D. Chung, *Chem. Commun.*, **2010**, *46*, 3863.

[72] A. Baber, J. G. de Vries, A. G. Orpen, P. G. Pringle and K. von der Luehe, *Dalton Trans.*, **2006**, 4821.

[73] A. Marra, S. Staderini, N. Berthet, P. Dumy, O. Renaudet and A. Dondoni, *Eur. J. Org. Chem.*, **2013**, 1144.

[74] P. G. M. Wuts and T. W. Greene, *Greene's protective groups in organic synthesis*, John Wiley & Sons Inc., Hoboken, New Jersey, 4th edition edition, **2007**.

[75] W. Steglich and B. Neises, *Angew. Chem. Int. Ed.*, **1978**, *17*, 552.

[76] K. C. Kress, M. Kaller, K. V. Axenov, S. Tussetschläger and S. Laschat, *Beilstein J. Org. Chem.*, **2012**, *8*, 371.

[77] A. Baron, C. Herrero, A. Quaranta, M.-F. Charlot, W. Leibl, B. Vauzeilles and A. Aukauloo, *Chem. Commun.*, **2011**, *47*, 11011.

[78] P. Y. Vuillaume, J.-C. Galin and C. G. Bazuin, *Macromolecules*, **2001**, *34*, 859.

[79] M. Wipf, R. L. Stoop, A. Tarasov, K. Bedner, W. Fu, I. A. Wright, C. J. Martin, E. C. Constable, M. Calame and C. Schönenberger, *ACS nano*, **2013**, *7*, 5978.

[80] T. Avellini, C. Lincheneau, M. La Rosa, A. Pertegas, H. J. Bolink, I. A. Wright, E. C. Constable, S. Silvi and A. Credi, *Chem. Commun.*, **2014**, *50*, 11020.

[81] Z.-H. Lin, S.-J. Ou, C.-Y. Duan, B.-G. Zhang and Z.-P. Bai, *Chem. Commun.*, **2006**, *2*, 624.

[82] Z.-H. Lin, Y.-G. Zhao, C.-Y. Duan, B.-G. Zhang and Z.-P. Bai, *Dalton Trans.*, **2006**, 3678.

[83] S. Khatua, D. Samanta, J. W. Bats and M. Schmittel, *Inorg. Chem.*, **2012**, *51*, 7075.

[84] K. L. Mulfort and D. M. Tiede, *J. Phys. Chem. B*, **2010**, *114*, 14572.

[85] M. O. Albers, T. V. Ashworth, H. E. Oosthuizen, E. Singleton, J. S. Merola and R. T. Kacmarcik, *Inorg. Synth.*, **1989**, *26*, 68.

[86] W. Paw and R. Eisenberg, *Inorg. Chem.*, **1997**, *36*, 2287.

[87] A. Ambroise, R. W. Wagner, P. D. Rao, J. A. Riggs, P. Hascoat, , J. S. Lindsey et al., *Chem. Mater.*, **2001**, *13*, 1023–1034.

[88] E. C. Constable and A. M. Cargill Thompson, *J. Chem. Soc., Dalton Trans.*, **1994**, 1409.

[89] E. C. Constable, C. E. Housecroft, A. M. Cargill Thompson, P. Passaniti, S. Silvi, M. Maestri and A. Credi, *Inorg. Chim. Acta*, **2007**, *360*, 1102.

[90] M. J. Hynes, *J. Chem. Soc., Dalton Trans.*, **1993**, 311.

[91] K. Hirose, *J. Inclusion Phenom. Macrocyclic Chem.*, **2001**, *39*, 193.

[92] M. Maestri, N. Armaroli, V. Balzani, E. C. Constable and A. M. W. Cargill Thompson, *Inorg. Chem.*, **1995**, *34*, 2759.

[93] P. Maccarthy, *Anal. Chem.*, **1978**, *50*, 2165.

[94] J. Shao, H. Lin, M. Yu, Z. Cai and H. Lin, *Talanta*, **2008**, *75*, 551.

[95] E. C. Constable, C. E. Housecroft, E. R. Schofield, S. Encinas et al., *Chem. Commun.*, **1999**, 869.

[96] M. Mariappan and B. G. Maiya, *Eur. J. Inorg. Chem.*, **2005**, 2164.

[97] B. Bozic-Weber, E. C. Constable, S. O. Fürer, C. E. Housecroft, L. J. Troxler and J. A. Zampese, *Chem. Commun.*, **2013**, *49*, 7222.

[98] J. E. Beves, P. Chwalisz, E. C. Constable, C. E. Housecroft, M. Neuburger, S. Schaffner and J. A. Zampese, *Inorg. Chem. Commun.*, **2008**, *11*, 1009.

[99] J. W. Slot and H. J. Geuze, *J. Cell Biol.*, **1981**, *90*, 533.

[100] S. Link and M. a. El-Sayed, *J. Phys. Chem. B*, **1999**, *103*, 4212.

[101] Y. Q. He, S. P. Liu, L. Kong and Z. F. Liu, *Spectrochim. Acta. A. Mol. Biomol. Spectrosc.*, **2005**, *61*, 2861.

[102] P. K. Jain, K. S. Lee, I. H. El-Sayed and M. a. El-Sayed, *J. Phys. Chem. B*, **2006**, *110*, 7238.

[103] http://www.cytodiagnostics.com, **03.10.2014**.

[104] X. Liu, M. Atwater, J. Wang and Q. Huo, *Colloids Surf., B*, **2007**, *58*, 3.

[105] E. C. Constable, C. D. Ertl, C. E. Housecroft and J. A. Zampese, *Dalton Trans.*, **2014**, *43*, 5343.

[106] J. Sun, F. Zhong and J. Zhao, *Dalton Trans.*, **2013**, *42*, 9595.

[107] G. Nasr, A. Guerlin, F. Dumur, S. a. Baudron, E. Dumas, F. Miomandre, G. Clavier, M. Sliwa and C. R. Mayer, *J. Am. Chem. Soc.*, **2011**, *133*, 6501.

[108] J.-J. Kim, K. Lim, H. Choi, S. Fan, M.-S. Kang, G. Gao, H. S. Kang and J. Ko, *Inorg. Chem.*, **2010**, *49*, 8351–7.

[109] H.-F. Huang, S.-H. Xu, Y.-B. He, C.-C. Zhu, H.-L. Fan, X.-H. Zhou, X.-C. Gao and Y.-F. Dai, *Dyes Pigm.*, **2013**, *96*, 705.

[110] M. Iyado, H. Otsuka, K. Sato, N. Nisato and M. Oda, *Bull. Chem. Soc. Jpn.*, **1990**, *63*, 80.

[111] E. Rajalakshmanan and V. Alexander, *Synth. Commun.*, **2005**, *35*, 891.

[112] F. Leroux, T. U. Hutschenreuter, C. Charriere, R. Scopelliti and R. W. Hartmann, *Helv. Chim. Acta*, **2003**, *86*, 2671.

[113] H. E. Katz, W. L. Wilson and G. Scheller, *J. Am. Chem. Soc.*, **1994**, *116*, 6636.

[114] H. E. Katz, S. F. Bent, L. W. William, M. L. Schilling and S. B. Ungashet, *J. Am. Chem. Soc.*, **1994**, *116*, 6631.

[115] K. Neuthe, F. Bittner, F. Stiemke, B. Ziem, J. Du, M. Zellner, M. Wark, T. Schubert and R. Haag, *Dyes Pigm.*, **2014**, *104*, 24.

[116] H. T. Uyeda, I. L. Medintz, J. K. Jaiswal, S. M. Simon and H. Mattoussi, *J. Am. Chem. Soc.*, **2005**, *127*, 3870.

[117] Y. Yan, Y. Hu, G. Zhao and X. Kou, *Dyes Pigm.*, **2008**, *79*, 210.

[118] F. Sancenón, R. Martínez-Mánez and J. Soto, *Angew. Chem. Int. Ed*, **2002**, *41*, 1416.

[119] H. G. O. Becker, W. Berger and G. Domschke, *Organikum*, Wiley-VCH Weinheim, 20. edition, **1998**.

[120] *APEX 2, version 2 User Manual, M86-E01078, Bruker Analytical X-ray Systems, Madison, 2006.*

[121] G. M. Sheldrick, *Acta Crystallogr. A*, **2008**, *64*, 112.

[122] J. Xu, R. Wang, Y. Li, Z. Gao, R. Yao, S. Wang and B. Wu, *Eur. J. Inorg. Chem.*, **2012**, 3349.

[123] T. Postma, W. Galloway, F. Cougnon, G. Pantos, J. Stokes and D. Spring, *Synlett*, **2013**, *24*, 765.

[124] J. S. Willemsen, J. C. M. van Hest and F. P. J. T. Rutjes, *Beilstein J. Org. Chem.*, **2013**, *9*, 960.

[125] A. Anthonysamy, S. Balasubramanian, V. Shanmugaiah and N. Mathivanan, *Dalton Trans.*, **2008**, *300*, 2136.

[126] E. Block, E. V. Dikarev, R. S. Glass, J. Jin, B. Li, X. Li and S.-Z. Zhang, *J. Am. Chem. Soc.*, **2006**, *128*, 14949.

[127] B. M. Adger, R. Bannister, N. J. Lewis and C. O. Farrell, *J. Chem. Soc., Perkin Trans. I*, **1988**, 2785.

[128] H.-C. Lin, H. Kim, S. Barlow, J. M. Hales, J. W. Perry and S. R. Marder, *Chem. Commun.*, **2011**, *47*, 782.

[129] C. A. Panetta, H. J. Kumpaty, N. E. Heimer and M. C. Leavy, *J. Org. Chem.*, **1999**, *64*, 1015.

[130] D. Wenkert and R. Woodward, *J. Org. Chem.*, **1983**, *48*, 283.

[131] T. Prakasam, M. Lusi, M. Elhabiri, C. Platas-Iglesias, J.-C. Olsen, Z. Asfari, S. Cianférani-Sanglier, F. Debaene, L. J. Charbonni and A. Trabolsi, *Angew. Chem.*, **2013**, *52*, 9956.

[132] L.-y. Liao, X.-r. Kong and X.-f. Duan, *J. Org. Chem.*, **2014**, *79*, 777.

[133] V.-M. Mukkala, *Helv. Chim. Acta*, **1992**, *75*, 1578.

[134] J. W. Walton, A. Bourdolle, S. J. Butler, M. Soulie et al., *Chem. Commun.*, **2013**, *49*, 1600.

[135] S.-W. Lin, Q. Sun, Z.-M. Ge, X. Wang, J. Ye and R.-T. Li, *Bioorg. Med. Chem. Lett.*, **2011**, *21*, 940.

[136] D. Jiménez, R. Martínez-Máñez, F. Sancenón, J. V. Ros-Lis, J. Soto, A. Benito and E. García-Breijo, *Eur. J. Inorg. Chem.*, **2005**, 2393.